Spatially and temporally scaled inverse hydraulic modelling, multi tracer transport modelling and interaction with geochemical processes at a highly transient bank filtration site

Dissertation

zur Erlangung des akademischen Grades
Doctor rerum naturalium
(Dr. rer. nat.)
im Fach Geographie

---

eingereicht an der
Mathematisch-Naturwissenschaftlichen Fakultät II
der Humboldt-Universität zu Berlin

von Dipl.-Ing. Bernd Ulrich Wiese M.Sc.

aus Berlin

Prof. Dr. Christoph Markschies
Präsident der Humboldt-Universität
zu Berlin

Prof. Dr. Wolfgang Coy
Dekan der Mathematisch-Naturwissenschaftlichen Fakultät

Gutachter:

1. Prof. Dr. Gunnar Nützmann, HU-Berlin

2. Prof. Dr. Reinhard Hinkelmann, TU-Berlin

3. Dr. habil. Ekkehard Holzbecher, WIAS-Berlin

Tag der Verteidigung: 20. Dezember 2006

Scientific Curriculum Vitae

Chronological itemisation

Since May 2002	Doctoral study at the IGB (Institut für Gewässerökologie und Binnenfischerei, Berlin)
Dec. 2001 – May 2002	Research Assistant at the IWS (Institut für Wasserbau, Universität Stuttgart), development of hydrologic software
May 2001	Degree: MSc. Water Resources and Engineering Management
Oct. 2000 – May 2001	Study course: WAREM (Water Resources and Engineering Management), Universität Stuttgart
Oct. 2000	Degree: Dipl.-Ing. Umweltschutztechnik
Oct. 1999 – Sept. 2000	Exchange study at the Universidad Complutense de Madrid and Diploma Thesis „Modelling the Entrepeñas Reservoir“
Oct. 1994 – Oct. 2000	Study course: Umweltschutztechnik, Universität Stuttgart
1993	Abitur, Auguste-Viktoria Schule, Itzehoe

Publications in international peer reviewed Journals

Bernd U. Wiese, María C. Palancar, José M. Aragón, Fernando Sánchez, Roberto Gil (2006), *Modelling the Entrepeñas Reservoir*, Water Environment Research, Vol. 78, No. 8, pp. 781-791

Dizer, H., Grützmacher, G., Bartel, H., Wiese, B., Szewzyk, R., Lopezpila, J. M. (2004), *Contribution of the colmation layer to the elimination of coliphages by slow sand filtration.* Water Science and Technology, 50, 211-214.

Conference Proceedings

Wiese, B. (2005), *Hydraulic and Transport Modelling of Bank Filtration at Lake Tegel (Berlin)*, ISMAR5, Proceedings of the 5th International Symposium on Management of Aquifer Recharge ISMAR5, Berlin, Germany, 11–16 June 2005, pp. 449-454

Grützmacher, G., Bartel, H., Wiese, B. (2005), *Simulating bank filtration and artificial recharge on a technical scale*, Proceedings of the 5th International Symposium on Management of Aquifer Recharge ISMAR5, Berlin, Germany, 11–16 June 2005, pp. 498-503

Licht E., Wiese B., Heberer T., Grützmacher G. (2005), Estimating of the solute transport parameters retardation factor and decay coefficient of pharmaceutical residues using the program Visual CXTFIT, Proceedings of the 5th International Symposium on Management of Aquifer Recharge ISMAR5, Berlin, Germany, 11–16 June 2005, pp. 399-404

Nützmann G., Holzbecher E., Wiese B., Licht E., Knappe A. (2005), Visual CXTFIT – a user friendly simulation tool for modelling one-dimensional transport, sorption and degradation processes during bank filtration, Proceedings of the 5th International Symposium on Management of Aquifer Recharge ISMAR5, Berlin, Germany, 11–16 June 2005, pp. 409-414

Greskowiak, J., Massmann, G., Wiese, B., Lewandowski, J., Nützmann, G., Pekdeger, A. (2004), Geochemical changes under alternating saturated and unsaturated conditions during artificial groundwater recharge via ponded infiltration of surface water - A field study, Saturated and Unsaturated Zone Workshop, Proc., Rome, p. 157-162

Wiese, B., Holzbecher, E., Rümmler, J., Nützmann, G. (2004), *Assessment of bank filtration pumping regimes on flow length and travel times: a case study*. In: KOVAR, K., HRKAL, Z.,.BRUTHANS, J. (eds.), FEM_MODFLOW, International Conference on Finite Elements Models, MODFLOW, and More: Solving Groundwater Problems, p. 411-414.

Palancar, M.-C., Aragón, J.-M., Wiese, B., Sánchez, F., (2001) *Modelling the active volume of reservoirs to predict the dispersion of pollutants*. Chem. Ing. Tech. 2001, 6, 602, 3rd European Congress of Chemical Engineering, Nürnberg, Germany, 26-28 June 2001

Other publications

Nützmann, G., Horner, C., Holzbecher, E., Wiese, B., Greskowiak, J., (2004) *Integrated modeling concepts and bank filtration processes: coupled groundwater transport and biogeochemical reactions*, 2nd NASRI intermediary Report, Kompetenzzentrum Wasser Berlin

Wiese, B., Rümmler, J., Holzbecher, E., Nützmann, G. (2003), *Assessing the effect of pumping regimes on bank filtration / Auswirkungen des Pumpregimes auf die Uferfiltration,* IGB Annual Report 2003 / IGB Jahresforschungsbericht 2003

Wiese, B., (2000) *Modelling the Entrepeñas Reservoir,* Universidad Complutense de Madrid and Universität Stuttgart, unpublished Diploma Thesis

Eidesstattliche Erklärung

Ich habe die vorgelegte Arbeit selbständig und ohne unerlaubte Hilfe angefertigt.

Ich reiche diese Arbeit erstmalig bei der Humboldt-Universität zu Berlin ein und besitze keinen entsprechenden Doktorgrad.

Der Inhalt der aktuellen Promotionsordnung (Nr. 34, 2006) ist mir bekannt.

Berlin, 6. 11. 2006 Bernd Wiese

Preface

The current study was scientifically enabled by previous investigations on bank filtration in general, and in particular on the current test site carried out by the Working Group Hydrogeology, FU Berlin, and long term data records provided for groundwater and technical operation by BWB (Berliner Wasser Betriebe), for ground- and surface water by SENSUT (Senatsverwaltung für Stadtentwicklung und Umweltschutz).

Large parts of the present work have been carried out with inverse modelling. Manual calibration was not necessary any more. It facilitated the hypothesis testing. It was annoying that often results were bad or even no convergent solution could be obtained, though fair manual calibration was possible. In many of these cases the model parameterisation was ill posed, i.e. deficiencies in the physical meaning of the incorporated processes existed. This points out a rarely discussed advantage of parameter estimation: The mentally unbiased consideration of the data on the base of processes included in the model. In this context the term “objective function” has a much deeper meaning than the mathematical process of its calculation, i.e. usually the sum of the squared residuals.

In the present work inverse modelling was the only way to distinguish a well posed conceptual model (the model represents the important system processes) from ill posed problems, (the parameters are just used in a non physical way to obtain a good curve fit). Ironically, many modellers believe just the opposite.

This potential of inverse modelling, to respect all data in an unbiased way, becomes the more important the more data are available. Often, much effort is put on the discussion why parts of the expensively collected and valuable data only partly provide a consistent picture with respect to the numerical model. The more data are available, the more difficult it is to find a consistent view and model concept. In this context the usual suspect of spatial heterogeneity is often used as a bulldozer in discussion. The potential benefit of inverse modelling, especially in problems with high amounts of available data, is still underestimated. It is not just a pathway to fit model curves, but enhances our ability to reject hypotheses, which Karl Popper identified as the essential way of progress in science.

Abstract

Several kinds of managed aquifer recharge techniques provide very good purification of surface water since more than 100 years. In order to maintain a reliable supply of clean water, they are becoming increasingly popular all over the world.

These methods require low technical effort. At Aquifer Storage and Recovery and ponded infiltration the recharged amounts are technically controlled. The infiltration water has to be pumped and often pretreated. At bank filtration this is dispensable, the approach, of using existing surface water bodies is even more consequent. Exemplarily, at a test site at Lake Tegel, Berlin, Germany, the hydraulic processes are modelled.

By means of 3D long term regional and transient hydraulic modelling it was detected that the existing approaches for determining the leakance induce large errors in the water balance and describe the infiltration zone insufficiently. The leakance could be identified to be triggered by the groundwater table, causing air exchange and intrusion of atmospheric oxygen, which reduces clogging by altered redox conditions by at least one order of magnitude. This causes that changes of the groundwater table are mitigated much more than previously assumed. Taking these findings into account, a transient water balance is determined and bank filtration ratios are quantified.

A new inverse modelling concept has been developed and applied to a 3D short term local and transient hydraulic model. It comprises spatially distributed pilot points and overparameterisation constrained by regularisation and calibration to head differences. Significance of the results is demonstrated by cross validation. With this approach the spatial distribution of an aquitard have been identified with high precision. The highly transient and heterogeneous flow conditions are specified and a new viewpoint on the geologic formation of Lake Tegel is obtained.

The good fit of modelled and observed breakthrough curves of ^{18}O, chloride and temperature by just using transferred parameters obtained with the previous hydraulic methods, show the very good model performance and predictive capabilities.

The intrusion of atmospheric oxygen into the unsaturated zone is identified to be the principal redox determining factor during infiltration. Previously inconsistent and also local geochemical conditions are identified to be determined by interaction of infiltration processes with the spatial extent of the aquitard. A theory for chemical clogging of abstraction wells is developed, identifying the strong vertical redox zoning as principal factor of influence.

Zusammenfassung

Seit mehr als 100 Jahren wird Oberflächenwasser mit verschiedenen Verfahren versickert, wobei sich dessen Qualität stark verbessert. Sie finden zunehmend weltweit Anwendung, um eine zuverlässige Versorgung mit sauberem Trinkwasser zu gewährleisten.

Solche Verfahren erfordern nur einen geringen technischen Aufwand. Während bei der Versicherung mit Schluckbrunnen und bei künstlichen Infiltrationsbecken das Wasser noch gepumpt und oft auch vorgereinigt werden muss, reduziert die Nutzung eines natürlichen Gewässers den Aufwand nochmals. Am Beispiel eines Untersuchungsgebiets am Tegeler See in Berlin werden die hydraulischen Prozesse modelliert.

Die regionale, instationäre und 3-dimensionale Modellierung eines langen Zeitraums zeigt, dass die bisher verwendeten linearen Ansätze zur Beschreibung der Durchlässigkeit der Kolmationsschicht sowohl die infiltrierten Wassermengen als auch die Infiltrationsprozesse nur unzureichend wiedergeben. Grundwasserpiegelschwankungen werden stärker als bisher angenommen gedämpft. Als Folge dieser Wasserspiegelschwankungen wird die Bodenluft in der ungesättigten Bodenzone ausgetauscht und Sauerstoff eingetragen. Auf diese Weise erhöht sich die Durchlässigkeit der Kolmationsschicht um mindestens eine Größenordnung. Auf Grundlage dieser Ergebnisse wurden eine instationäre Wasserbilanz aufgestellt und die Uferfiltratanteile bestimmt.

Die genaue lokale Lage eines Grundwasserstauers wird mit Hilfe eines neu entwickelten inversen Modellkonzeptes bestimmt. Er wird mit räumlich verteilten Pilot Points und Überparameterisierung unter Nebenbedingungen kalibriert. Die Zielgröße sind Piezometerhöhenschwankungen. Kreuzvalidierung bestätigt, dass die Lage des Grundwasserstauers präzise bestimmt wird. Diese hat einen entscheidenden Einfluss auf das räumliche Strömungsfeld und liefert neue Anhaltspunkte zur Genese des Tegeler Sees.

Ein Transportmodell liefert lediglich mit den hydraulisch kalibrierten Parametern eine genaue Anpassung der Durchbruchskurven von Chlorid, ^{18}O und Temperatur. Dies kann als Vorhersage angesehen werden und zeigt die Güte des Modells.

Es konnte gezeigt werden, dass der Sauerstoffeintrag die Redoxprozesse in der Infiltrationszone dominiert. In Kombination mit der Lage des Grundwasserstauers können so auch zuvor widersprüchliche und lokale geochemische Verhältnisse schlüssig interpretiert werden. Es wird eine Theorie entwickelt, die erklärt, wie die vertikale Schichtung von oxidiertem und reduziertem Wasser zu starker Verockerung der Brunnen führt.

Index

1. Introduction

Definition

Bank filtration is the process of abstracting water, using vertical or horizontal collector wells adjacent to rivers or lakes. The wells induce a hydraulic gradient which causes infiltration of surface water into the aquifer. During the underground passage mechanical as well as biogeochemical reactions proceed, substantially improving the water quality regarding suspended solids, algae, pathogens and other bacteria, algal toxins, dissolved organic carbon, nitrate, organic pollutants and pharmaceutical residues. These constituents are eliminated or significantly reduced, peak concentrations of the surface water are mitigated. It is an effective and cost-efficient pretreatment, applied in many parts of the world, mainly for drinking water production. The term bank filtrate is used in two ways:

i. With respect to water supply it denotes the total amount of water which is produced by a waterworks which is affected by bank filtration.
ii. At the scale of a well only the part which infiltrated by surface water is called bank filtrate, in contrast to inland water recharged by precipitation.

Worldwide Relevance

Bank filtration is predominantly applied in Europe. Usually vertical collector wells are located about 30 to 300 m from surface waters. Large plants exist in the following countries, the percentage denotes the ratio of nationwide consumed water: Netherlands (7%), Hungary (40%), Finland (48%), France (50%), Switzerland (80%) and Germany (16%). In Germany big plants exist in Düsseldorf, Dortmund, Dresden and Berlin. In the USA it is rarely applied, big plants are located at the Plate River, Nebraska. In contrast to Europe, in the USA wells are located much closer to the rivers, often horizontal collector wells are located directly beneath the lake bed. Distances between 3 m and 30 m are usual with higher water abstraction rates, as consequence abstracted amounts are higher, travel times are shorter and purification capacity is lower.

Bank Filtration Berlin

Rivers act as exfiltrating surface waters for bank filtration in most parts of the world. In Berlin the surface waters have hydrologic behaviour of lakes, though they form part of river systems. Bank filtration under a similar hydrologic setting is only found to exist in Finland (Miettinen et. al. 1997). In Berlin bank filtration solely is used for drinking water production.

Because of good surface water quality and purification efficiency further pretreatment is dispensable. Normally, after aeration the raw water can be discharged to the consumer.

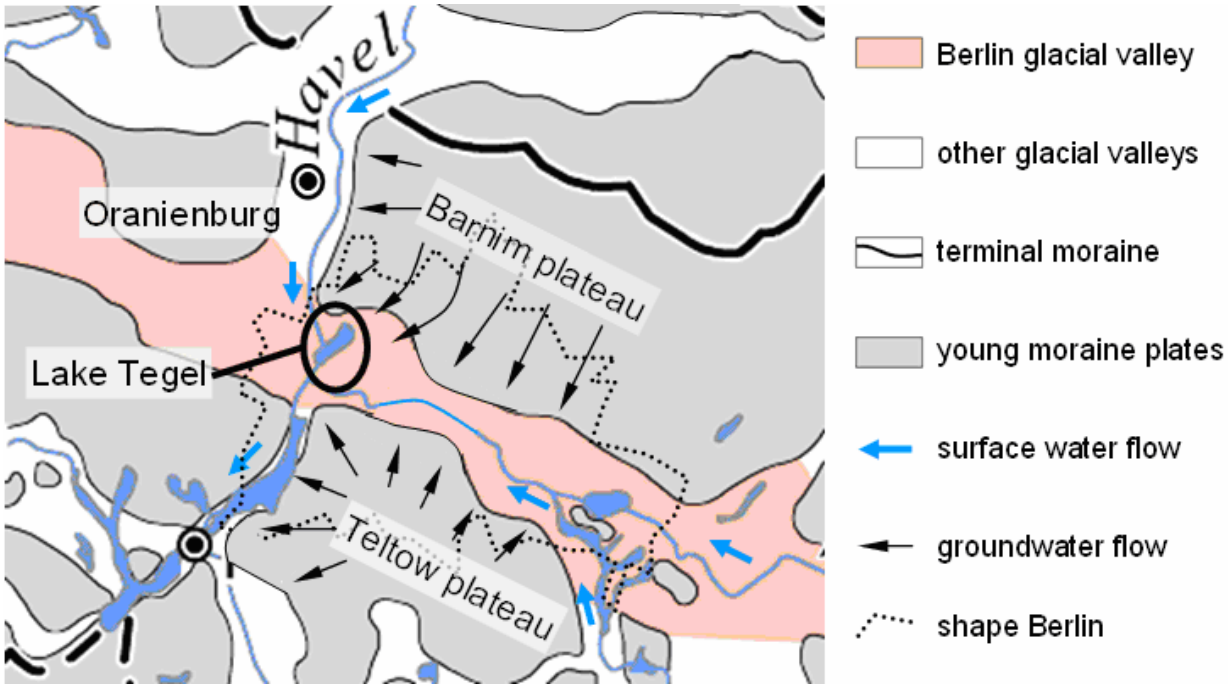

Figure 1: Lake Tegel and its connection to the regional surface and groundwater flow The map is adapted from Wikipedia.

In general the water quality is only a little worse than groundwater recharged by precipitation, but the amount of available water is much higher. In case of the studied Well Field West (fig. 2) the inland catchment comprises an area of a few square kilometres up to the Barnim plateau (fig. 1). The maximum amount of groundwater which may be extracted is limited to the recharge in this area. However, operating the wells such that surface water infiltrates into the aquifer, the well catchment comprises the entire surface water catchment, which is the Havel upstream of Lake Tegel, about 15000 km². The benefit of having water disposable from a huge area is paid with the price that every mayor process affecting the water quality within this area potentially has an impact on the drinking water quality. Of particular importance is the anthropogenic affected part of the water cycle, in the present case these are:

i. the effluents from wastewater treatment plants, partly forming a cycle with the drinking water production (Ziegler 2001),
ii. residues from a former pharmaceutical plant in Oranienburg (fig. 1).

Bank filtration acts as sink for most of these constituents of Lake Tegel which are undesired in drinking water. The efficiency of removal is documented in numerous studies and reports, for many substances the removal mechanisms are studied on phenomenological level. Most of the modelling studies however only regard steady-state hydraulic and/or hydrogeochemical boundary conditions and also only address a sparse set of possible

hydrogeochemical interactions (Greskowiak et al. 2005). At the present field site at the Well Field West hydraulic and geochemical conditions are highly transient. In order to ensure physically meaningful modelling the model should account for

i. transient hydraulic conditions,
ii. heterogeneity of the aquifer,
iii. transient geochemical conditions and boundary conditions.

Points (i) and (ii) shall be clarified, and phenomenological description of point (iii) will be attempted.

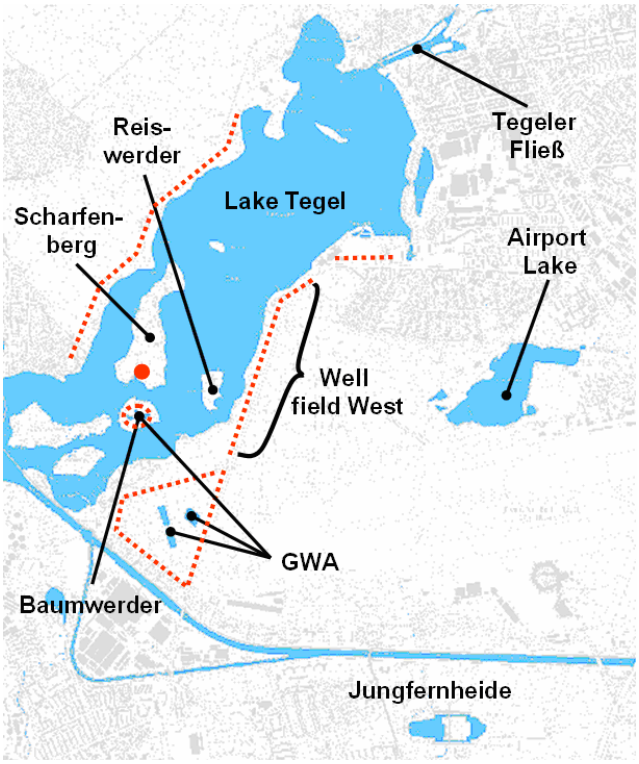

Figure 2: Map of the region around Lake Tegel. Red dotted lines indicate well fields, the red circle a horizontal well, GWA denotes the ponds of the artificial groundwater recharge (GrundWasserAnreicherung). The waterworks Jungfernheide is located slightly south of the map.

Hydraulics

Due to highly transient well operation and spatial heterogeneity the flow field at the transect strongly changes. The interpretation of available tracer data without a sophisticated hydraulic model does not allow a sufficiently accurate description of the flow conditions.

Models which are capable of resolving flow field, travel time and geochemical reactions exist for similar techniques like artificial groundwater recharge (infiltration of water by ponds) (e.g. Greskowiak 2005) or ASR (aquifer storage and recovery, infiltration by injection wells) (e.g. Prommer and Stuyfzand 2005). The hydraulics of these systems are technically controlled from two sides: The amounts may be controlled and monitored as well for recharge as for abstraction. Bank filtration in contrast is technically only controlled by abstraction, from the

viewpoint of system description however the infiltration is of identical importance. Numerous studies, including modelling exist, which describe the interaction of surface water and groundwater (Kühn and Müller 2000, Hiscock and Grischek 2002, Ray et al. 2004). However, the exchange between Lake Tegel and the adjacent aquifer neither can be described transiently using the traditional linear exchange, applying boundary conditions of 2nd or 3rd type (Shaw et al. 1990, Rümmler 2003, WASY 2004, Holzbecher 2005). Previously applied nonlinear mechanisms (Bouwer and Rice 1989, Schubert 2002, Lin et al. 2003, Holzbecher 2006) could not describe the behaviour satisfactory. Here a gap in the scientific knowledge of exchange between surface- and groundwater exists.

Though many aquifer recharge techniques are similar, infiltration is controlled by different processes: Usually, rivers or streams feed bank filtration facilities. The hydraulic resistance of river beds is known to be temporally variant since a river is subject of continuous change by shear stress, bed load transport, discharge, water level, reversed hyporheic flow direction and wetted perimeter. Artificial recharge ponds normally have water depth smaller than 1.5 m, are operated intermittently, algal growth plays an important role, often the clogging layer is removed. Exchange coefficients between lakes and groundwater are not reported to be affected by transient hydraulics, neither under natural conditions nor at bank filtration. Nevertheless, possibly nonlinear leakance appears here and affects in- and exfiltration. Generally applied boundary conditions are 1st type, 3rd type or 2nd/3rd type, the latter alternating depending on whether saturated or unsaturated conditions exist below the infiltration area. All types mitigate the head error by stable behaviour. It only could be detected if the flow rates would be known with high accuracy which is normally not possible in a natural system. Furthermore, usually gradients are such small that other factors control the system behaviour, the transient character of lake bed hydraulic conductivity is not detected.

The revelation of the transient character is based on two prerequisites:

i. At the investigation area the hydraulic head difference between lake and groundwater varies between 1 m and 7 m, the magnitude is large enough that the nonlinear effects occur, and the head variation is high enough to detect their transient character.
ii. A transient conceptual model which comprises a sufficient long interval that the deviations to the existing linear and non-linear transfer concepts can not be compensated by storage, accumulate and become obvious.

The precise knowledge of the water balance is essential for the reliability of the results. It is ensured since the abstracted amounts can be determined precisely by operating data of the

waterworks. The region is hydrogeologically explored very well and continuously hydraulically monitored such that a numerical model of sufficient accuracy can be set up.

The transfer rate of surface water to the groundwater affects several aspects of water management. The ratio of infiltrated water to total abstraction is the key parameter for assessing mixing and dilution, flow velocity and elevation of the groundwater table affect the biogeochemical reactions which purify the bank filtrate. Also inland groundwater levels are affected. In areas with naturally low water table depth, decreasing groundwater levels adversely affect vegetation and small ponds and may cause subsidence, possibly leading to structural damages of buildings or infrastructure. Between 1989 and 2002 the water consumption in Berlin decreased by 42% (Umweltatlas Berlin 2005). Though the water demand decreases, water quantity is an important issue. In order to manage shrinking demand and predict increasing water levels, the exchange between surface- and groundwater should be understood. The decreasing abstraction already affects large areas in Tegel and the southeast with increased levels of more than 0.5 m, partially more than 1 m (Umweltatlas Berlin 2005). As consequence deep cellars become wet, and vegetation may be subject of succession, like it is the case at the park Jungfernheide (fig. 2)

Reactive Processes

Apart from the consequences directly following from changing amounts and inaccuracy of modelled and predicted hydraulic heads, the discovered nonlinearity of bank conductivity shows that central processes in the hyporheic zone are not understood. The hyporheic zone is the upper zone of a lake/river bed which is in close hydraulic, chemical and biological contact to the surface water. Since the most important biogeochemical changes occur within the first meter after infiltration, the impact on the water quality is potentially high.

The quality of abstracted water mainly depends on the composition of the surface water, biogeochemical reactions in the hyporheic and unsaturated zone, but also on biogeochemical reactions in the aquifer and thus on hydrogeologic formations and travel time.

The identification of surface water is covered by the measurements performed during the NASRI project (Natural and Artificial Systems for Recharge and Infiltration, Pekdeger 2006, Nützmann 2006, Jekel 2006, Chorus and Bartel 2006) and by SENSUT (Senatsverwaltung für Stadtentwicklung und Umweltschutz des Landes Berlin). Further investigations have been carried out by Richter (2003), which reveal that the tracers which are most important for this study are distributed almost homogeneously in the main basin of Lake Tegel. It is an important simplification that the area of interest, forming the surface water boundary condition, can be treated as spatially homogeneous.

Though the most important geochemical changes occur immediately after infiltration (e.g. Bourg and Bertain 1993, von Gunten et al. 1994, Ludwig et al. 1997, Grünheid 2005) this region is considered geochemically only in a qualitative way. Further investigations within the NASRI project about the infiltration zone are carried out in column studies (Chorus and Bartel 2006, Jekel 2006) and on a artificial groundwater recharge test site (Greskowiak et al. 2005). In contrast to the latter test site only at the bank filtration facility an extended area of iron reducing conditions could be observed, which is of importance for degradation processes.

Heterogeneity

The subsurface at the investigation transect has been interpreted mainly by Fritz (2002), Voigt et al. (2000), Hannappel et al. (2002) and Pekdeger et al. (2004). The main results which concern the transect are that a glacial till divides the groundwater body horizontally. The upper aquifer has mainly aerobic conditions and only contains young bank filtrate, the lower is anaerobic and contains waters from different sources. The aquifers however show significant heterogeneities. While aquifer hydraulic conductivities vary within 1 order of magnitude, the leakage between the aquifers, determined by the distribution of the glacial till, varies within 5 orders of magnitude (Fritz 2002) and thus is the principal geological factor determining the hydraulic properties at the transect. The structure how the upper and lower aquifers are divided, affects flow conditions and is probably of importance for purification capacity and crucial for the interpretation of observed chemical composition at observations wells. Around Lake Tegel the glacial till is believed to be nonexistent (Voigt et al. 2000).

In order to obtain an insight to the biogeochemical reactions controlling the purification during bank filtration a test site has been installed and sampled (Fritz 2002) and an extended campaign has been carried out within the NASRI project (KWB 2005). The approach was based on the assumption that the flow and transport conditions could be approximated with a vertical cross section and explore it by installation of a transect. This concept has been applied at numerous test sites (Ludwig et al. 1997, Massmann et al. 2004, Grünheid et al. 2005), also in conjunction with the conceptual approach of modelling a 2-D vertical cross section (Bourg and Bertain 1993, Doussan et al. 1994, Schubert 2002, Greskowiak 2005). For the transect at Lake Tegel the general behaviour is met, but considerable gaps can only be filled with a 3D approach.

Tracers and Redox Conditions

The interpretation of tracer data forms the base for understanding a hydraulic system. Since the field site is located in the most restricted areas for water protection, zone 1 and 2, (Wasserschutzgebietsverordnung Tegel 1995) tracer tests can not be carried out. Instead, so

called environmental tracers, already present in the natural environment, are analysed. The tracers should fulfil several criteria:

i. the existence of a pronounced input signal
ii. ideally: conservative
iii. ideally: non retarding
iv. If point ii and/or iii are not fulfilled, the mechanisms of degradation and matrix interaction have to be known.
v. Analytics should be sufficiently precise for the existing concentrations, and the analytical effort shall be reasonable.

The tracer which fulfils all criteria still awaits for its detection. In the present study information is obtained from 6 non reactive tracers: Chloride and ^{18}O are conservative and non retarding, the analytical effort for chloride is reasonable but it only shows one significant signal (spring 2003), ^{18}O in contrast shows a pronounced seasonal signal, but the analytical effort is high. Temperature shows a pronounced seasonal signal and the measurement just requires a thermometer, but it is retarding and the signal attenuates. Boron is conservative, but retarding (De Simone et al. 1997) and below detection level in some observation wells. AMDOPH as a degradation product of phenazone is very useful for determining source and age on the decadal scale, since Tritium/Helium age dating requires extremely high analytical effort and has been carried out only once. Apart from the physical properties none of the tracers can be regarded as ideal. For revealing the hydraulic properties of the transect, each tracer provides a smaller or larger piece of information, only a combination in conjunction with hydraulic data provides an optimal result. Anticipated results are the determination of the water source, determining the travel times and setting up a reliable hydraulic and transport model which

i. fills the gaps within measured data,
ii. assists in analysing and understanding complex environmental systems (Prommer and Barry 2005).

Though tracer breakthrough curves suggest such a cross sectional groundwater model could sufficiently describe flow and transport, a closer view reveals considerable obstacles. Observed concentrations show anomalies, indicating a deficient current picture of the flow conditions. Between 2002 and 2004 at the transect Tegel AMDOPH is an indicator for old bank filtrate which is known to be present at the bottom of the lower aquifer. However it is found in observation wells at the top of the lower aquifer, for which ^{18}O and temperature suggest containing young bank filtrate with an age of about 1-3 months. Concentrations of chloride and boron also suggest that these observation wells contain a mixture of at least 2 different waters.

The origin and flowpaths of at least one water are unknown. Temperature data also show anomalies. In some observation wells the extremes of the breakthrough curves are not symmetrical to the annual mean temperature of about 10 °C, some minima are considerably higher, in one case the minimum is 11°C. Additionally, the phase shift of temperature breakthrough could not be modelled correctly, the conclusions drawn about the flow field using the ideal tracer ^{18}O are considerably different.

These anomalies only occur in the observation wells in the second aquifer. They are of outstanding relevance in order to comprehend the system bank filtration and have to be included in modelling:

i. It is the main aquifer where most water flows.
ii. They could be sampled continuously, most wells above fell dry at low water levels.
iii. The low redox state of iron reducing environment is an important characteristic of bank filtration sites. In the upper aquifer hardly manganese is found.

By inspection of the redox sensitive geochemical data of the observation wells in the second aquifer, it becomes obvious that the locations with presumably short travel time close to the bank are much more reducing than the observation wells with longer travel time close to the abstraction well. Bourg and Bertain (1993) document such a reversed redox zoning by re-oxidation through the unsaturated zone. However, in the present field site a 4 m thick glacial till with conductivities of $2*10^{-8}$ m/s and lower (Fritz 2002) prevents re-oxidation. Hydraulics are extremely complicated, a pumping pattern highly alternating on different scales induces a highly transient flow field affecting two irregularly separated aquifers. The present study is carried out in order to identify the mechanisms, which apparently have hydraulic reasons.

Investigation Concept

The present study shall provide a comprehensive view of hydraulic behaviour of a bank filtration system which is extremely affected by hydraulics of largest waterworks, showing highly transient behaviour on different temporal and spatial scales. The water balance shall be determined with high temporal resolution with special respect to the dynamics of infiltration. Hydrogeologic conditions shall be identified at the field site. A transport model, capable of reproducing the observed tracer data, shall be established. These findings shall be combined in order to describe the field sites particularities and to show the impact of hydraulics on the interpretation of transport and geochemical conditions.

Inverse modelling is essential for the investigation concept. The model contains a huge amount of data which have to be considered unbiased and contains many parameters to estimate. This can not be ensured with manual calibration, consequently, this task is carried out

by inverse modelling. This means that a computer code fits the model parameters in such a way that deviations between the results and the observations are minimised. This method is called inverse modelling or automated parameter calibration. Further advantages are the higher accuracy of the solution and reduced effort for calibration. However, the danger of unphysical calibration or overfitting always has to be considered.

The investigated bank filtration system is subject of an alternating well operation scheme, large amounts of water are transiently exchanged between different hydrological and hydrogeological formations. The resulting transient flow in 3 dimensions, temporally and spatially scale dependent, interacting with biogeochemical processes might be unique worldwide. Consequently, the interdependence of multiple dynamic processes on different scales is analysed by different model concepts; ensuring to simulate appropriately as many physical properties as possible. It is assessed how much informational value can be extracted with methodical different approaches and models, namely: ´

i. ireview of hydrogeology and previous modelling
ii. hydraulic modelling with the key issues:
    a) determination of the boundary conditions with focus on the leakance
    b) determination of a transient water balance
    c) identification of local flow patterns
iii. multi tracer transport modelling at the transect
iv. determination of spatial aquifer structures
v. assessment of the impact of hydraulics on sampling and geochemical conditions

Depending on the approach, the spatial and temporal scale is different. Long term hydraulics are relevant on a regional scale. The relevant transport length is much smaller. The temporal scale of the short term hydraulic effects is smaller than the latter two, with a spatial extent similar to the transport. The different approaches require modelling on different scales and with adapted concepts. The results are different viewpoints on one system and provide different pictures of the same physical processes. They are highly interconnected and iteratively analysed under the consequent application of inverse modelling. Hydraulic system analysis on such a level of integration probably has not been performed in any previous study.

2. Material and Methods

The bank filtration system at Lake Tegel has been build around 1900, but unfortunately there is no information available about the hydraulic situation under natural conditions because the piezometric heads have not been documented prior to the beginning of the groundwater extraction. The current total extraction amount of all 8 well fields is 50 million m³ of drinking water per year. The bank filtration system, i.e. the Waterworks Tegel, affects a region of about 50 km².

Subject of the present study is the bank filtration of Well Field West (fig. 2) with the focus on a transect located between the Well Field West and Lake Tegel. For an adequate description and appropriate boundary conditions, the model domain had to be considerably increased in comparison to previous models. The hydrogeological situation in the study area as well as the integrated data approach using piezometric heads, environmental tracers, infiltration measurements will be described in the following sections.

2.1. Hydrogeology

The two upper aquifers in the model domain as well as Lake Tegel itself are formed during the quaternary Saale ice-age (Hannappel and Asbrand 2002). Lake Tegel (fig. 3, fig. 13) actually has a maximum depth of 14 m, with the deeper regions already being filled up with thick sediments and mud, decreasing and vanishing towards the bank (Brühl et al. 1986, Pachur and Haberland 1977). Hydraulic conductivity of the mud ranges from $2.1*10^{-7}$ m/s for the upper and $2.8*10^{-9}$ m/s for the lower mud layers (Schley 1981). The two upper aquifers, where the waterworks Tegel abstracts drinking water, are sealed to the bottom by thick Pleistocene mud and silt layers (Pachur and Haberland 1977).

The upper aquifer (1st aquifer) is formed by glaciofluviative fine to coarse sand and has a thickness of about 10 m, half of which is saturated. k_f values are of about $3.5*10^{-4}$ m/s (fig. 4). The main aquifer (2nd aquifer), where the wells are screened, is about 30 m thick and predominantly covered by glacial till of about 4 m thickness. It is also formed by glaciofluviative fine to coarse sand. k_f values calculated from the transmissivity and thickness (Fugro 2000) result in values between $2*10^{-4}$ m/s below Lake Tegel to $5.5*10^{-4}$ m/s near observation well TEG051 (fig. 5).

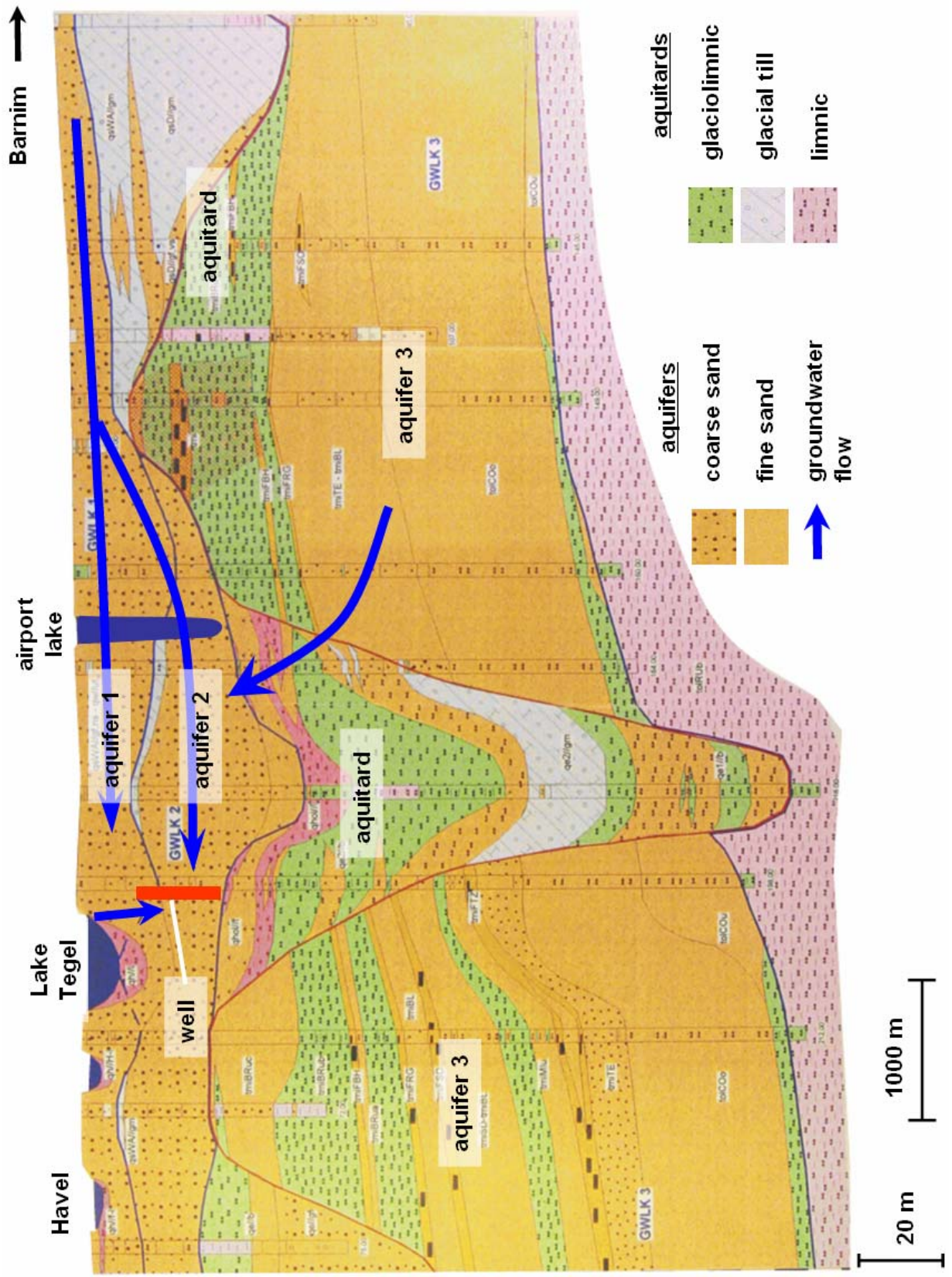

Figure 3: Vertical geologic cross section of the Tegel area by Voigt et al. 2000, slightly modified.

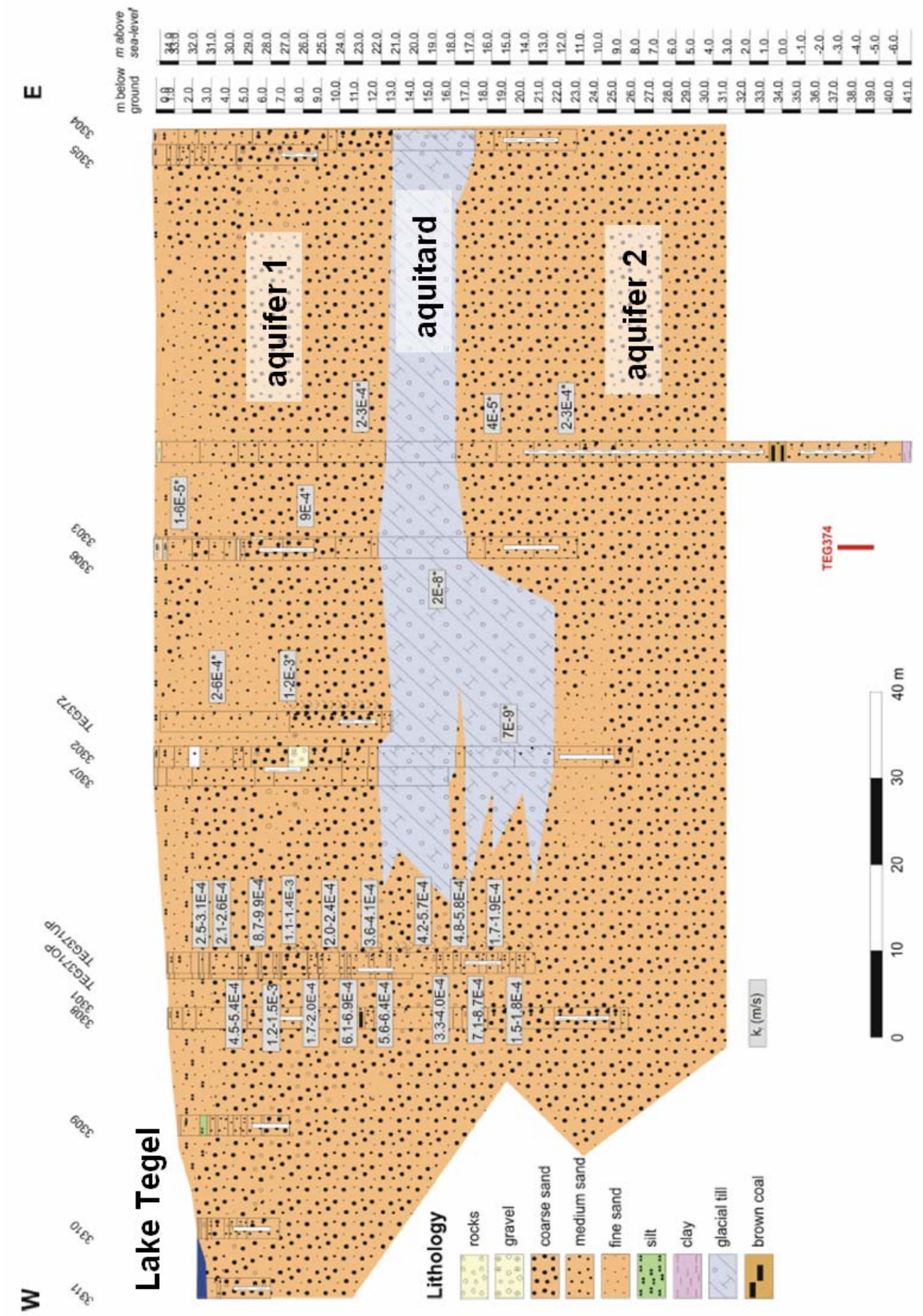

Figure 4: Geological cross section of the transect (Pekdeger et al. 2004). The conductivities in the grey boxes are derived from sieve analyses.

At observation wells 3301, 3302 and 3303, which are part of the transect (tab. 1, fig. 6), the analysis of sieve curves result in a mean k_f value of $2.9*10^{-4}$ m/s (Fritz 2002). A geological cross section of the transect was set up (Pekdeger et al. 2004, fig. 4). A tertiary fine sand aquifer with 70 m thickness (3rd aquifer, fig. 3) lies below, separated by 20 to 30 m thick glaciofluvial silt and clay of the Holstein interglacial (Hannappel and Asbrand, 2002, Voigt et al. 2000, fig. 3). However, by comparing piezometric heads of the 3rd aquifer with heads of the 2nd aquifer and pumping rates of the waterworks, some extent of hydraulic connection is evident (fig. 15).

The Airport Lake (fig. 3, fig. 13) has a depth of 40 m and thus penetrates both upper aquifers. The water level of the lake is quite similar to the piezometric heads of the aquifers. Due to stormwater discharge from adjacent quartiers, a water level of 30 cm above the groundwater level might temporally occur.

Tab. 1: Observation wells incorporated into the model either for boundary conditions or as observation. The coordinates use the Soldner88 system.

Name of Piezometer	Aquifer #	Screen top [m NN]	Screen bottom [m NN]	Soldner coordinates easting [m]	Soldner coordinates northing [m]
3301	2	13.4	10.4	15065	27064
3302	2	12.7	9.7	15096	27044
3303	2	15.9	12.9	15113	27015
3304	2	15.9	12.9	15167	26989
3305	1	27.9	25.9	15166	26991
3306	1	29.2	26.2	15114	27016
3307	1	28.7	26.7	15095	27045
3308	1	28.6	26.6	15065	27065
3309	1	29.8	27.8	15053	27075
3310	1	30.2	27.7	15043	27086
3311	1	29.9	27.9	15032	27087
3312	1			15071	26954
3313	1			15130	27146
BR13	2	15	-4	15120	27001
TEG050	1	22	21	15681	27027
TEG051	1-2	29	-33	16302	26787
TEG053	2	13	10	17061	27155
TEG103	2	12	11	15010	26222
TEG142	2	6	-3	26031	15193
TEG149	1-2	29	-16	15872	26332
TEG233	1	24	23	15550	27794
TEG242	1	29	28	15532	27717
TEG243	1	20	19	15622	27728
TEG339	1	24	15	16685	27073
TEG340	1	22	12	15715	27387
TEG341	1	15	14	15663	26759
TEG343	1	13	12	14650	26411
TEG347	1			14123	26874
TEG350	1-2	25	-8	15368	26338
TEG363	2	8	5	14784	26226
TEG371OP	2	23.7	21.7	15073	27061
TEG371UP	1	17.9	15.9	15072	27061
TEG372	1	24.7	22.7	15103	27043
TEG374	2			15113	27015
TEG6034	2	-3	-25	16249	26397
TEG6035	3	-99	-143	16249	26397
TEG6053	2			14148	27033

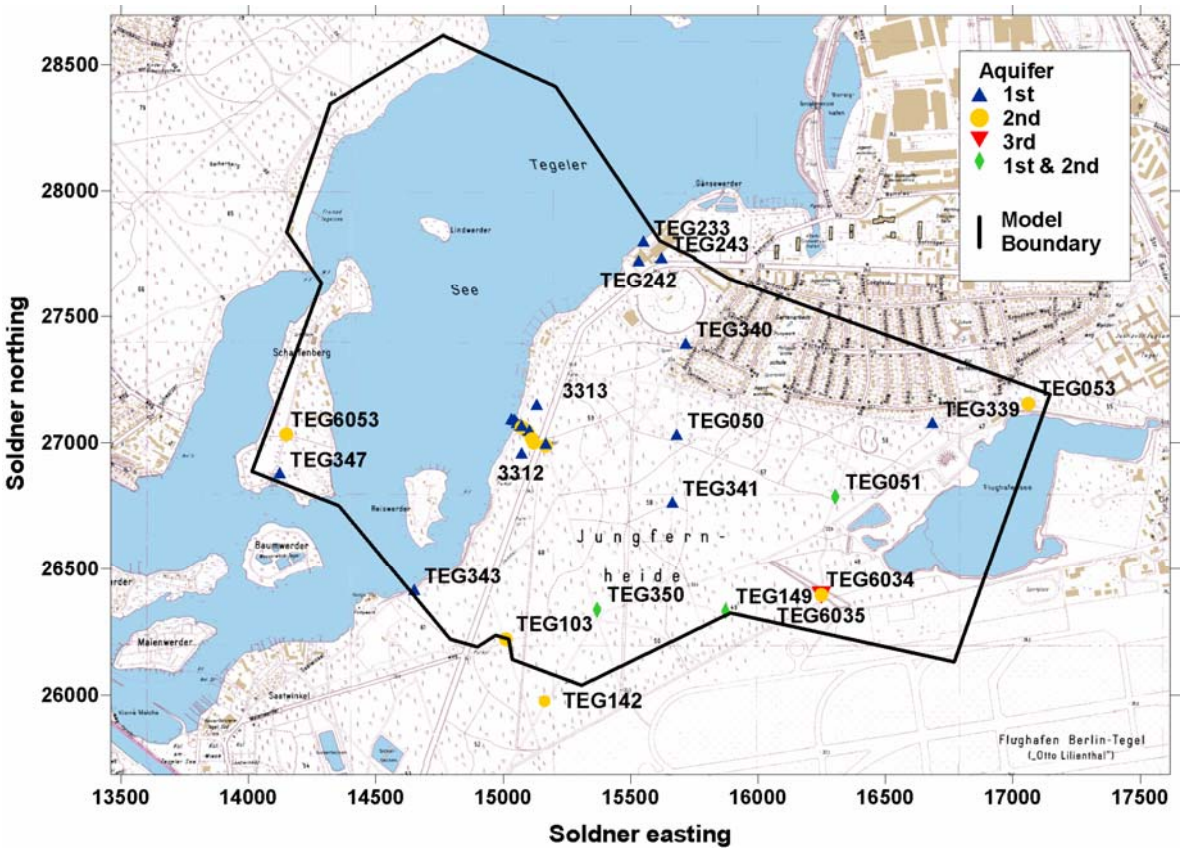

Figure 5: Location of the observation wells: Blue upside triangles represent wells screened in the first aquifer, yellow circles represent wells screened in the second aquifer, the downside red triangle represents TEG6035 in the 3rd aquifer. Green diamonds represent wells screened as well in the first as in the second aquifer. The bold black line defines the model domain (chapter 4.1.1). Soldner coordinates are metres.

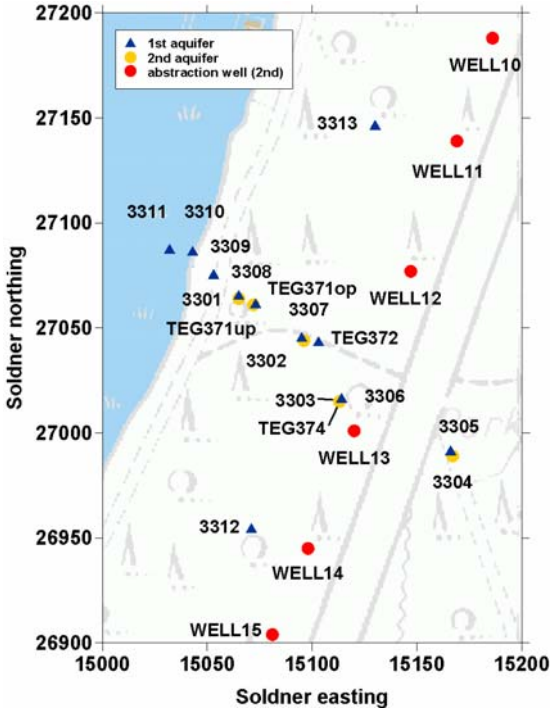

Figure 6: Location of the observation and abstraction wells at the transect: Blue triangles represent observation wells screened in the first aquifer, yellow circles represent observation wells screened in the second aquifer and red circles represent abstraction wells screened in the second aquifer. Soldner coordinates are metres.

The bathymetry of Lake Tegel is available, the origin of the data is not known.

Sieve analyses of the lake bottom in front of the transect (Sievers 2001) result in a k_f value of $5.4*10^{-6}$ m/s for the upper 12 cm of sediment, infiltration measurements of Hoffmann and Gunkel (2006) indicate a leakance of $4.5*10^{-6}$ s^{-1}. Modelling of Eichhorn (2000) results in leakance of $2*10^{-6}$ s^{-1} for shallow water and $3*10^{-8}$ s^{-1} for the deeper regions. Rümmler (2003) calibrated leakance at the transect at Lake Tegel in 3 water depths: shallower than 60 cm (30.80 m NN) a value of $1.2*10^{-6}$ s^{-1}, between 60 cm and 3.9 m (30.80 n NN to 27.50 m NN) a leakance of 10^{-7} s^{-1}, below 3.9 m (27.5 m NN) a value of $4*10^{-8}$ s^{-1}. The coordinates and positions of the screens are listed in Table 1.

For further information about the hydrogeology see HSM Tegel (Hydrogeological Structural Model, Fugro 2000), and geological profiles (Voigt et al. 2000).

2.2. Data

Within the investigated time span between January 1998 and April 2005, different measurement campaigns were carried out within the work of Pekdeger et al. (2004), BWB (2005) (Berliner Wasser Betriebe / Berlin Water Works), SENSUT (2005), Jekel et al. (2004) and Richter (2003). However, some locations are not sampled during the whole time span, data have different time intervals and measured parameters may be temporally variant. In order to come to a comprehensive understanding of the way the modelled area is embedded in the hydraulic context of the catchment, data outside of the model domain have been also included into the analyses.

To avoid inflating this section, only the main characteristics of model relevant data are documented. Note that data without temporal annotation cover the entire time span between January 1998 and April 2005.

Piezometric Heads

- of 17 observation wells, abstraction wells 12 to 14 and for Lake Tegel with either monthly, daily or hourly intervals were provided within NASRI (KWB 2005) and Fritz (2002),
- of 15 observation wells with usually monthly intervals were provided by BWB (2005),
- of Well Field West, 2 to 4 times per year, at the dates of pumpage tests, by BWB (2005),
- of Lake Tegel, Airport Lake and 4 observation wells with usually daily intervals were provided by SENSUT (2005),
- of several observation wells at the transect between 1999 and 2002 with 4 to 6 week intervals were provided by Pekdeger (2003).

Temperature

- of 17 observation wells, 3 abstraction wells and Lake Tegel with usually monthly intervals (May 2002 – Aug 2004) were provided within NASRI (KWB 2005),
- of Lake Tegel with usually monthly time intervals was provided by SENSUT (2003),
- of well 13 between 2000 and 2002 were provided by BWB (2004).

Tracer Data

- of chloride, boron, AMDOPH, ^{18}O, ^{2}H were provided by NASRI between May 2002 and August 2004 (KWB 2005),
- of chloride and boron of Lake Tegel were provided by SENSUT (2003),
- of chloride and ^{18}O (May 2001 – May 2002) were extracted from Richter (2003).

Composition Lake Tegel

- of the parameters pH, electrical conductivity, O_2 content, O_2 saturation, total colloids, Secchi Depth, BOD 1, BOD 5, DOC, loss on ignition of DOC, organic nitrogen, ammonium, total P, ortophosphate, inorganic carbon, sulphate, chloride, silicon, sodium, calcium, potassium, magnesium, total phytoplankton biovolume, chlorophyll-A, phaeophytin, zooplankton biomass between January 1998 and April 2005 were provided by SENSUT (2005).

Well Data

- of daily operational hours (Jun 1999- Apr 2005), well switching times (Mar - Oct 2004), pumpage test data (2 to 4 times per year) for the Well Field West were provided by BWB (2005),
- of monthly sums of abstracted water for 8 well fields and amounts of artificially recharged water for 2 facilities were provided by BWB (2004).

Precipitation

- of daily precipitation data for waterworks Tegel were provided by BWB (2004).

Geochemical Data

- of O_2, NO_3^-, Mn_2^+, Fe_2^+, NH_4^+, Ca^{2+}, Mg^{2+}, K^+, Na^+, SO_4^{2-}, redox potential, electrical conductivity, pH, DOC, HCO_3^-, AMDOPH, phenazone, propyphenazone, and others are provided within NASRI between May 2002 and August 2004 (see appendix fig. App8 to App29, KWB 2005),
- of DOC, SUVA were extracted from Grünheid (2005), and Jekel (2006).

2.3. Infiltration Measurements

Since the thickness of the lake bed with a high resistance is unknown and may vary, a lumped parameter of the hydraulic conductivity and bed thickness is used:

$$L[s^{-1}] = \frac{k_f[m/s]}{M[m]} \quad \text{eq. 1}$$

where L is the leakance, k_f the hydraulic conductivity and M the thickness of the clogging layer. The Darcy velocity v_f is calculated by:

$v_f = L * \Delta h$ eq. 2

The pore space of this clogging layer usually is water saturated wherefore the driving head difference Δh is defined as:

$\Delta h = h_w + M$ eq. 3

with h_w as the level of surface water above the water/sediment interface. If $M << h_w$, as it is usually the case, it can be neglected and lumped to the leakance.

In order to obtain the lake bed leakance, a simple in situ infiltration measurement method is applied. Amounts of infiltrated water are measured directly under natural field conditions. The measuring setup consists of a cylinder, a hose and a reservoir bag (fig. 7). The cylinder is open at the bottom and closed at the top, leaving a small hole at a flange where a hose can be put up (fig. 8).

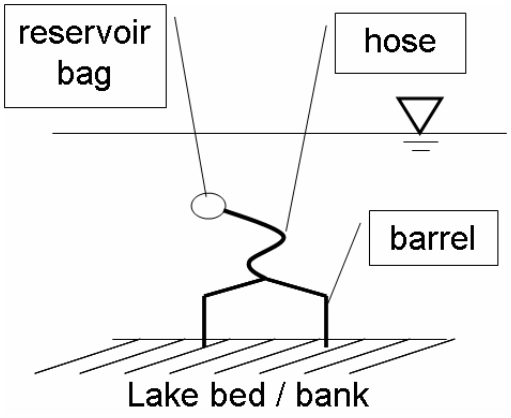

Figure 7: Vertical cross section through an infiltration barrel during infiltration measurement

The bottom of the cylinder is inserted a few cm into the lake bed, to the flange on the top a hose is put up (fig. 7). The water filled bag at the end of the hose acts as a reservoir, the difference in volume of the reservoir bag within a defined time is equal to the amount of infiltrated water. As the pressure inside and outside of the barrel is identical, the water infiltrates under natural field pressure conditions.

Figure 8: Cylinder used for direct infiltration measurements. A hose with the reservoir bag is plugged to the flange at the top.

Hoffmann and Gunkel (2006) carried out infiltration experiments in Lake Tegel in front of the transect (in water depth of 40/80 cm) which are evaluated by the method described above. Piezometric heads measured in about 5 cm depth indicate that the hydraulic active thickness of the lake bed is considerably higher.

For infiltration measurements, Hoffmann and Gunkel (2006) applied similar measuring setup as shown in figure 7. The cap is detachable, the cylinder stayed in the ground when the campaigns have been carried out at subsequent days, and the cover was only attached during the measurements. Around the barrel, hydraulic heads in 2 cm depth have been measured by 3 piezometers. The same principle has been developed by KUP (2006) for the application in rivers.

The repeat accuracy of the measurements by Hoffmann and Gunkel is within the outer limits ± 30%, the absolute accuracy is unknown. Accuracy is higher than the "Open End Test" (Langguth and Voigt 1980), applied by Nogeitzig (2005). The area is larger and thus the boundary effects are smaller and the hydraulic gradient across the interface is not affected.

2.4. Previous Modelling

The transect at Well 13 (fig. 6) has been included within few models which widely vary in the model concept, purpose and scale. Although the model concepts applied in previous studies are not adequate for answering the questions of this study, they have brought a significant portion of useful information. In the following paragraphs a short summary of the major properties of the previous models will be presented.

(a) A steady state model by Eichhorn (2000) was set up to quantify the bank filtrate ratio, flow paths and travel times at the transect. The calibration period is 1^{st}-30^{th} June 1999. The model extent is shown in figure 9. The benefit from this study is an estimation of the k_f values of the Lake Tegel bed. Travel time information is neither detailed enough, as the model is steady state, nor applicable, as the study is carried out for the hydraulic situation in 1999. Due to the fact that the boundary conditions in the north, south and west are not suitable for transient conditions, the results of this study have a limited significance.

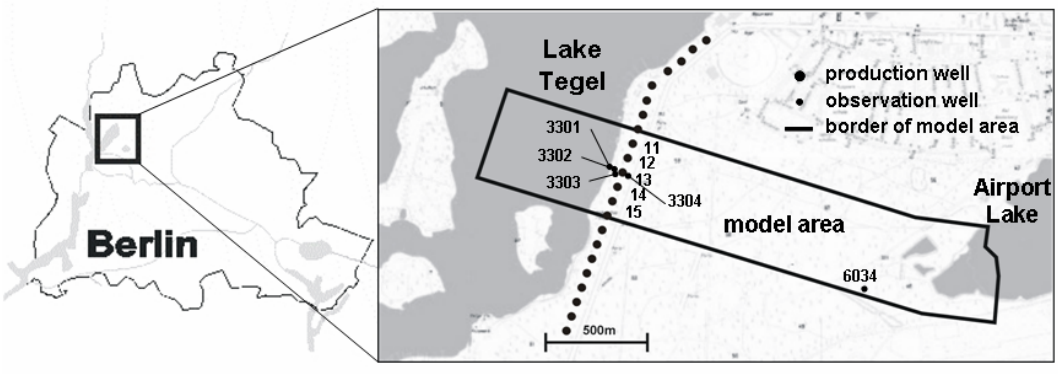

Figure 9: Model domain of the steady state hydraulic model by Eichhorn (2000)

(b) In order to evaluate the impact of different pumping scenarios on the water resources and to give recommendations for future water management, WASY (2004) set up a steady state as well as a transient catchment model (fig. 10). A special issue herein is the behaviour of contaminated sites. The benefit is the specification of the steady state watershed between Well Field West and the adjacent well fields, namely the no flow boundary between the Well Field West and the Well Field East. This model also approves the postulation of the existence of old bank filtrate at the bottom of the main aquifer (Pekdeger et al. 2004). According to WASY (2004), this water infiltrated at the eastern bank of Scharfenberg (fig. 12) and at the western bank of Lake Tegel at the height of Well Field North.

The model is calibrated for steady state, to data of 2002, and is run transiently for the entire year 2002. This period is much shorter than the sampling period of the NASRI project (May 2002 - September 2004) and not sufficient to detect long term effects. The temporal and spatial discretisation is too coarse to give a detailed description of the transect, besides, the model is too bulky/extensive and hardly manageable for the present purpose.

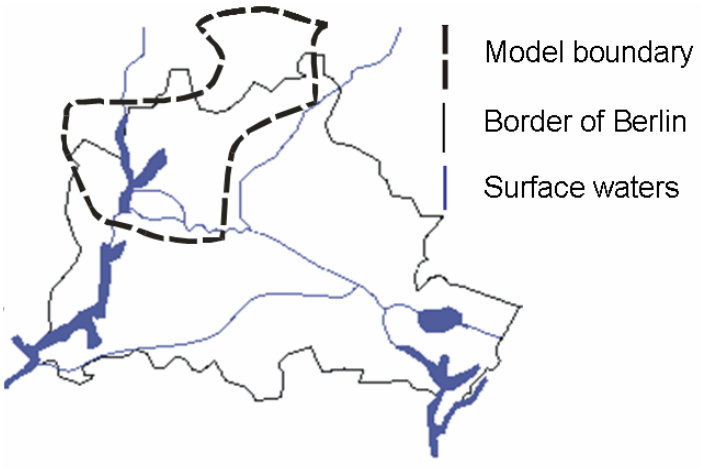

Figure 10: Model domain of the catchment model (dashed line) for waterworks Tegel, Spandau and part of the catchment of the former waterworks Jungfernheide (WASY 2004)

(c) Rümmler (2003) and Wiese et al. (2004) set up a transient two-dimensional model to assess the effects of oscillating pumping regimes on bank filtrate with real hydrogeology and

hypothetical pumping rates and -patterns (fig. 11). The leakance could be roughly estimated with this model. Although the applied well field operation mode is only a hypothetical mode, the pumping rates are within real range. It could be detected that the boundary conditions (fig. 11) are not suitable for transient conditions in the north, west and south leading to the conclusion that the model domain has to be enlarged. It is extended to the model presented in this thesis.

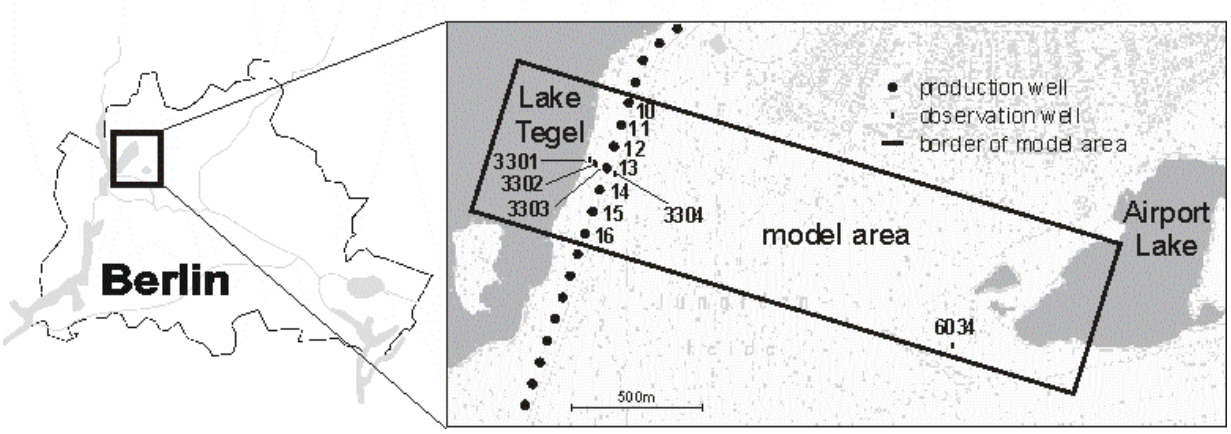

Figure 11: Model domain of Rümmler (2003) and Wiese et al. (2004)

Previous models showed that the entire Well Field West should be included into the model as well as bigger regions of Lake Tegel, including Reiswerder and Scharfenberg. (fig. 2, fig. 12). The order of magnitude of the leakance of the bank could be obtained.

2.5. Groundwater Flow and Transport Representation

The physical processes of the bank filtration system are of such a complexity that only numerical modelling can give a correct representation. Various groundwater flow and transport models exist. The choice was made based on the criteria:

i. iprocess representation
ii. Reliability
    a) accuracy
    b) numerical stability
    c) documentation
iii. possibility for modifications
iv. coupling
v. user-friendliness

The first point is essential, the model has to be capable to simulate the processes which may occur. The second point means that the model shall be established and intensively tested at practical applications, it is a tool for representation and quantification of the processes. It

should work stable and accurate such that it should not become necessary to shift the investigation effort from the physical problem to the model itself. Usually, the numerical accuracy of a groundwater model is higher than the accuracy of the system description by the available data. The model shall be stable under all possible states the system may take. A documentation of the numerical methods is necessary to estimate errors and to apply the model appropriately. A wider definition of documentation comprises the existence of comparison with analytical methods, previously documented test cases etc. Scientific work on a problem always comprises the possibility of new processes appearing to be of importance. Point 3 is of special importance in a scientific context. In case modifications become necessary open source codes are essential. Point 4 is of special importance for combined ground- and surface water interaction and as well for geochemical modelling. In case the important processes can be described with different models, appropriate coupling is indispensable. In order to concentrate the effort on the problem itself, existing solutions should be preferred. Good documentation and open source code is a great help in case coupling becomes necessary. Last but not least, the extremely unscientific issue of user-friendliness should be taken into account. The more convenient the handling is, the more time can be spent to investigate and the better the situation can be understood. In this context an adequate pre- and postprocessing is of high importance.

To summarize, modelling shall be a tool to facilitate the researcher to focus on the problem itself. Many points listed above gain importance with increasing amounts of data. Since the present study requires large amounts of data, of which many are variant on temporal and/or spatial scale, a careful assessment of these points seriously affects the scientific outcome.

2.5.1. Flow Modelling

The equation which describes the groundwater flow is obtained by combining the Darcy equation with the continuity equation. The latter can be written as:

$$\nabla \vec{v}_f = S_0 \frac{\partial h}{\partial t} - W_0 \quad \text{eq. 4}$$

where ∇ is the nabla operator applied to $\vec{v}_f$, which is the vector of the filter velocity, the result is the divergence of the velocity field. S_0 is the storage coefficient h is the pressure head, t the time, W_0 is the source and sink term. The Darcy equation can be written as:

$$\nabla \vec{v}_f = -k_f \nabla h \quad \text{eq. 5}$$

where k_f is the hydraulic conductivity, and h the hydraulic potential. The combination results in the groundwater flow equation:

$$\nabla(-k_f \nabla h) = S_0 \frac{\partial h}{\partial t} - W_0 \quad \text{eq. 6}$$

Written in Cartesian coordinates:

$$\frac{\partial}{\partial x}\left(k_x \frac{\partial h}{\partial x}\right) + \frac{\partial}{\partial y}\left(k_y \frac{\partial h}{\partial y}\right) + \frac{\partial}{\partial z}\left(k_z \frac{\partial h}{\partial z}\right) = S_0 \frac{\partial h}{\partial t} + W_0 \quad \text{eq. 7}$$

Where k_x, k_y, k_z are the hydraulic conductivities in the 3 spatial dimensions. These coordinates are more intuitive for models which perform the solution on a regular grid. The hydraulic conductivities between neighboured cells are calculated with the harmonic mean by Finite Difference Methods and Finite Volume Methods. Finite Element Methods only calculate the arithmetic mean, which is a disadvantage since hydraulic conductivities are distributed logarithmically. In the present work the aquifer is horizontally isotropic, such that:

$$k_x = k_y \quad \text{eq. 8}$$

The Darcy's Law is valid only for small velocities, i.e., for flow whose inherent kinetic energy is negligible. The validity of the Darcy's Law can be estimated using the Reynolds number. Darcy's Law is valid for laminar flow which means the Reynolds number (eq. 9) should have values smaller than 1 but values of up to 10 are also acceptable (Bear 1972).

$$\mathrm{Re} = \frac{v_a L \rho}{\eta} \quad \text{eq. 9}$$

with v_a [m/s] as the pore velocity, L [m] as characteristic length which is D_{10} (the 10 % percentile of the grain size distribution) for groundwater systems, ρ [kg/m³] as the density and η [kg/(m*s)] as dynamic viscosity of water depending on the temperature. For the centre of the investigation area (fig. 13), the flow field between Well 13 and Lake Tegel, Re has a maximum value of 0.001 (v=1m/day, T=10°C, D_{10}=0.1mm). For pore diameters lower than the $5*10^{-6}$ m, electrostatic interactions become important and such that the Darcy law overestimates the flow.

The equations above are only valid for the saturated zone. The unsaturated zone is not simulated.

Choice of the Flow Model

Evaluating the criterion of reliability in a restrictive way, the large number of flow models can be reduced to 2: MODLFOW (McDonald et al. 1988, Harbaugh et al. 2000) and FEFLOW (Diersch 2002). The latter was rejected because it is a commercial product, the source code is not accessible and the model can not be modified. At the starting point of this work it was objected to simulate geochemical reactions. The reactive capabilities of FEFLOW are limited and coupling to models was not available. Thus MODFLOW is chosen. Furthermore, as a Finite Volume/ Finite Difference Method, it has the advantage of being mass conservative on

the scale of cells and calculates harmonic means, while FEFLOW as a finite element method is only globally mass conservative and dummy layers have to be introduced to represent structures with large differences of hydraulic conductivities. The main advantage of Finite Element methods is the possibility of using an irregular horizontal grid.

MODFLOW modules for coupling transport, geochemical reaction and parameter estimation models already exist. Several versions exist, in this work MODFLOW2000 (Harbaugh et al. 2000) is applied, because it allows the combined simulation of steady state and transient stress periods (intervals of constant boundary conditions).

MODFLOW comprises several packages to define appropriate boundary conditions for a wide range of applications. In the present work, the following are applied:

i. time variant specified head – used to introduce a time variant 1st type boundary at arbitrary position
ii. recharge package – used to introduce a 2nd type boundary to the top of the model
iii. general head boundary package – used to introduce a 3rd type boundary at arbitrary position
iv. reservoir package – used to introduce a boundary to a surface water, automatically switches between a 2nd/3rd type boundary depending on the existence of an unsaturated zone below the infiltration area
v. river package – the same function like the latter boundary, with the disadvantage of being not as user friendly but the possibility of also defining transport boundary conditions
vi. well package – used to define a 2nd type boundary at arbitrary position
vii. rewetting package – MOFLOW sets dry cells inactive, used to reactivate dry cells at changing water tables
viii. solver - PCG2 in conjunction with Jacobi preconditioning

Modifications

In order to manage the model size and number of boundary conditions MODFLOW had to be recompiled with redimensioned array parameters in order to extend the storage. Temporally variant leakance was introduced into the reservoir package, head dependent leakance was introduced into the reservoir and river package. The well package was extended to abstraction rates which depend on the hydraulic head in the well.

2.5.2. Transport Modelling

The transport model has to be capable of simulating the transport of different substances. The simulation of conservative and non retarding advective transport is essential, also the modelling of dispersion and molecular diffusion. The possibility of temperature transport would be very advantageous. Often these processes are described by the transport equation, reading with transport in x – direction:

$$\frac{\partial c}{\partial t} = -v_a \frac{\partial c}{\partial x} + D_L \frac{\partial^2 c}{\partial x^2} + D_T \left(\frac{\partial^2 c}{\partial y^2} + \frac{\partial^2 c}{\partial z^2} \right) \quad \text{eq. 10}$$

with c as the concentration, t as the time, v_a as flow velocity, D_L as longitudinal dispersivity (x-direction), D_T as transversal dispersivity (y and z direction). This is an Euler approach.

Another method for transport simulation is particle tracking (Langange approach). Here the concentration is assigned to discrete particles which are transported in the flow field. Particle tracking methods have a higher numerical stability, and their representation of sharp fronts and is better.

Apart from the numerical solutions, the present work requires other processes:

The age of the infiltrated water is a key parameter in assessing bank filtration. Most transport models are not capable of direct determination of the age but capable of modelling first order decay. A small trick enables a rather precise dating: Two species are used. Species one, corresponding to concentration c_0 is conservative, the second, corresponding to concentration c_1 decays with a first order rate (eq. 11):

$$t = \frac{\ln\left(\frac{c_1}{c_0}\right)}{-\lambda} \quad \text{eq. 11}$$

where t is the residence time, and λ the first order decay constant. If mixing of water of different ages occurs, the mixing age is underestimated in comparison to the arithmetic mean. The effect depends on the mixing conditions and appropriate choice of λ, in the present model the age in the observation wells is only slightly affected. Since degradation processes in bank filtration follow more a first order approach than zero order approach, the calculated mixing age is more significant than the arithmetic mean of the age of two waters.

Temperature is an important tracer in subsurface systems which are in contact with surface waters. The model shall be capable of simulating heat transport. Unlike all other tracers, heat is not only transported by advection, diffusion and dispersion, but it is also transported by heat conduction in the water and in the matrix. This is described by Fourier's Law of Conduction:

$$\vec{q} = -k \nabla T \quad \text{eq. 12}$$

where $\vec{q}$ [J m^{-2} s^{-1}] is the heat flux vector, k [W m^{-1} K^{-1}] the thermal conductivity and T [K] the temperature. It is identical to Darcy's law. The thermal conductivity for the two phase system of sand with water filled pores is about k_w = 2.7 [J m^{-2} s^{-1}]. The heat capacity of a saturated sand can be calculated by the heat capacity of pure water c_w = 4184 [J kg^{-1} K^{-1}] and a density of approximately ρ_w = 1000 [kg/m³] and quartz sand with c_s = 800 [J kg^{-1} K^{-1}] and a density of approximately ρ_s = 1820 [kg/m³]. Direct heat transport is not possible for most transport models, but again a small trick can be used. The diffusion equation can be used to simulated heat conduction:

$$J = -D\frac{\partial c}{\partial x} \quad \text{eq. 13}$$

where J [mol m^{-2} s^{-1}] is diffusive flux and the c [mol/m³] is the concentration and D [m²/s] is the diffusivity. Equations 12 and 13 are of the same type, in order to model the temperature D can be calculated as:

$$D = \frac{k_w}{c_{wet}} \quad \text{eq. 14}$$

At a porosity Θ = 0.23 [-] the heat capacity of a saturated sand is about c_{wet} = 2083 [J kg^{-1} K^{-1}], resulting in a diffusivity of 1.3*10^{-6} [m²/s].

Delayed transport of substances and also of temperature can be described by retardation:

$$v_T = \frac{v_a}{R} \quad \text{eq. 15}$$

The retardation factor R denotes the ratio between the pore velocity of water, v_a and the transport velocity of temperature, v_T.

The delayed temperature transport can be simulated by using a linear absorption isotherm. The temperature can be expressed by concentrations, the heat capacities by the distribution coefficient. R can simply be calculated by the ratio of the heat capacity of the mobile and immobile phase:

$$R = \frac{\theta c_w \rho_w}{(1-\theta) c_s \rho_s} \quad \text{eq. 16}$$

It has to be taken into account that both, heat conduction as well as delayed transport (retardation) depend on the porosity.

The characteristic length L_c is a useful parameter to estimate the spatial scale of a diffusion or dispersion process. Assuming the erosion of a sharp concentration front, L_c denotes the distance where the tracer concentration is between 0.16 and 0.5 respectively between 0.5 and 0.84 of the maximum concentration. It is calculated by eq. 17:

$$L_c = \sqrt{Dt} \quad \text{eq. 17}$$

MT3DMS

MT3DMS (Zheng et al. 1998) is chosen as transport code as it comprises the required capability of first order decay and linear equilibrium sorption. Furthermore it is reliable and yet coupled to MODFLOW. It provides several solution algorithms: upstream finite differences (Eulerian method), MOC (method of characteristics, mixed Eulerian-Lagrangian method), MMOC (modified method of characteristics, mixed Eulerian-Lagrangian method), HMOC (hybrid scheme switching between MOC and MMOC, and 3rd oder TVD scheme.

The advective step of the MOC scheme is performed by moving particles. A discrete or random particle distribution within each cell is transported forward in time. MOC is free of numerical dispersion, but may show some oscillations. Under certain conditions, especially irregular grids, it is locally not mass conservative and considerable mass balance errors may occur. The alternative would be a finite difference or TVD scheme, but these have considerable numerical diffusion. MOC is memory intensive and tends to be slower than MMOC.

Instead of using a large number of particles, MMOC uses one particle, placed at the nodal point of the model grid. This particle is tracked backward in time. According to the simulated starting position the concentration of the particle is interpolated to the adjacent cells. This scheme requires considerable less memory and computational time, since only one particle per cell is simulated and the pattern is reset for each time step. The lower order interpolation scheme prevents numerical oscillations but induces some numerical diffusion.

MOC and MMOC are mixed methods because the diffusion/dispersion is simulated after transport by a finite difference step. The HMOC scheme is applied because it combines the advantages of MOC and MMOC. It uses MOC for sharp fronts where high accuracy and low numerical disperions is required. For low gradients the MMOC scheme is applied because numerical disperion is not of concern and the solution is much faster. The scheme of combining MOC and HMOC within MT3DMS is very similar to a method proposed by Neumann (1984). Some effort had to be put on the choice and parameterisation of the solving algorithm in order to find the appropriate criterions to find a setting where the HMOC scheme optimally combines the advantages and minimise the disadvantages of the two transport methods and not vice versa.

2.5.3. Parameter Estimation

Automated parameter estimation may provide substantial benefit to the outcome of a model. Indubitable, parameters estimated by a inverse modelling routine provide a closer

model fit, i.e. more accurate values than manual calibration. Upon adaptation of the parameter estimation routine to the model, numerous different parameterisations can be tested within a short time compared to time needed to perform manual calibration.

Usually the basic process of parameter estimation is the calculation of the Jacobi Matrix, i.e. the matrix containing the sensitivities of the observed values with respect to the parameters which should be estimated. It is the problem of finding a global minimum in a *n*-dimensional parameter space, where *n* is the number of estimated parameters. Usually only one global minimum exists, but often only a local minimum may be found. Numerical parameter insensitivities, more than one local minimum or poor preconditioning may inhibit a solution. The goodness of fit is assessed with the objective function Φ. During parameter estimation the task is to minimise the objective function Φ, defined as:

$$\Phi = \left(\underline{c} - \underline{\underline{X}}\underline{b}\right)^t \underline{\underline{Q}} \left(\underline{c} - \underline{\underline{X}}\underline{b}\right) \quad \text{eq. 18}$$

where $\underline{c}$ is a vector containing the observations, which usually are in case of groundwater modelling hydraulic heads but also could be fluxes, concentrations or travel times, $\underline{\underline{X}}$ a matrix representing the model, $\underline{b}$ is the vector containing the model parameters and $\underline{\underline{Q}}$ the weight matrix. The vector $\underline{b}$ which minimises Φ is defined as:

$$\underline{b} = (\underline{\underline{X}}^t \underline{\underline{X}})^{-1} \underline{\underline{X}}\underline{c} \quad \text{eq. 19}$$

the Jacobi matrix $\underline{\underline{J}}$ can be calculated by the equation:

$$\underline{c} = \underline{c}_0 + \underline{\underline{J}}(\underline{b} - \underline{b}_0) \quad \text{eq. 20}$$

where c_0 is the vector of the model generated observations, and b_0 in proximity to b. For further details please refer e.g. to Doherty (2004).

It may be distinguished between the modellers experience or prejudice on the one hand, and the model performance, measured by statistical indicators on the other hand. Inverse modelling may result in far different values than expected. This may have a physical reason but this also may be result of an ill posed regression problem, not accounting for the relevant processes. Such parameter estimates often point to problems in the model setup and/or the model significance with respect to the observations. However, after a careful review of the model structure, input data etc. the unexpected output may also be true (Hill 1998).

The principle of parameter parsimony is an important point to consider in order to obtain a unique and meaningful solution (Hill 1998, Doherty 2005). This just means that the number of parameters should be kept small, some degree of decreased fit with a model with less parameters is acceptable. The right choice of parameters may be achieved by careful model

evaluation towards obtaining more relevant output and possibly even better fit (Olsthoorn et al. 2002). For calibration of spatially distributed parameters this means that a smaller number of pilot points (see below) or zones should be preferred.

Parameterisation

To get benefit of inverse modelling routines, the flow model has to be parameterised, i.e. identification of unknown coefficients of the relevant physical processes. As the flow model takes about 50 to 90 min computational time on a Pentium 4 with 3 MHZ, and 5 to 10, sometimes more than 30 calculations of the Jacobi matrix are required, with at least one model run for each parameter, the number of parameters should be kept small by the mere limit of computational time, which matches to the principle of parsimony (Hill 1998, Doherty 2005). Only those parameters which are not known by reliable measurements should be included in order to avoid physically meaningless overfitting (Brusseau 1998, Oreskes and Belitz 2001). The inverse modelling routine is only the tool for fitting curves, whereas the result's physical interpretation is the modeller's task. Estimating too many parameters might be problematic for the inversion process. Especially, insensitive parameters should be taken out, as the estimation slows down since more parameters and more steps require more computation time, and additionally, the matrix inversion might have poor results with adverse effects on the necessary number of iterations and precision of the solution. Anyway, insensitively estimated parameters provide only very few and unreliable information about the system. However, it has to be taken into account that previously insensitive parameters might become sensitive, thus the sensitivity of the parameters should be checked periodically.

Calculation of sensitivities is a useful task in highly parameterised models. Especially, detecting parameter correlation either by inspection of the parameter correlation coefficient matrix (if only 2 parameters are correlated) or by inspecting the Eigenvector matrix. Highly correlated parameters show up in substantial contribution to the largest Eigenvector (Doherty 2005).

Choice of Observations and Weighting

The weight matrix $\underline{\underline{Q}}$ is commonly a diagonal matrix. This means that all observations are assumed to be independent of each other, Φ is calculated according to the equation:

$$\Phi = \sum_{i=1}^{n} (r_i w_i)^2 \quad \text{eq. 21}$$

where Φ is the measurement objective function, n the number of observations, r the residual for each observation and w the corresponding weight. The weighting function shall

provide that the summands of the objective function have the same units despite observations of different types and should account for the measurement errors of the observations (Hill 1998, Doherty 2005). In the present study, only the hydraulic heads are studied implying that only the measurement part is of importance. The assumption of the errors being normally distributed however is hardly applicable, as errors are often systematic, due to wrong reference heights and the fact that the standard deviations of logger data are almost as difficult to obtain as standard deviations of manual measurements. Besides, these errors may be small because the hydrographs vary by 1 to 6 meters.

Usually, the stage hydrograph observations are not independent of each other. A properly chosen measurement interval allows following trends and oscillations of the piezometric heads. Otherwise too few measurements exist, the hydrograph would look like white noise. Thus, an observation covariance matrix should be used according to the equation:

$$\Phi = \begin{bmatrix} r_1 & r_2 & \cdots & r_n \end{bmatrix} \times \begin{bmatrix} w_{11}^{\,2} & w_{12}^{\,2} & \cdots & w_{1n}^{\,2} \\ w_{21}^{\,2} & w_{22}^{\,2} & \cdots & w_{2n}^{\,2} \\ \vdots & \vdots & & \vdots \\ w_{n1}^{\,2} & w_{n2}^{\,2} & \cdots & w_{nn}^{\,2} \end{bmatrix} \times \begin{bmatrix} r_1 \\ r_2 \\ \vdots \\ r_n \end{bmatrix} \quad \text{eq. 22}$$

where r_i are the residuals for each observation, w_{ij} are the elements of the weight matrix. When the statistical assumptions for using a diagonal weight matrix are not fulfilled, the interdependence between two single observations may be judged by statistical methods, which, however, do not necessarily represent a physical interdependence. In the present study a physical interdependence is not known a priori, and could be therefore reconstructed only by statistical methods or by the model itself. Using a full weight matrix would mean statistical correlations which might be a result of different processes and consequently a virtual interdepence. In order to separate the information introduced into the model and the results, the model itself should not be used to determine such interdependence. In this particular case, the matrix would have 10 million elements and would be very laborious to set up, as well as a possible source of errors. Therefore the data are weighted according to its structure and information content. Weighting reflects the following aspects:

i. Hydraulic heads may be recorded with different intervals. To avoid a period with dense measurements having a much higher impact on the objective function than a period with scarce measurements, each single measurement is weighted according to the time for which it represents the hydraulic head, usually, the measurement interval. However, if the interval gets too long this may not be the case anymore. The

maximum time for which the measurement is representative is determined using the correlation time of a variogram.

ii. Hydrographs of different piezometers have a different range of variation, thus a different standard deviation. Consequently, the residuals are different at the different measurement locations. As the calibrated model should represent the temporal behaviour at all measurement locations equally well, the relative deviation is regarded as residual. To accomplish this, the single observations of each piezometer are divided by the standard deviation of all observations of the particular piezometer.

iii. Near the transect the spatial density of piezometers is much higher than in the rest of the model and hydraulic heads are very similar (fig. 5). Due to the small distance, the similarity can be assumed to be systematic. Instead of using a weight matrix and in order to obtain an spatially and temporally balanced model output, only observation from piezometer 3301 (fig. 6), where the time series is longest, is included in the inversion process. As the hydraulic heads are very similar, the loss of information in comparison to using a weight matrix is small. Alternatively, the piezometers could be weighted according to the area they represent. Analogue at the northern boundary only observation well TEG243 (fig. 5) has been included in parameter estimation.

iv. In order to have the same units as the weighted hydraulic heads, prior information has to be weighted. The prior information about the spatial structure of the depth dependent infiltration introduced into the present model could also be called initial guess or prejudice. Thus, the weighting is carried out manually and iteratively, ensuring that its contribution to the objective function is not too high. This could be called prejudice or expert knowledge.

Excluding Observations

Similar to weighting, the choice of observation wells also affects the model result. Item (iii) of the last list illustrates why it is a possible to omit certain observation wells, making the modellers life easier, without loosing relevant information. In fact the quality of the results and stability can be improved because:

i. No parameter estimation tool does not have any physical comprehension. If the model set up and parameterisation do not meet the physical requirements, any inverse modelling routine tries to adjust other parameters instead, with physically senseless results (Oreskes and Belitz 2001).

ii. The differences of hydraulic heads at the transect are strongly affected by spatially and temporally highly variant well switching. This problem arises when no logger

data but only single measurements are available. The observation wells react very quickly to well switching, especially the piezometers in the second aquifer. Several hours might elapse between the first and the last measurement with the result that the hydraulic situation already changed. These single measurements, normally carried out once in a month, have a high weight. Since the temporal discretisation is one week but the hydraulics change within hourly scale, the parameter estimation tool tries to obtain a model fit without the possibility of adjusting the corresponding physical parameters.

iii. Different piezometers are sampled with different intervals and within different periods because they may fall dry or the sampling pattern may change. Due to the effects under (i) and (ii) local effects may introduce substantial differences in hydraulic heads between observed values of neighboured piezometers. When observations of one piezometer begin or end, the parameter estimation tool tries to introduce a shift to the hydraulic heads which does not exist in the continuous time series. In order to maintain the correct temporal dynamic only the longest time series is used.

By excluding observations from the calibration process, the absolute deviation might be increased, from the point of view of random measurement errors. But the price is small in relation to the correct description of the temporal dynamic and inversion stability. For these reasons only observation well 3301 from the transect is included and observation wells TEG233, TEG242, TEG243 (fig. 5) are excluded. The reasons are further discussed in chapter 4.3.

Sensitivity Analysis

The parameter covariance matrix is a by product of the parameter estimation. It is a square symmetric matrix with as many rows/columns as there are adjustable parameters. The diagonal elements of the covariance matrix are the variances of the adjustable parameters. The off-diagonal elements of the covariance matrix represent the covariances between parameter pairs. Under the assumption of linear relationships between the parameters, this matrix contains information about parameter correlation and uncertainty (Doherty 2005). In order to enable a more intuitive inspection independent of the corresponding parameter values, the parameter correlation coefficient matrix is calculated by:

$$\underline{\underline{\rho}}_{ij} = \frac{\underline{\underline{\sigma}}_{ij}}{\sqrt{\underline{\underline{\sigma}}_{ii}\,\underline{\underline{\sigma}}_{jj}}} \quad \text{eq. 23}$$

where $\underline{\underline{\rho}}_{ij}$ are the elements of the parameter correlation coefficient matrix, $\underline{\underline{\sigma}}_{ij}$ are the elements of the parameter covariance matrix and the counters *i*, *j* denote the row, column, respectively. Like the covariance matrix the parameter correlation coefficient matrix is always symmetric. The diagonal elements of the correlation coefficient matrix are always unity, the off diagonal elements always are between 1 and -1. The closer that an off-diagonal element is to 1 or -1, the more highly correlated are the parameters.

The Eigenvector matrix and Eigenvalues are also calculated from the parameter covariance matrix. The Eigenvalues can be calculated from the equation:

$$\det(\rho - \lambda E) = 0 \quad \text{eq. 24}$$

with det denoting the calculation of the determinant, λ is the Eigenvalue and *E* the identity matrix. For each Eigenvalue λ an Eigenvector can be calculated by the equation:

$$(\rho - \lambda E)\vec{x} = 0 \quad \text{eq. 25}$$

where $\vec{x}$ is the Eigenvector. Numerically Eigenvalues and Eigenvectors can be calculated as the Potence Method, Inverse Iteration, Lanczos Method or Arnoldi Method.

The Eigenvectors span up the probability ellipsoid in the n-dimensional parameter space, the square root of each Eigenvalues is the length of the corresponding semiaxis of the ellipsoid. If the ratio of a particular Eigenvalue to the lowest Eigenvalue is particular large, then the respective Eigenvector defines a direction of relative insensitivity in parameter space. The Eigenvector with the largest Eigenvalue defines the maximum model insensitivity. If this Eigenvector is dominated by a single element, then the parameter associated with that element may be quite insensitive. If this Eigenvector contains a group of parameters with significant components, then this is an indication of correlation within this group (Doherty 2005).

For the present problem, where spatially distributed parameters are of high importance, the method of regularisation allows to use a huge number of parameters while maintaining numerical stability as well as a meaningful output. The model may be physically and mathematically overparameterised. Regularisation in this context means imposing a target function to spatially or temporally distributed parameters. It represents our previous knowledge about the system and often is a smoothing function. Heterogeneity only is introduced when observations indicate that the parameter is sensitive. It constrains the parameters which are insensitive to the previous knowledge, allows the sensitive parameters to change and thus introduces heterogeneity only where/when required to explain the observations (Doherty 2005). The decision, if the calibrated parameter indeed represent the physical process has to be

made by the modeller. Regularisation only inhibits numerical problems of overparameterisation.

PEST is chosen for parameter estimation as it is capable of regularisation, in contrast to other parameter estimation programs as MODFLOW2000 (Harbaugh et al. 2000) or UCODE (Poeter 1998). It is reliable and many tools for coupling to MODFLOW already exist.

PEST

Regularisation

In order to identify spatial structures, the regularisation function of PEST is used. In this case the objective function Φ_{tot} consists of two parts:

$$\Phi_{tot} = \gamma * \Phi_{meas} + \Phi_{regul} \quad \text{eq. 26}$$

where γ is a Lagrange multiplier, chosen such that the regularisation part Φ_{regul} of the objective function Φ_{tot} does not dominate the measurement part Φ_{meas}. Additionally it is ensured that the measurements' objective function does not increase during parameter estimation, Φ_{meas} is calculated according to equation 21 or 22, and Φ_{regul} according to the users definition. By this way a model may be highly overparameterised, constraining insensitive parameters with respect to Φ_{meas} with Φ_{regul}. Numerical stability is maintained and only the model parameters sensitive to the observations are adjusted. Smoothing is a common way of regularisation, it means assuming neighboured parameters have the same value, unless measurements indicate they are different. A similar effect could be achieved by ordinary prior information, the advantage of PEST's regularisation is that the Lagrange factor γ is calculated automatically and it is ensured that the measurement part does not increase during iteration. Furthermore a threshold value for the measurement function can be set, at which the regularisation function is minimised. For further information see Doherty (2005).

Parallelisation

Each partial derivative for an estimated parameter is calculated in a separate model run, called coarse grained parallelisation. A modified version of PEST exists, called Parallel PEST, which can distribute the model runs of the Jakobi matrix calculation and Marquardt lambda search to different machines and processors. This way the process can sped up several times. Within this work computations have been carried out on up to 19 Pentium 4 processors between 1.6 and 3 Ghz.

2.5.4. Pre- and Postprocessing

Without suitable pre- and postprocessor the present work could not have been carried out. PMWIN is chosen, it couples MODFLOW with MT3DMS. Though implemented, PMWIN only partially serves as preprocessor for PEST. The parameterisation is limited, some files are generated incorrectly. Additionally, various utilities for data conversion and model coupling are required. Most are already available together with PEST, others have been created as executables within this work in Visual Basic, Fortran or as batch files. Furthermore, as it was intended to perform geochemical modelling, PMWIN also is a user interface for PHT3D (Prommer 2002), which itself is a coupling routine between MT3DMS and PHREEQC (Parkhurst and Appelo 1999).

General Data Handling

Large amounts of data had to be converted, summed up, weighted and preconditioned. Most of this work was carried out by macros in VBA (Visual Basic for Applications) under EXCEL, written within this work, or utilities by other authors. The conversion of time dependent data would have meant a significantly increased effort with less precision, data being as well temporally and spatially dependent could not have been converted with existing preprocessing software. On the way of defining the boundaries and testing hypotheses, various models have been set up, usually each with many subsequent modifications. Only using the automation routines the work could be carried out.

Spatial data could be post processed with PMWIN (Pre and Postprocessor for MODFLOW, WebTech360, 2005) or SURFER (contouring and mapping), temporal dependent data required EXCEL or MATLAB (language for scientific programming).

Water Budget

The water balance is calculated using the program PMWBLF (Chiang 1993) in conjunction with a program extending the applicability to transient calculations (written within this study).

The discharge into the Airport Lake is calculated by subtracting the variations of the groundwater (TEG053, fig. 5) from the daily Airport Lake water level. Thus, the rapid increase of the water level after rainfall by surface runoff is multiplied with the surface area of the Airport Lake resulting in the discharge from the adjacent areas. The amounts of groundwater passing through the lake are not considered by this method.

2.6. "Validation"

A critical review of models is indispensable in groundwater modelling having in mind that even with a model which is physically totally wrong, the fitting of the output values may be excellent. The central problem is that absolute validity of a model never can be determined (National Research Council 1990). Numerous authors reject the terminology validation and verification as these lead to false impression of the model capabilities (Konikow et al. 1992, Morel-Seytoux 2001) and introduce different terminologies. The process of transferring parameters obtained by modelling an interval to another interval, traditionally is called validation. Since only the correctness of output for a certain interval can be approved but the word validation implies the correctness of the processes and parameters, the transfer of parameters obtained modelling an interval to another interval is named according to Morel-Seytoux (2001) "performance check". Such a check may only be applied if the parameters should be basically the same for the 2 different time spans. As the hydraulic conductivity of the bank is identified to be a function of time and the value of this function is determined with the model, the performance check is not possible. The correctness of the temporal behaviour is demonstrated by excluding other possible factors of influence.

Especially regarding groundwater modelling, concerning the high degree of physical uncertainty which always results more or less in parameter uncertainty and nonuniqueness, a model can never be validated, only falsified, and the chance for falsification must always exist (Popper 1959, Lane et al. 2001, Bates and Anderson 2001). However, the term "validation" may serve as a keyword to summarize the different methods of model testing.

Apart from statistical tests, good modelling practice means essentially development of a meaningful model. These principles have been described e.g. by Hill (1998). Four of them are of special importance for the present work:

i. Principle of parsimony: Start with simple parameterisation and add complexity only as warranted by the hydrogeology or the inability of the model to reproduce observations. Using PEST's regularisation to constrain parameters a higher complexity may be introduced from the beginning.
ii. Use a broad range of information to constrain the problem. In the present study piezometric heads, abstraction rates of wells and tracer data for transport are included.
iii. Use prior information carefully. Begin without prior information to see the information content of the observations, add carefully later.

iv. Evaluate optimised parameter values: unreasonable parameter values might indicate a model error and identify highly correlated parameter values.

Cross Validation

Morel-Seytoux (2001) calls the transfer of model parameters performance test, if they are determined for one period and applied to a second period,. If parameters are also determined with the second period and transferred to the first it is named cross validation. The data set may be split up in 2 parts or more, either temporally, spatially or by other criteria. The resulting parameter combination of each run is compared to the parameter combination of all other runs.The goodness all fits is the criterion for the correctness of the model.

3. Results and Discussion

The results presented in the following chapter are the outcome of an iterative process of model development. The regional model (chapter 4.1) itself is a result of flow modelling (chapter 4.3), data pretreatment (chapter 4.2) and transport modelling (chapter 4.6) strongly depends on the results of the telescope model (chapter 4.7). Many results of later chapters act as indication for the correctness of the previous findings. The following structure however represents the general trend of the improvement in perception.

3.1. Regional Model

The centre of the investigation is the transect at Well 13 of Well Field West (fig. 5, 6, 19). It consists of 14 observation wells roughly installed along the flow direction between bank and well. A necessary prerequisite for a comprehensive understanding of the transect is a correct flow description. Well defined boundary conditions have to be found, while keeping the model domain as small as possible. Previous studies from Eichhorn (2000) and Wiese et al. (2004) defined boundary conditions a priori perpendicular to the Well Field West and below Lake Tegel through the interpretation of the hydrogeological situation and arrangement of the well field. This interpretation does not hold as the entire area around Lake Tegel is strongly affected by the waterworks with several meters of drawdown. Hydraulic contact of Lake Tegel can not be regarded as good and thus is introduced as $2^{nd}/3^{rd}$ type boundary. This means Lake Tegel may only slightly mitigate the alternating pumping regime within Well Field West and between Well Field West and the adjacent well fields (fig. 12). Moreover, with increasing drawdown the interaction between the well fields also increases.

In addition to the described necessary modifications regarding boundary conditions, the present model indicates that the existence of a water divide below Lake Tegel (Fritz 2002) can be rejected and in contrast to a study of WASY (2004) it could be shown that significant amounts of water come up from the 3^{rd} aquifer. Probably the most important finding here is the detection of the leakance which determines the infiltration of lake water into the aquifer and which depends on the pumping rates of the well field.

The test site has been modelled with different model concepts. The final version was obtained by iterative variation of the boundary conditions, temporal steps and the model extent. In figure 13, the basic specifications of the final version are presented.

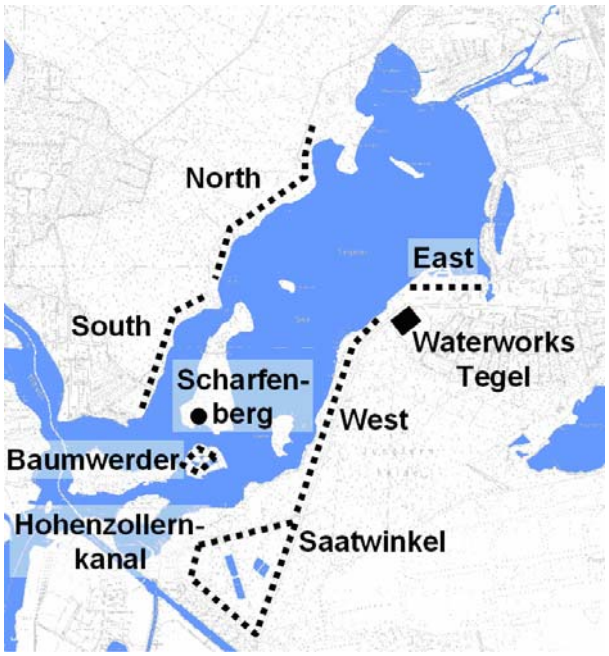

Figure 12: Location of the well fields pertaining to the waterworks Tegel. The dotted lines represent vertical abstraction wells, the black dot represents the horizontal well at Scharfenberg

3.1.1. Boundaries

As the study region is strongly affected by waterworks Tegel, it is not possible to set time invariant boundary conditions without modelling the entire catchment. Fortunately, a dense net of piezometers with monthly observation exists. These transient hydraulic heads are introduced as time variant specified head boundaries, interpolated linearly in time and space where necessary. The boundaries where no hydraulic heads are available are chosen in such a way that no flow appears to be a reasonable assumption.

The model comprises an area of 4.1 km². In the following, a description of the applied boundary conditions will be given.

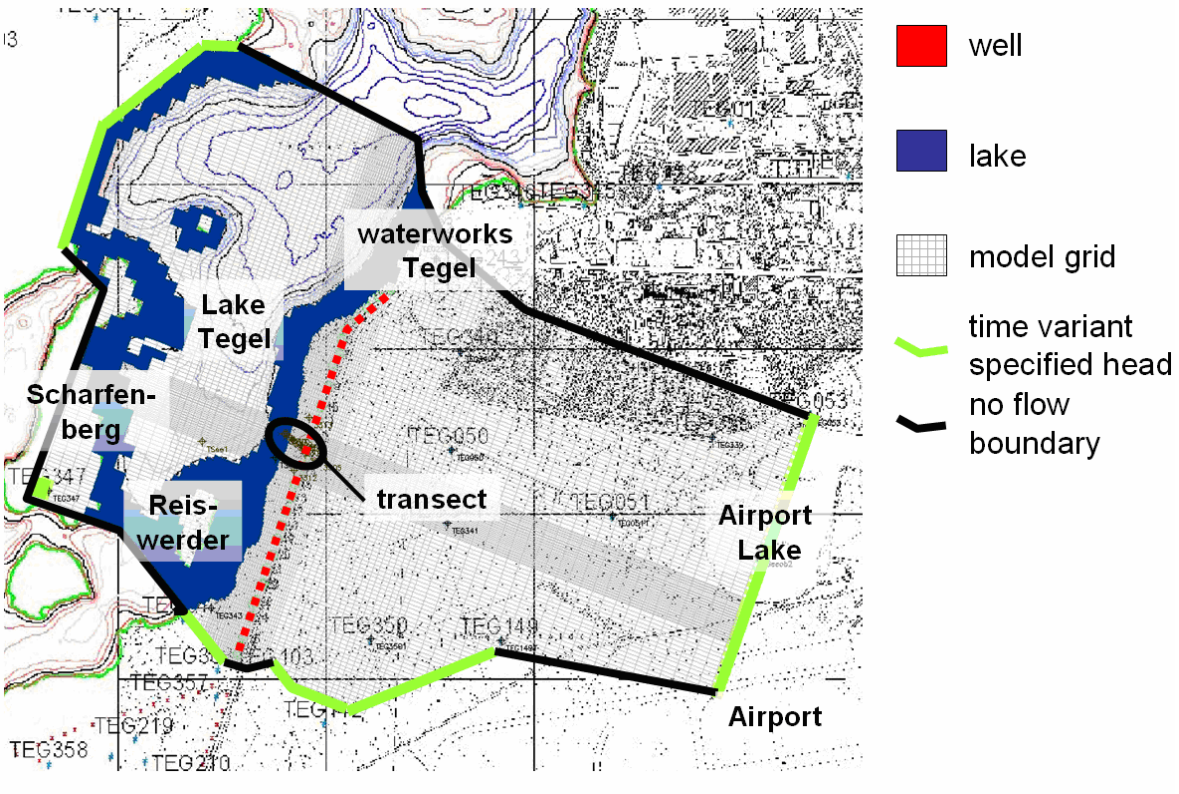

Figure 13: Top view on the boundary conditions of the model domain, wells of the Well Field West are marked red, Lake Tegel introduced as 2nd/3rd type boundary is marked blue, time variant specified head boundaries use green. Please note that boundaries are not assigned to every layer (see Fig. BC2). All borders with no value assigned are “no flow” boundaries. Tiny grey lines represent the model grid. The bathymetry of Lake Tegel is indicated with isolines of 1 m distance, above 25m NN in red colour, partially covered by the shape of the boundary condition of Lake Tegel.

North

At the deepest regions of Lake Tegel limnic mud and silt form a hydraulic barrier as they are located up to a depth of 10 m below sea level, at the same depth already Holstein silt occurs. The location of the deepest sediments roughly coincides with the catchment of Well Field West (fig. 13).

As the ratio of abstracted water between the adjacent Well Field East and Well Field West (fig. 6) roughly stays constant (fig. 14), a no flow boundary is applicable between waterworks Tegel and the Airport Lake.

Additional confirmation of the no flow boundary assumption is that the flow direction remains almost constant within the entire investigated period. It is determined using hydraulic heads of observation wells TEG233, TEG243, TEG242 (fig. 5), located between Well Field West and East and forming a triangle. These observation wells are screened in the first aquifer. According to adjacent deeper bore profiles the glacial till does not exist here, so hydraulic heads and flow direction in the first and second aquifer are probably identical. If a layer of glacial till would exist below these piezometers, the hydraulic heads would lead to a false

impression. The close fit of observed and modelled hydraulic heads of observation wells near the boundary TEG233, TEG243, TEG242, TEG340 (hydraulic heads in fig. 26, fig. 27), (location of observation wells in fig. 5) is a further indication that a no flow boundary is the appropriate choice.

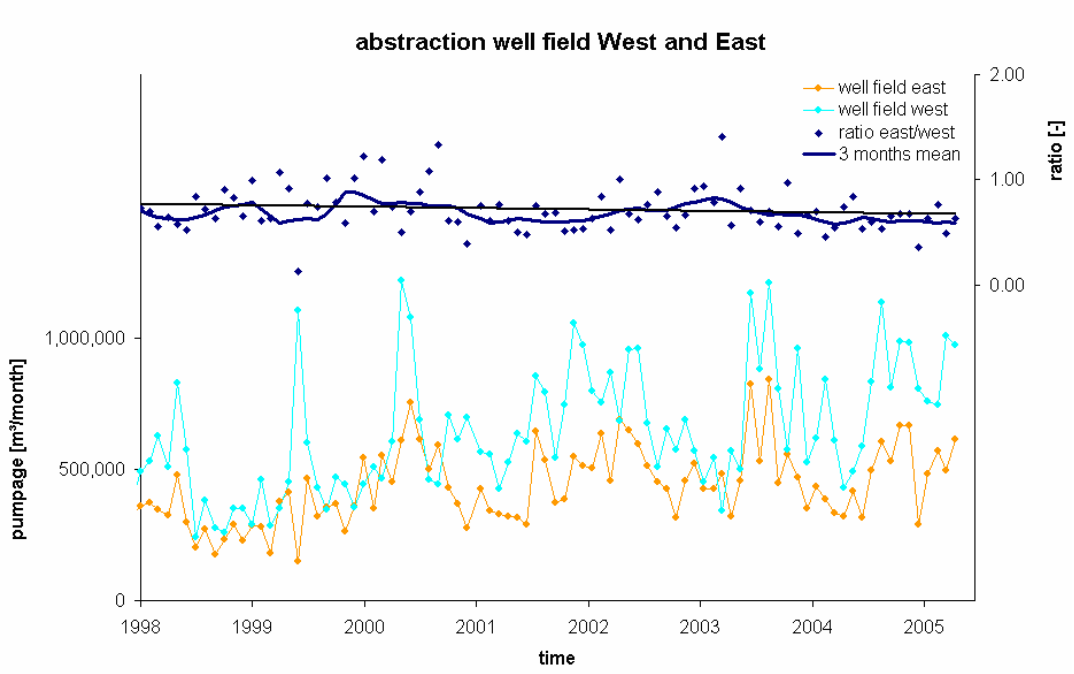

Figure 14: The turquoise and orange line show abstraction of Well Field East and west. The blue dots show the ratios, the blue line the 3 month moving average. All values have monthly interval.

However, modelling also showed that the no flow boundary north of Well Field West has to be shifted from directly between the well fields to the north, because hydraulic heads indicate that Well Field West extract water from the extended regions of shallow water next to the waterworks Tegel (fig. 13).

East

Piezometers in the model domain screened in different aquifers suggest that the upper and the lower aquifer have the same head at the Airport Lake. The Airport Lake penetrates both aquifers and is well connected to both since is formerly was a gravel pit. Consequently, the same boundary condition is assigned to both aquifers. The piezometers TEG053, TEG339, TEG051 (fig. 5) also show that they are located sufficiently far enough away from the well fields implying a constant flow direction. Due to stormwater runoff, the water level of the Airport Lake temporarily exceeds the groundwater level by a few centimetres wherefore the piezometric head of the observation well TEG339 is used for the model setup.

The study of WASY (2004) has shown that during the year 2002 the no flow boundary between observation well TEG149 (fig. 5) and the airport follows steady state conditions.

Inaccuracy for the present model is mitigated by the adjacent time variant constant head boundaries.

South

At the southern model boundary the ratio of extraction amounts between the Well Field West and adjacent Saatwinkel (fig. 12) varies by factor 3, implying highly variable flow directions and water levels, which consequently have to be respected with time variant specified head boundaries. The boundary is interpolated using piezometers TEG103, TEG142, TEG149 (fig. 5). It might appear strange that piezometer TEG142 is not located within the model domain. Hydraulic heads are interpolated by triangulation to the outer model cells. Unfortunately, it is not possible to set the boundary further to the south because there are no available data from the airport (fig. 13). But at least piezometer TEG350 allows to check correct hydraulic description since it is located between the well field and the boundary.

South of the Well Field West a short no flow boundary is introduced, because interpolation between observation wells TEG363 and TEG103 is not possible due to an abstraction well in between. Inaccuracies are mitigated by the 2 adjacent time variant specified head boundaries.

Southeast of the Well Field West, between TEG 363 and TEG 343 (fig. 5) the interpolated hydraulic heads form a time variant hydraulic head boundary. Though the hydraulic heads of TEG343 vary with high frequency due to the neighboured well fields with about 1 m, the long term variations of up to 7 m are representative as they coincide with other observation wells which are not affected by the wells with such a high frequency, e.g. TEG350.

West

Between Scharfenberg and Reiswerder a no flow boundary is applied according to the flow paths extracted from WASY (2004). They are only valid for steady state conditions, however it is the best estimation available for conditions below Lake Tegel. Inaccuracy is mitigated by the time variant specified head boundary between the Lake Tegel and Well Field West.

On Scharfenberg a piezometer exists at the horizontal well. To avoid setting a time invariant watershed between Scharfenberg and Well Field South, the well is introduced as time variant specified head. In this manner the influence of the well fields Baumwerder and South (fig. 12) are included in the model. Assuming radial pathlines towards the horizontal well in combination with a 1st type boundary the 90° sector, which is included from Scharfenberg, can be regarded independently when the well is switched on. This approach is feasible as the calculated abstraction from this sector is 17% of the nominal abstraction, and the distance to the bank is higher than in other directions. Hydraulic heads of piezometer 6053 (fig. 5) normally are matched with a deviation of 20 cm or less, however differences of up to 1.1 m

occur from time to time and suggest that the hydraulic situation is not represented entirely correct. Possible reasons are the unknown leakance of Lake Tegel, and unknown distribution of the glacial till below Scharfenberg. With respect to the entire model and the region around the transect these deviations are regarded to be acceptable. As there are not any observation wells between the Well Field North and the lake, also not in the lake the boundary condition here is less well defined than the other boundaries.

Estimated by the pumping rates of Well Field North a mean head of 29 m until September 2002 and 28 m beginning from October 2002 represents the hydraulic situation. The abstraction from this boundary is 79% of the well fields nominal abstraction. This is equivalent with a bank filtration ratio of 79%. This is probably a little high but the impact of the boundary on hydraulics at Well Field West is small. It is mitigated by the infiltration in front of the well fields North, West and north of Scharfenberg and as well by deep lake sediments in the middle of the lake.

An increase of 1 m of the hydraulic head at Well Field North increases heads north of Well Field West (observation well TEG223) by 14 cm at the beginning of 1998, the difference diminishes to 5-8 cm between 2001 and 2005. At the transect (observation well 3301) the differences diminish from 11 cm in 1998 to 3-7 cm between 2001 and 2005.

Lake Tegel

Unlike the k_f value, the leakage includes the unknown thickness of the clogging layer, wherefore two unknown parameters are lumped to one parameter and i.e. conveniently only one parameter has to be estimated. The leakance is related to the k_f value according to equation 1.

Characteristics of infiltration of lake water to the aquifer are widely unknown, some constraints however can be set: Sievers (2001) showed that sulphate is reduced within the upper few centimetres of mud. As sulphate concentrations are almost the same in Lake Tegel and the adjacent groundwater, it is a strong indication that mud inhibits infiltration of lake water. Thus infiltration is assigned only to the shallow regions above 25 m above sea level, where the mud is absent according to Parchur (1977), Brühl et al. (1986) and Ripl et al. (1987). The mud itself is impermeable with a k_f of $2.8*10^{-9}$ m/s (Schley 1981). The average surface water level is approximately 31.45 m above sea level, with about 31.30 m in summer and 31.55 m in winter. Infiltration measurements indicate that the leakance is highest in a water depth of 1.5 m to 2 m (fig. 39). However the spatial and temporal variability is high. Some modelling indicates a relatively homogeneous distribution over the depth, with values about factor 2

higher in shallow than in deep regions. Two possible distributions of the leakance by depth are shown in figure 44.

The leakance of Lake Tegel to the aquifer is identified to be temporally variant by means of exclusion. For the entire model period no reasonable parameterisation could be found using a constant leakance. Two possible calibrated characteristics are shown in figure 43.

The depth of the lake bed, where saturated conditions below Lake Tegel exist, is not known. By modelling within this study the thickness is a very insensitive parameter between, equally good fits may be obtained with a thickness between 0 and 2 m. Core samples (Hoffmann and Gunkel 2006) indicate 5 to 22 cm saturated thickness in a water depth of about 50 cm. The MODFLOW Reservoir Package is used for flow calculations, it enables defining the bed thickness, but transport boundaries may not be assigned. Transport boundaries can be assigned using the river package, but it is not possible to simulate the bed thickness. Except for calibration runs of the bed thickness, a bed thickness of 1 cm is applied in order to enable transferring values from the flow to the transport model.

Recharge

Mean annual groundwater recharge is 125 mm/a (Umweltatlas Berlin Version 2003) which is 21% of the annual precipitation (measured at waterworks Tegel). Recharge values applied to the model is assumed to be also 21% of annual precipitation, with 75% in winter and 25% in summer. Values are calculated with about weekly intervals, according to the present discretisation of the model. With exception of Lake Tegel and the islands, recharge is assigned everywhere. However the magnitude and temporal distribution is not of major importance since it is only 4% to the abstraction amount of Well Field West (tab. 5). The area to which recharge is applied has a size of 2.4 km²

Bottom Water

The lower face of the model is generally a no flow boundary, as tertiary and quaternary glaciofluviatile silt and clay layers (Fugro 2000) act as aquitard. However a quaternary glacial trough (Frey 1975) direction from NNW to SSE, with observation wells TEG051 and 6034 (fig. 5) roughly located on its axis, penetrates deep into tertiary sediments. Observation well 6035 is located at the same place as 6034, but screened in the third aquifer. The hydrograph of 6035, which is 80 cm to 1.60 m above the hydrograph of observation well 6034 suggests hydraulic contact between the 2nd and the 3rd aquifer (fig. 15). For accuracy of the further modelling it should be respected, that hydraulic heads in 1998 and beginning of 1999 appear to be subject of some systematic measurement error. The upcoming water is introduced by a 3rd type boundary. It is located where the base of the aquifer 2 is lower than 28 m below sea level

(fig. 16). The head is taken from the hydrograph of 6034, the transfer factor is calibrated. The model structure differs from the hydrogeological structural model at this item.

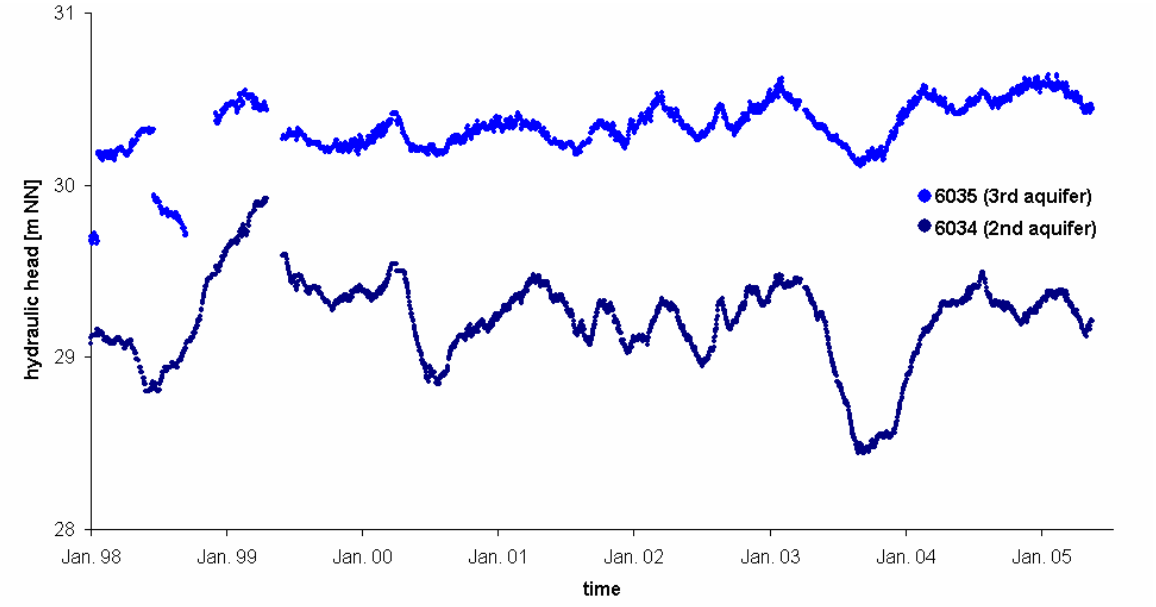

Figure 15: Measured piezometric heads in observation wells of the second aquifer represented by 6034 and the third aquifer, represented by 6035. Both piezometers show identical fluctuations, the gradient is directed bottom up. In January and autumn 1998 data appear to contain errors.

Without taking into account this bottom water, the piezometric heads of observation wells 6034, TEG051 and TEG339 would be between 2000 and 2005 continuously 10 cm to 30 cm lower than observed. This is a strong indication for large amounts of upcoming water as these observation wells are in vicinity of time variant specified head boundary conditions and modelled piezometric gradients would be 30% to 50% higher than observed. It has to be pointed out that this deviation still exists after automatic calibration when the bottom water is not included.

A better fit in periods of low groundwater levels is obtained when no bottom water is introduced, in particular regarding observation well 3301. The better fit inland results in a worse fit at the lake side of the well field. Surely, hydraulic conductivities could have been increased near the boundary and varied spatially to obtain a better fit, but at this point further calibration was stopped as the physical indication for a different parameterisation has to be paid with high degrees of nonuniqueness of the solution.

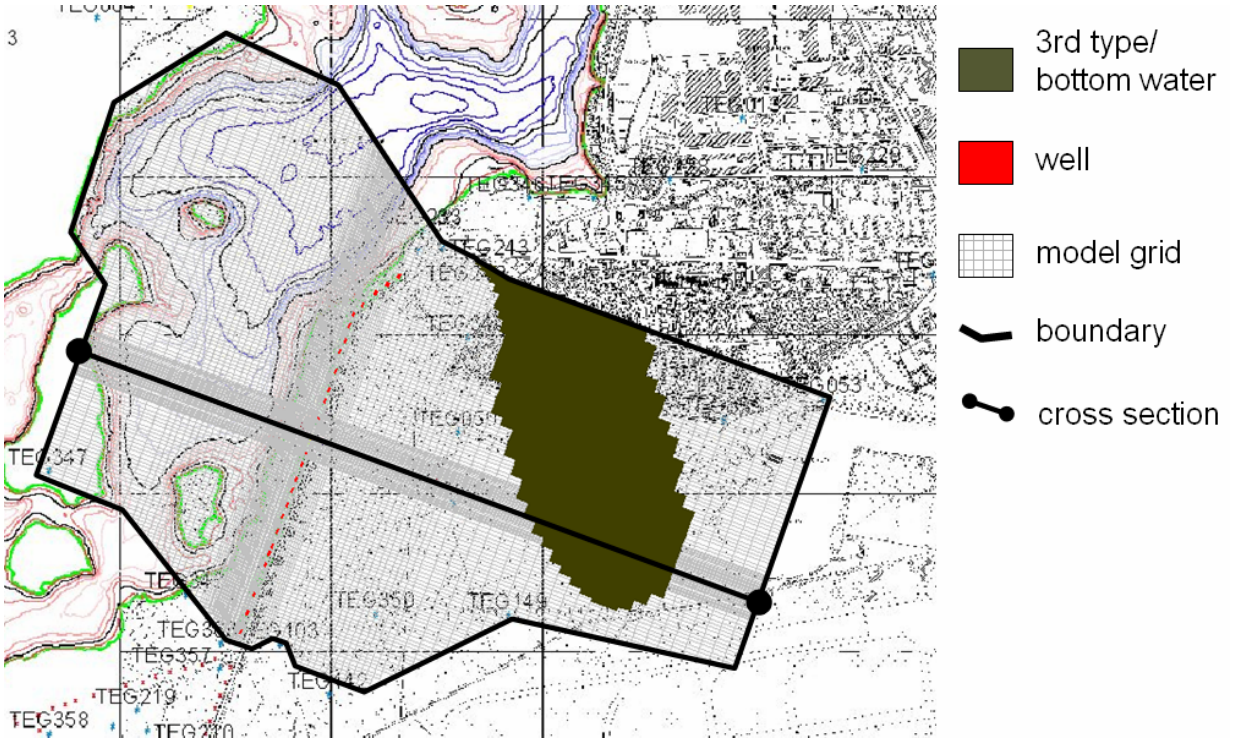

Figure 16: the brown area indicates where a 3rd type boundary represents the weak zone between the 2nd and the 3rd aquifer, resulting in upcoming water. Red dots indicate the Well Field West, grey lines the model grid and a, the cross section of fig. 17 is indicated by the black line between the circles. The other bold black line defines the shape of the model domain.

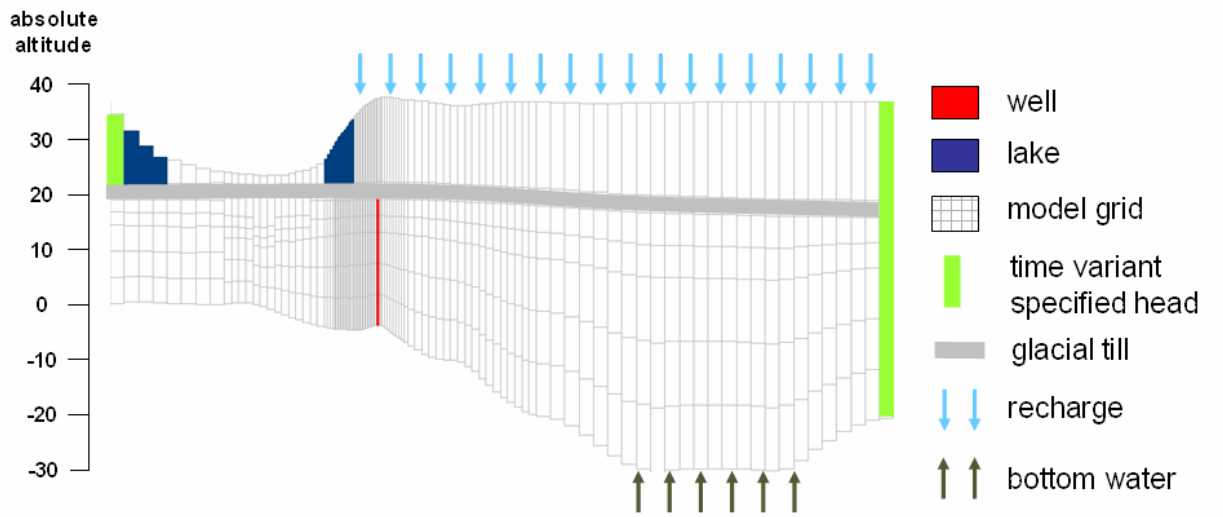

Figure 17: Vertical cross section of the boundary conditions at Well 13. The screened part of the well is marked red, Lake Tegel is marked with dark blue, tiny grey lines represent the model grid, time variant specified head boundaries are marked with a light green. The time variant specified head at the left is a projection of the horizontal well Scharfenberg. The grey line indicates the position of the glacial till layer, recharge by precipitation is indicated by blue arrows, the 3rd type boundary introduced for intruding water from the 3rd aquifer is indicated by brown arrows.

Wells

The pumping rates are calculated through the use of the daily well operation time and pumpage. Amounts are checked using the sums from the water meters and hours of well operation, both registered at the well capacity measurements which take place between 2 and 4

times a year. Wells are only screened in the second aquifer. Different pumping rates for each well from 10 to 16 are split up to the model layers according to the screen depth as vertical flow might affect the conditions at the transect. For the other wells, due to the distance to the transect, the Dupuit assumption is applied and the pumping rates are simply partitioned according to the layer thickness.

3.1.2. Aquifer Parameters

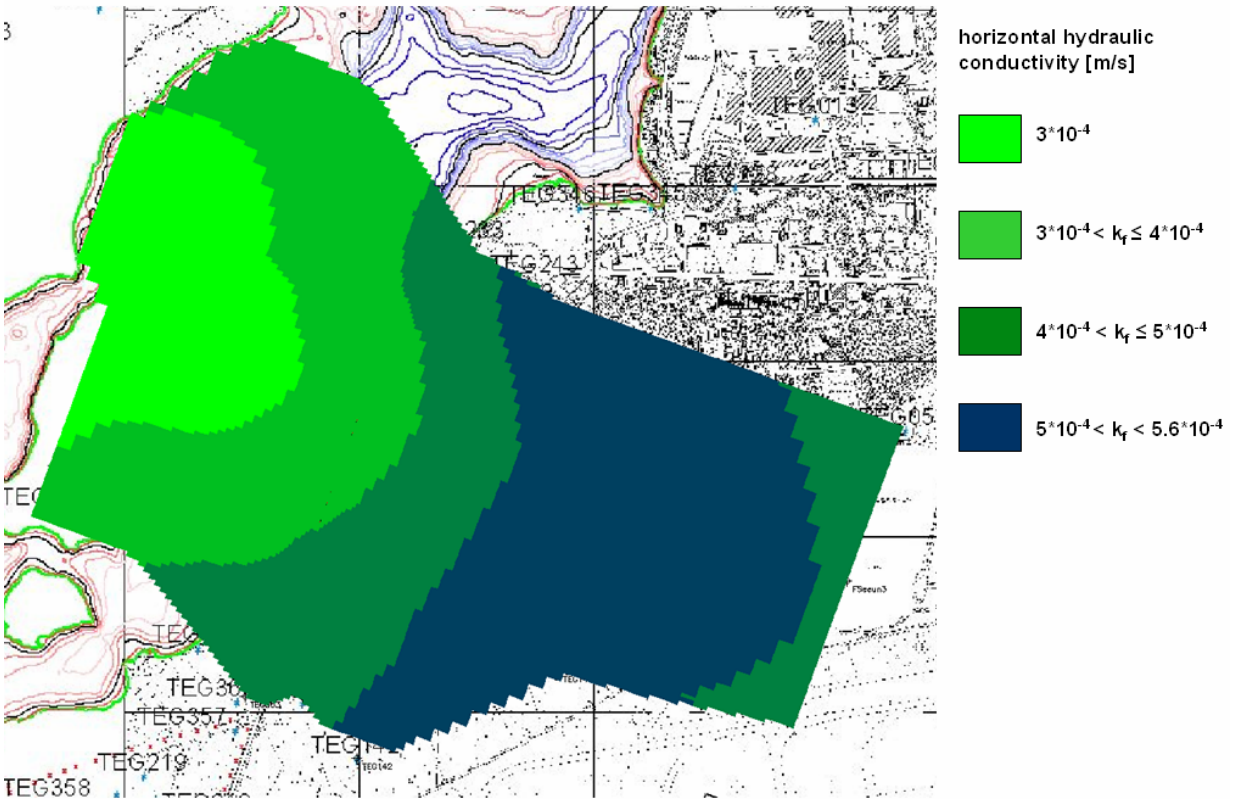

Figure 18: Horizontal conductivity of the second aquifer.

Horizontal hydraulic conductivity is calculated from the transmissivity and thickness of the 2nd aquifer according to the HSM (Hydrogeological Structural Model, Fugro 2000), resulting in k_f of $3*10^{-4}$ m/s below Lake Tegel and at Well Field West to about $5*10^{-4}$ m/s at the Airport Lake (fig. 18). Values at the transect of $3.5*10^{-4}$ m/s by Fugro (2000) and $2.9*10^{-4}$ m/s by Fritz (2002) are almost identical.

Specific yield (sy) denotes the pore space which is subject of variable saturation. It is set to sy=0.2 [-] by calibrating the velocity of propagation of drawdown events induced by the Well Field West. The value corresponds well with values measured at the artificial recharge site (Greskowiak 2005) in the triangle of well fields Saatwinkel and Hohenzollernkanal (fig. 12). The specific storage coefficient is set to s= 10^{-4} [-] for the entire model. It only represents the confined part of the storage. Its hydraulic impact is negligible as overlaid by the specific yield.

3.1.3. Discretisation

The interval between the Jan. 1st 1998 and Apr. 30th 2005 is modelled, including thus the entire duration of the NASRI project. At the beginning of the simulation a steady state stress period of 3 months duration is introduced, the step size afterwards is one week. In total the model comprises 370 stress periods.

Spatially the model is discretised in 174 rows, 117 columns, 7 layers. The rows are either 15 or 5 m wide, the columns have a width between 5 and 50 m. At the transect the resolution is highest with a block size of 5 m. The layer thickness of the two upper layers is set according to geologic formations and land surface elevation. (fig. 17). The 2nd aquifer is represented through 5 layers, the lower 3 represent each ¼ with a vertical length of about 6 m at the transect up to a maximum of 10 m. The uppermost 2 model layers of the 2nd aquifer comprise each $^1/_8$ of its thickness in order to represent transport processes at the transect more accurately, resuling in a vertical block length of about 3 m at the transect to a maximum of about 5 m. Exchange between neighboured cells is calculated applying the harmonic mean.

3.1.4. Transport Boundaries and Parameters

Transport is only modelled on a small part of the regional model in order to keep the computational effort low. Besides, results could not be improved with a larger area, because the known boundary conditions are located within a distance of 2 years travel time. The next travel time of known boundary conditions would be in a distance of more than 10 years. These would not affect the area of interest at the transect since the modelled interval only comprises 7 years.

Minimisation of the boundary effects on the transect is achieved through ensuring that the transport boundaries have such a distance from the transect, that all lateral effects are taken into account within the domain and that only inland water and old bank filtrate coming from Scharfenberg enter the transport domain. These sources can not be modelled because the model period is not long enough. However, most observation wells of the transect are located within flowpaths coming from the eastern bank of Lake Tegel. All flowpaths which affect the transect and have their origin at the eastern bank of Lake Tegel are included. It is an important simplification that the main basin of Lake Tegel can be assumed as homogeneous (Richter 2003).

The tracers should have a significant signal in the surface water, which is the case for ^{18}O and temperature with seasonal variations. Chloride concentrations decrease slowly from the beginning of 2001 with a sharp increase in spring 2003. By combining the short and long term

behaviour travel times of different scales may be identified. However, only ^{18}O and chloride are not retarding. Data of Deuterium is available but not used in an explicit way, as it basically shows the same behaviour as ^{18}O with increased scattering. Data of boron is available but not included in later modelling stage as boron shows retardation with R varying from R=1.3 to R=2.1 (De Simone et al. 1997). It may only be used in a qualitative way, simulations carried out with preceding models showed varying retardation also at the transect of R=1 to R=1.3.

Three physical species are assigned:

i. chloride - 1998 to Aug. 2004 to Lake Tegel, data from NASRI (KWB 2005) and SENSUT (2005)
ii. ^{18}O - May 2001 to Aug. 2004 to Lake Tegel, data from Pekdeger et al. (2004) and Richter (2003)
iii. temperature - 1998 to Aug. 2004, data from NASRI (KWB 2005), SENSUT (2005)

These species are assigned to Lake Tegel, temperature is also assigned to the fixed concentration boundary, in contrast to other tracers it can be estimated quite precisely, 10 °C is a good estimation.

For impact assessment of unknown concentrations as well as for a water balance estimation at the transect and the wells the following 7 dummy species are assigned:

i. BF_TOT total ratio of bank filtrate
ii. BF_YOUNG ratio of Lake Tegel in front of transect
iii. BF_REIS ratio of Lake Tegel around Reiswerder
iv. BF_OLD lake side fixed concentration boundary
v. LAND initial condition inland, fixed concentration boundary inland
vi. species with first order decay for the age assessment:
vii. AGE_YOUNG corresponding to BF_YOUNG
viii. AGE_REIS corresponding to BF_REIS

A bulk density of 1820 kg/m³ and a distribution coefficient k_d of $1.97*10^{-4}$ m³/kg is assigned to the aquifer matrix. A thermal conductivity of 10^{-6} m²/s is assigned to the entire aquifer.

The transport boundaries (fig. 19, fig. 20) are assigned such that all relevant flow paths are included.

Only inland groundwater and old bank filtrate enter the model across the outer transport boundaries. Young and medium bank filtrate are recharged within the transport boundaries. Intrusion of bank filtrate which passes the well field does not touch the boundary. A larger area

would not improve the physical meaning of the results, travel times in the model would be longer than the model interval and computational effort would be seriously increased.

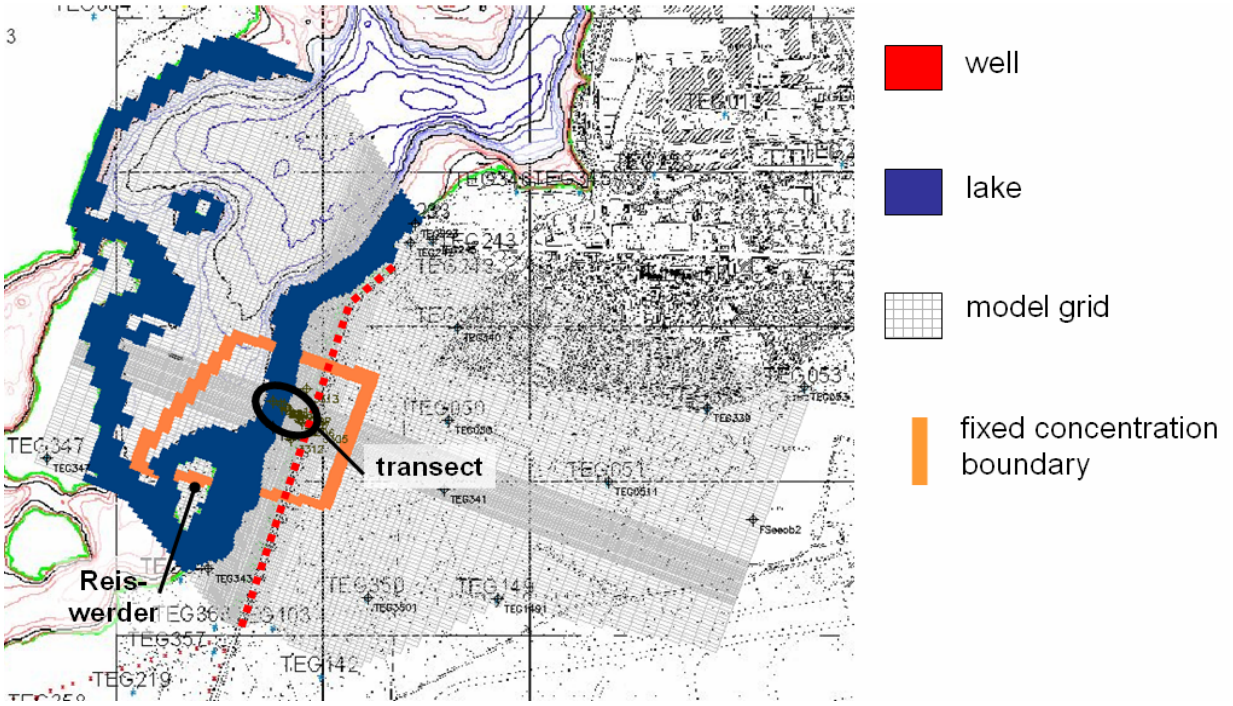

Figure 19: Model domain with transport boundaries for all species. The orange line represents a fixed concentration boundary. The transport is simulated inside the boundaries, while the outside cells are inactive. To the lake cells the concentrations of Lake Tegel are assigned. The fixed concentration boundary is not displayed where the lake boundary is present.

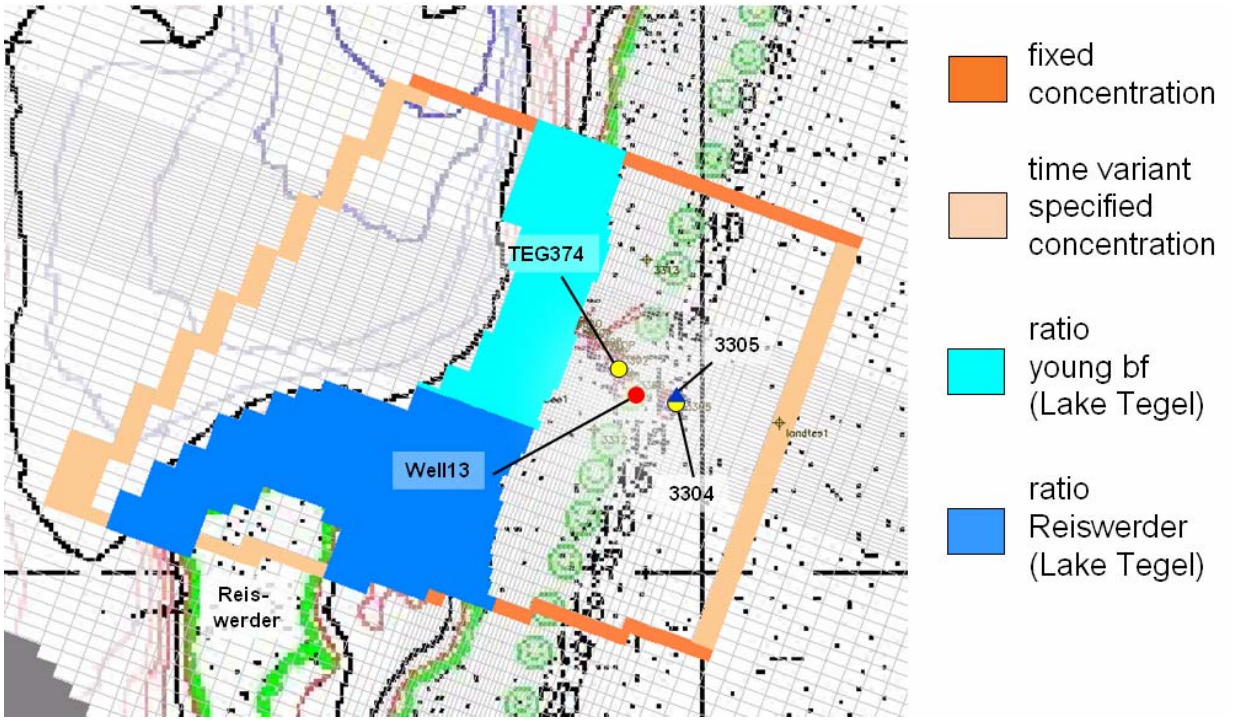

Figure 20: Transport boundaries for all species. Outside the boundaries no transport is simulated. The time variant specified concentration is in the foreground, the fixed concentration is behind, fixed concentration is only visible where none of the other boundaries are present, it forms a closed tetragon. Dark orange shows fixed (time invariant) concentration, light orange shows time variant specified concentrations, Lake Tegel is represented by blue colour, light blue shows dummy species indicating young bank filtrate, dark blue shows dummy species Reiswerder.

Concentrations of Lake Tegel are applied to the boundary using measurements carried out within NASRI (KWB 2005), Richter (2003) and SENSUT (2002-2005), the values are interpolated and assigned to the lake boundary. For ^{18}O measurements are available since spring 2001, whereas the monthly mean is assigned for the preceding period (fig. 22). Regarding the lake, due to the known concentrations and known place where to apply them, the situation is quite easy. For inland groundwater and old bank filtrate the situation is not as comfortable. Here, through the use of the observation wells 3304, 3305 and TEG374 (fig. 6), only point values exist. Concentrations on the outer boundary conditions are not known. They are assigned with a phase shift of the flow time, such that downstream, in the observation well itself, the simulated and observed concentrations coincide well. For preceding times, values are extrapolated within a reasonable scale (fig. 22, fig. 23). Mean ^{18}O concentration of groundwater recharge through precipitation between 1978 and 1990 is -9.3 $^{0}/_{00}$ vs. SMOW, between 1991 and 2001 -8.2 $^{0}/_{00}$ vs. SMOW (fig. 21). The unit [$^{0}/_{00}$ vs. SMOW] denotes the content of an isotope in relation to standard ocean water. Values are calculated from precipitation data measured in Berlin (IAEO, 2006) in the same manner groundwater recharge is calculated from precipitation. After August 2004 values are simply held constant.

Three different source concentrations are distinguished:

i. old bank filtrate (TEG374)
ii. inland groundwater of the first aquifer (3305)
iii. inland groundwater of the second aquifer (3304).

The concentration of the latter probably varies by depth, but since only observation well 3304 at the top of the second aquifer exists, the best estimation is to assume aquifer 2 as homogenous. The assigned values are shown in figure 22 and figure 23.

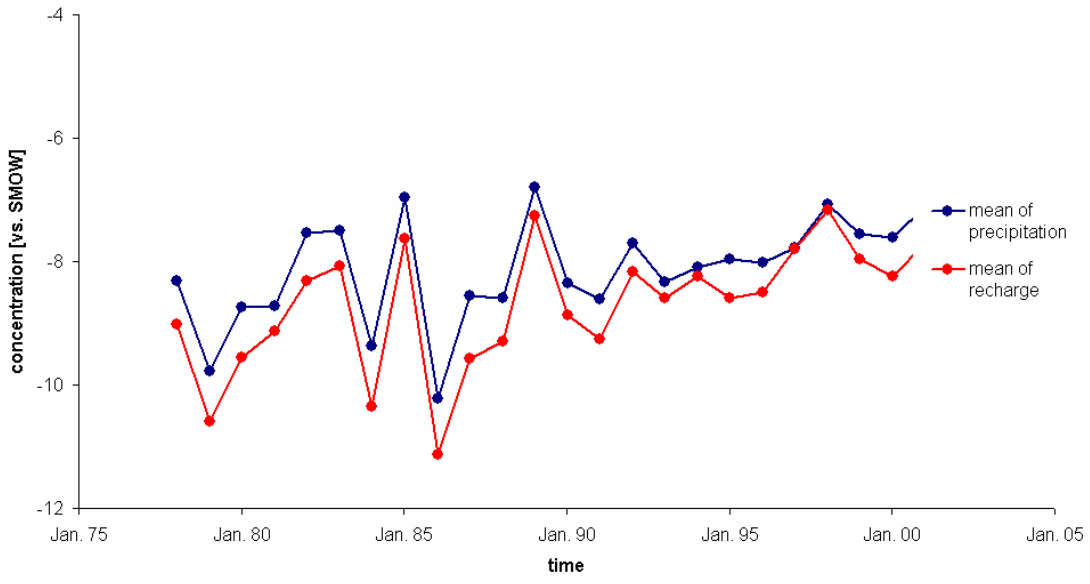

Figure 21: Mean annual concentrations of ^{18}O in precipitation in Berlin. The mean of the recharge is lower since most groundwater is recharged in winter. Fractionation due to transpiration and evaporation is not considered. Data kindly provided by IAEO (2006).

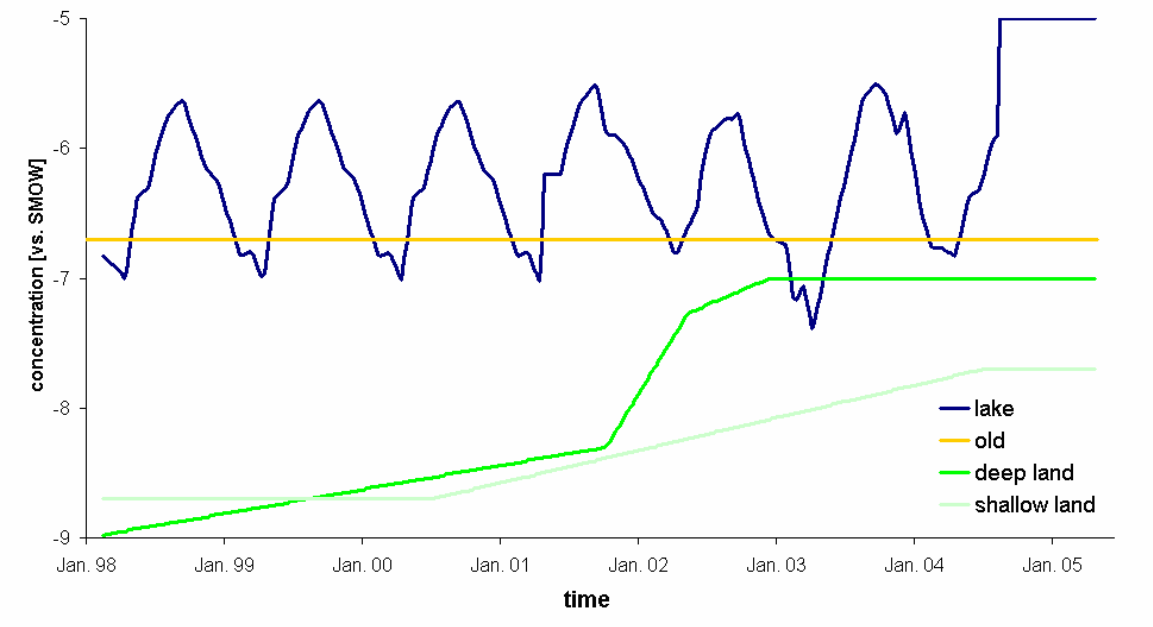

Figure 22: ^{18}O values of the concentration boundaries. The blue curve represents the lake concentration, the orange line represents old bank filtrate coming from lakeside, the dark green curve represents inland concentration of the first aquifer, the light green curve represents inland concentration of the second aquifer.

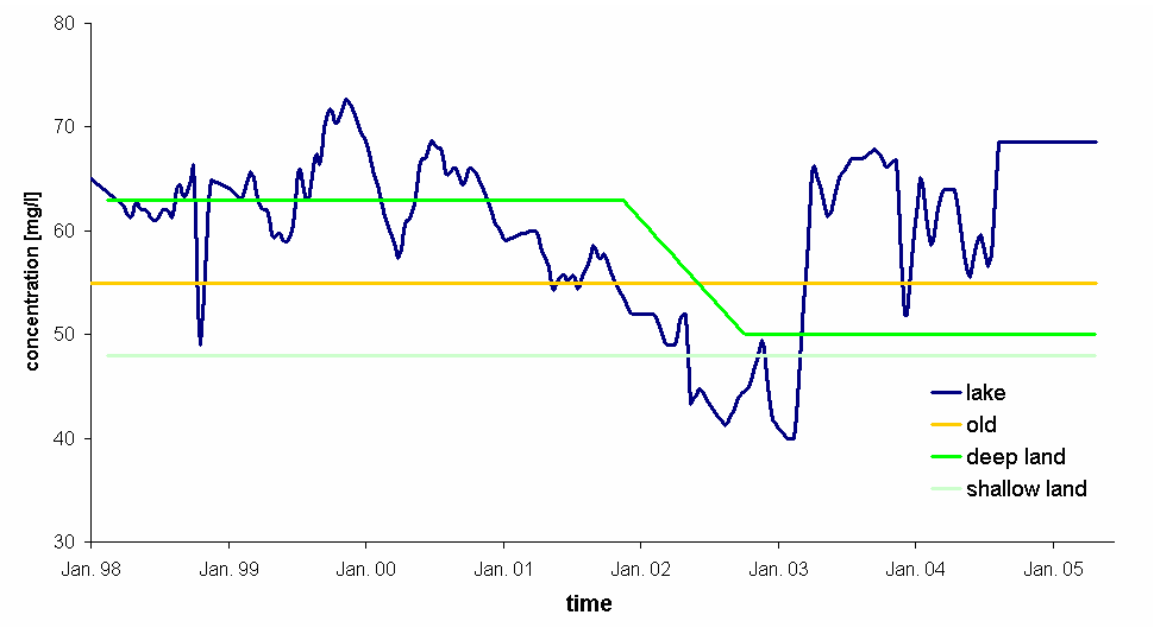

Figure 23: Chloride values of the concentration boundaries. The blue curve represents the lake concentration, the orange line represents old bank filtrate, the dark green curve represents inland concentration of the first aquifer, the light green curve represents inland concentration of the second aquifer.

The average groundwater temperature in Berlin is 10°C, affirmed by measurements in observation wells 3304 and 3305. TEG374 shows variant temperature since it is affected by young bank filtrate. The value of 10°C is assigned to all outer boundaries. The lake

temperature is assigned according to the water temperature measurements within NASRI (KWB 2005) and SENSUT (2005) (fig. 24).

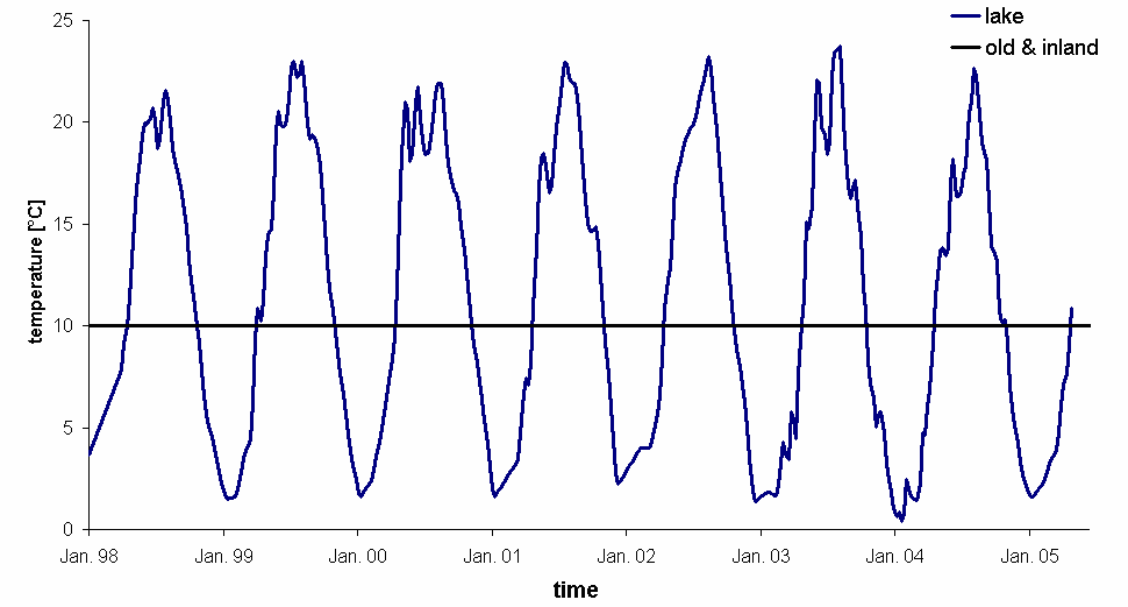

Figure 24: Temperature assigned to the boundary at Lake Tegel is represented by the blue curve, the black line represents boundary concentrations at the outer boundaries.

3.2. Data Pretreatment

All data previously mentioned and incorporated into this study were usually available in the required format or could be transformed to the required units by simple calculation. In general, the quality of the data is good, however, some special pretreatment was necessary and punctual errors have been detected.

3.2.1. Pumping Rates

The calculation of abstraction rates for single wells is an extremely important issue within this work. Some grade of deviations are acceptable if the temporal trend of the real values is matched, but errors will definitely lead to a poor model fit or in the more unpleasant case to wrong parameters. In order to obtain as much and as precise information as possible, the calculation of the well operation data has been the most extensive data pretreatment. BWB (2002-2005) provides many data of potential relevance for the computation of abstraction rates:

Performance test are carried out 3 to 4 times per year. The data comprise current pumping rate, average pumping rate since the last test, nominal pumping rate, operational hours since the last test, amounts of abstracted water since the last test, piezometric heads of the inner tube and of the piezometer in the well filter. In principle, several ways to calculate the daily well discharge exist. The following appears to be most reliable:

The wells either operate on full power or are switched off. The pumping rate is determined using a combination of the mean and the current pumping rate. Both values are plotted and normally the deviation between them is smaller than 5%, then the mean of the two values is taken. Sometimes higher deviations of either values occur. Outliers are identified by assuming the smoother temporal development as correct. The maximal daily abstraction is calculated by linear interpolation between these values, discontinuities because of changed pumps are respected. The maximal daily abstraction rate is multiplied with the daily operational hours, the real abstraction for each well is obtained with daily intervals.

An attempt was made to scale daily abstraction with the total amounts of abstracted water recorded with a water meter at the wellhead for each well. These recorded values accord only fairly with the calculated, some are missing, some are negative and the deviations are high. A scaling using these values would decrease the accuracy. Another scaling was attempted using the amounts for the entire Well Field West which are provided by BWB, calculated by using the operational data of the entire waterworks. Since the exact method of calculation is not known, this approach is not assumed to be more precise than the method described above.

No operational times are available for single wells for the period between January 1998 and June 1999, thus the amount for the entire Well Field West has to be used instead. It is split up to each well, the amount of the entire well field is distributed to the single wells by the ratio of their pump power. The method implies that shifts in abstraction within the well field are not represented, but since these shifts roughly level out on monthly scale, this procedure is appropriate for representing flow conditions for the entire well field at the beginning of the model period. Between 1999 and 2005 the amount for the entire Well Field West is about 11% lower than the amount calculated from the single wells (fig. 45). This is introduced as correction factor for the first period before June 1999.

3.2.2. Observation Well 3301

The hydraulic situation at the transect is represented by observation well 3301, mainly because the latter has the longest time-series of observations with few gaps. It is screened at about 11 m NN, two observation wells exist within a distance of 2 m, TEG371up in the same aquifer screened at about 17 m NN and TEG371op (fig. 6) in the aquifer above screened at about 22 m NN (tab. 1). The head difference to these wells can be used for a plausibility check.

Regarding the differences between 3301 and TEG371up (differences in fig. 25, locations in fig. 6) a mismatch is obvious. Normally the recorded heads are almost identical, but from August till September 2003 a difference of about 20 cm occurs, in August 2004 it grows up to

55 cm. Both piezometers are located within the same aquifer, implying that the previous should be regarded as an error of the reference height. The identification to which well the error belongs is not as obvious. Since hydraulic heads can change up to 1.5 m within a few hours, the time when the offset of 20 cm appears can not be detected in a single head curve.

Regarding the differences between TEG371op and TEG371up and between both to 3301 (yellow and red points) the existence of an offset can not be detected that easily. The piezometers are screened in different aquifers, a hydraulic gradient from above to below exists. This gradient increases up to 1.5 m when the wells are in operation (from September 2003 it is about 20 cm when the wells are switched off), the lower envelope of the TEG371op-TEG371up (yellow points) then is about 20 cm. On the first sight this seems plausible, since water infiltrates to the first aquifer and is extracted from the second. However, an estimation of the amounts of water flowing downwards reveals that the storage coefficient of the lower aquifer is too low to maintain such a current when wells are switched off. This is approved with the telescope model (chapter 4.7) which takes into account exact well operation.

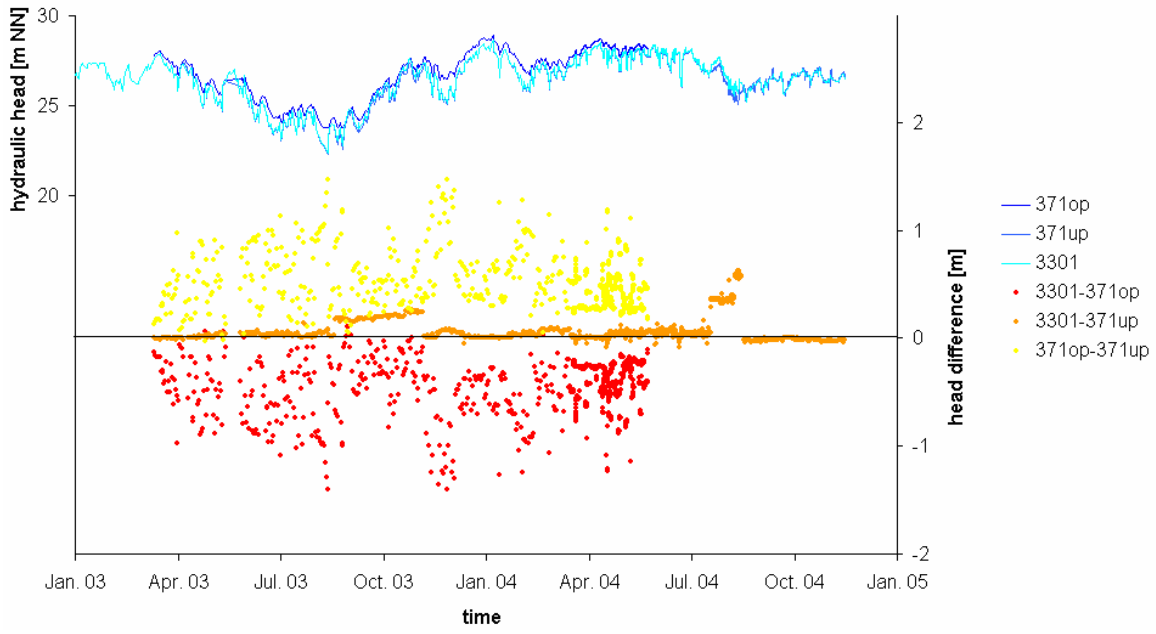

Figure 25: Hydraulic heads of observation wells TEG371op, TEG371up and 3301 which are located at the same position and are screened in different depth. The blue lines belong to the observed heads and the left axis, the red, orange and yellow lines belong to the differences and the right axis.

The errors of reference height occur when the data loggers are changed and recalibrated. By careful evaluation of the exchange dates and the differences of the envelopes a correction function for observation well 3301 is set up. However, outside the period where heads of more than one piezometer are available, errors of this magnitude remain undetected. Regarding the dynamic of several meters and with respect to the hydraulic situation seen on the scale of the entire model domain the deviations are considered as acceptable.

Sometimes a trend in the differences can be observed, e.g. 3301-371up starting from August 2003 in 3 consecutive months a drift of 10 cm occurs. The maximum absolute logger accuracy is within this range.

3.3. Flow Modelling: Parameterisation, Statistical Properties and Sensitivity Analysis

This subsection contains three different components, which can not be assessed separately: Namely a sensitivity analysis should not only be based on statistical properties but rather interpreted with respect to the physical parameter meaning, implying that the results can not be discussed separately. The parameterisation depends on the parameter sensitivities and model results, ranking the importance of the physical processes already included in the model or suggesting whether some are still missing. Finally, in order to judge physical correctness as well as analytical and predictive model capabilities, all three points of the title should be considered together.

3.3.1. Results

In general simulated and observed hydraulic heads coincide very well. The most important criterion for the goodness of a model fit usually is somehow subjective: the inspection and judgement of simulated time series with respect to the observations. At each piezometer the curves show the same trend, additionally the short term dynamic is generally met. For all observation wells which are included in inverse modelling, the statistical parameters of the residuals (fig. 28, fig. 29, R^2) and hydraulic head time series (fig. 26, fig. 27) show a very good match with a deviation from the mean of less than 7 cm, except for the standard deviation of observation well 3301. However, considering that heads change within the range of 7 m, which is much more than at the other observation wells, the deviation from the mean nevertheless is low. The most important statistical parameters for the discrepancy between observed and simulated hydraulic heads are: The deviation from the mean $\bar{\mu} \leq 7$ cm, the standard deviation $\bar{S} \leq 20$ cm, squared regression coefficients $0.91 \leq R^2 \leq 1$. The fit is not perfect but it is an unavoidable compromise between an acceptable fit and an overparameterised model. Thus, the statistical parameters point to some inaccuracies and model limitations.

Visual inspection of simulated and observed heads show the most important deviations at TEG233, TEG242, TEG243 which is also reflected in the statistical properties (fig. 28, fig. 29, fig. 30). These piezometers are located next to the northern boundary which is introduced as “no flow”, only strictly valid for a long time average (fig. 14). Differences occur due to

changing ratios between the Well Fields West and East in general, especially because of shifting abstraction within the well fields. Nevertheless the statistical parameters indicate an acceptable fit for observation wells TEG233, TEG242, TEG243. The difference of mean values is 10 cm $\leq \bar{\mu} \leq$ 35 cm, standard deviations $\bar{S} \approx 45$ cm and the squared regression coefficient $R^2 \approx 0.7$ appear to be acceptable respecting the conditions at the northern boundary. The inspection of the time series supports the correct description, since the level and the dynamics are normally met, the main differences occur within short periods like at the beginning of 2000 and in winter 2001/2002. Because of these differences, the observations of TEG233, TEG242, TEG243 are not included into the objective function of parameter estimation. Otherwise, a physically meaningless curve fit would have been obtained because the Well Field East is the reason for the deviations and not included into the model. The nearest piezometer included is TEG340. Considering the latter, the fit at TEG233, TEG242, TEG243 can be described even as good, and is an indication for the correctness of the boundary conditions.

At an early stage of parameter estimation, observation well TEG243 was included. Visual inspection of the hydraulic heads show TEG233 and TEG242 do not contain extra information than TEG243 and additionally TEG233 does not cover the entire model period and shows 4 outliers where heads are too low. However, it turned out that including TEG243 into the objective function seriously degrades the quality of the results and degrades the inversion stability, since not only Well Field West but also Well Field East, which is not included into the model, affects the heads. Additionally, it may be the case that the temporal characteristic of the leakance in the north is different compared to the transect, but the entire lake is simulated using only one temporal characteristic. Nevertheless, the temporal dynamic of observed heads is met quite well (fig. 26, fig. 27), surprisingly it improved even at TEG243 when the latter was taken out of the parameter estimation process, since the parameterisation of the inversion process is now in agreement with the physical processes, the problem is well posed (Hill 1998), and does not try to obtain a senseless fit for the influence of the Well Field East.

Statistical parameters of piezometer 3311 (location in fig. 6) have only fair values. The deviation from the mean is about 30 cm, the standard deviation 30 cm $\leq \bar{S} \leq$ 1.3 m, the coefficient of determination R^2 is 0.77. Several reasons exist for the poor fit. The piezometer 3311 is not included into parameter estimation, the nearest piezometer included is 3301. Since these two piezometers are screened in different aquifers and have a different distance from the well field, local aquifer properties induce different hydraulic behaviour. These local properties could be partly calibrated with the telescope model, but data from piezometer 3311 could not

be included into this calibration. The misfit is reason of the unresolved local differences. Another reason is that during the almost 3 year long period between July 1999 and June 2002 only 22 head measurements at observation well 3301 exist. Since observation well 3301 reacts confined and thus quickly and strongly to well operation, the model with weekly discretisation can not resolve the misfit between variability of the hydraulic heads on hourly scale. But in order to benefit from the fact that hydraulic heads of observation well 3311 are less affected by well operation than observation well 3301 and thus give a more general picture of the hydraulic situation, these values have been included in inverse modelling of the regional flow model. However, the damage exceeded the benefit. Temporal variant leakance showed oscillating behaviour and the stability of the inversion process decreased for the following reasons:

i. Local aquifer properties and the confined reaction of observation well 3301 to well operation induce differences to observation well 3311 which can not be calibrated within the regional flow model.
ii. Only manual measurements exist after July 1999 and it falls dry if piezometric heads are low, thus the time series is interrupted.
iii. Since the single measurements have a high weight, the parameter estimation routine tries to meet heads at the exact measurement time, not caring if heads before and after are reasonable, and as it does not have the right handle of local aquifer properties it just uses the temporal variant leakance or different parameters.

In order to prevent these effects, piezometer 3311 is taken out from the objective function.

Observation wells 3301, 3311, TEG233, TEG242, TEG243 show differences between statistical parameters of weighted and unweighted residuals since the heads of these piezometers are monitored in variable temporal steps. Usually the weighted parameters show a better fit, which just means the fit during dense measurements is worse than average. The weighted values are the better indicator for the goodness of fit.

The statistical parameters are calculated twice, for the entire model period and from June 1999 till the end, because until June 1999 only the total amount of the well field is known while the abstraction of each single well is unknown. The distribution of the abstraction had to be guessed which is done by weighting with the nominal pumping rate. Thus, unlike in reality, the abstraction of each well is assumed to be always proportional to the abstraction of the entire well field. At observation wells 3301, 3311, TEG233, TEG242 and TEG243 differences between weighted mean and weighted standard deviation exist, depending on whether the period until May 1999 is included or not (fig. 28, fig. 29). The mean stays rather constant which supports the assumption that the average abstraction of each well can be estimated by

the nominal output. This is additionally supported since the statistical parameters of the observation wells located farer from the well field are practical independent whether the beginning period is included or not. The standard deviation of the wells close to the well field however decreases, indicating that the abstraction shifts affect these wells.

It is somehow surprising that observation well TEG339 (fig. 28) shows the highest deviation of the mean with simulated heads being 7 cm below the observed although its standard deviation is one of the lowest with also 7 cm. This is especially remarkable as it is very near to the time variant specified head boundary in the east. Piezometer TEG053 used for specifying the level is very near. The model has been set up under the premise of hydraulic heads being parallel to the eastern boundary. This assumption is apparently not strictly valid, possible reasons are:

i. Large amounts of water infiltrate into the Airport Lake, resulting in a radial component of hydraulic heads around. TEG053 is affected more because it is located much nearer to the lake than TEG339.
ii. The area where bottom water intrudes has a larger extend to the north and east than introduced in the model.
iii. Between TEG053 and TEG339 the hydraulic conductivity is lower than average and taken from the HSM.

Item (i) is less probable than (ii) and (iii) because the infiltration of stormwater is highly time variant, with the relatively low standard deviation.

The standard deviation of TEG340 (fig. 29) is the second highest of the observation wells included in the objective function, the R^2 the second lowest. This is probably based on the neighbourhood of the northern no flow boundary condition only representing a watershed for steady state conditions. The reasons are the same as concerning TEG233, TEG242, TEG243. The fit of the mean is however very good, because the magnitude of the leakance in the north is calibrated with an extra parameter.

Initial values are matched well. A steady state model for the time between January and March is always run prior to the transient model, resulting in a good match of the first simulation values to the observations (fig. 26, fig. 27). The contribution to statistical differences, depending on whether the time until May 1999 is included or not, is not substantial.

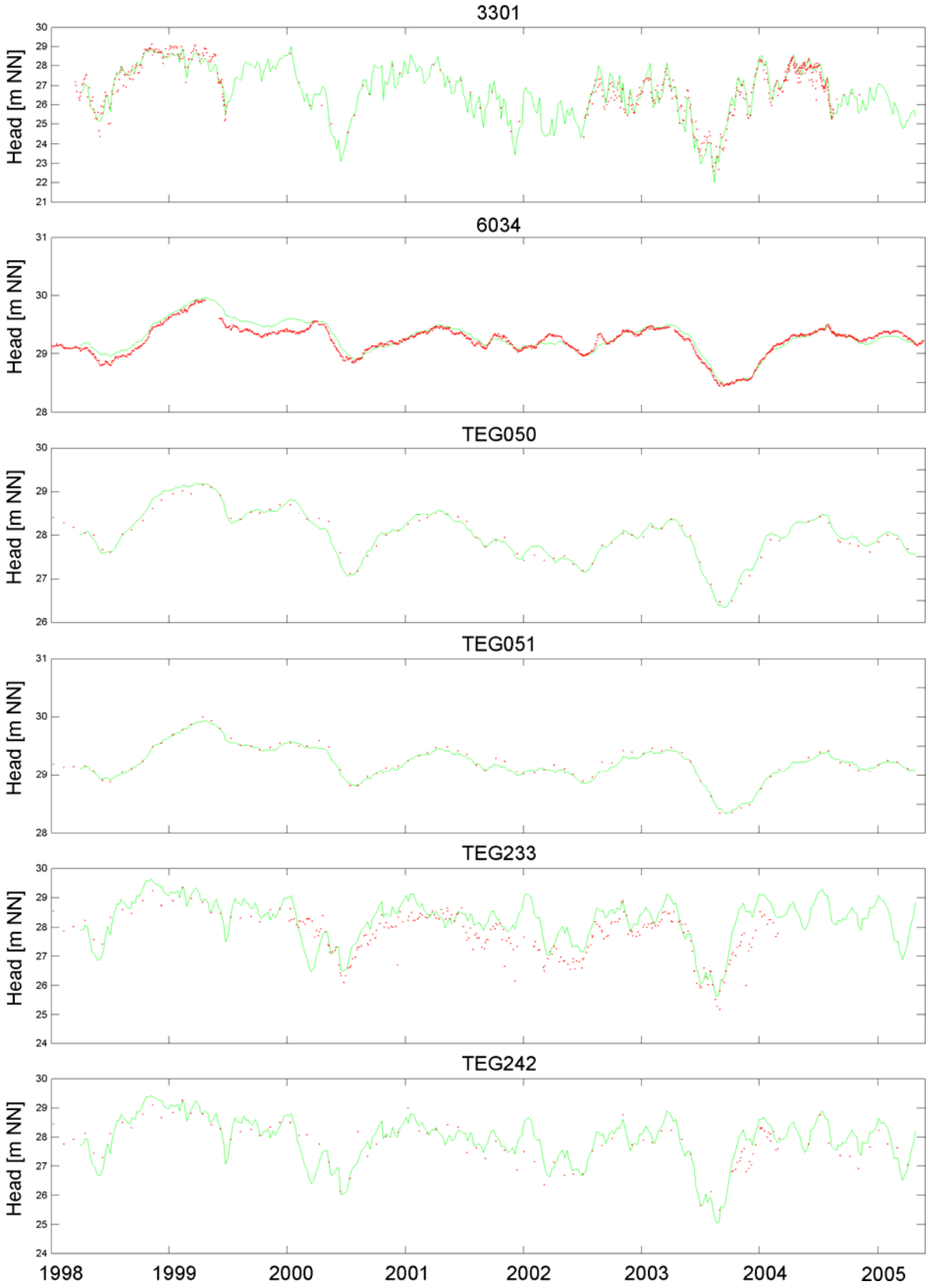

Figure 26: Observed and simulated piezometric heads for observation wells included in inverse modelling and additionally the observation wells near the northern boundary TEG233, TEG242. Each red dot indicates a head measurement, the green line represents the simulated values.

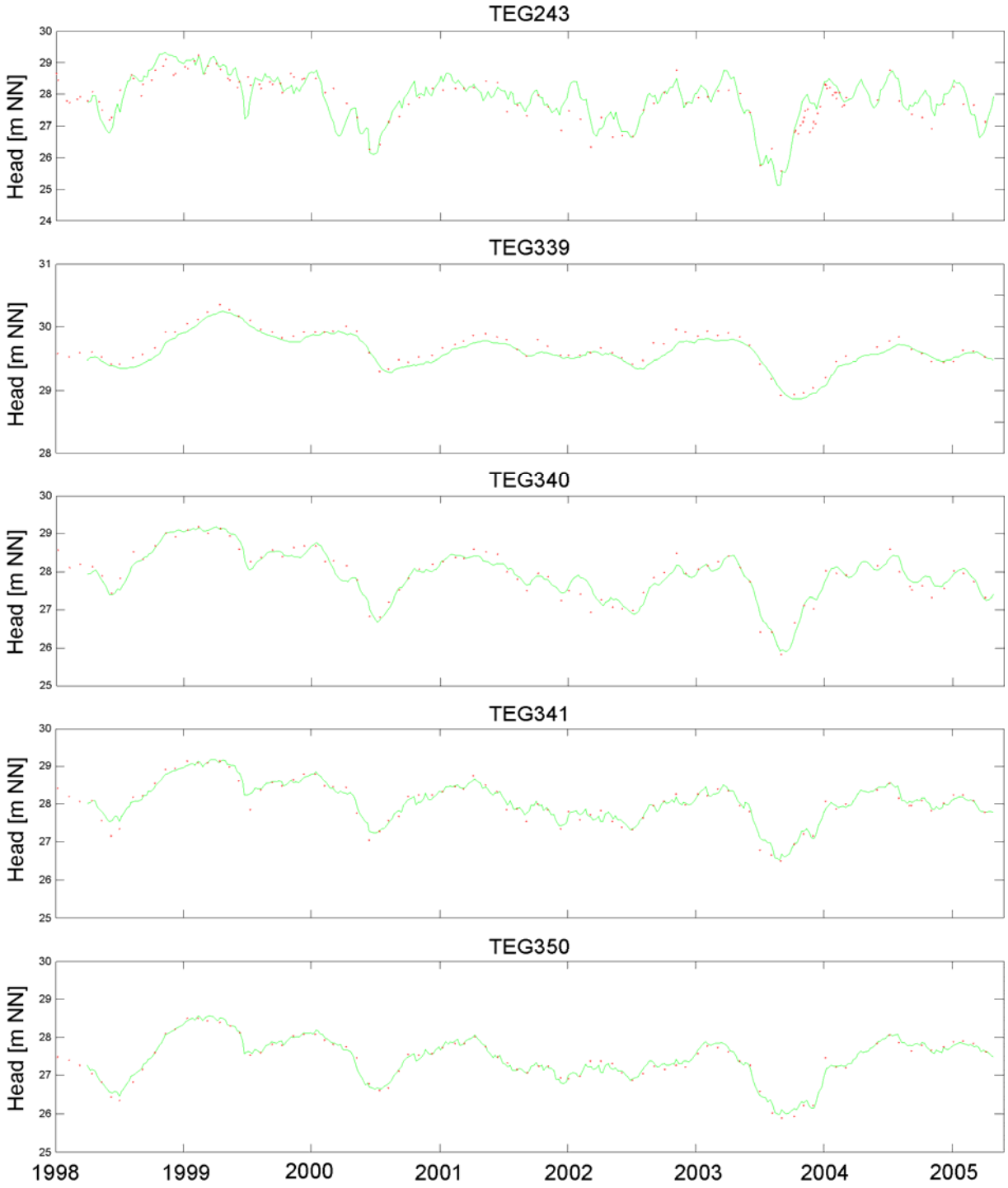

Figure 27: Observed and simulated piezometric heads for observation wells included in inverse modelling and additionally the observation wells near the northern boundary TEG243. Each red dot indicates a head measurement, the green line represents the simulated values.

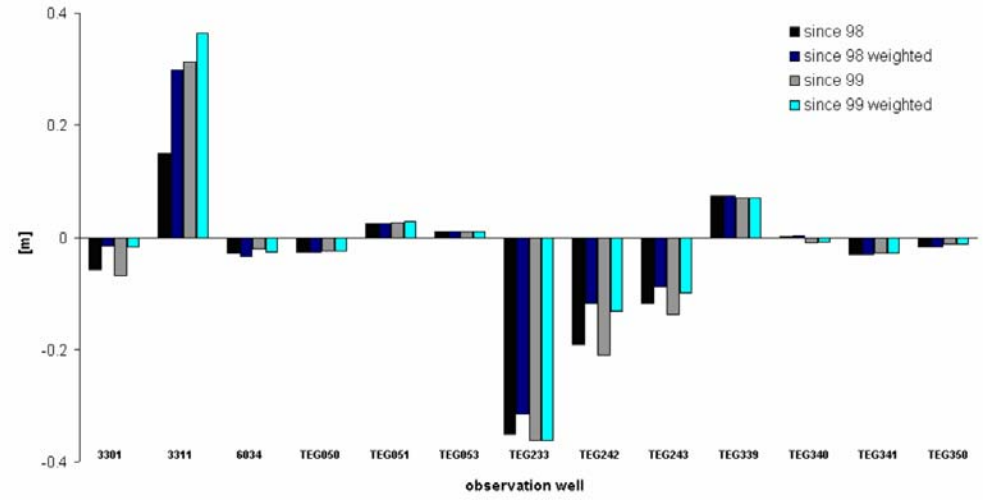

Figure 28: Mean of the residuals. The black bars are calculated from the unweighted values for the entire model period, the dark blue bars are calculated from residuals of the entire model. The contribution of each residual is weighted with the measurement interval. The grey and light blue curves are calculated in the same way, but the first year is excluded in order to minimise the influence of initial conditions.

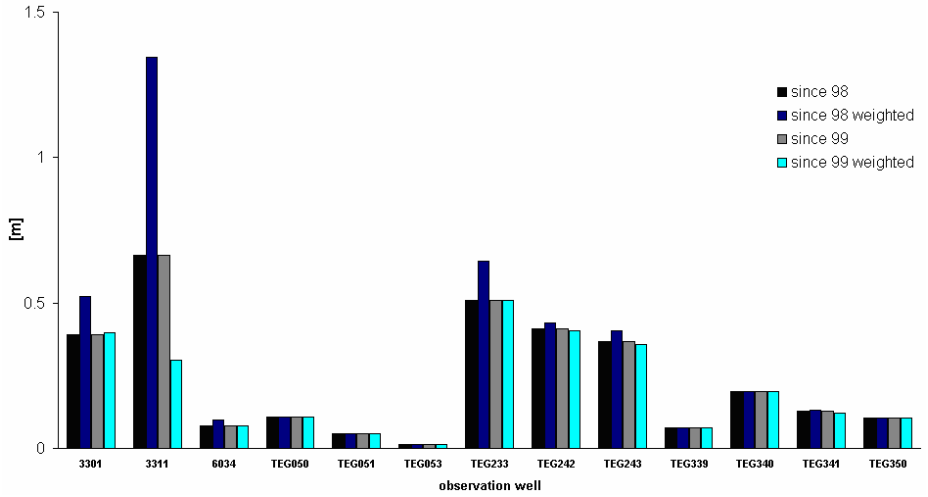

Figure 29: Standard deviation of the residuals. The black bars are calculated from the unweighted values for the entire model period, the dark blue bars are calculated from residuals of the entire model. The contribution of each residual is weighted with the measurement interval. The grey and light blue curves are calculated in the same way, but the first year is excluded in order to minimise the influence that the spatial and temporal distribution of pumping of Well Field West is not known.

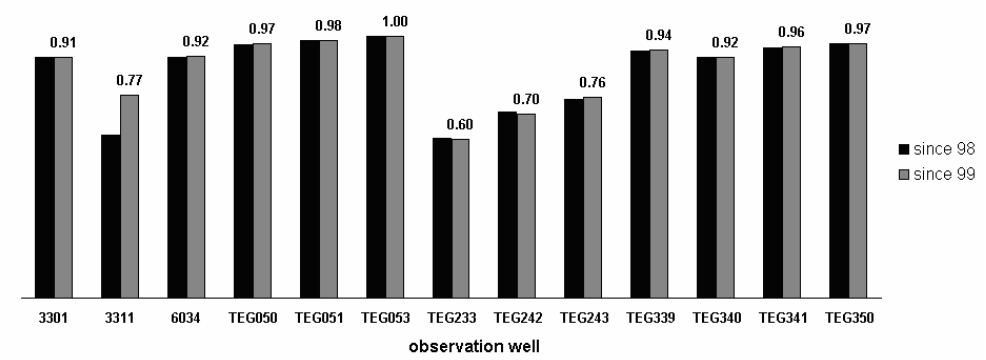

Figure 30: Unweighted regression coefficient of simulated versus observed piezometric heads. The black bar is calculated using the entire model period, for the grey curve the first year is excluded in order to minimise the influence of initial conditions.

Observation well 3301 is chosen to represent the hydraulic situation at the transect. It is the longest time series available and has always been included in the sampling campaigns at the transect, such that the other observations do not contain extra information relevant apart from local aquifer characteristics (chapter 2.5.2). It has been tried to include observation well 3311 since it does not react confined and is affected less by short term well operation. However, this concept has failed as described above. Consequently, all other observations of the transect are not included directly. However, they are used to detect inconsistencies in piezometric head data.

Scharfenberg

The horizontal well is introduced as time dependent constant head using hydraulic heads of TEG347. (fig. 5) This piezometer is highly affected whether the horizontal well is operating or not, within 1 day the heads may vary by 1.2 m, within 4 days by 2 m. In this context the variation of the residuals at observation well 6053 between zero and 1m is sufficient. However, the value heads are systematically overestimated by 42 cm (fig. 31).

The short term oscillations of the observed values occur due to weekly alternating operation of the horizontal well. The boundary is simulated with monthly averages and thus the heads show a smooth behaviour (fig. 31).

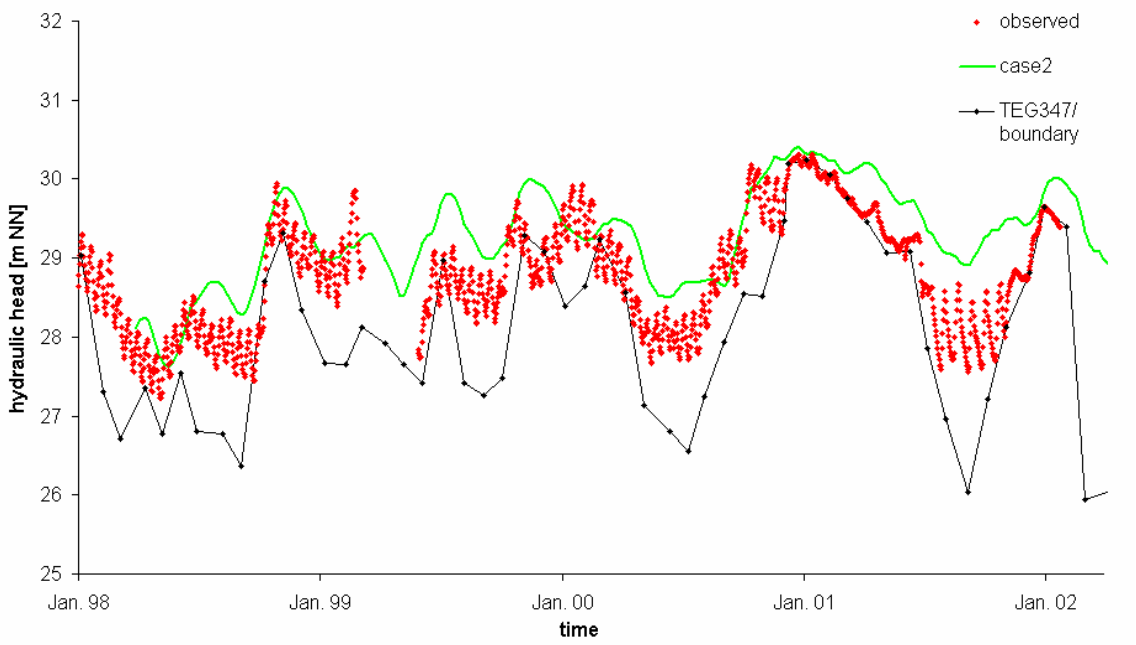

Figure 31 Observed (red dots) and simulated (green line) hydraulic heads of piezometer 6053, located on Scharfenberg. The black line shows observed piezometric heads of TEG347, located in direct vicinity of the horizontal well. Between 1st Apr. 1998 and 28th Jan. 2002 the arithmetic mean of 6053 is $\overline{\mu} = 28.81$ for observed and $\overline{\mu} = 29.23$ for simulated heads.

3.3.2. Parameterisation

The parameterisation is a mirror of the entire model. It depends on the processes and their sensitivities. In the current study, with increased knowledge about the system the parameterisation was changed fundamentally. Parameters had to be introduced, others became insensitive and obsolete, the model domain had to be enlarged. This process of refusing the former model version in favour of another hypothesis is the essential scientific process (Popper 1959, Bates and Anderson 2001). Consequently the final configuration of sensitive parameters represents the important processes and is thus a central result of the model.

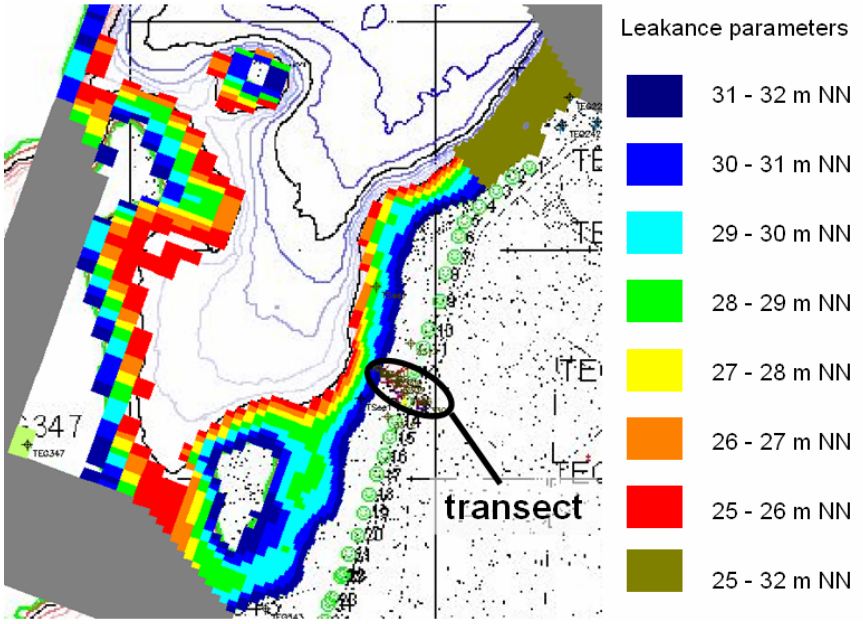

Figure 32: Spatial distribution of the depth dependent leakance. Each colour represents one parameter. North of well 3 the leakance is independent of the depth, represented by only one parameter.

Spatially, the leakance of the Lake Tegel is defined by 8 parameters (fig. 32). The depth distribution is resolved with 7 parameters, each valid for 1 m range of lake bed elevation. In order to account for local heterogeneities of infiltration characteristics an extra parameter is introduced to the small region in front of the Well Field West, north of well No. 3, which is the third well from the top in figure 32. For reason of simplicity the leakance there has the same value in all depths, which is justifiable since the parameter correlation of the depth distribution is very high.

Due to high parameter correlation between the parameters of depth dependent leakance, a smoothing function is introduced as prior information. It is constraining the results only weakly, since it contributes less than 1% to the minimised objective function.

The magnitude of these 8 parameters has been found to be temporally variant. The temporal behaviour is approximated by a continuous function of linear trends with 2 month intervals. The values at the limits of these intervals, in total 45, are calibrated.

The specific yield is assumed to be similar in the entire model, it is approximated by one parameter and distributed homogeneously.

The intrusion of bottom water is introduced as third type boundary condition. The hydraulic head of the underlying aquifer is known, the transfer rate is approximated as one parameter.

3.3.3. Sensitivity Analysis

The parameterisation described above only comprises the sensitive parameters which are included in the inversion process of the final model version. On the way to this parameterisation other parameters could be excluded from the inversion process in order to save computational time and to increase the stability of the inversion. In order to give a comprehensive picture of the physical interactions, though not determined with inverse modelling, the hydraulic conductivity of aquifer 1 and 2, recharge by precipitation and the leakage of the glacial till are also included into the inverse modelling based sensitivity analysis.

Storage Coefficient

The confined part of the storage coefficient has shown to be an insensitive parameter. With total aquifer thickness of 40-60 m an assumed upper bound of the confined specific storage coefficient of 10^{-3} m^{-1}, the total confined storage would have a maximum of $6*10^{-2}$ [-] which is three times less than about 0.2 [-] for the unconfined storage coefficient.

Reservoir Thickness

The thickness of the saturated layer below the lake bottom, also called bed thickness, affects the amounts of infiltration since

i. it is a multiplier of the hydraulic conductivity,
ii. it changes the hydraulic gradient (eq. 3).

Simulations revealed that the physical influence of the thickness is small, even considering conservatively an upper bound of 1 m. It is almost ideally cross correlated to the depth dependent leakance and time variant leakance. Values were quite insensitive and show oscillations during parameter estimation. Measurements of Hoffmann and Gunkel (2006) indicate a saturated thickness of 22 cm, which is the depth introduced into the model. It is not included into the numerical sensitivity analysis since its sensitivity is almost entirely based on cross correlation to the spatial and temporal leakance factors.

Statistical Parameters

The statistical parameters from table 2, table 3 and table 4 can be only interpreted in a physical way, considering that the achieved model fit is very close. Even when the objective

function is doubled, the fits quality would be optically still good, additionally figures 35 and 36 illustrate that a different parameterisation only leads to optically slightly different results.

Regarding the table 3, the threshold for correlations to be significant is set to R = 0.5, though this corresponds to a R^2 of only 0.25. The correlation coefficients are calculated with respect to the similarity of the models output and not with respect of similarity to the observations. This means, a different parameter set may result in an identical objective function but the regression between the two fits may be considerably lower than 1. With the knowledge of different parameterisations resulting in a similar goodness of the model fit, i.e. objective function or optical fit, also lower R values (around 0.5) might indicate cross correlation, since particular parameters, like ghb1 (bottom water) mainly affect observation wells close to the Airport Lake.

The following parameters are discussed with regard to their physical meaning and statistical properties. The values and the sensitivity is listed in table 2, the parameter correlation matrix is shown table 3, the Eigenvectors and the contribution of the parameters is shown in table 4.

Recharge (parameter name: rca1, tab 2)

Within the model domain, recharge by precipitation contributes only 4% to the water budget. The values are available by Umweltatlas Berlin (2003). Other factors determine the models behaviour, like temporal and spatially variant leakance or intrusion of bottom water, the magnitude of the latter however is known with less precision. To avoid physically meaningless parameter fitting (Brusseau 1998, Oreskes and Belitz 2001), though sensitive, recharge is not included into parameter estimation (tab. 2), in order to determine the factor of influence which is known with less precision (Oreskes and Belitz 2001). Including recharge would be a possible danger since a cross correlation (R= -0.54, fig. 3) to intrusion of bottom water (ghb_1) exists and can be explained physically. The hydraulic conductivity of the glacial till between the two aquifers is not high enough to allow high differences in hydraulic head. Thus it is of minor importance if the water comes from above (recharge) or below (bottom water). The correlation is weak, because recharge occurs within the entire model, bottom water only intrudes across a smaller area in the east.

Glacial Till Inland (parameter name: leak_1)

The calibration and sensitivity analysis of the inland glacial till which divides the first from the second aquifer can be only performed manually. An automatic calibration is not possible since a variation does not lead to a better fit expressed with least squares, but can be seen at the structure of the time series. The glacial tills conductivity (fig. 33) mainly affects short term

fluctuation in the scale of days or weeks (fig. 34), but the sum of the squared residuals is determined by the misfit in 1999, the small oscillations are negligible. Because the heads are observed daily and the model has weekly discretisation, the structure of the finest oscillations can not be reproduced. The coarser oscillations sometimes match low till conductivities, e.g. the nose in autumn 2003, sometimes high till conductivities like at the minimum in autumn 2003 (fig. 34). This is probably caused by the real spatially heterogeneous till distribution which is however modelled almost homogeneously. Taking a reasonable mean value, the till has a conductivity between 10^{-7} m/s and $2*10^{-7}$ m/s. Though the 10^{-7} m/s shows the better curve fit, the value is finally set to $2*10^{-7}$ m/s because observation well 6034 is close to the eastern 1st type boundary condition which is mitigating the models reaction.

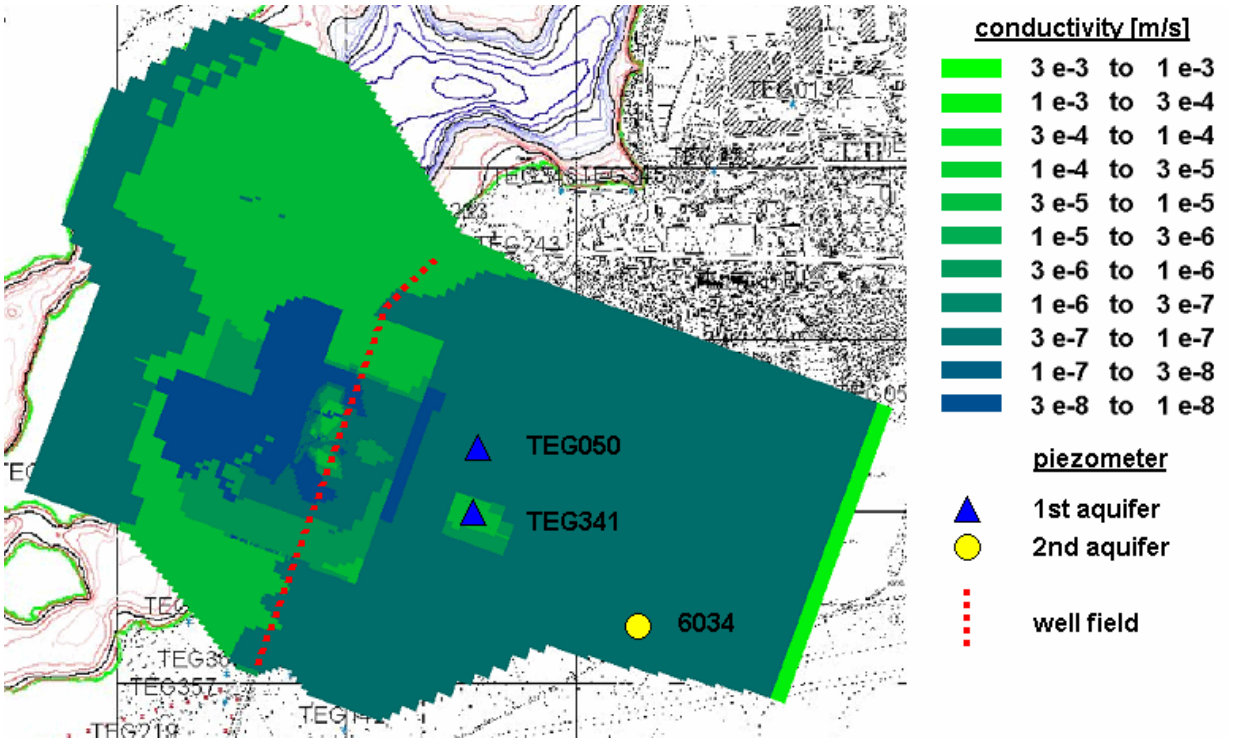

Figure 33: Distribution of the glacial till, based on bore logs and modelling results. The distribution near the transect is determined in a telescope model, the high conductivity at the eastern boundary is a trick to provide identical hydraulic heads in both aquifers at the eastern boundary condition. The thickness is 4m.

Just at one location, at TEG341 (fig. 5) the piezometric heads strongly indicate the existence of a hole in the till. Regarding figure 35 it can be observed that the hydraulic conductivity of $2*10^{-7}$ m/s is too low, though it is appropriate for the other observation wells like e.g. for the near located TEG050 (fig. 36), which almost has the same distance to the well field. Setting the k_f to 10^{-6} m/s (green curve) produces similar results like introducing a hole (blue curve) around TEG341. The structure with the hole produces even the better results with respect to drawdown and phase shift, since the pressure difference between the aquifers is

higher which locally can lead to higher variations. In reality this effect is even much more pronounced, regarding the low observed heads in summer 1998, 1999 and 2000.

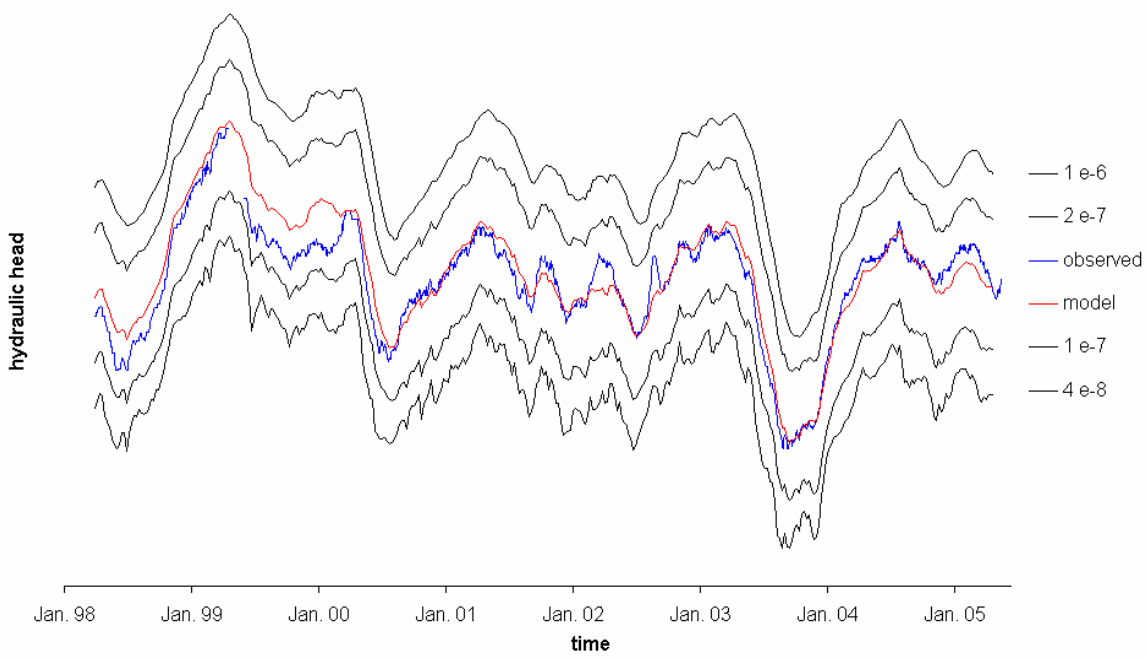

Figure 34: Observed and simulated hydraulic heads at observation well 6034 (2nd aquifer) in dependence of the glacial tills conductivity. The blue line shows observed hydraulic heads, the read line the hydraulic heads modelled with the final till configuration. The black lines show hydraulic heads for different conductivity of the glacial till. The important information are the short term structures. The absolute values are within a few cm differences, thus the curves are shifted on the ordinate by 20 cm each to enable a comparison of the short term structures.

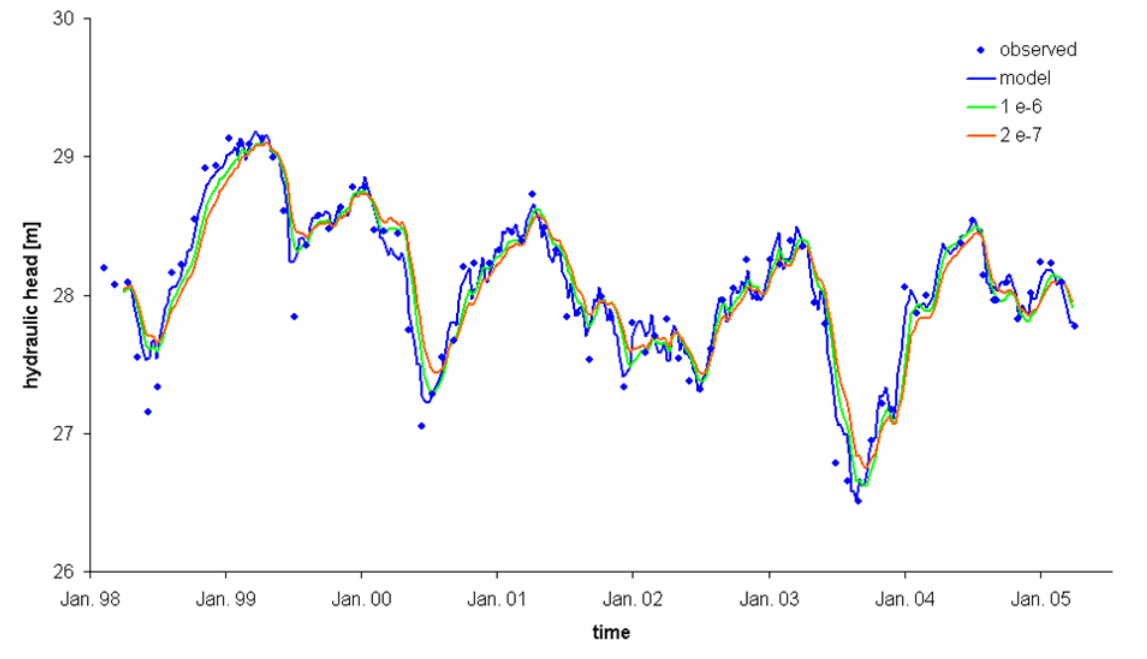

Figure 35: Observed and simulated hydraulic heads at observation well TEG341 (first aquifer), in dependence of the glacial tills conductivity. The blue dots show observed hydraulic heads, the blue line shows modelled hydraulic heads with the final glacial till configuration. The green and orange line show hydraulic heads for the tills k_f of 10^{-6} m/s and $2*10^{-7}$ m/s without the hole at TEG341.

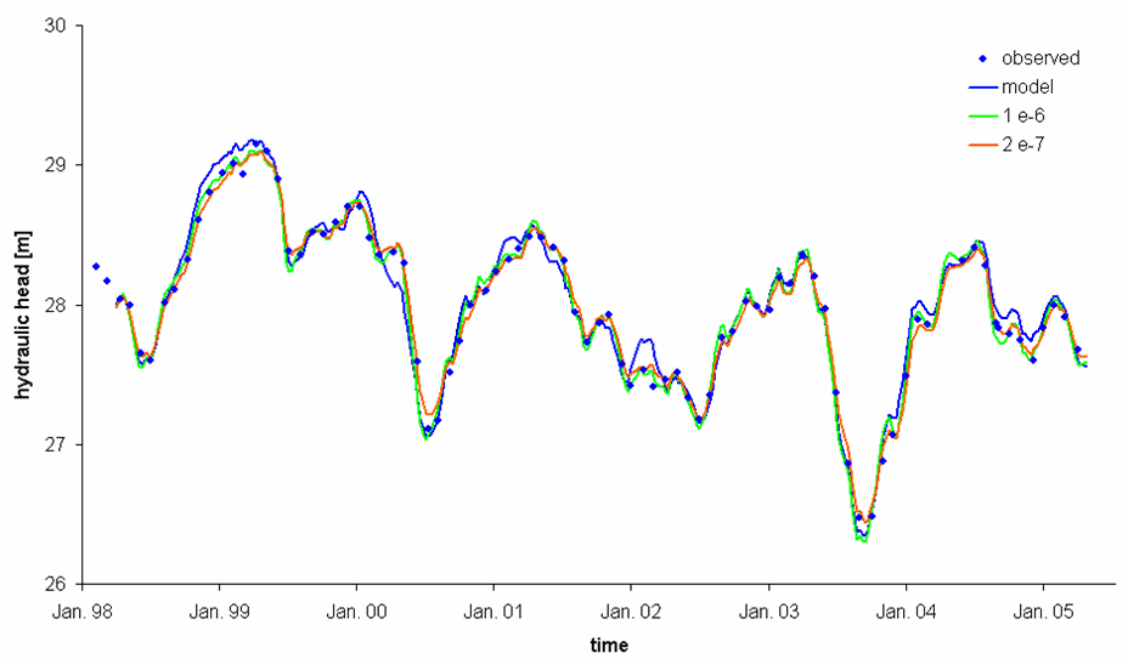

Figure 36: Observed and simulated hydraulic heads at observation well TEG050 (first aquifer), in dependence of the glacial tills conductivity. The blue dots show observed hydraulic heads, the blue line shows modelled hydraulic heads with the final glacial till configuration. The green and orange line show hydraulic heads for the tills k_f of 10^{-6} m/s and $2*10^{-7}$ m/s without the hole at TEG341.

Observation wells above and below the till react reversed on the change of the leakage. The wells are screened below. Thus a high conductivity leads to high drawdown and fast reactions above, and low drawdown and slow reactions below and vice versa. Since no individual heads for the first and second aquifer are available at the same location and specific yield affects the hydraulic heads in a similar way, the solution is not unique. This is reflected by a correlation coefficient of R = 0.56 to the specific yield (sy_1). The correlation of the conductivity of aquifer 1 (hk_aq1) is negative because when increasing the conductivity of aquifer 1 the propagation velocity of a drawdown incident increases. However, the cross sensitivities and lack of correct description of the spatial distribution is of minor importance, since its sensitivity is low (tab. 2).

Specific Yield (parameter name: sy_1)

The specific yield is calibrated to 0.22, depending on different parameterisations and weighting, values lie between 0.18 and 0.22. This coincides well with values of 0.2 (Greskowiak 2005) obtained in the same geological formation at the GWA Tegel (Artificial Groundwater Recharge / GrundWasserAnreicherung). The relative sensitivity of the parameter is relatively high (tab. 2) but considering the narrow range of physically meaningful calibration the differences of the curve fit within this range is small. Some cross sensitivity to the conductivity of the glacial till exists, both parameters affect the phase shift of drawdown

events, like in summer 2000 or summer 2003. The nonuniqueness is reflected in the weak correlation of 0.57 in the correlation coefficient matrix (tab. 3).

The velocity of wave propagation and the magnitude of drawdown events is mainly affected by the specific yield, the propagation is visible very well at the extreme drawdown 2003, (fig. 37).

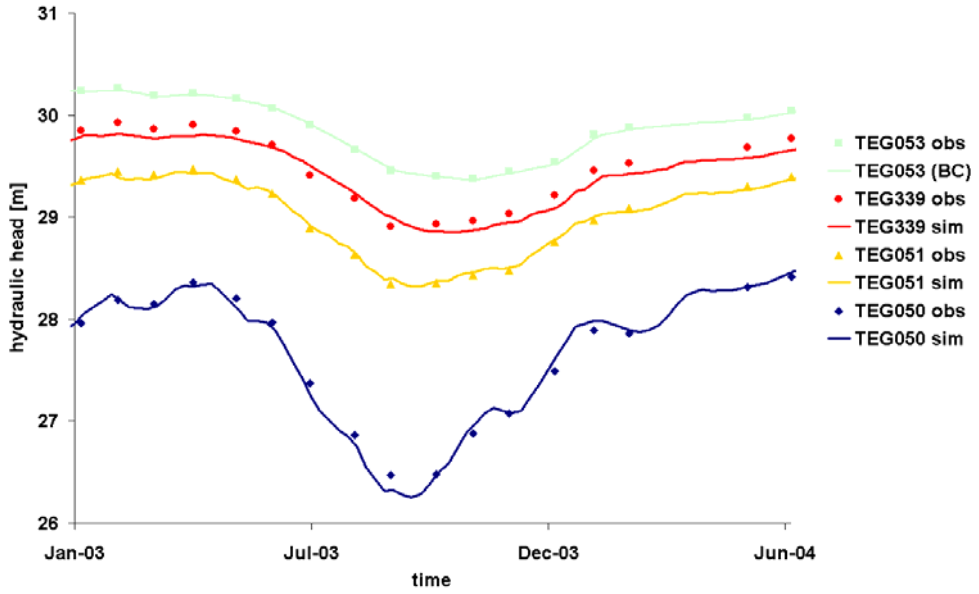

Figure 37: Observed and simulated hydraulic heads at the observation wells TEG050, TEG051, TEG339. Heads at TEG053 show a perfect match as it is the boundary condition. A phase shift of 50 days exists between TEG050 and TEG053.

Aquifer Hydraulic Conductivity (parameter names: hk_aq1, hk_aq2)

Though they are sensitive, calibrated hydraulic conductivities are not introduced into the model. Instead values calculated from bore profiles are taken. Though the hydraulic conductivity of aquifer 2 is even the most sensitive single parameter (tab. 2), however, the model does not allow a precise determination of the hydraulic conductivity. Namely, the leakance and the glacial till around the well field have such a high influence and unknown distribution that the hydraulic conductivity can not be calibrated. The flow from inland to the well field is itself matter of calibration, thinking about the continuous discussion about bank filtrate ratios. Following the Darcy's law for a given gradient, flow and conductivity are ideally cross correlated. Furthermore bottom water intrudes between Well Field West and eastern boundary and thus affects the hydraulic heads, which is reflected by the cross correlation of $R = 0.57$. Fortunately, bore logs of several boreholes (BWB 2005) give a good impression of the hydraulic conductivity. The results are aggregated in the geological profiles by Voigt et al. (2000), and provide values of $3*10^{-4}$ m/s to $5.5*10^{-4}$ m/s. Sieve analysis by Fritz (2003) results in a mean hydraulic conductivity of $3.6*10^{-4}$ m/s. Sand is the principal component of the aquifers. Cross sensitivities of horizontal hydraulic conductivity of aquifer 1 (hk_aq1) to the

specific yield (sy_1) and leakage of the glacial till (leak_1) exist, and horizontal hydraulic conductivity of aquifer 2 (hk_aq2) is cross sensitive to the intrusion of bottom water (ghb_1). Thus the results for calibrated hydraulic conductivity of $6*10^{-4}$ m/s can not be called definitely wrong but are unrealistic from the viewpoint of the measurements, however measurements are still realistic from the viewpoint of the calibrated values, since the values are not too far away and the cross correlations have to be taken into account.

Leakance (parameter names: res_1 to res_7, res_21, r_1 to r_45)

In order to describe its temporal and spatial characteristics, the leakance is parameterised in two groups. The temporal behaviour is described by 44 sections of continuous linear trends, implying that 45 start and end points which define the sections are calibrated. The first and last point are the least sensitive (tab. 2) and dominate the three largest Eigenvectors due to the fact that only very few observed values lie within the corresponding sections. To these vectors the maximum model insensitivity, defined by the three largest Eigenvalues (tab. 4) belong. The results, however, are only slightly affected, the observed heads begin 1 day before the first section ends, the results of the last section neither affect the rest of the model, nor they are of special importance in interpretation. In parameter estimation the insensitivity is partially compensated by prior information imposing a smoothing constraint.

Parameters r_2 to r_45 are almost ideally positively cross correlated with correlations higher than 0.94, normally higher than 0.99 (tab. 3). This is not physically based, but it just reflects that the leakance is calculated from the product of the spatial and the temporal component. Under the premise that all temporal parameters are increased by a certain factor and the spatial values are divided by the same value, model results are identical. This behaviour can be seen through the negative ideal cross correlation to parameter res_21 (tab. 3), which represents the depth independent leakance between 25 and 32 m NN north of the Lake Tegel. The depth dependent leakance for the rest of the model (res_1 to res_7) shows different behaviour. Between 31 m NN and 32 m NN (res_1) the leakance is insensitive, since the maximum hydraulic head difference is 0.55 m in winter and 0.3 m in summer and thus infiltration is small due to a small head difference and a small area. The depth dependent leakance is constrained by a smoothing function. Without this function the leakance varies irregularly by depth with differences of factor 6. Though this constraint only contributes less than 1% to the final objective function, values vary less than factor 2 and show a smooth depth distribution, though parameters only show low cross correlations with a maximum R of 0.7 (tab. 3). But regarding the Eigenvectors 2, 3 and 5 to 10 (tab. 4) which contain several significant non-zero components pertaining to spatial leakance parameters, the high parameter

correlation becomes obvious. The cross correlation is not ideal, since depending on time and space the boundary conditions of Lake Tegel changes between 2nd and 3rd type, resulting in different infiltration characteristics.

Bottom Water (parameter name: ghb_1)

The intrusion of bottom water has been detected within this model. Hydraulic heads of observation wells TEG050, TEG051, TEG339, TEG340, TEG341 between the eastern boundary condition and the well field would have been too low with a no flow boundary at the bottom. The hydraulic gradient is varies, relatively low near the eastern boundary and increases toward the well field. Several hydraulic characteristics contribute to this behaviour:

i. the unconfined water table,
ii. groundwater recharge and
iii. hydraulic conductivity is high in the east and low near the well field.

Though groundwater recharge is already included and though the hydraulic conductivity is almost twice as high in the east compared to the west, these reasons only partly explain the variable gradient. The similarity of their impact like bottom water (ghb_1) is reflected by positive cross correlation of R= 0.54 to recharge (rca1) and negative cross correlation to the hydraulic conductivity (R= -0.57). Furthermore the hydraulic heads of the third aquifer are clearly correlated to the heads of the second aquifer (fig. 15).

Tab. 2: Parameters included in the sensitivity analysis, the asterisk denotes, the estimated parameter is a parent parameter, to which tied parameters are linked with a constant ratio, preserving a given spatial or temporal distribution. Hydraulic conductivity of aquifer 2 ranges from $3*10^{-7}$ m/s to $5.5*10^{-7}$ m/s. The recharge is calculated weekly, the value in the table is the mean. The parameters res_1 to res_7 and r_1 to r_45 are plotted as Case2 in figures 43 and 44.

Parameter	Description		value	unit	relative sensitivity
hk_aq1	kf aquifer 1		3.5 e-4	m/s	1.14
hk_aq2 *	kf aquifer 2		4.2 e-4	m/s	6.89
leak_1	leakage glacial till		2.0 e-7	1/s	0.65
rca1 *	recharge by precipitation		4.6 e-9	m/s	1.19
ghb_1	conductance bottom water		2.4 e-8	1/s	1.94
sy_1	specific yield		2.2 e-1	-	3.00
res_1	leakance Lake Tegel	32 - 31 m NN	3.2 e-7	1/s	0.06
res_2	leakance Lake Tegel	31 - 30 m NN	3.3 e-7	1/s	0.68
res_3	leakance Lake Tegel	30 - 29 m NN	3.5 e-7	1/s	1.85
res_4	leakance Lake Tegel	29 - 28 m NN	3.1 e-7	1/s	1.81
res_5	leakance Lake Tegel	28 - 27 m NN	2.5 e-7	1/s	0.86
res_6	leakance Lake Tegel	27 - 26 m NN	2.3 e-7	1/s	0.87
res_7	leakance Lake Tegel	26 - 25 m NN	2.1 e-7	1/s	0.82
res_21	leakance Lake Tegel north	32 - 25 m NN	2.9 e-7	1/s	4.24
r_1	temporal variant leakance	01.01.1998	0.04	-	0.02
r_2	temporal variant leakance	01.03.1998	0.58	-	1.05
r_3	temporal variant leakance	01.05.1998	0.22	-	0.30
r_4	temporal variant leakance	01.07.1998	0.86	-	0.90
r_5	temporal variant leakance	01.09.1998	0.57	-	0.50
r_6	temporal variant leakance	01.11.1998	0.89	-	0.64
r_7	temporal variant leakance	01.01.1999	0.33	-	0.32
r_8	temporal variant leakance	01.03.1999	0.59	-	0.59
r_9	temporal variant leakance	01.05.1999	0.14	-	0.16
r_10	temporal variant leakance	01.07.1999	1.31	-	0.97
r_11	temporal variant leakance	01.09.1999	0.77	-	0.49
r_12	temporal variant leakance	01.11.1999	0.68	-	0.53
r_13	temporal variant leakance	01.01.2000	0.91	-	1.18
r_14	temporal variant leakance	01.03.2000	0.07	-	0.16
r_15	temporal variant leakance	01.05.2000	0.92	-	1.59
r_16	temporal variant leakance	01.07.2000	1.14	-	2.14
r_17	temporal variant leakance	01.09.2000	0.87	-	1.13
r_18	temporal variant leakance	01.11.2000	1.06	-	1.12
r_19	temporal variant leakance	01.01.2001	1.37	-	0.93
r_20	temporal variant leakance	01.03.2001	0.72	-	0.89
r_21	temporal variant leakance	01.05.2001	0.67	-	0.96
r_22	temporal variant leakance	01.07.2001	1.01	-	1.39
r_23	temporal variant leakance	01.09.2001	1.12	-	1.51
r_24	temporal variant leakance	01.11.2001	0.90	-	1.34
r_25	temporal variant leakance	01.01.2002	1.89	-	1.53
r_26	temporal variant leakance	01.03.2002	0.81	-	0.69
r_27	temporal variant leakance	01.05.2002	1.30	-	1.12
r_28	temporal variant leakance	01.07.2002	1.15	-	1.21
r_29	temporal variant leakance	01.09.2002	1.56	-	1.09
r_30	temporal variant leakance	01.11.2002	0.86	-	0.77
r_31	temporal variant leakance	01.01.2003	0.93	-	0.88
r_32	temporal variant leakance	01.03.2003	0.85	-	0.81
r_33	temporal variant leakance	01.05.2003	0.70	-	0.80
r_34	temporal variant leakance	01.07.2003	0.95	-	1.18
r_35	temporal variant leakance	01.09.2003	1.55	-	1.50
r_36	temporal variant leakance	01.11.2003	1.89	-	1.15
r_37	temporal variant leakance	01.01.2004	1.61	-	0.86
r_38	temporal variant leakance	01.03.2004	1.29	-	0.65
r_39	temporal variant leakance	01.05.2004	0.83	-	0.48
r_40	temporal variant leakance	01.07.2004	1.83	-	0.96
r_41	temporal variant leakance	01.09.2004	1.39	-	1.57
r_42	temporal variant leakance	01.11.2004	1.33	-	1.05
r_43	temporal variant leakance	01.01.2005	1.63	-	0.83
r_44	temporal variant leakance	01.03.2005	0.47	-	0.18
r_45	temporal variant leakance	01.05.2005	2.46	-	0.12

Table 3: Parameter correlations: the first row and column contain the parameter names, each field the correlation between two parameters. Yellow colour indicates weak, red colour strong correlation.

Table 4: Matrix of the normalised Eigenvectors: the first column contains the parameter names, the first row the parameter number. Values above 0.3 are marked yellow, above 0.5 orange and above 0.9 red.

3.3.4. Numerical Reliability

The numerical convergence and the model reliability are tested by the following criteria:

i. The error of the water balance is determined for all 370 stress periods. The balance is carried out setting different regions: the entire model, west of Well Field West, east of Well Field West and regions around each of the 26 wells. The error is calculated for each layer, and is always smaller than 0.01% (which is the detection limit).
ii. Temporal convergence is fulfilled. By increasing the number of time steps by factor 10, the difference in solution is for all observation wells incorporated in the model always smaller than 2 cm. This appears to be an uncritical value regarding that changes of up to 7 m occur.
iii. Grid convergence could not be tested. The model is too big so that PMWIN was not capable to convert it to a finer spatial distribution, because the model is too big.

3.4. Leakance

The determination of the leakance is a central point of the present work. It has been tried to resolve the question by measurements on the one hand and modelling on the other. Results give a new insight in infiltration dynamics of lake bank filtration and possibly also of riverbank filtration though some processes only could be described with limited uniqueness.

3.4.1. Measurements

In order to determine the leakance (eq. 1) infiltration has been measured as described in chapter 3.3. Three campaigns have been carried out at several locations in front of the transect, near observation well 3311 (fig. 6) and in water depths between 60 cm and 3.5 m.

The spatial variability of the leakance is high. Infiltration measured at the 4 corners of a square (Pos1 to Pos4) within a radius of 75 cm shows a variability of factor 4 between the lowest and the highest values, in water depth between 90 cm and 120 cm (fig. 38).

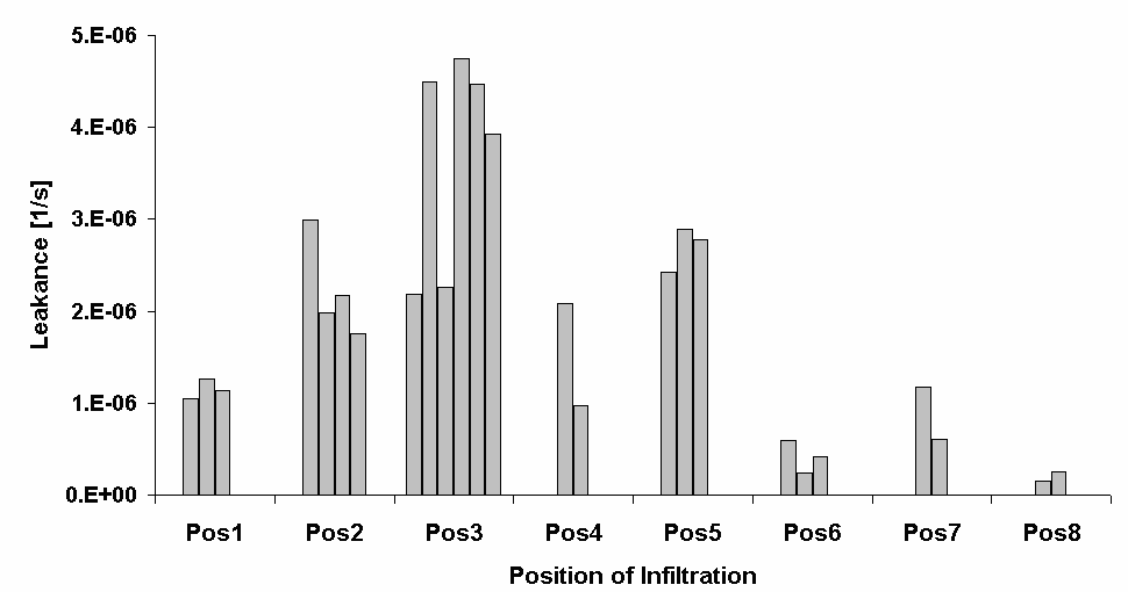

Figure 38: Leakance calculated from infiltration measurements. Each position is sampled subsequently at one day without moving the barrel. Pos1 to Pos4 are measured simultaneously at the corners of a square of 1.5x1.5m, with Position 1 and 3 as 2 and 4 at opposite corners. The water depth of Pos1 is 92 cm, Pos2 120 cm, Pos3 118 cm, Pos4 100 cm, Pos5 180 cm, Pos6 185 cm, Pos7 235 cm, Pos8 350 cm. Each bar represents one measurement. The hydraulically active sediment is assumed to have a thickness of 1 m.

Temporal variations of the leakance in subsequent measurements of about 100% occur at Pos3, Pos4, Pos6, Pos7, Pos8 (fig. 38). The reason for this behaviour is not known. It is conjectured that the mechanical stress on the barrel or the water body inside the barrel either changes the barrels connection to the sediment or changes the structure of the sediment itself. However, the possibility of oscillating infiltration appears improbable but cannot be rejected to exist also under field conditions unaffected by measurements.

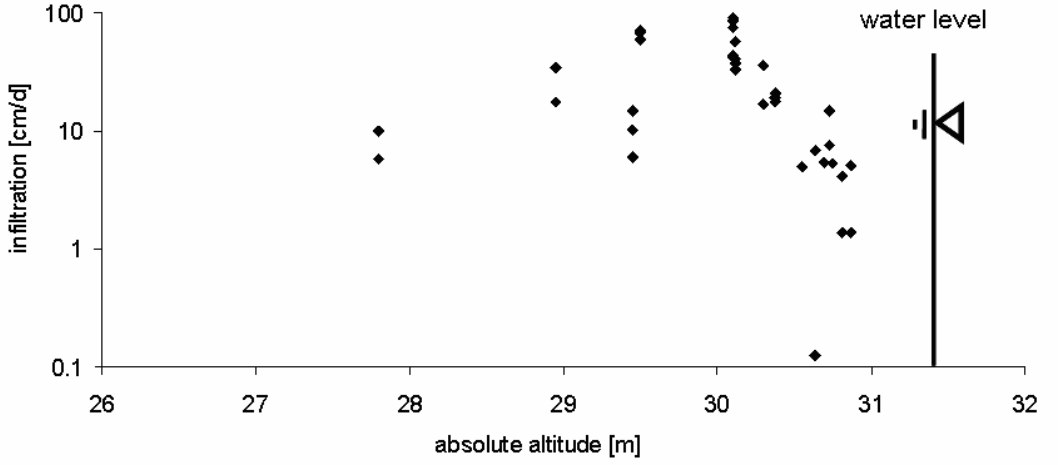

Figure 39: Infiltration for all infiltration measurements, each point represents one measurement, ordered by the elevation of the infiltration position.

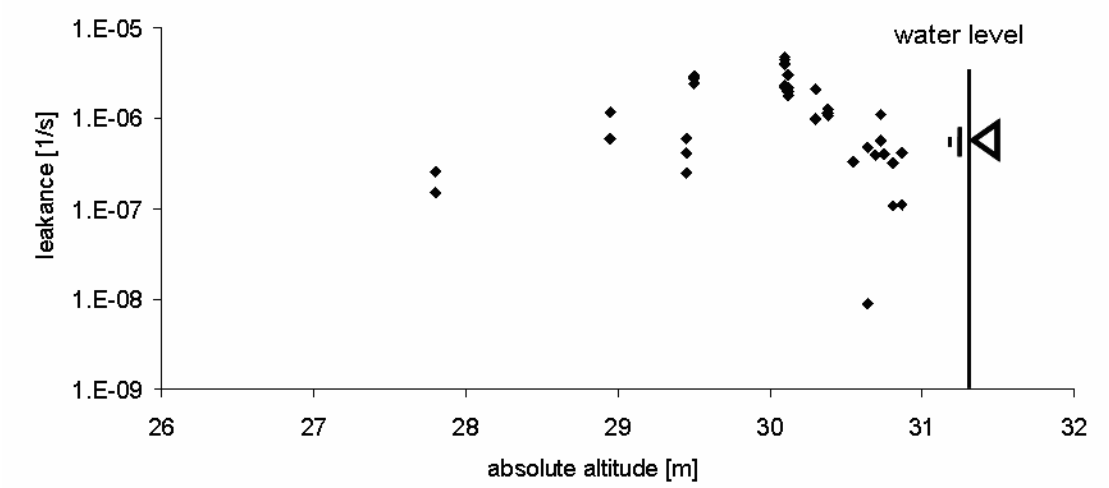

Figure 40: Leakance for all infiltration measurements, each point represents one measurement, ordered by the elevation of the infiltration position. The bed thickness is assumed to be 1m.

Most water infiltrates at 1.5 m water depth (fig. 39), decreasing by about one order of magnitude towards the highest and lowest sampled elevations. The leakance (fig. 40) shows the same behaviour. The higher values have much more hydraulic impact on the infiltration characteristic, the mean values are close to the highest as the scale is logarithmic.

Measurements have been carried out at a small region, just in front of the transect, and only cover a small part of the model domain and thus might not be representative. The shallow part here (> 1m water depth) is not protected by palisades, unlike at most other parts of the lake bank. The main benefit is not obtaining hard values for infiltration characteristics but gaining an idea of the spatial and temporal variability.

3.4.2. Modelling

The determination of the leakance is a crucial point in setting up a model, it affects strongly the hydraulic situation. The measurements which have been carried out provide an idea of the variability and an indication of the magnitude, a direct transfer is not possible.

Eichhorn (2000), Rümmler (2003) and Holzbecher (2006) applied leakance decreasing by about factor 10 between shallow water and the maximal infiltration depth of about 5 m. Applying these values and distribution transient modelling is impossible. Either heads are at least 1.5 m too high or the entire model is drained.

WASY (2004) applied a constant leakance of $7*10^{-5}$ s^{-1}on a width of about 100 m from the fringe, which enabled transient modelling in 2002.

Even better results are obtained with a rather homogeneous depth distribution not varying more than factor 3 between the fringe up to the beginning of the mud in a depth of 7 m, covering the lake bed until a distance of about 100 m from the bank (fig. 41). With this

configuration the trend can be reproduced fairly with high leakance, but the absolute value of the heads is about 70 cm too high. When the leakance is lowered, the mean of simulated and hydraulic heads is identical, but the simulated trend is too steep (fig. 41). During the simulation heads decrease 1 m too much. This might sound not so much within 7.5 years, but taking into account the mitigating effect of the $2^{nd}/3^{rd}$ type boundaries, this is not acceptable. Besides, measurements indicate that the highest leakance should occur at about 30 m NN, decreasing towards the deeper regions. The mismatch of the temporal dynamics using time invariant leakance is shown exemplarily at TEG050. It is too far away from the boundaries to show the mismatch and as well far away from the well field that short term fluctuations do not distract the spectators eye. Observation well 3301 shows a very similar behaviour. Fitting the observed data is not achievable using time invariant leakance, it is like trying to cover a big table with a small tablecloth. With a high leakance in shallow water, decreasing towards nil at 5 m depth it is not possible at all, heads are much too high or the model is entirely drained.

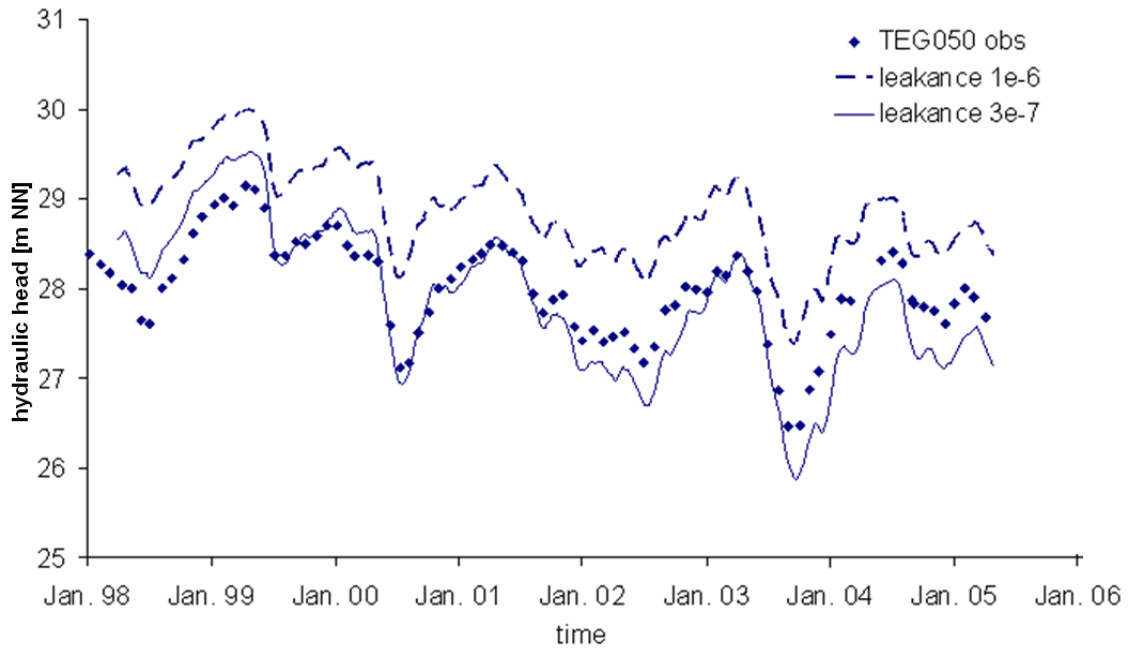

Figure 41: Observed and simulated hydraulic heads of observation well TEG050, with constant leakance in depth between 25 m NN and water surface (~31.45 m NN) and during the entire simulation. The thick dashed curve stands for simulated water levels with a leakance of 10^{-6} s^{-1} and shows the trend, but not the dynamic: in phases with high drawdown as in summer 2000 and 2003 it's about 1 m above observed, before and after drawdown events only about 0.6 m. The tiny solid curve stands for simulated water levels with a leakance of $3*10^{-7}$ s^{-1}. The dynamic during drawdown events is reproduced correctly, but the heads decrease faster than observed.

Two ways exist to handle this problem hydraulically:

i. Case1: The leakance is assumed to have a linear temporal trend. The slope of the trend as well as the depth dependence are simultaneously determined by inverse modelling (fig. 43).

ii. Case2: The leakance is assumed to be temporally variant, approximated with a continuous curve consisting of linear sections with 2 months length. This curve is simultaneously estimated with the depth dependent leakance (fig. 43).

In order to enable temporal variant leakance as well as easy communication with PEST, the MODFLOW2000 code has been modified. The resulting hydraulic heads are quite similar for both cases (fig. 42), though the parameterisation is quite different (fig. 43, fig. 44). Under the premise of a linear temporal behaviour, the leakance is higher in greater depth. If the temporal behaviour is not forced to be linear, measurements indicate that the pattern is quite variable (fig. 43) and the leakance is higher in shallow water (fig. 44). A higher temporal resolution neither led to a considerably lower objective function nor resulted in a significantly different temporal behaviour.

The depth distribution of the leakance is in both cases subject of high parameter cross correlation and nonuniqueness. In Case1 7 Eigenvectors contain 7 depth zones of infiltration as significant non-zero elements with values between 0.12 and 0.62, in Case2 the values vary between 0.01 and 0.86 (tab. 4).

In order to override numerical problems and meaningless results due to the high parameter correlation, the leakance is constrained in both cases to be identical by depth, introduced as prior information into the parameter estimation process:

$$\Phi_{pri} = \sum_{i=1}^{n-1} \left| \log(leak_i) - \log(leak_{i+1}) \right| \quad \text{eq. 27}$$

with Φ_{pri} as the contribution to the objective function, i the counter and n the number of depth zones, $leak_i$ as the leakance of a certain depth. The constraint is however only weak, contributing less than 1% to the minimised objective function. This means, the depth distribution shown in figure 44 may only be seen as an indication. However, regularisation without prior information gives the same results as ordinary parameter estimation. This shows that the depth dependent leakance, as calculated (fig. 44), is based on field observations and is not entirely a matter of parameter nonuniqueness.

In between these two cases an unlimited number of parameter combinations might exist, all giving an appropriate reproduction of the measured hydraulic heads. The parameter describing the temporal variation is named relative leakance.

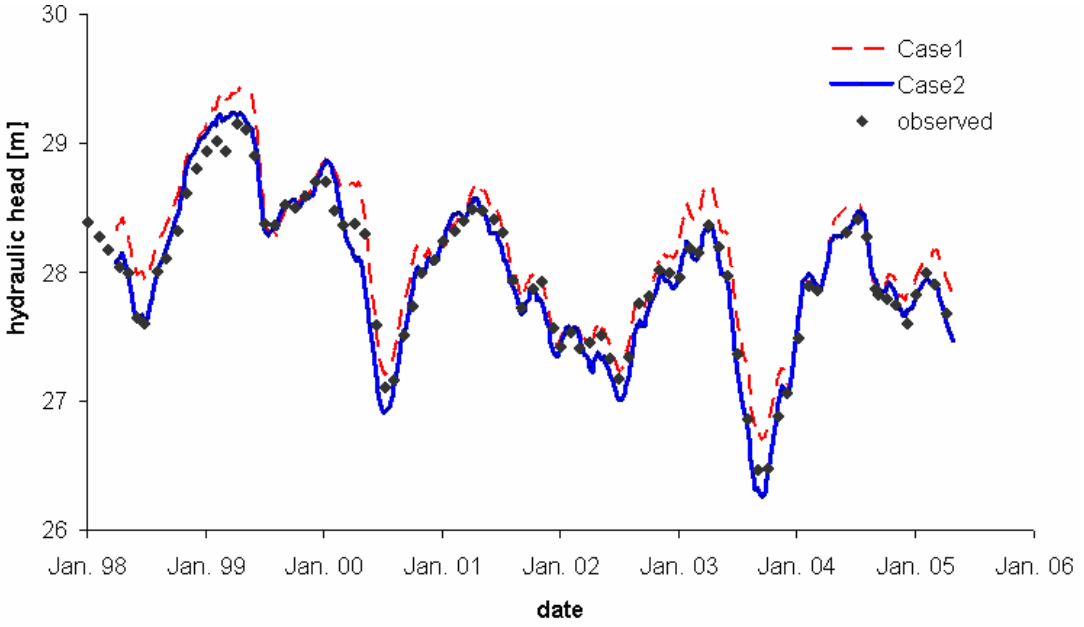

Figure 42: Hydraulic heads at TEG050, Case1 represented by tiny red dashed line, Case2 represented by thick solid blue line. Observed values are represented by black diamonds. Both cases give a very good representation of the system.

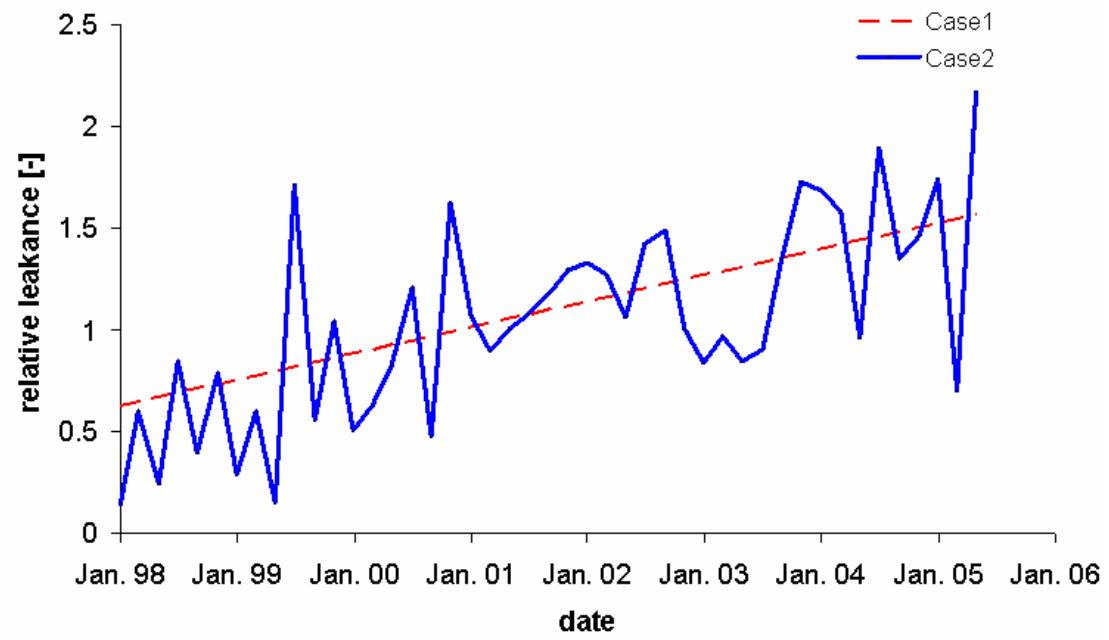

Figure 43: temporal behaviour of the relative leakance, multiplied with the leakance shown in figure 44. At Case1, represented by a red dashed line, leakance increases linearly, at Case2, represented by a solid blue line, linear trends of 2 months length from a continuous curve.

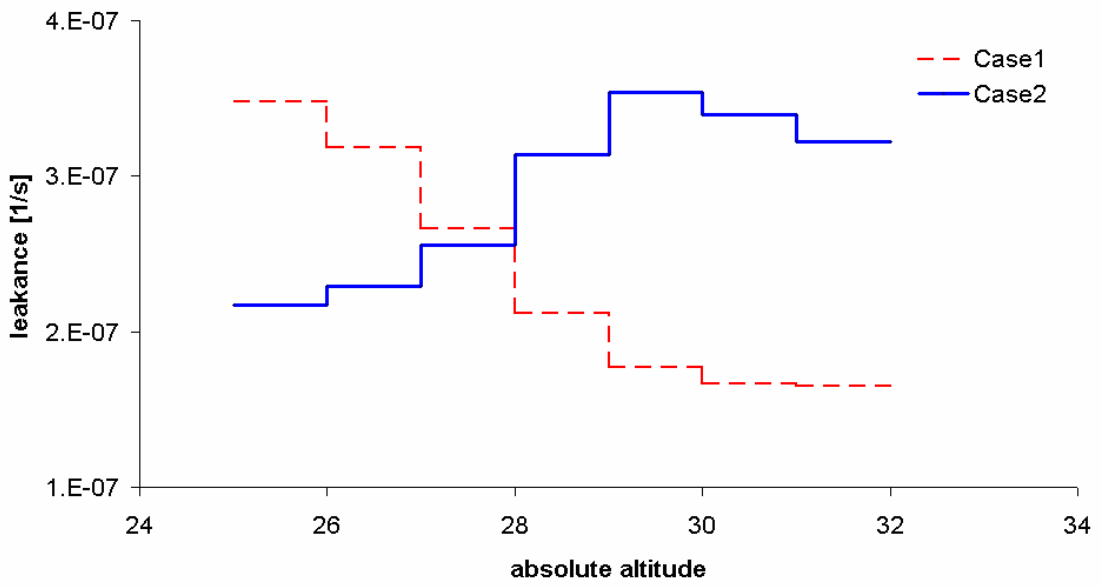

Figure 44: Distribution of the leakance by bathimetric steps of 1 m. Multiplied with the relative leakance from fig. 43, the leakance at a certain time is obtained. In Case1, represented by a red dashed line leakance is high in deeper regions and decreases towards the bank. In Case2, represented by a solid blue line leakance tend to be lower in deeper regions, increasing towards the bank.

Preliminary Upshot Temporal Variant Leakance

There are several mechanisms, which could affect hydraulics and potentially could also explain the observed piezometric heads, the corresponding hypotheses 1 to 8 could all be rejected, because no satisfying fit of hydraulic heads could be obtained using a time invariant leakance. The variability of the leakance is revealed, but hypothesis 9, 11.1 and 11.2 do not explain the behaviour. Hypothesis 10 may suggests a contribution to the time variant leakance, hypothesis 11.3 explains most of it.

Hypothesis 1: The variant piezometric heads inland, with changes between 3.5 m (piezometer TEG343) and 1 m (piezometer 6034), lead to changes in pore space and compaction or swelling processes of fine grained layers which release or absorb considerable amounts of water.

Compaction and swelling denotes the reduction/increase of the pore space of a fine grained soil as clay or silt which may be provoked by mechanical compression/decompression and may be reversible or irreversible. Such sediments exist as aquitard between aquifer 1 and 2 with a thickness of 4 m as between aquifer 2 and 3 with a thickness of 30 m.

This behaviour can be simulated using MODFLOW's interbed storage package. However, even with a change of pore space by factor 2 of compaction or swelling, no significant increase in model performance could be achieved.

Hypothesis 2: Variant groundwater recharge leads to the observed dynamics of hydraulic heads.

The weekly groundwater recharge is estimated on the basis of the precipitation data, with regard to the corresponding season. The Umweltatlas Berlin (2005) denotes an annual recharge of 125 mm. Even different annual recharge, chosen in the wide range between 50 and 300 mm, with different temporal dynamics, does not improve the temporal behaviour of modelled hydraulic heads.

Hypothesis 3: The pine forest transpirates considerable amounts of water.

This could be rejected without running the model. The unsaturated zone is about 5 m thick and pine trees have a maximal root depth of 1.2 m (Kuhr 2001). With sand as the main constituent of the matrix in the unsaturated zone, the capillary pressure is not high enough to bridge the difference.

Hypothesis 4: The spatial distribution of the leakance, especially the distribution by depth, induces substantially different infiltration dynamics than homogeneously distributed leakance and leads to the observed dynamics of hydraulic heads.

Different spatial distributions have been applied manually, with respecting the measured infiltration values, and the magnitude has been estimated using PEST.

The behaviour described above could be mitigated through the application of low leakance in shallow and high leakance in deep parts of Lake Tegel. As result variations on monthly scale coincide with observed values, but the modelled trend still decreases too fast. Even assuming the mud of Lake Tegel being well permeable, a match of the trend can not be achieved. Also inverse modelling failed, cells with observations went dry in summer 2000 or summer 2003. The Jacobi matrix could not be computed and parameter estimation has been thus terminated.

Hypothesis 5: Due to increasing delivery height of the pumps during periods with low piezometric heads, the amounts of abstracted water are reduced and the observed hydraulic heads could be reproduced.

The pumpage is regulated by a gate between the pump and the collector pipe of the Well Field West. This inhibits assessing the effect using the manufacturers pump characteristic. Linear and quadratic relations have been applied to a modified version of MODFLOW2000 resulting in a total change of 20 % of abstraction amounts for typically occurring head differences of 5 m. The simulated results have not been improved significantly. Besides, though considerable variations between calculated abstraction and the amounts recorded by

water meters of the pumps occur, no systematic deviations between periods of high and low piezometric heads are detectable.

Hypothesis 6: The amounts of abstracted water applied to the model are not correct. A different way of calculation aligns observed and modelled hydraulic heads.

Unfortunately, direct measurements of abstracted water in high temporal resolution are not available. The quantification of the abstraction for the entire well field and single wells can be calculated using different methods. Amounts are calculated by multiplying daily operational hours with the pumpage. The values of the operational hours seem to be correct, electronic data coincides almost always with the sheets for well switching times filled in by hand (BWB 2005). Discrepancies are detected with the telescope model (chapter 4.7). Stress periods are set to the exact times of well switching, some differences between the recorded switching cycle and the real switching could be detected through discrepancies in the hydraulic heads. Either the wells are switched at different times or different wells are switched or not switched. But within the 7 months long simulation period of the telescope model only 5 to 10 times such errors could be identified. Even during these phases piezometers do not show substantially different hydraulic heads. This indicates the operational time more precise than the pumpage.

Two kinds of pumpage information exists (BWB 2005):

i. the current pumpage while the test is conducted and
ii. the average pumpage between the last and the actual pumping test.

For most wells these values show a discrepancy less than 5 % during the entire period, very rarely more than 10 %, neither the values nor the discrepancies show a trend. Discrepancies between these values may not be the reason for the observed behaviour of hydraulic heads.

The daily amounts of extracted water for each well field are provided by BWB (2005). These amounts are calculated using the time of well operation and pumpage, and scaled to the raw water produced by Waterworks Tegel. The modelled values are on average 16 % higher than the values for the entire well field, the ratio varies over time (fig. 45). In summer 2003 the discrepancy is highest. However, scaling the calculated pumping rates with the pumping rates provided by BWB, the discrepancy between observed and calculated hydraulic heads could not be reduced.

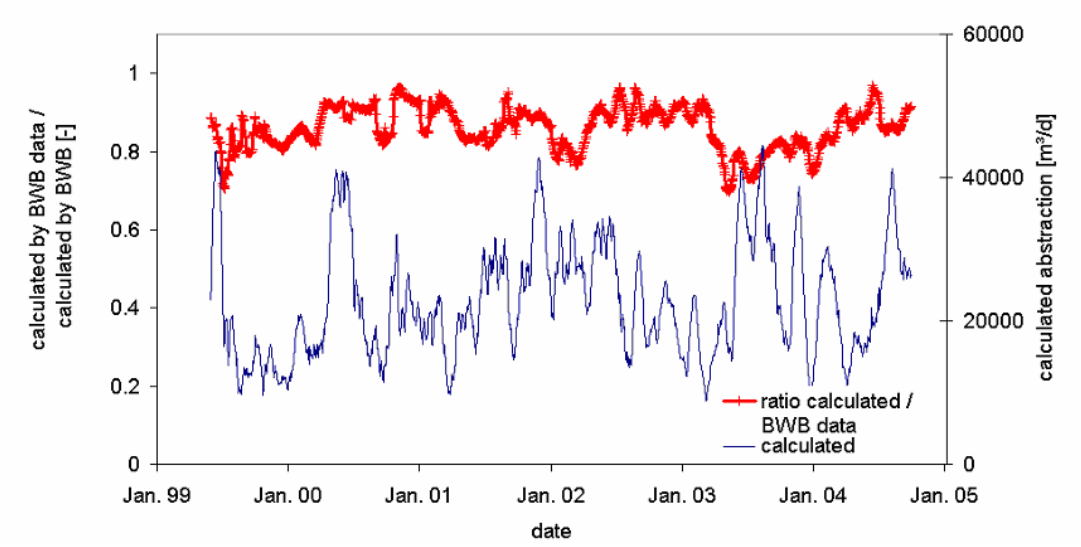

Figure 45: Abstraction by Well Field West. The thick red line (left axis) is the ratio of values calculated by pumpage test data and time of well operation divided by a value scaled by the entire raw water of waterworks Tegel, provided by BWB. The tiny blue line represents the abstraction calculated by pumpage test data and time of well operation. Both curves are the moving average of 20 days.

Hypothesis 7: The interaction between the upper 2 inland aquifers is the reason for the observed dynamics of hydraulic heads.

For the check of the model performance 7 inland observation wells are available. 4 are screened in the first aquifer, 1 is screened in the second aquifer and 2 are screened as well in the first as in the second aquifer. Consequently, most information and a clear spatial picture is available only from the first aquifer. If this aquifer whose saturated thickness is smaller than 10 m, would have only weak hydraulic contact to the aquifer beneath, the hydraulic heads of the lower aquifer, with a thickness of 25-45 m, would be poorly known. Additionally, the observation well which is screened only in the second aquifer is located quite near to the boundary condition. This means that the hydraulic state of the main aquifer inland is unknown without further information. The available observed hydraulic heads are possibly not significant with respect to the water flowing towards Well Field West.

Several aquifer parameters are only roughly known. The specific yield may have a value between 0.1 and 0.3 [-] (of importance only for the upper aquifer), the confined storage coefficient may have values between $5*10^{-4}$ [-] and 10^{-6} [-] (of importance for the lower aquifer), the hydraulic conductivity of the 2nd aquifer has a possible range aquifer between 10^{-4} m/s and $6*10^{-4}$ m/s. The spatial distribution of the glacial till is unknown. Depending on the ratio of holes, it may divide the two aquifers effectively. A combination of parameters may exist which aligns observed and simulated hydraulic heads (fig. 41). Especially the distribution of observation wells introduces uncertainty. Heads at 6 of the 7 observation wells only are provided with monthly intervals and have hydraulic contact to the first aquifer. Only in piezometer 6034, which is located close to the boundary condition, daily values are recorded.

Small storage coefficients and low leakage between aquifer 1 and 2 could not be identified easily. Short term changes (daily/weekly) of the hydraulic heads may fall in the unobserved months between two observations or in case of observation well 6034 may be mitigated by the vicinity of the boundary condition.

However, no parameter combination could be found which aligns the observed and simulated hydraulic heads of the inland observation wells and also at the transect without introducing time variant hydraulic leakance. With the variant leakance introduced, the best fit is obtained with the glacial till having such a leakage factor that hydraulic heads in the upper and lower aquifer do not differ more than 30 cm (chapter 4.3.3).

Hypothesis 8: Bottom water from the third aquifer supplies the missing water, the leakance is time invariant.

At the deepest point of Lake Tegel sandy sediments are found in a depth of -15 m NN, the drilling is sunk up to -20 m NN. Like the "Tegeler Rinne" (Frey 1975), the formation of the former trough, now filled up with Lake Tegel and its sediments, might have disturbed the underlying tertiary aquitard, which could lead to hydraulic contact between the aquifers.

Water would intrude from the 3rd aquifer and only show up in the northern part of Well Field West, near the deepest point of Lake Tegel. At the transect such water is not detected, at the bottom of the 2nd aquifer, observation well TEG374 shows old bank filtrate (Pekdeger et al. 2006). Chemical composition of the water abstracted by wells 1 to 26, as values of chloride, sodium, calcium and others do not give a hint to water coming up. Introducing a 3rd type boundary between the northern part of Well Field West and the deepest point of Lake Tegel, a parameter combination where leakance is time invariant with satisfying hydraulic heads could not be found.

Intermediary Result

The previous hypotheses were stated under the assumption of time invariant leakance. As they had to be rejected, it has to be assumed the leakance is time variant. Possible reasons are analysed:

Hypothesis 9: The annual cycle of water temperatures leads to temporal variant leakance.

Between 0 °C and 25 °C the viscosity of water varies by factor 2. Assuming a constant permeability, temperature dependent viscosity causes temperature dependent k_f values. This would result in a seasonal curve having in principal a sinusoidal shape following the water temperature. This is definitely not the case. However, a previous model of the interval between

2001 and 2004 showed in every summer an increase of bank conductivity, also visible in fig. 43. Between 1998 and 2001 however this effect can not be observed. The pumping regime in these years is acyclic with respect to the seasonal water demand.

The water temperature is known to affect the k_f values by viscosity effects, (Lin et al. 2003, Müller 1999). At 25°C the k_f is two times higher than at 0°C. Under influence of bioclogging the effect may be reversed. At 5°C infiltration is 2.5 times higher than at 25°C (Okubo and Matsumoto 1983). A correlation analysis of the observed temporal dependent leakance and water temperature results in an insignificantly positive correlation (fig. 46). The seasonal effects appear to neutralise each other or are dominated by different mechanisms.

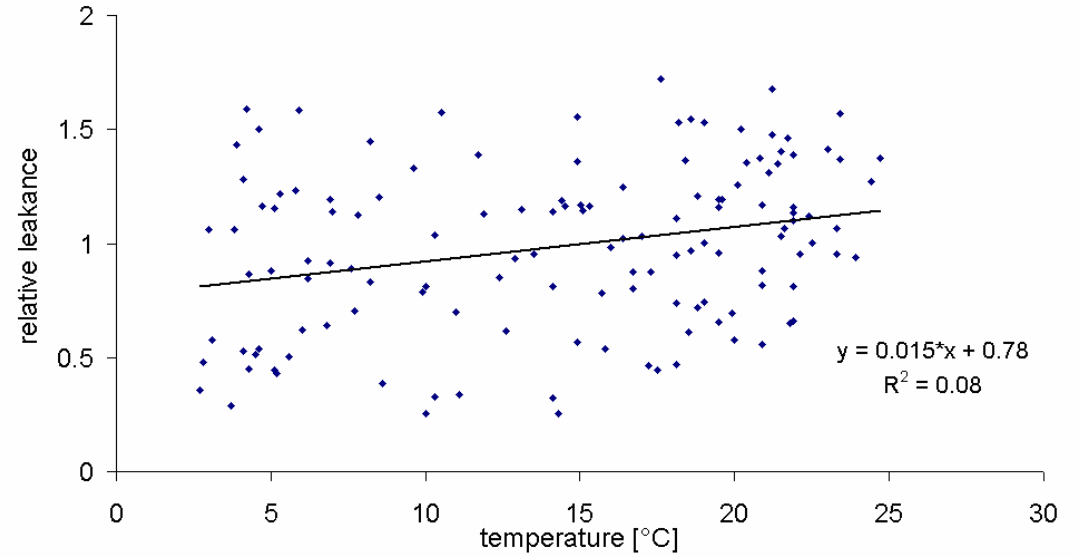

Figure 46: Blue diamonds represent the relative leakance against the water temperature. A linear regression between water temperature and leakance is indicated by a black line. The correlation is positive and the coefficient of determination is 0.08.

Hypothesis 10: The composition of water of Lake Tegel determines the time variant infiltration.

Correlations between the time variant leakance from Case2 and the physico-chemical parameters have coefficients R^2 smaller than 0.1. The studied parameters are: pH, electrical conductivity, O_2 content, O_2 saturation, total colloids, Secchi Depth (measure for turbidity), BOD 1 (biological oxygen demand within 1 day), BOD 5, DOC, loss on ignition of DOC, organic nitrogen, ammonium, total P, ortophospate, inorganic carbon, sulphate, chloride, silicon, sodium, calcium, potassium, magnesium, total phytoplankton biovolume, chlorophyll-A, phaeophytin, zooplankton biomass. The lack of significant correlations suggests that clogging is rather independent on surface water quality but does not necessarily mean the hypothesis can be rejected. More complex interactions between several of the different physico-chemical water parameters and the leakance may exist.

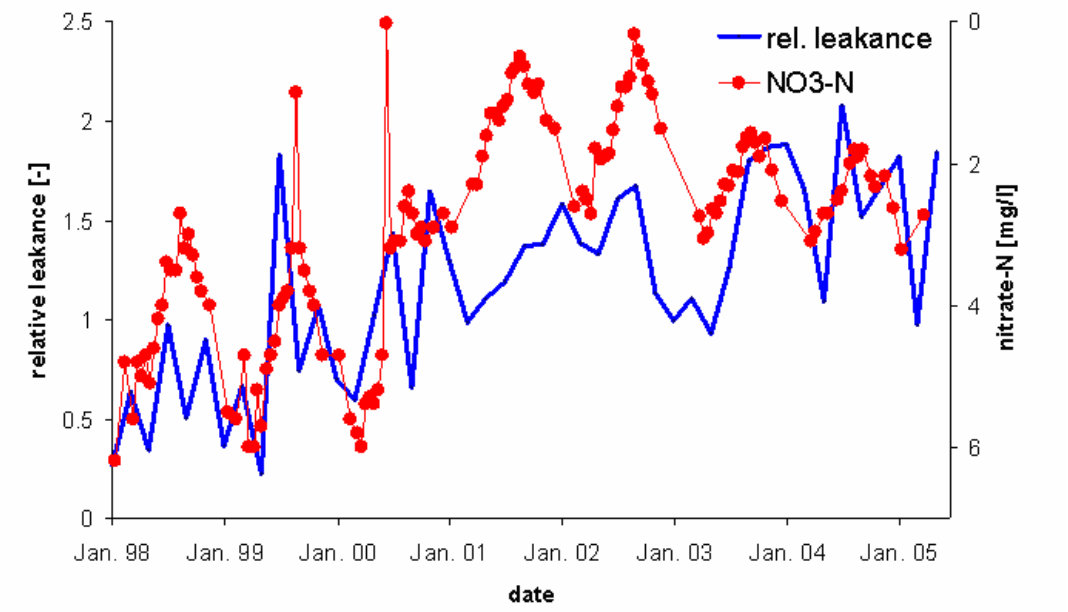

Figure 47: The solid blue curve (left axis) represents calibrated time variant leakance according to Case2, the red circles on a tiny red line (right axis) represent the measured NO_3-N concentration. Please note the reversed axis for the nitrate concentration.

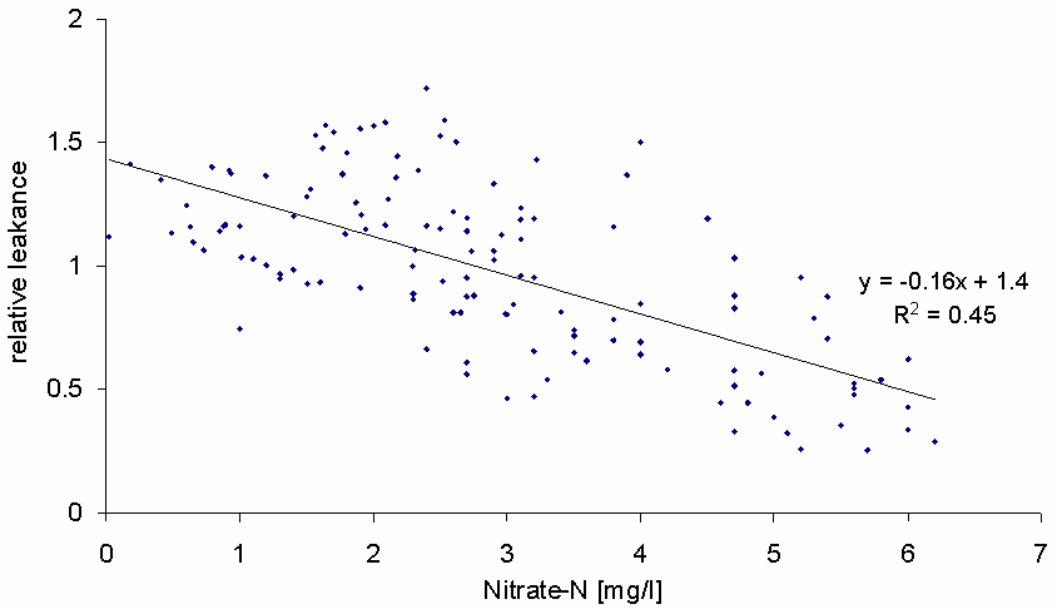

Figure 48: Blue diamonds represent the relative leakance against the nitrate nitrogen. A linear trend is indicated by a black line. The correlation is negative and the coefficient of determination is 0.45.

Nitrate however is clearly negatively correlated to the leakance with R^2 of 0.45 (fig. 48). Regarding the temporal match of the curves (fig. 47) the correlation is less obvious than regarding the regression analysis. Literature which reports reduced clogging with increasing nitrate concentrations has not been found, but anaerobic conditions generally enhance the production of extracellular polymers (Vandevivere and Baveye 1992) or lead to precipitation of minerals (Schubert 2002). Further significance and possible reasons of the correlation are considered in the discussion part.

Hypothesis 11: The hydraulic dynamics at the infiltration zone induces time variant leakance

The pumping rate affects the leakance via the hydraulic heads below Lake Tegel. Hydraulic heads in this zone vary rapidly and nonuniform along the bank. Head data with high temporal resolution are only available at the transect. Thus, instead of hydraulic heads, the pumping rate of Well Field West is an integral value for the entire bank and is continuously recorded. Thus it is considered as more reliable parameter and used for the comparison with the temporal variant leakance. Values have been found to coincide temporally (fig. 49). The correlation coefficient of the pumping rate to temporal variant leakance is 0.42 (fig. 50), slightly lower than the correlation coefficient of nitrate, the temporal behaviour however coincides better than for the nitrate concentration (fig. 47). Regarding the peak of relative leakance and pumping rate in 2000, and the behaviour between 2001 and 2004, it appears that the leakance reacts with a small delay. This is coherent with the law of cause and effect, but decreases the regression coefficient.

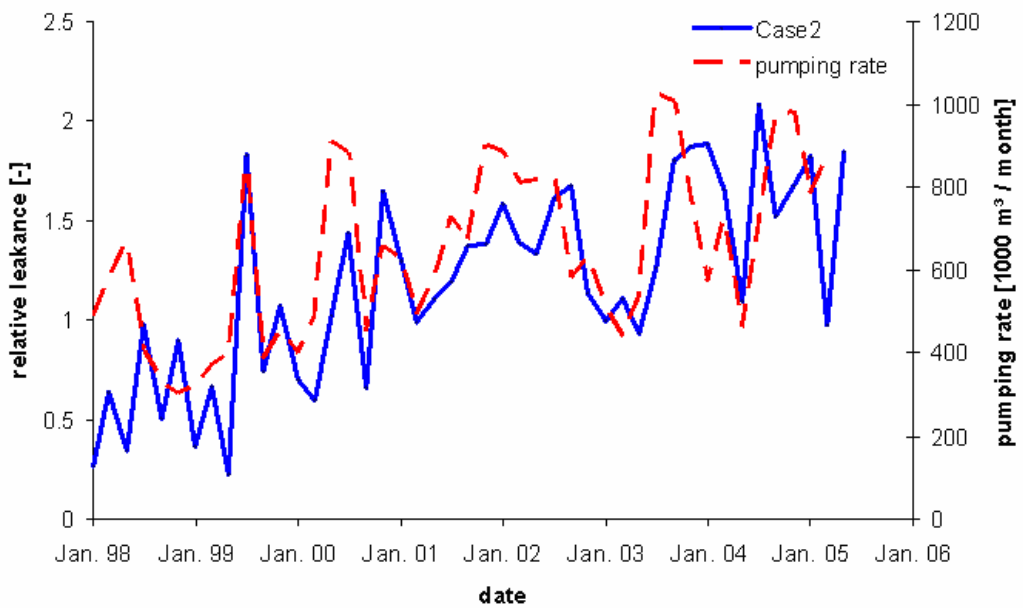

Figure 49: Temporal variant leakance of Case2 (solid blue line, left axis) and pumping rate of Well Field West (dashed red line, right axis).

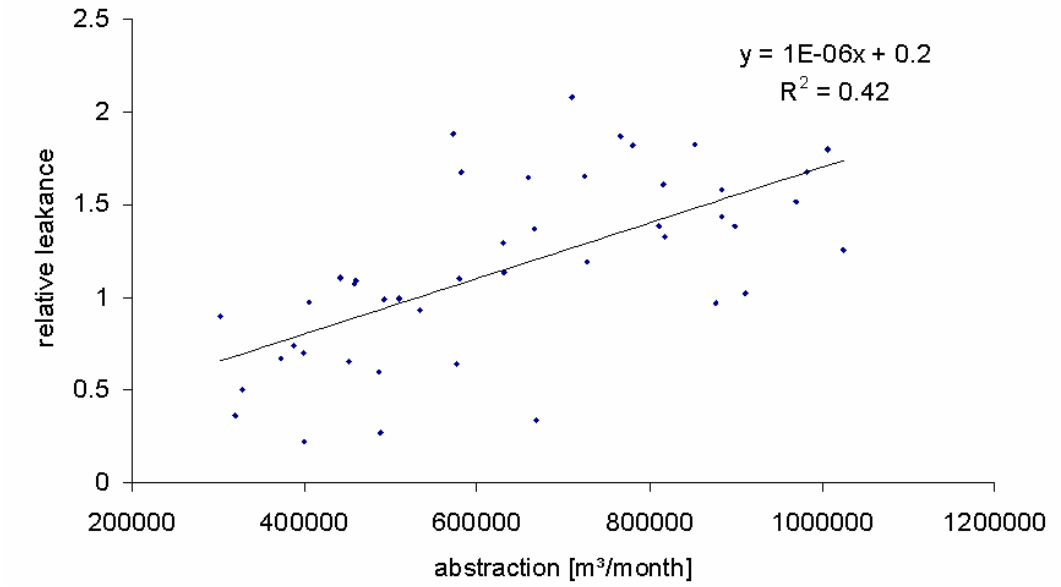

Figure 50: Scatter plot of figure 49, each dot represents the temporal leakance factor above the mean of the pumping rate for two month.

Hypothesis 11.1: A zone below Lake Tegel provides hydraulic contact to the groundwater. By this way the leakance, calculated with a small saturated depth would appear to increase.

The leakance is correlated with the pumping rate, but the hydraulic heads of the groundwater indicate an unsaturated zone for the shallower regions of Lake Tegel, which would cause the hydraulical independence of the infiltration to the groundwater table. Two ways might exist to bridge the unsaturated zone:

i. As the pressure head in the unsaturated zone may not have a discrete step but rather a transition zone between saturated conditions above and unsaturated conditions of gravity flow below, a gradient in pressure head may suck water downwards.
ii. Alternatively fine particles/bacteria/precipitated minerals/gas bubbles in the lake bed provide the smallest kf and thus the control of infiltration in a depth much deeper than the water sediment interface, also leading to suction.

Both scenarios would enhance infiltration at low groundwater levels as the pressure gradient across the water sediment interface would increase. These mechanisms might exist in parallel, but even if they would bridge 2 m between lake bottom and groundwater table, the temporal dynamic of the modelled hydraulic heads would only slightly improve. For water depths of about 30 to 80 cm the saturated zone below Lake Tegel has a depth of maximal 22 cm (Hoffmann and Gunkel 2006).

Hypothesis 11.2: The variable hydraulic head difference between surface and groundwater affects the hydraulic conductivity of the lake bed.

Since the previous hypotheses could be rejected, it is reasonable that the thickness of the clogging layer is small, relatively to the hydraulic head difference. Thus the infiltration velocity is given by eq. 28:

$$v_f = \Delta h * L \quad \text{eq. 28}$$

where v_f is the Darcy velocity, L the leakance [s^{-1}]. The variable Δh [m] is the driving head difference, calculated by eq. 29:

$$\Delta h = \begin{cases} h_{ow} - h_{gw}, & h_{gw} > h_{bot} \\ h_{ow} - h_{bot}, & h_{gw} \le h_{bot} \end{cases} \quad \text{eq. 29}$$

Where h_{gw} is the hydraulic head of the groundwater, h_{ow} is the water table of the lake and h_{bot} is the elevation of the lake bottom.

High infiltration rates stabilise themselves, leading to a pronounced spatial pattern rather than to spatially similar values (chapter 4.4.3.1). Thus it is reasonable, that an increased hydraulic gradient across the clogging layer increases infiltration more than proportional. Two approaches have been applied. In the first, the leakance L is related to the difference in hydraulic head by an exponential fitting function:

$$L = L_0 * (p_1 + p_2 * \Delta h^{p_3}) \quad \text{eq. 30}$$

where L is the momentary, spatially and temporally distributed leakance, L_0 is the leakance without head difference as function of the lake bed elevation, p_1, p_2 and p_3 are parameters of the fitting function. Analogue a second fitting function is applied:

$$L = L_0 * (p_1 + p_2 * v_f^{p_3}) \quad \text{eq. 31}$$

where v_f is the Darcy velocity in the lake bed. Both equations are not physically based. They have been added to the source code of the reservoir package of MODFLOW2000.

The principal dilemma that the trend of the hydraulic heads either decreases too fast or heads are too high could not be resolved with any of the equations. Even in combination with setting the bed of Lake Tegel permeable up to an elevation of 20 m NN (12.5 m water depth) only a mitigating effect is achieved.

Hypothesis 11.3: The infiltration increases with the extent and thickness of the unsaturated zone (Case3).

In case that the subsurface below Lake Tegel is unsaturated, no hydraulic contact exists between the lake and the groundwater table. The capillary potential of the sandy aquifer may

bridge only a few cm. A significant portion of fine sediments which may cause a higher capillary potential does not exist (Sievers 2001).

Analogous to the hypothesis 11.2, the leakance is assumed to be a function of the thickness of the unsaturated zone. A simple, not physically based function is assumed:

$$L = L_0 * (p_1 + p_2 * h_{usat}^{\ p_3}) \quad \text{eq. 32}$$

where L is the momentary, spatially and temporally distributed leakance, L_0 is the saturated leakance as function of the lake bed elevation, p_1 and p_2 are parameters of the fitting function:

$$h_{usat} = \begin{cases} h_{bot} - h_{gw}, h_{bot} > h_{gw} \\ 0 \quad , h_{bot} \le h_{gwt} \end{cases} \quad \text{eq. 33}$$

The eq. 32 and 33 have been added to the source code of the reservoir package of MODFLOW2000. The principal hydraulic behaviour could be reproduced. The trend of the simulated and observed hydraulic heads is identical, the mean hydraulic heads are similar.

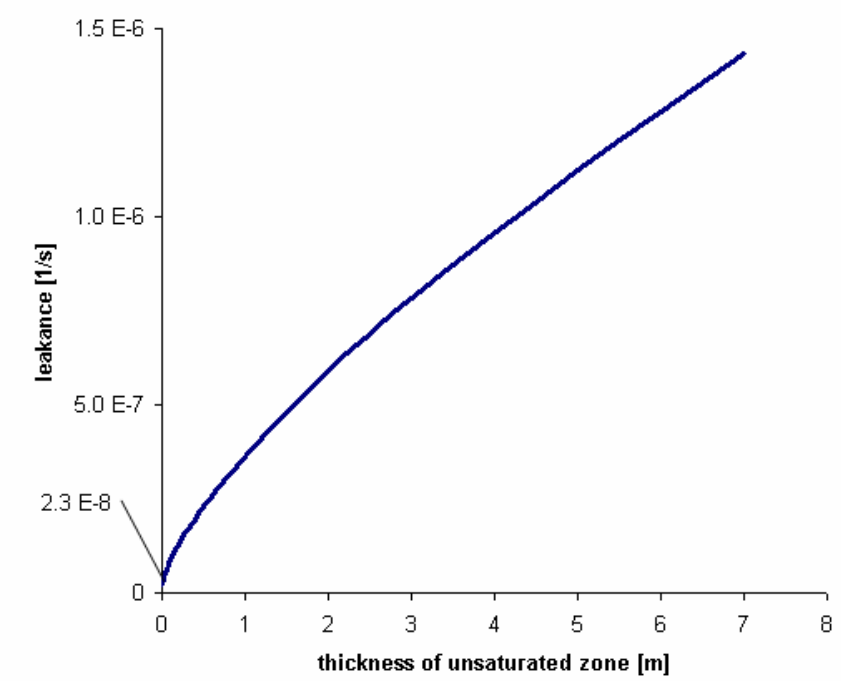

Figure 51: Leakance of Lake Tegel as function of the thickness of the unsaturated zone, calculated with equation 32 (p_1= 14.8, p_2= 0.78). The maximum unsaturated thickness between 1998 and 2005 is 7 m. The leakance in the saturated zone is $2.3*10^{-8}$ s^{-1}.

Calibrated values of the parameters are: $2.6*10^{-8}$ $s^{-1} \ge L_0 \ge 2*10^{-8}$ s^{-1}, p_1 = 14.8, p_2 = 0.78. The leakance L_0 with a saturated zone below is similar in all water depths and does not have a trend. Figure 51 shows the leakance as function of the thickness of the unsaturated zone. The simulated hydraulic heads at observation wells TEG050 and 3301 are plotted in figures 52 and 53.

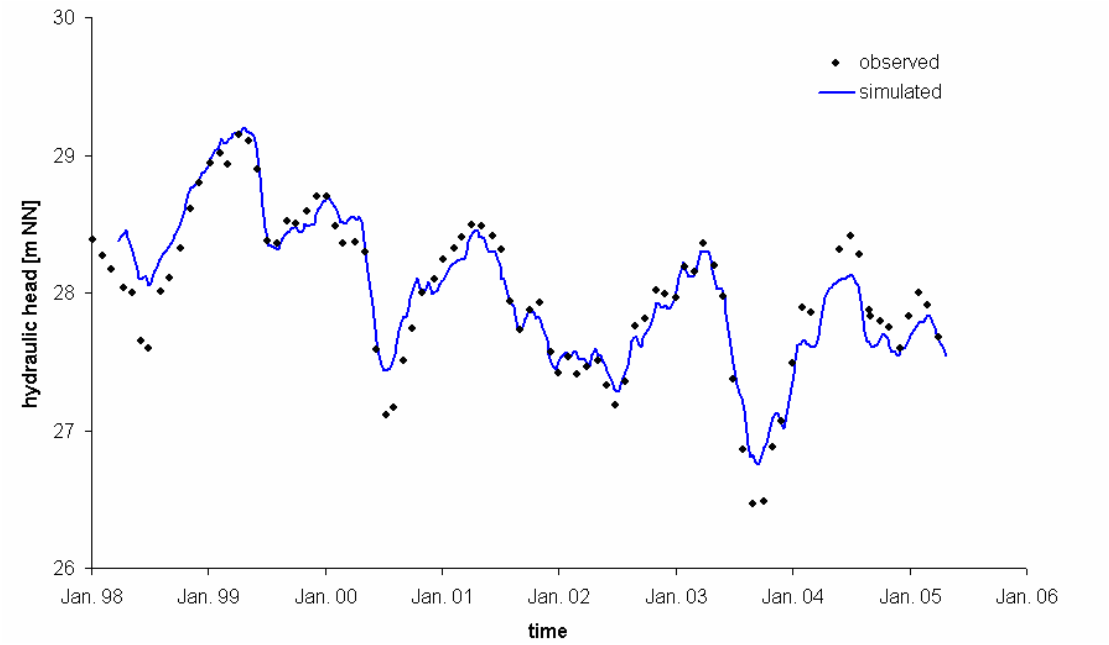

Figure 52: Observed (black dots) and simulated (blue line) hydraulic heads at TEG050 with the conductivity of the lake bed following Case3.

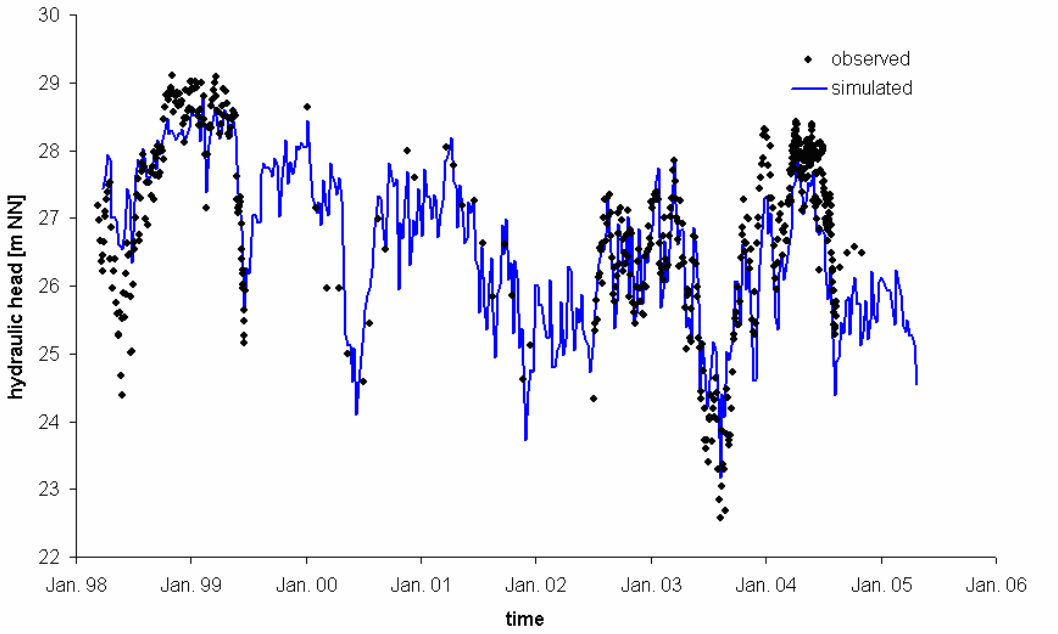

Figure 53: Observed (black dots) and simulated (blue line) hydraulic heads at observation well 3301 with the conductivity of the lake bed following Case3.

For Case2 the leakance of the bank is calibrated temporally to the observed heads of the corresponding piezometers. This is only valid for the eastern bank of Lake Tegel which is primarily affected by Well Field West. In the model however, the same leakance is also applied to the bank around Scharfenberg. The application of Case3 instead of Case2 improves the fit of observed and simulated hydraulic heads. The temporal dynamic coincides better (fig. 54). Also the mean $\bar{\mu} = 28.84$ m NN of Case3 is much closer to the observed mean $\bar{\mu} = 28.81$ m NN than Case2 $\bar{\mu} = 29.23$ m NN. It is astonishing that observed heads in January 2001 and January

2002 are lower than the boundary conditions of the wells and of Lake Tegel. This is a shortcoming of the model. A sector of 90°C from Scharfenberg is included into the model. When the well is switched on, the flowpaths are almost radial. When the well is switched off, the sector of 90°C does not represent the hydraulic situation correctly, the area of the sector is too big in relation to its bank length, the modelled heads increase too slow.

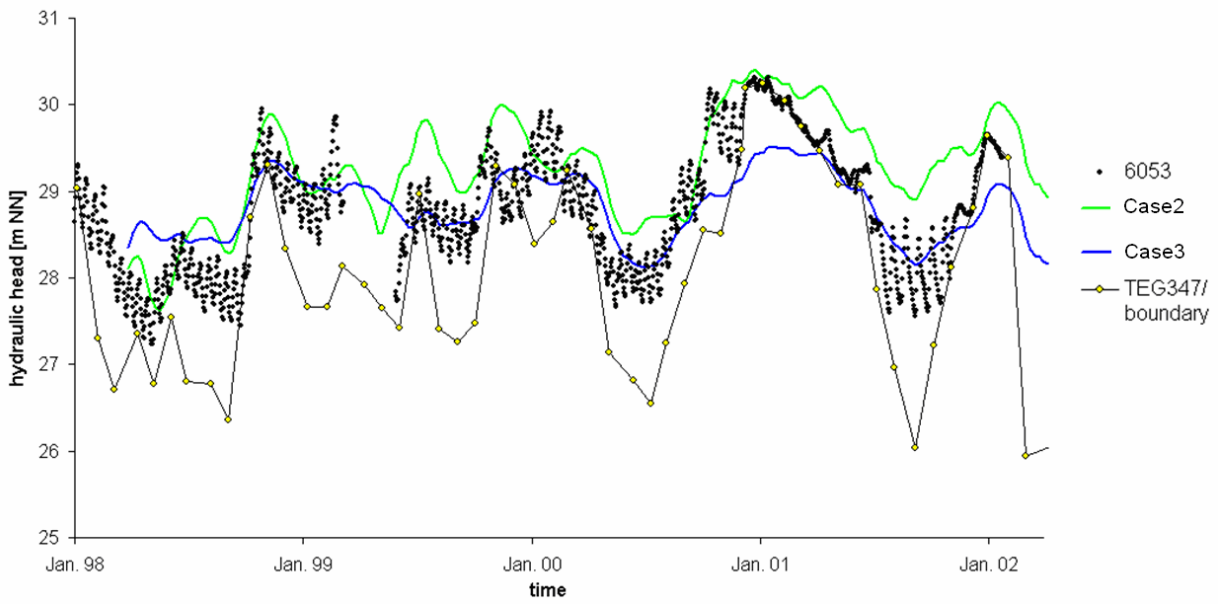

Figure 54: Observed (black dots) and simulated (blue line) hydraulic heads at observation well 3301 with the conductivity of the lake bed following Case3. The green line are simulated hydraulic heads with Case2, the black line with the yellow dots are observed heads at TEG347 which are introduced as 1st type boundary condition. The arithmetic mean of observation well 6053 between 1st Apr. 1998 and 28th Jan. 2002 is $\overline{\mu} = 28.81$ m NN for observed heads, $\overline{\mu} = 29.23$ m NN for Case2 and $\overline{\mu} = 28.84$ for Case3.

The current parameterisation reproduces the most important temporal behaviour. However, 2 items are not reproduced satisfactory: On the one hand, at very high pumpage, like in Summer 2000 or in summer 2003 the drawdown is slightly too small, on the other hand in 2004 the heads increase too slow and the trend of the measured hydraulic heads is still too steep. Compared to time invariant leakance however (fig. 41), the temporal behaviour is significantly improved. Though the fit is not as close like using a temporal function of Case2, the objective function increases from about $\Phi \approx 50$ [-] to $\Phi \approx 110$ [-], but the reduction from 45 to 2 parameters is a significant improvement in parameter parsimony and solution uniqueness.

3.4.3. Discussion Leakance

The infiltration from Lake Tegel into the aquifer is the most uncertain hydraulic process within the current model. It is determined by clogging processes, about which numerous studies exist, still with increasing trend of publications. This illustrates the relevance of the issue, the variability of system behaviour and the lack of a coherent theory. On

phenomenological level, five mechanisms are distinguished (Dillon et al. 1999), and their relevance is assessed. The spatial distribution is poorly known. Until 2004, only scarce measurements had been carried out (Sievers 2001). Previous modelling studies determined leakance under steady state conditions (Eichhorn 2000, Rümmler 2003).

Measurements

Clogging processes control the magnitude and dynamic of infiltration. The sandy lake bottom with grain sizes of 0.2 to 0.3 mm (Sievers 2001, Hoffmann and Gunkel 2006) would result in leakance 50 to 100 times higher than measured by the author within this study and Hoffmann and Gunkel (2006) und up to 1000 times higher than modelled values. Thus clogging processes determine the infiltration. A thorough analysis of these processes is essential for understanding bank filtration, for quantity aspects and especially under conditions of low groundwater levels, when hydraulic contact between surface water and groundwater is cut off and infiltration is hydraulically independent of the groundwater table. Field measurements of infiltration have been carried out by the author in summer 2004. At the end of 2004, when NASRI field measurements stopped, it turned out that leakance is temporal variant and seriously affects infiltration. At this point it was too late to initiate further measurements in order to identify temporal and spatial infiltration characteristics. This gap is partly closed by measurements by Hoffmann and Gunkel (2006), started March 2004 until February 2005, which are included in this discussion. Some characteristics are revealed and indications for the importance of controlling mechanisms are drawn.

Hoffmann and Gunkel (2006) carried out infiltration measurements from March 2004 to February 2005 at seven locations. Every three weeks the devices for infiltration measurement have been installed at identical positions. During 4 subsequent days infiltration and hydraulic heads in 2 cm depth have been measured. The leakance obtained is presented in figure 55. The magnitude and variability of the values are comparable to measurements carried out within this study. The minimum of $2*10^{-7}$ s^{-1} is identical, the maximum of $2.4*10^{-5}$ s^{-1} (Hoffmann and Gunkel (2006) is only slightly higher than $7.5*10^{-6}$ s^{-1} measured in this study. The arithmetic mean of Hoffmann and Gunkel's measurements is $4.5*10^{-6}$ s^{-1}, similar to $2.3*10^{-6}$ s^{-1} obtained within this study. Taking into account the variability and temporal dynamic in conjunction with the logarithmic behaviour of the leakance the difference of factor 2 between the measurements is considered to be not significant.

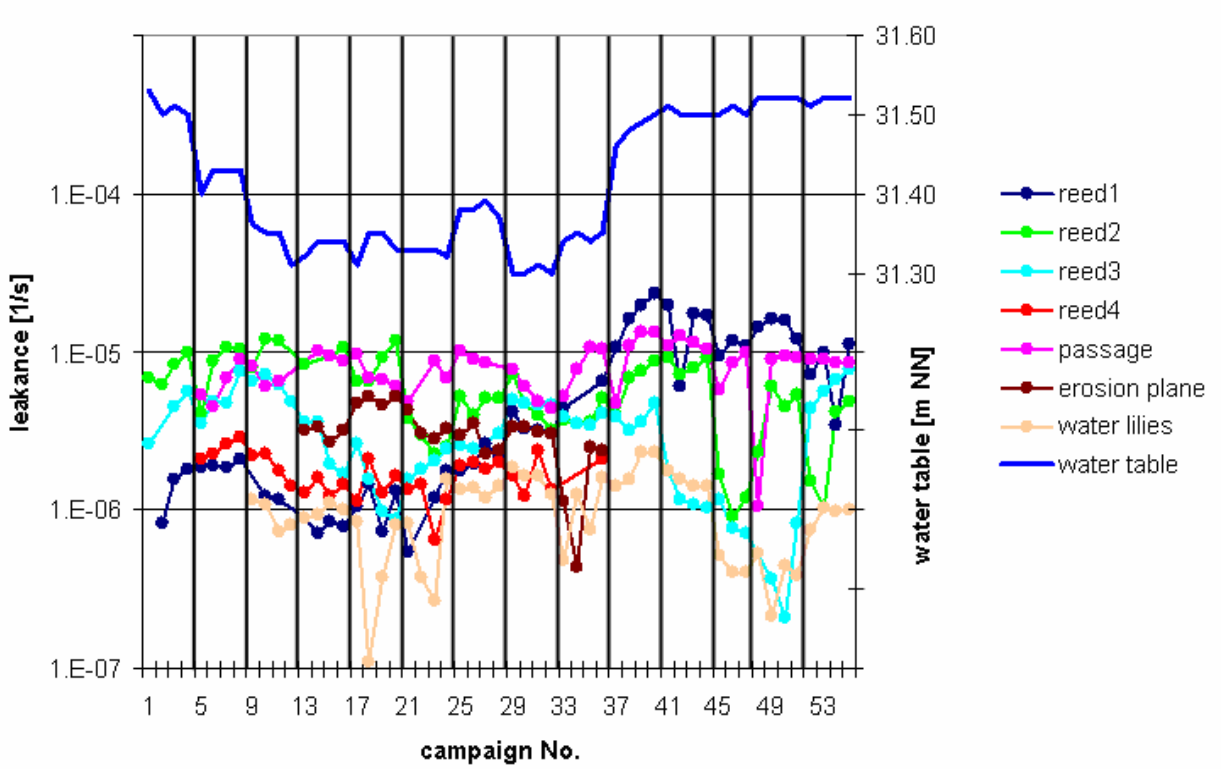

Figure 55: Leakance calculated with infiltration measurements of Hoffmann and Gunkel (2006). Measurements have been carried out between March 2004 and February 2005. The blue line without markers represents the water table (right axis). The lines with markers represent the temporal development of the leakance at 7 measurement locations and belong to the left y-axis. The x-axis represents the campaigns. Black vertical lines indicate an interval of 17 days without measurements, otherwise measurements are carried out at subsequent days.

The ratio between a theoretical leakance, calculated by the hydraulic head loss of the upper 2 cm and the total leakance, is shown in figure 56. This ratio is manifestly less variable at the timescale of days than the leakance itself. The reason may lie in the clogging processes themselves as they change the hydraulic conductivity in different depths in the same manner. But probably the short term variations shown in figure 55 occur due to measurement errors affecting both, the calculation of leakance of the upper 2 cm and total leakance, thus the ratio stays constant. The most pronounced example occurred at the position “water lilies” between campaign 17 and 20. The interval between the daily subsequent campaigns usually is 17 days, indicated by black vertical lines. Within this time, the change of the ratio is higher than within subsequent campaigns, probably due to the change of subsurface properties. The ratio can be regarded as an indication for the controlling depth of infiltration, between campaign 29 and 37 (Aug. 17th 2004 and Oct. 18th 2004) the controlling depth moves upwards towards the water sediment interface. Groundwater level drops about 75 cm between the beginning of July and middle of August. As in this period the reduced zone below Lake Tegel shrinks from about 20 cm to about 5 cm (Hoffmann and Gunkel 2006). Either an aeration by falling groundwater levels may occur or the decreasing water temperature in this period may slow down biological

metabolism and increase the oxidation potential. Since increased clogging leads to low redox states and vice versa (Styfzand et al. 2004), the two processes probably affect each other. However, neither measurements nor modelling with Case2 indicate that the leakance increases during this period.

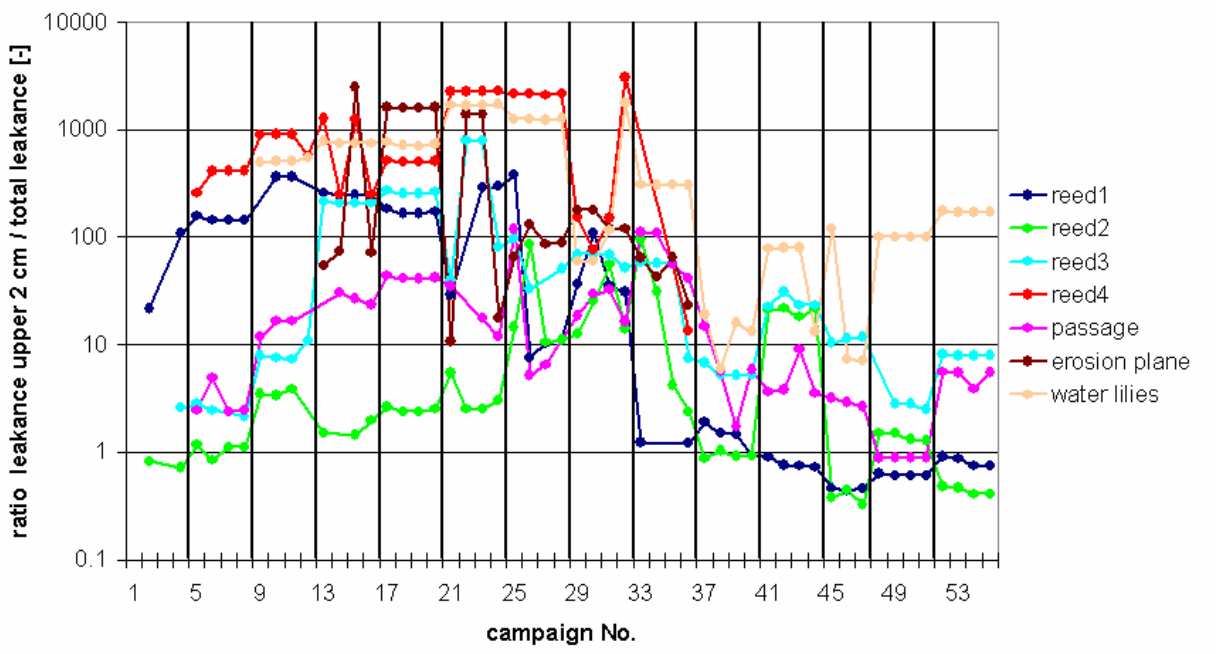

Figure 56: Ratio of leakance calculated by k_f values for the upper 2 cm and (total) leakance obtained by measurements of Hoffmann and Gunkel (2006). The x axis represents the campaigns. Black vertical lines represent an interval of three weeks where no measurements have been carried out, otherwise measurements are carried out at subsequent days. The colours and positions are identical to figure 55.

Most studies on clogging about water recharge refer to aquifer storage and recovery, soil columns, infiltration ponds or rivers, while most publications for the latter are limited to the description of physical clogging (eg. Stuyfzand et al. 2004, Schubert 2002) These publications report the effect of physical clogging by river sediment and bed load transport. Spatially distributed infiltration by bioclogging in a 2D laboratory experiment is described by Seifert et al. (2005). A comprehensive investigation of clogging and geochemical processes during infiltration in Lake Tegel actually is subject of investigation by Hoffmann and Gunkel (2006). Clogging during ASR (Aquifer Storage and Recovery) is a more intensive subject of investigation, Dillon et al. (1999) assume the principal processes to be the same as clogging at infiltration areas with free surface. Dillon et al. (1999) classify the following clogging processes:

1. physical clogging by suspended solids and organic matter
2. dispersion of clay minerals or rearrangement of fine material within the aquifer
3. chemical clogging by precipitation of minerals on the surface of aquifer materials
4. biological clogging due to growth of micro-organisms and associated polysaccharides,
5. gas binding through release of entrained air or production of gases

Item 1 and 2

Unlike infiltration velocities the leakance of figure 40 and 55 can be regarded as a property of the subsurface. The high spatial variation shows that physical clogging (item 1) does not determine infiltration, this would reduce the permeability at zones of high infiltration by inclusion of particular matter and lead to spatially similar values. Besides it would be almost irreversible which is in contradiction to the long history of bank filtration at Lake Tegel since 1900 and the temporal variant leakance as reported within this study and measured by Hoffmann and Gunkel (2006) (fig. 55). Core samples by Sievers (2001) gave no hint for internal physical clogging. No correlation to suspended matter or algal biomass could be found. The spatial and temporal variability is an indication for pore flushing, the opposite effect of pore congestion. High infiltration rates seem to stabilize themselves.

Item 3

During ASR chemical clogging is known to occur e.g. Dillon et al. (1999). Schubert (2002) mentions the possibility of precipitation of e.g. $FeCO_3$ under anaerobic conditions. Nevertheless, it probably affects the infiltration characteristics. Sievers (2001) measured calcium concentrations of 10 to 16 mg/g in the grain size fraction smaller than 0.02 mm. Values in the bigger fraction probably are lower, but in the same order of magnitude. For a significant clogging concentrations appear to be too low.

Hoffmann (2006) measured significant calcium concentrations in a sequence of core samples taken in the upper 5 cm of the sediment with concentrations between 5 and 50 mg/g. These would result in calcite concentrations between 12.5 and 125 mg/g or gypsum between 17 and 170 mg/g, the higher values may affect infiltration. Surface water quality does not seem to affect leakance via chemical clogging as no significant correlation to concentrations could be found.

Item 4

Preferential flow by bioclogging in 2-D laboratory experiments is described by Seifert et al. (2005). Permeability may be reduced by factor 1000 with a pronounced spatial pattern which reason could not be identified. High spatial variability on a short distance (fig. 38) is a hint that

spatially distributed bioclogging occurs. Hoffmann and Gunkel (2006) detects several biogeochemical reactions in the lake bed which suggest that chemical or bioclogging occur, partially 50% of the pore space is filled with biomass, however direct effects on leakance and infiltration can not be quantified yet. Significant correlations to leakance could only be found at nitrate and pumping rate. Mechanisms relating these points to bioclogging are not obvious, a detailed analysis would exceed this study.

Item 5

Gas bubbles were not detected as infiltration was measured in this study, nor by Sievers (2001). Hoffmann and Gunkel (2006) rarely observed big amounts of entrapped air in the sediment, especially in spring. Concentrations of other gases were very low. Normally no gas was detected. Presumably only in spring, gas concentrations may affect infiltration, which is in accordance with temporal variant leakance being low in May 2004, see figure 43.

Synthesis

The variability of the measured leakance covers 2 orders of magnitude. By means of modelling it could be demonstrated that the leakance of the entire infiltration area varies by factor 4 (Case2), but it is not necessarily a contradiction. For determining a mean leakance, the arithmetic mean has to be applied but the distribution is of a logarithmic kind, so the highest values are most important for the mean. Only the number, not the value, of low leakance measurements affect the mean value. Single measurements on a small area always vary more than spatial average values.

For steady state models a good fit with high leakance at low depths can be obtained, e.g. Eichhorn (2000), Rümmler (2003), Wolf (2004), Holzbecher (2006). At lake Stechlin constant leakance appears to be applicable (Nützmann et al. 2003). Representing the bank with a 3rd type boundary condition, WASY (2004) achieves a fair fit for transient modelling of the year 2002. However, since the groundwater table usually is at least 2 m below the surface water table the boundary condition changes from 3rd type to 2nd type, transient modelling becomes impossible under these conditions. Either the heads are far too high or the model totally drains.

However, the measurements may systematically overestimate the leakance. Leakance measurements by Nogeitzig (2005) with the open end test following Langguth and Voigt (1980) at Lake Wannsee give the impression of a patchwork with only weak depth dependence (fig. 57), a distinct decrease in conductivity is only visible in the transition zone where the mud begins. The measured leakance has values between 10^{-6} s^{-1} and 10^{-4} s^{-1} and a mean of $5*10^{-5}$ s^{-1} up to a water depth of 6 m. Modelling in that area in contrast results in values between $2*10^{-7}$

s^1 and $3*10^{-6}$ s^{-1} (Holzbecher 2006) and $1.5*10^{-6}$ s^{-1} (Wolf 2004), while the high values are only applied at water depth smaller than 2 m. The water budget errors can not be assessed. Very conservatively the water budget error is assumed to be less than factor 2. The measurements have been carried out thoroughly with a high density on a large area up to high water depths. A statistical error can be excluded, the possible influence of the water budget error is not sufficient, the measurements can be identified as systematically overestimating the leakance by 1 or 2 orders of magnitude. Probably the clogging layer is disturbed due to the penetration of the measurement device. In the same way the measurements at Lake Tegel may overestimate the leakance. Here the usual suspect of spatial heterogeneity shows up. All measurements have been carried out along a 150 m long bank section just in front of the transect. Modelled values are valid for the entire bank with a length of 1.5 km and additionally the bank of Reiswerder and Scharfenberg. Leakance might be locally higher in the region where the measurements have been carried out.

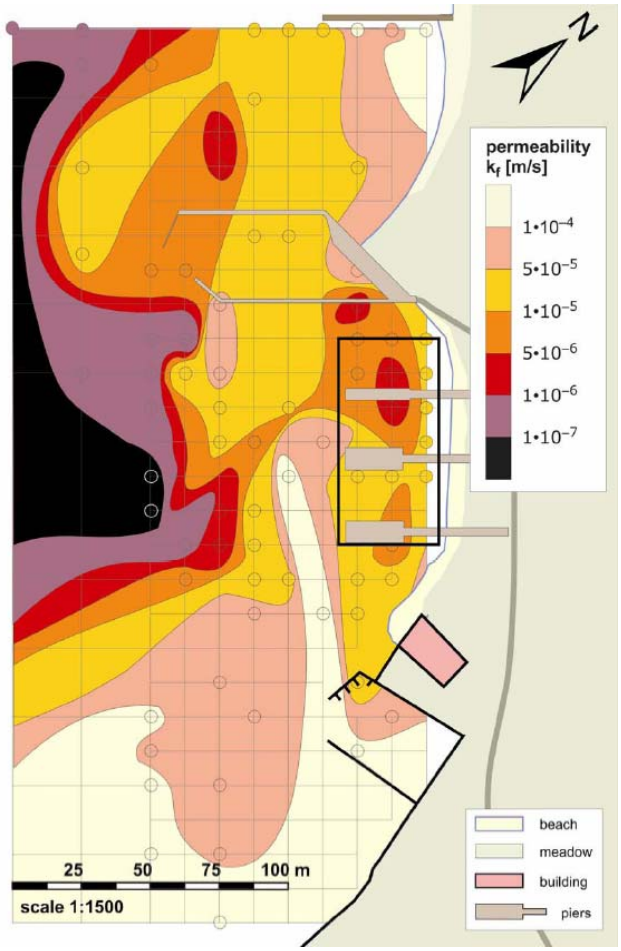

Figure 57: Hydraulic conductivity at the bank filtration site Lake Wannsee, determined with transient permeability tests. Circles indicate that measured k_f values are identical to leakance as the reference depth is 1m, see Nogeitzig (2005)

Just considering hydraulic factors of influence, a fair fit (fig. 41) only can be obtained by decreasing the magnitude of the leakance and applying similar values to the mud free zone of

Lake Tegel up to a depth of 7 m (Parchur 1977, Brühl et al. 1986, Ripl. et al. 1987). This couples the amounts of infiltrated water to the groundwater table. Just with 2 or 3 years of transient modelling, possibly the leakance would not have been detected to be temporally variant. However, no good fit can be obtained with a temporally constant leakance. Several parameter combinations between Case1 and Case2 of depth distribution and temporal variance of the leakance provide the correct water balance and lead to good fits of observed and simulated hydraulic heads. It is a nice example, how a model provides a good fit and meaningful results with a process which is described physically totally wrong. At Case2 the infiltration just follows a temporally fitted curve, without physical sense. The depth dependence of infiltration velocity is far too high in deep regions (fig. 70, fig. 71). But the important point for the entire model is that the amounts of infiltrating water are rather correct.

Several counter-indications exist that the leakance measurements at Lake Tegel highly deviate from the real values. The infiltration for the determination of the leakance by Hoffmann and Gunkel (2006) and within this study is measured applied a different principle than measurements by Nogeitzig (2005) with less disturbance of the clogging layer. The devices of Hoffmann and Gunkel stayed 4 days in the ground, the leakance does not show a decreasing trend, which would be an indication for reestablishing of a damaged clogging layer. Measurements carried out within this study additionally indicate leakance decreases with water depth, however only 2 values at one location exist for a water column of more than 3 m.

In comparison to temporally constant leakance, Case3 is the only approach which significantly reduces the difference between observed and simulated hydraulic heads. Simulated values for the leakance are closer to the measurements, the difference is reduced from factor 5-10 to only 1.5-3 and moreover it suggests a mechanism how the groundwater table might affect the clogging layer. The hypothesis is that temporal variant leakance occurs due to a change of the pore structure of the clogging layer due to aeration from below. In contrast to the mathematical formulation of Case3 (eq. 32) the assumed reason which changes the pore structure is not the thickness of the unsaturated zone, but intrusion of oxygen. This oxygen is consumed by the DOC reduction during infiltration. The decrease of redox potential has been observed at O_2, NO_3 and less pronounced at other species, between observation wells 3310 and 3311 (fig. 6), 3310 located at the fringe of Lake Tegel, 3311 about 8 m away towards the middle of the lake. Okubo and Matsumoto (1979, 1983) observe rapid reduction of hydraulic conductivity in column experiments when the milieu becomes anoxic, Wood and Basset (1975) observed a dramatic decrease in infiltration rate in artificial recharge ponds when sulphate reducing conditions occur. Hoelen et al. (2006) observed significantly reduced

hydraulic conductivity in a bioremediation site when sulphate reduction occurs. Schubert (2002) reports the possibility of chemical clogging under anaerobic conditions, e.g. through the precipitation of $FeCO_3$. High oxygen concentrations presumably only occur near the fringe between water and bank and increase the leakance here. Short term variations of the water table do not allow air to penetrate to deeper regions, it can only be exchanged near the fringe, similar to a diver who has a too long snorkel. The unsaturated zone below the lake can be compared to the lung volume. The leakance increases at low groundwater tables, because the unsaturated volume below the lake also increases and more oxygen can be sucked below the lake. Possibly deeper regions are also affected, but the increase in leakance is less pronounced since oxygen concentrations are lower. This behaviour is approximated with Case3, but since it only accounts for the magnitude and not the variation of the unsaturated zone the description is inaccurate. In 1998 the simulated heads at 3301 are about 1 m too high, from summer 2003 on about 0.5 m too low. The heads at the drawdown events in 2000 and 2003 are simulated a little too high. Possibly, other mechanisms, e.g. the temperature dependence of the k_f and clogging, nitrate concentration or microfauna also affect the leakance.

Interpreting the temporal variant leakance mainly as the result of processes within the unsaturated zone, the modelled hydraulic heads, the measured values and physical mechanism give a coherent picture. However, one counter-indication exists: In summer 2004 the water table drops by 2 m (fig. 53), which is not reflected by the measurements (fig. 55). This would mean the high spatial and temporal variability masks the effect or the significant changes occur in deeper regions. The thickness of the saturated zone below Lake Tegel, where the clogging occurs, however decreases in this time, supporting the aeration hypothesis.

At artificial recharge ponds infiltration strongly decreases upon the formation of an unsaturated zone (Greskowiak et al. 2005). In contrast to the present field site infiltration dynamics at the particular system is controlled by physical clogging, fine grained matter and organics form the low permeable layer. The pore structure is much finer than the clogging layer at the transect, the matrix potential is high and inhibits the intrusion of air.

Except for the pumping rate also nitrate is identified to show a significant positive correlation to the magnitude of the leakance. Since the clogging processes appear to be triggered by the alternation between saturated and unsaturated conditions and thus the redox state, and nitrate acts as terminal electron acceptor, it might lift the redox potential and this way negatively affects clogging. Concentrations in 1998/1999 are much lower than 2004/2005 and the leakance using Case3 is overestimated in 1998/1999 and underestimated it 2004/2005. This supports the hypothesis. A counter-indication however is that oxygen concentrations in

contrast are not correlated to the leakance though the temporal variation in useable terminal electron acceptors is similar to the variation of those by nitrate. Oxygen shows strong seasonal behaviour so its influence may be masked by other seasonal effects. Within this study however it can not be judged whether nitrates affects the leakance or just an illusory correlation exists.

Alternating and discontinuous well operation causes increased atmospheric exchange of the unsaturated zone and a higher redox state below the lake and as a consequence higher infiltration rates and less drawdown compared to a uniform pumping regime.

The mechanism that the leakance is triggered by the unsaturated zone also would explain observed infiltration of Schubert (2002) on the cross section of the river bed. Most water infiltrates at the shallow area. Probably the zone is unsaturated, but no information is given about this topic.

Upshot

Leakance has been identified to be temporally variable. Physical clogging, dispersion of clay minerals or rearrangement of fine particles can be rejected. Gas bubbles have been detected only in spring, their impact near the bank is probably small. Chemical and/or bioclogging appears to be of importance, triggered by the existence of an unsaturated zone and/or aeration from below, infiltration increases when the extent of the unsaturated zone increases. Nitrate possibly decreases clogging, its impact should be further investigated. Holländer et al. (2005) found the same ranking of the processes.

Though it might appear strange that the leakance is time variant and infiltration is higher where the bank below the lake is unsaturated though head differences are smaller, all other hypotheses could be eliminated as impossible, whatever remains, however improbable, must be the truth (Doyle 1890).

This behaviour probably causes increased groundwater levels at alternating and discontinuous pumping regimes compared to smooth and uniform pumping regimes.

Confidence about the mechanisms of temporal variant leakance may only be obtained in further studies. More measurements should be carried out, especially in water depths considerably deeper than 1 m, but up to 7 m and, if possible, in zones where plant roots of reed or water lilies penetrate the bank.

For the following calculations the parameterisation of bank conductivity follows Case2. Though Case3 gives a better representation from the mechanistical point of view, the process understanding is rudimentary and considerable deviations occur. The amounts of infiltrated water are correct with applying Case2. Consequently, since the water balance is of higher

priority to the performance of the model than the position of infiltration, all computations are carried out using Case2.

3.5. Water Balance

The source of abstracted water is a key question and topic of continuous discussion of scientists and waterworks. Looking directly at the Well Field West we have the special situation of some water infiltrating at the opposite bank flowing below the lake towards the wells (fig. 58, fig. 59). This study provides estimates for these ratios, the first time determined transiently and taking into account the temporal variation of the leakance.

The sources of water at Well Field West are bank filtrate and inland water. Bank filtrate can be classified to young water infiltrated directly in front of the transect, medium aged water infiltrated near Reiswerder and old water infiltrated at Scharfenberg and the western bank. This results in the remarkable situation that the bank filtrate catchment of Well 13 consists of 3 spatially separated areas (fig. 59). The old water has an age of more than 10 years, containing elevated concentrations of phenazone and its degradation products, e.g. AMDOPH. The existence of the fraction is verified by chemical composition in TEG374 (fig. 59). At Well 12 and 13 the medium aged fraction can be distinguished because the distance to Reiswerder is large enough to induce a gap in the residence time of the two fractions. Due to the proximity to Reiswerder, this is not possible in Well 14, the areas which are separated for Well 13 merge. The flow lateral to the bank is induced by the large areas of shallow water around Reiswerder.

Observation well 3301 contains young and medium bank filtrate in temporally variant fractions. Travel times of the young fraction are about 3 to 4 months (Massmann et al. 2004) obtained by evaluating the time shift of ^{18}O and deuterium. Numerical simulations show an age varying between 80 and 150 days between spring 2002 and summer 2004 (chapter 4.6., fig. 76). The ages coincide quite well, but numerical results show a larger variability as weekly intervals allow higher temporal resolution than tracer data with a seasonal signal. However, age dating by Tritium-Helium method shows an age of 20 month in observation well 3301 (Pekdeger 2006). As a large portion is young bank filtrate with 3-4 month age, the smaller portion is considerably older. NASRI (2004) considers the difference in age as result of 3% of old bank filtrate. Simulations and tracer data additionally suggest a large ratio of medium aged bank filtrate.

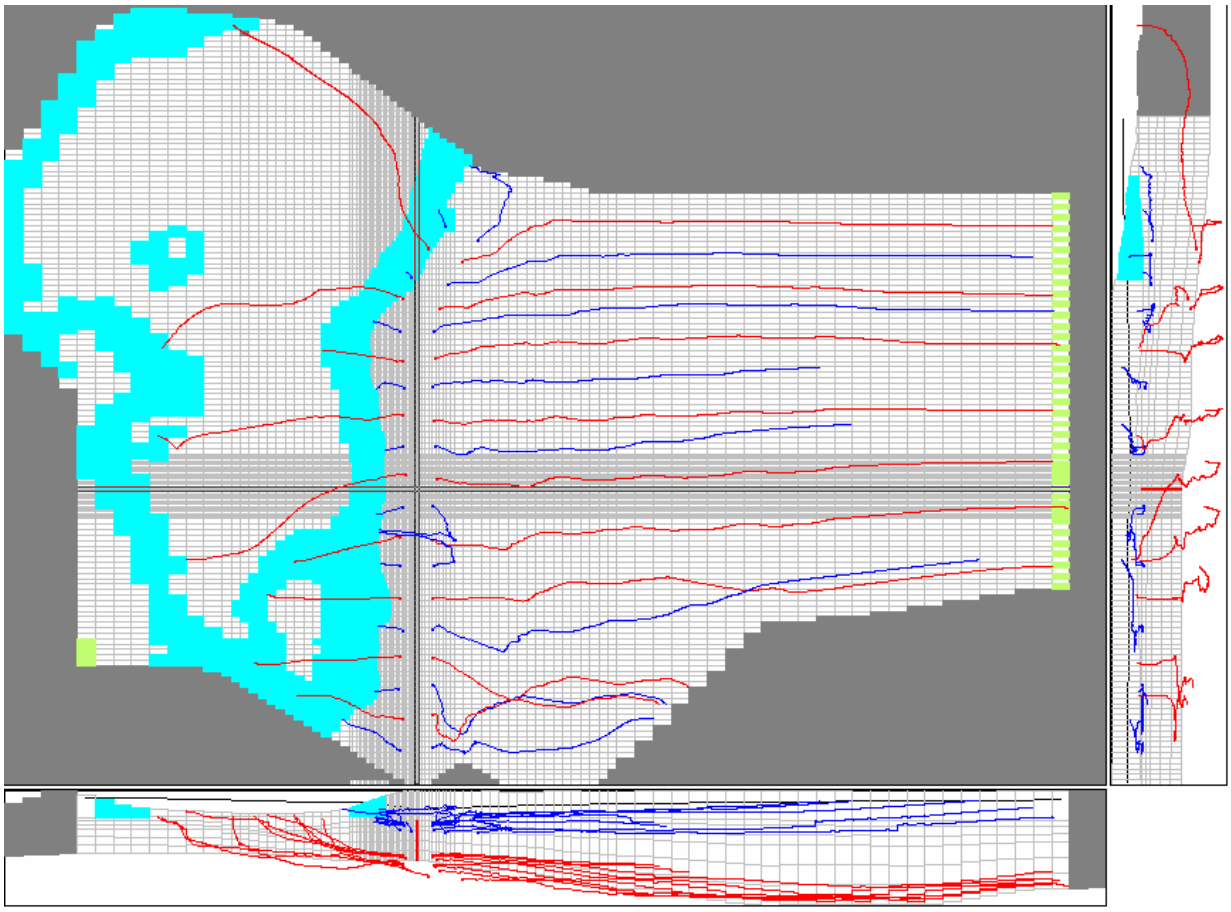

Figure 58: Backward pathlines from the April 30th 2005, until the particles reach a cell with a source. The rectangular pictures at the right and at the bottom show cross-sectional views. Red lines are started in the lowest model layer, directly above the lower aquitard, blue lines are started in the third model, directly below the glacial till. Usually flow is perpendicular to the well field. However, especially inland in direct vicinity of the well field the directions change considerably, but these changes level out in average. The 5th and 6th (counted from below) shallow (blue) inland flowline come show that bank filtrate penetrates inland passes by holes in the glacial till and flows to the abstraction well from behind. The inland flowlines at the bottom show that this area, neighboured to well field Saatwinkel, is subject of strong variations in flow direction, almost up to 180°. Regarding the bank filtrate it is obvious that the shallow water always is young bank filtrate, the water at the bottom of the aquifer partly derives from the opposite bank of Lake Tegel.

Concentrations of chloride (fig. 61), boron (fig. 62) and sodium (fig. App26, appendix) in observation well 3301 are significantly higher than concentrations in Lake Tegel 3 to 4 months ago. This is an indication for the presence of medium aged bank filtrate. Assuming chloride as being unretarded and taking into account a retardation factor of boron of 1.3 to 2.1 (De Simone et al. 1997), the water has a minimum age of 1 year if it is not diluted. Observation well 3301 shows a clear temperature and ^{18}O signal, thus still containing considerable amounts of young bank filtrate and it only contains a small ratio of medium bank filtrate. Probably it is older and less than 50% of total water derive from Reiswerder. This infiltrated when concentrations of chloride (fig. 61) and boron (fig. 62) have been higher than the observed 59 mg/l chloride and 290 µg/l boron in May 2002. The long term concentrations in Lake Tegel of chloride and boron are plotted in the appendix, (fig. App5 and fig. App6).

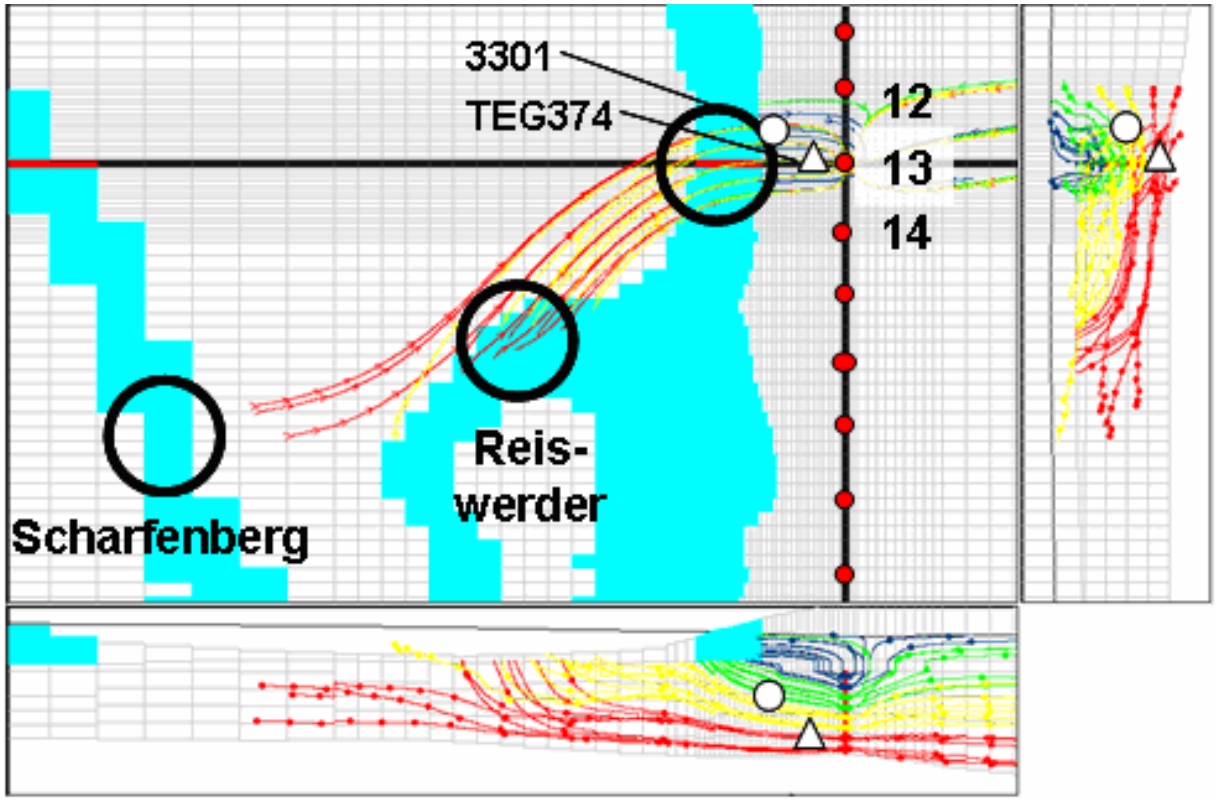

Figure 59: Backward flowlines from Well 13, view from top (big image), and two cross sections along the black cross on the top view (right and bottom image). Total simulation length is 10 years, tick labels mark an interval of 1 year. The lower and right cross sections are projections along the axes of the black lines. A stationary flow field between January and March 2001 is extrapolated to the duration of 10 years. A colour ramp from blue to red is used to mark particles arriving in different depths of Well 13, big black circles indicate their infiltration area. Small red circles indicate wells, the white circle indicates observation well 3301, the white triangle observation well TEG374. The turquoise areas indicate leakance from Lake Tegel into the groundwater. The top view is a zoom of figure 13.

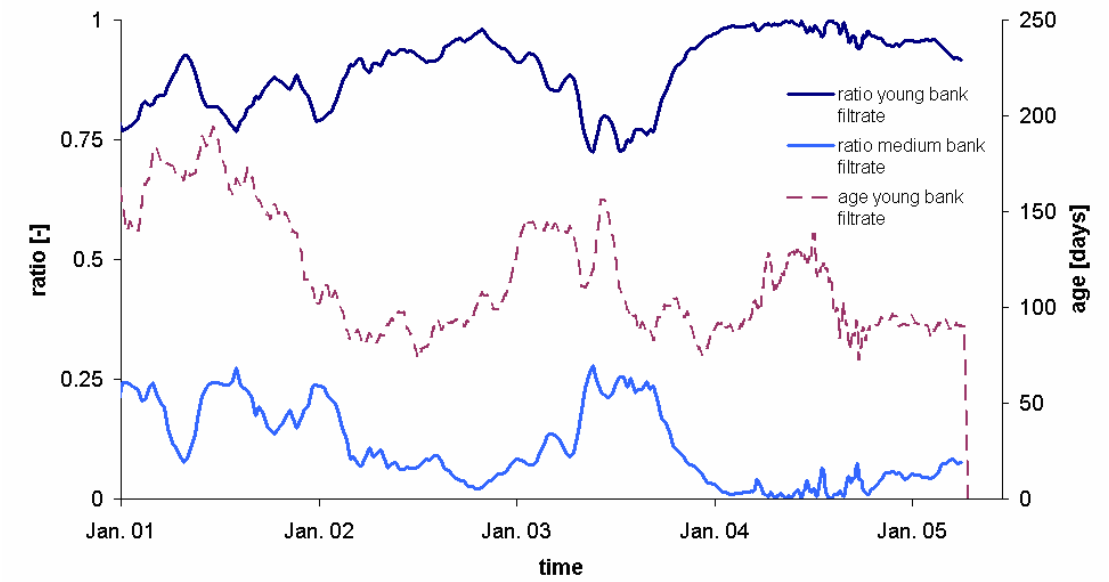

Figure 60: Dark blue and light blue curves show ratios of young and medium bank filtrate in observation well 3301. The violet dashed curve shows the age of the young bank filtrate.

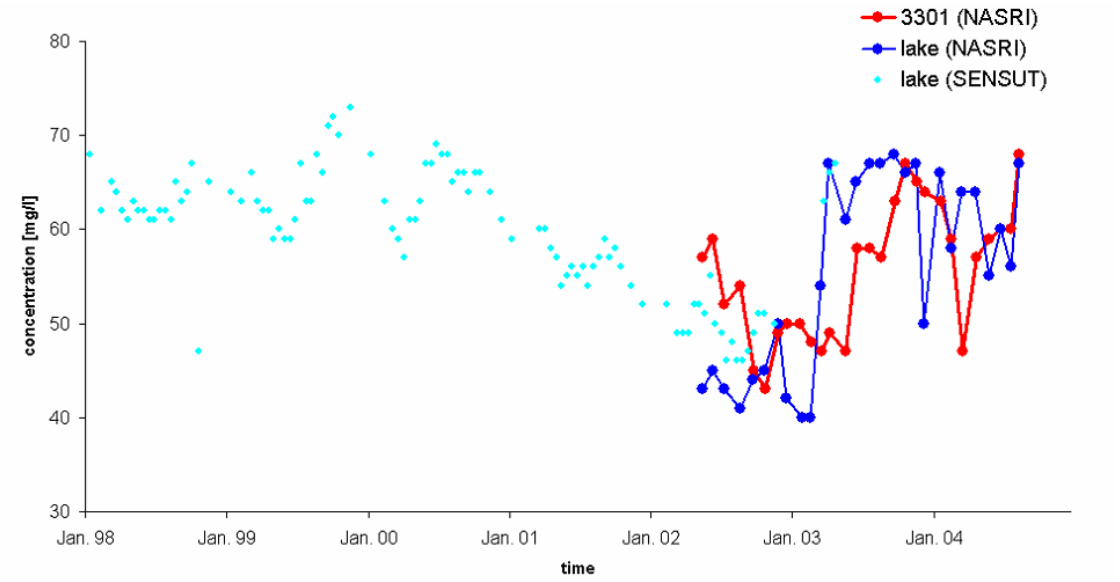

Figure 61: Chloride concentration in observation well 3301 and Lake Tegel. The red line represents the concentration in observation well 3301, the dark blue line represents the concentration in Lake Tegel in front of the transect, (KWB2005). The light blue circles indicate concentrations measured north of waterworks Tegel by SENSUT (2004). In summer 2002 concentrations in observation well 3301 correspond to concentrations in Lake Tegel in winter 2000/01.

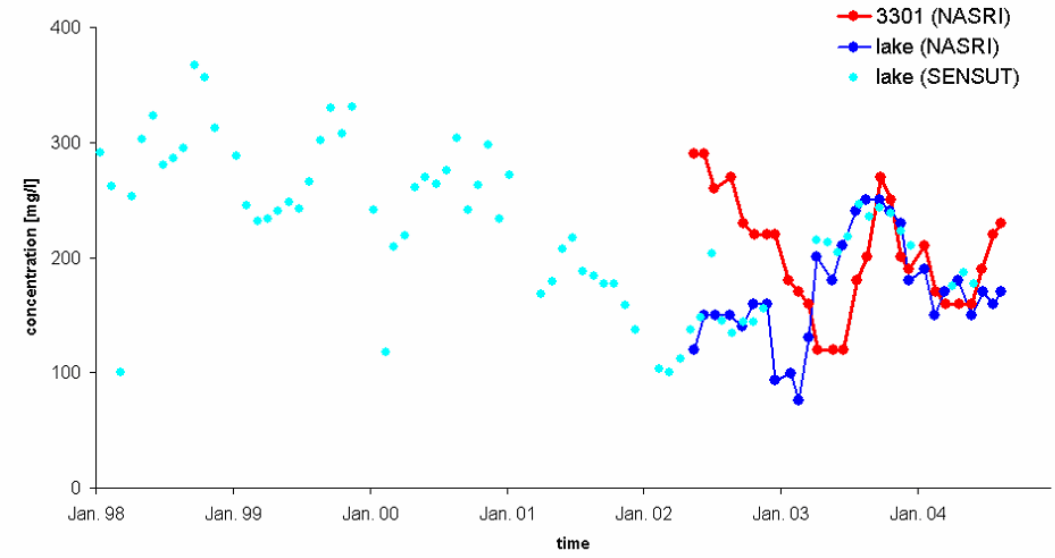

Figure 62: Boron concentration in observation well 3301 and Lake Tegel. The red line represents the concentration in observation well 3301, the dark blue line represents the concentration in Lake Tegel in front of the transect (KWB2005). The light blue circles indicate concentrations measured north of waterworks Tegel by SENSUT . Until 2003 concentrations in observation well 3301 correspond to lake concentrations in 2000 (2004). Taking into account a retardation factor of boron of 1.3 to 2.1 flow times are at least 20 month.

In observation well 3301 simulation results in 20% medium aged bank filtrate between 2001 until February 2002 and decrease in March until April 2003 to values of about 7% (fig. 60). These ratios are too low to match the high concentrations of chloride and boron. Additionally the simulated values decrease 5 months earlier for chloride and 8 months for boron compared to the measurements. The mismatch probably occurs because the exact configuration of the glacial till being present below the infiltration area is not known. The

principal behaviour however, of observation well 3301 containing a portion of medium bank filtrate is shown.

In 2002 and beginning of 2003 AMDOPH concentrations in observation wells 3301, 3302 and TEG371up are also elevated. For observation well 3301 Pekdeger (2006) assumes small portions of old bank filtrate as reason and calculates a ratio of 3% in 3301.

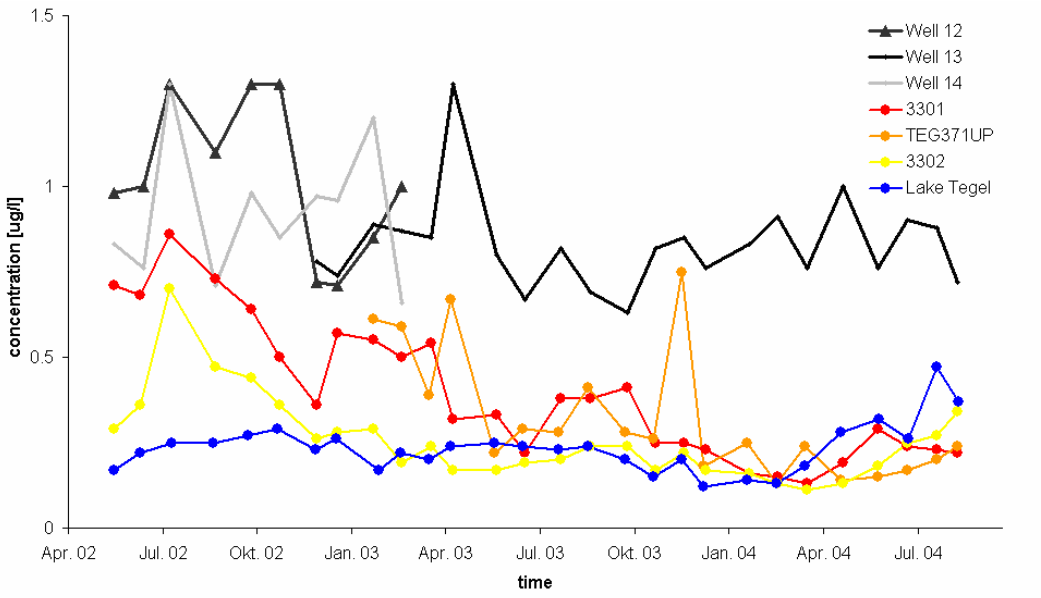

Figure 63: Observation and abstraction wells containing elevated concentrations of AMDOPH (KWB 2005) which are significantly higher than concentrations of young bank filtrate.

It is surprising to find AMDOPH as indicator for old bank filtrate in the transition zone of young and medium bank filtrate. Three reasons seem to be possible:

i. In the subduction zone of medium and old bank filtrate north of Reiswerder (fig. 66) and the highly transient pumping regime all 3 waters mix and are present within observation well 3301. Simulations show 0% to 1% old bank filtrate, but regarding the spatial discretisation and the accuracy of the transport model it could be caused by numerical dispersion. In reality the transition zone probably is sharper and the variation of the ratios is probably higher. Numerical dispersion occurs, as layers have a thickness of up to 6 m. In front of the infiltration zone, the layer structure is adapted to the bathymetry of Lake Tegel (fig. 17) which causes considerable inaccuracy in transport calculations using MT3DMS.

ii. It is possible as well that phenazone and its derivates as the precursors of AMDOPH are present in high concentrations in the medium aged bank filtrate, as lake concentrations before spring 2002 are unknown. The production site where phenazone comes from is located upstream of Lake Tegel directly at the Havel (fig. 1) and has been closed about in 1998 (Dünnbier 2005), but in the subsurface

extremely high concentrations are still present. The legacy is subject of remediation, and spilling of extracted water can not be excluded.

iii. As observation well 3301 is just located in the transition zone between young and medium bank filtrate, model results may not reproduce the exact behaviour. Dissolved substances as chloride, boron, sodium show different retardation and interaction with the aquifer matrix leading to a mixture which can not be described by one ratio because the different constituents behave differently. Thus mixing calculations with chloride, boron, 18O and sodium result in different ratios. Concentrations of boron (fig. 62) suggest 100% medium aged water while concentrations of 18O suggest almost all water derives from young bank filtrate (fig. 74). Three observation wells (fig. 63FIG) show elevated concentrations of AMDOPH, but only observation well 3301 shows old bank filtrate in simulations. Observation well TEG371up is located 10 m higher than observation well 3301 and shows until April 2003 even higher concentrations (fig. 63). Observation well TEG371up shows similar behaviour for boron and chloride. This observation well is much higher than the depths where medium or even old bank filtrate might appear. Mixing behaviour at the transition zone can not be the reason. Geological profiles of Voigt et al. (2000) show the direct vicinity of Lake Tegel being free of the glacial till which separates the first and the second aquifer, the hydraulic conductivity below the lake is homogeneous and vertically well permeable. Using this geological model, the old and medium aged bank filtrate is pressed to the lowest regions of the aquifer by infiltration in front of the transect (fig. 66).

Regarding the formation of Lake Tegel as result of a glacier excavating the till from the former ice age and subsequent melting of residual ice (Pachur 1987), it can not be justified why 10th of metres sand should have been sedimentated around the former lake bed and then suddenly sedimentation of mud began. It seems more reasonable that the till only is excavated up to Lake Tegels deepest extent, the geologic structure of the adjacent aquifers is not disturbed by formation of Lake Tegel . Thus the till is connected to the former lake bed and thus also to the sediments. However, it probably still is not homogeneous, but similar to the region around the transect a patchwork with different conductivities. Such impermeable layers would shield the pressure of infiltration and as well old as medium aged bank filtrate could flow directly below or above towards the transect. Regarding the observations of AMDOPH, chloride, boron, sodium etc. in observation wells 3301, 3302 and TEG371up in 2002 the

hypothesis seems to be resonable. Especially observations at TEG371up, located at an elevation of 22.7 m directly below the glacial till and far away from modelled mixing zones support this hypothesis. Introducing glacial till below Lake Tegel into the model changes the flow regime such that a ratio of old bank filtrate reaching observation wells TEG371up and 3301.

With the presently used hydrogeological model, where no till is present below Lake Tegel, the old bank filtrate mainly is extracted at wells 12, 13, 14 (fig. 66) because the hydraulic potential created by the large regions of infiltration around Reiswerder causes displacement of old bank filtrate and the ratio in wells 16 to 24 is nil or very low. Observed concentrations of phenazone around 1 mg/l at the transect and e.g. in Well 20 to 24 (located directly in front of Reiswerder) suggest the old bank filtrate is not entirely replaced by water from Reiswerder. Two possibilities exist: (i) The pressure from the shallow regions is sheltered by the glacial till. (ii) Computing the infiltration dynamics according to Case3 the reduced hydraulic gradient between groundwater and surface in larger distance from the well field causes disproportionately low leakance there. A combination of both reasons is possible.

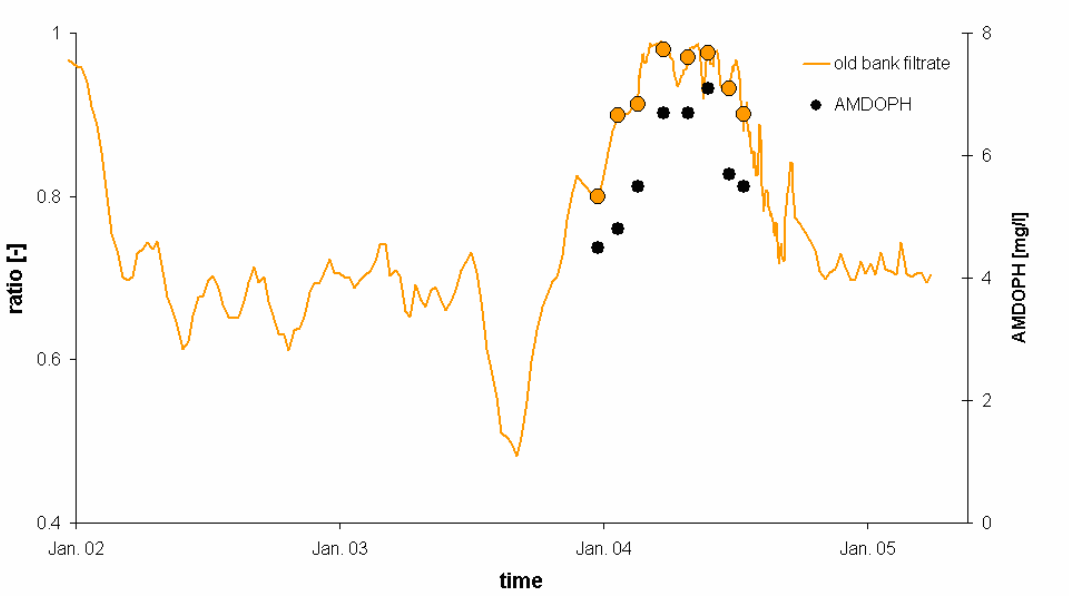

Figure 64: The orange line represents the ratio of old bank filtrate in observation well 3301. Black circles indicate the concentration of AMDOPH. Orange circles with black border indicate the ratios of old bank filtrate at the corresponding sampling dates. The water which is missing to complete the ratio of 1 is medium aged or young bank filtrate.

Observation well TEG374 also shows transient ratios of water with a different source. As the well was drilled in 2003, only 8 months of observations exist. During this time the ratio of old bank filtrate varies between 78% and 98% (fig. 64). The concentrations of AMDOPH vary in the same manner, with the maximum between April and June 2004. Using the ratios to

calculate conservative mixing would result in negative AMDOPH concentrations for the medium bank filtrate. Retardation processes might be responsible for this mismatch. Since the temporal variant AMDOPH concentration is not result of a classical breakthrough curve but of a vertically moving interface between old and medium bank filtrate, retardation only affects the magnitude of the concentration and not the peak location.

3.5.1. Long Term Behaviour

Inland water may be classified in 3 groups. Most water is recharged by precipitation and percolation in the catchment outside the model domain, smaller portions infiltrate in the Airport Lake due to discharge of stormwater runoff, a third part intrudes from the underlying (third) aquifer.

The water balance is obtained with Case2. Cumulative values of Case1 differ by maximum 1 percentage point. Between 1998 and 2004 72 % of the abstracted water is bank filtrate, of which 66 percentage points infiltrated at the eastern and 6 percentage points at the western bank of Lake Tegel. Thus 28 % are inland water, of which 24 percentage points originate from the 2 upper aquifers, 4 percentage points come from the 3rd aquifer. According to a conservative calculation from water level changes 5 percentage points are recharged in the Airport Lake. Using amounts of stormwater runoff data of Umweltatlas Berlin (2004) even 10 percentage points of the water which is abstracted at Well Field West is recharged in the Airport Lake.

Correlating the pumping rate with the amounts of water entering the model, columns 2 and 3 of table RATIO are obtained. While the ratios of inland water and bankfiltrate strongly correlate to abstraction ($R^2 \geq 0.8$) the coefficients of determination of bottom water and old bank filtrate are considerably smaller $R^2=0.48$ and $R^2=0.58$, respectively. The ratio of bottom water depends on the hydraulic head in the 3rd aquifer, which is affected by many factors except Well Field West, the ratio of old bank filtrate depends considerably on the hydraulic head at the opposite bank of Lake Tegel and thus on abstraction at Well Field North, Scharfenberg and Baumwerder.

Table 5: Water balance terms for Well Field West between 1998 and 2005. The first column contains average values for the entire period, column 2 and 3 are obtained by linear regressions of the pumping rate with the corresponding balance term over the entire simulation period, the coefficient of determination is listed in column 4. The bottom water, recharge and water recharged in the Airport Lake are subsets of inland water, as the old bank filtrate is a subset of bank filtrate. The first part of the flow to the Airport Lake is determined using the water level peaks by rainfall events the second value is taken from Umweltatlas Berlin (2004), the other values are obtained from Case2.

	mean 1998-2005	low pumpage	high pumpage	R^2
pumpage [m^3/month]	736000	250000	1300000	1
landside [%]	28	47	25	0.8
bottom water [%]	4	9	3	0.48
recharge [%]	4	12	2	independent
airport lake [%]	5 / 10	16 / 31	3 / 6	independent
bank filtrate [%]	72	53	75	0.82
old bank filtrate [%]	6	6	6	0.58

Regarding the terms of the inland water, 3 points are notable:

i. The recharge by the Airport Lake is higher than groundwater recharge in the model domain. Thus the water quality of the surface water runoff from the Airport Lake is of high importance for the quality of the inland water in the future. For mean conditions the mean travel time (without dispersion) between the Airport Lake and Well Field West is 13 years.

ii. The ratio of bank filtrate highly increases from 53% to 11% from low to medium pumpage, but only slightly to 75% for high pumpage.

iii. The amount of inland water from outside the model domain in the upper 2 aquifers increases strongly with higher pumping rates. This results in a theoretical catchment of 2 km² for low, 7 km² for mean and 13 km² for high pumpage. Probably the catchments size does not change as much, since neither storage effects outside the model are respected nor it is taken into account that inland surface waters as the Tegeler Fließ (fig. 2) mitigate falling groundwater tables by enhanced recharge. Most of the changes of the catchment probably occur due to relocation of the watershed to other well fields.

Regarding the bank filtrate it is notable that the ratio of old bank filtrate is independent of the pumpage of Well Field West. This ratio may change however in case that Well Field North and Scharfenberg strongly increase or decrease pumpage. In the present model using Case2 the leakance of the bank sediments have identical temporal behaviour at all parts of the Lake Tegel bank. However, the leakance at Scharfenberg and Well Field North probably mainly depends

on the pumping rate of the corresponding well fields. Thus the ratio probably is not constantly 6% but much more variable.

The coefficients of determination between pumping rate and bank filtrate and inland water is $R^2 \approx 0.8$ suggesting a close correlation, the coefficient for bottom water and old bank filtrate only has a value of $R^2 \leq 0.6$, as the corresponding boundary conditions are in a greater distance to the well field and depend on different boundary conditions, as head of aquifer 3 and pumpage of Scharfenberg.

At this point it shall be emphasised again, that the values from table 5 as discussed above are related to the hydraulic situation during the model period. Considering pumping scenarios, the results may only be regarded as hints.

3.5.2. Short Term Behaviour

The bank filtrate ratio of water abstracted at Well Field West varies between 52% and 88% (fig. 65). On the monthly scale, bank filtration ratios and pumping rates generally show reversed behaviour, an increase of abstraction causes a decrease of bank filtrate ratio, observable in spring and summer 1998, spring 2000, autumn 2001, between summer 2002 and autumn 2003 and in summer 2004. The reason is that between the well field and Lake Tegel only a band of 100 m aquifer may act as unconfined storage capacity for bank filtrate, inland the distance is much larger.

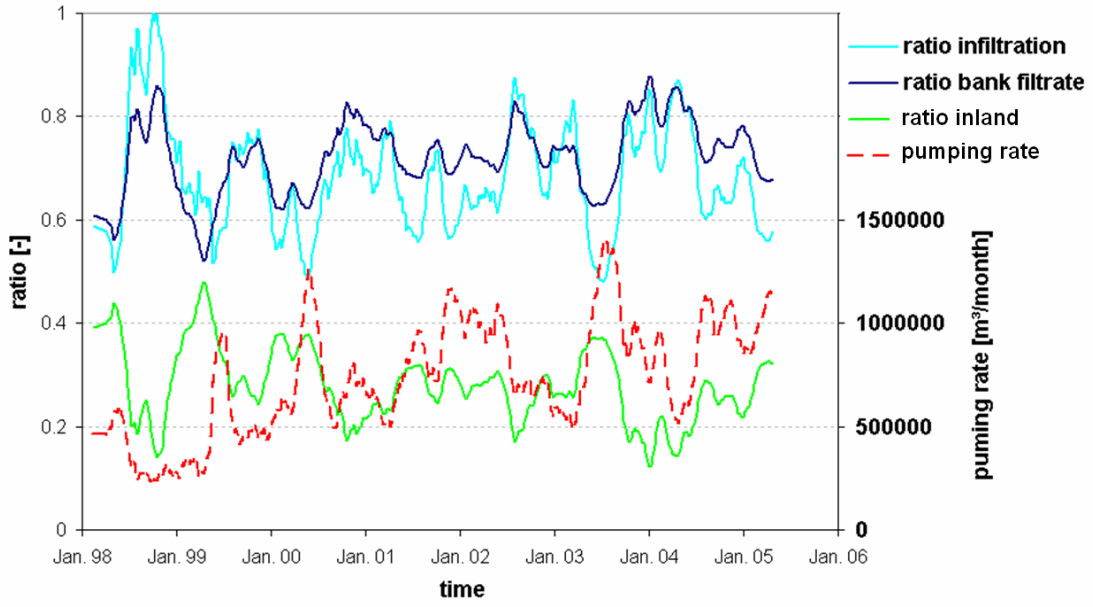

Figure 65: Transient parts of the water balance as ratio of the pumping rate of Well Field West, and the pumping rate itself. The ratios belong to the left axis, the pumping rate to the right axis. Light blue represents the ratio of infiltration in front of the Well Field West (eastern part of Lake Tegel), dark blue represents the ratio of bank filtrate, green represents the ratio of inland water. All curves are the moving average of 2 months, calculated following Case2.

However, in spring/summer 1999 and winter 2000/2001 bank filtrate ratios increase with increasing pumping rates, in spring/summer 2000 the bank filtration ratio almost stays constant though the pumping rate doubles. In winter 1999/2000 the ratio of inland water increases about 4 months before the pumping rate. The reasons is not obvious, probably a combination of several factors.

It is remarkable that the ratio of inland water may varies by factor 2 within a few months, as seen in spring 1998, winter 1998/1999, summer 1999, summer 2000, summer 2003. Calculating bank filtrate ratios based on tracer mixing calculations this should be taken into account.

In Wells 12, 13, 14 about 70% of the abstracted water is bank filtrate, which is almost the average value for the entire well field. The young fraction (~4-6 month age) and the medium fraction infiltrated near Reiswerder (~ 2 years age) can only be distinguished in Well 12 and 13. Well 14 (tab. 6) and wells in the south also show up water of different ages with the oldest of several years, but it is not possible to distinguish different fractions, as it is a continuous age distribution. Only ⅔ of the bank filtrate extracted at these wells pertains to the young fraction, ⅓ is considerably older. It is not surprising to find less water from Reiswerder in Well 12 than in Well 13 as it is farer away.

Somehow surprising is to find old water infiltrated near Scharfenberg instead. Around Reiswerder we find elevated hydraulic heads which partially inhibit the old water taking the direct way but deviating it to the north (fig. 66). This is indicated by higher AMDOPH concentrations in Well 12 than in Well 14. In the field the effect is probably weaker than in the simulation, since a glacial till, which is not respected in the model, partially protects the old and bank filtrate in the second aquifer from being replaced and Case2 overestimates the infiltration around Reiswerder.

Between Well 12 and Well 13 old and medium aged bank filtrate substitute each other, also temporally one fraction increases as the other decreases, the ratio of young bank filtrate to total bank filtrate stays constant (tab. 7).

As it could be expected, ratios of bank filtrate for each well vary temporally wider than for the entire well field. Lower ratios are only 50%, but upper ratios increase up to 95% or even 100% after Well 13 has been out of operation during 5 months in 2002. Chemical analyses of sampled water however does not show this behaviour as sampling started 6 weeks after the well restarted pumping.

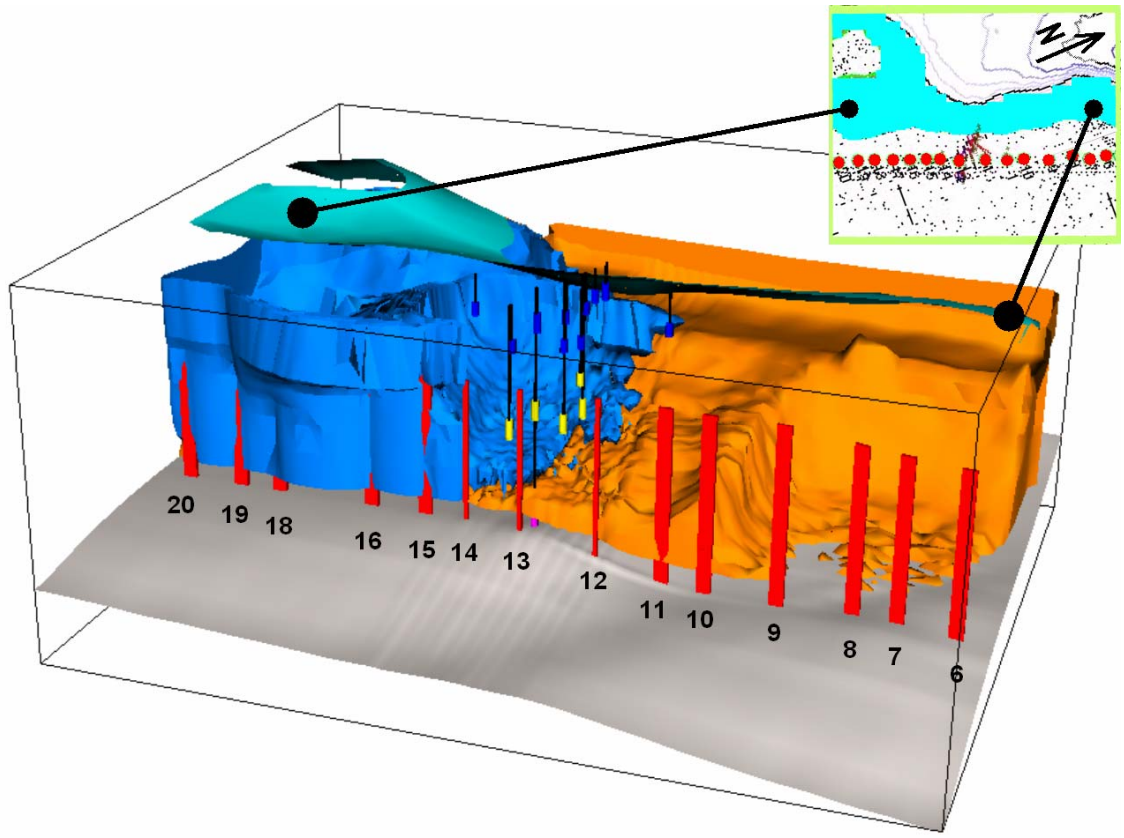

Figure 66: Visualisation of the spatial distribution of bank filtrate which infiltrated near Reiswerder (blue) and old bank filtrate infiltrated near Scharfenberg (orange) from the 2nd week in January 2002, inland water and young bank filtrate are invisible. Abstraction wells are represented by red vertical bars. The turquoise (partially shaded) plane represents the infiltration area of Lake Tegel, black vertical lines show positions of observation wells, blue filters are located in the first aquifer, yellow filters are located in the upper half of the second aquifer, the purple filter in front of Well 13 belongs to TEG374 and is located directly above the bottom of the 2nd aquifer, shown by the grey plane. The glacial till is invisible, it is located directly above the wells, between Well 15 and Well 20 bank filtrate above the till in the first aquifer penetrates farer inland than in the second aquifer. The view is vertically 7 times exaggerated, calculation without glacial till below Lake Tegel

The transient behaviour of the different ratios in Well 13 is illustrated in figure 67. Compared to the behaviour of the entire well field, the ratios show less obvious reactions to the pumping rates, as neighboured wells also affect these ratios (ratios for wells 12 and 14 in fig. App1 and App2, appendix). During the downtime in 2002 when Well 13 was out of operation, bank filtrate replaced the inland water, afterwards it takes some weeks to normalise the bank filtrate ratio. The hydraulic gradient of the bank filtrate is higher than the hydraulic gradient of inland water with opposite direction. The interface separating these 2 fractions is not a vertical plane comprising the wells. Cushions of bank filtrate form in between two active wells, which can be observed in figure 66 e.g. between Well 15 and 20 and especially across Well 17, which is switched of. Here Well 17 is out of operation, also during the last month, the cushion between the adjacent penetrates much deeper inland.

Table 6: Mean fractions of abstracted water at wells 12 to 14 between 2000 and 2005, "bf" denotes bank filtrate. Young bf infiltrated directly in front of the well (~6 month age), medium bf infiltrated north of Reiswerder (~2-5 years age). Well 14 is located too close to Reiswerder to distinguish these fractions. Old bf infiltrated near Scharfenberg (>10 years age). The sum of bf and inland water should be 100%, error bf denotes the difference between total bf and the sum of young, medium and old bf. Pumpage is in m³/month.

	well 12	well 13	well 14
total bf	72%	69%	76%
landside	30%	36%	26%
young bf	49%	45%	
medium bf	5%	13%	
old bf	18%	11%	7%
young bf / total bf	68%	65%	
error bf+land	102%	105%	103%
error bf	-1%	0%	
pumpage	27566	42710	31763

Table 7: Minimum and maximum fractions of abstracted water at wells 12 to 14 between 2000 and 2005, obtained by moving average values of 2 months. "bf" denotes bank filtrate. Young bf infiltrated directly in front of the well (~6 month age), medium bf infiltrated north of Reiswerder (~2-5 years age). Well 14 is located too close to Reiswerder to distinguish these fractions. Old bf infiltrated near Scharfenberg (>10 years age). The sum of bf and inland water should be 100%, error bf denotes the difference between total bf and the sum of young, medium and old bf.

	well 12	well 13	well 14
total bf	53 - 96%	50 - 100%	65 - 94%
landside	4 - 47%	0 - 50%	6 - 35%
young bf	35 - 69%	35 - 67%	
medium bf	2 - 12%	5 - 26%	
old bf	14 - 27%	6 - 17%	2 - 13%
young bf / total bf	66 - 73%	63 - 67%	
error bf+land	97 - 108%	99 - 107%	100 - 110%
error bf	99%	-5 - 5%	
pumpage	11000-130000 m³/month	0-200000 m³/month	11000-122000 m³/month

The concentration of old bank filtrate is almost nil in January 2000 because the transport species by which it is represented has not yet arrived at the well. Regarding the error of the checksum for total bank filtrate "error bf" in figure 67, this becomes obvious. As the transport model takes longer time to reach initial equilibrium than the flow model, which started in 1998 all transport results are presented from 2000.

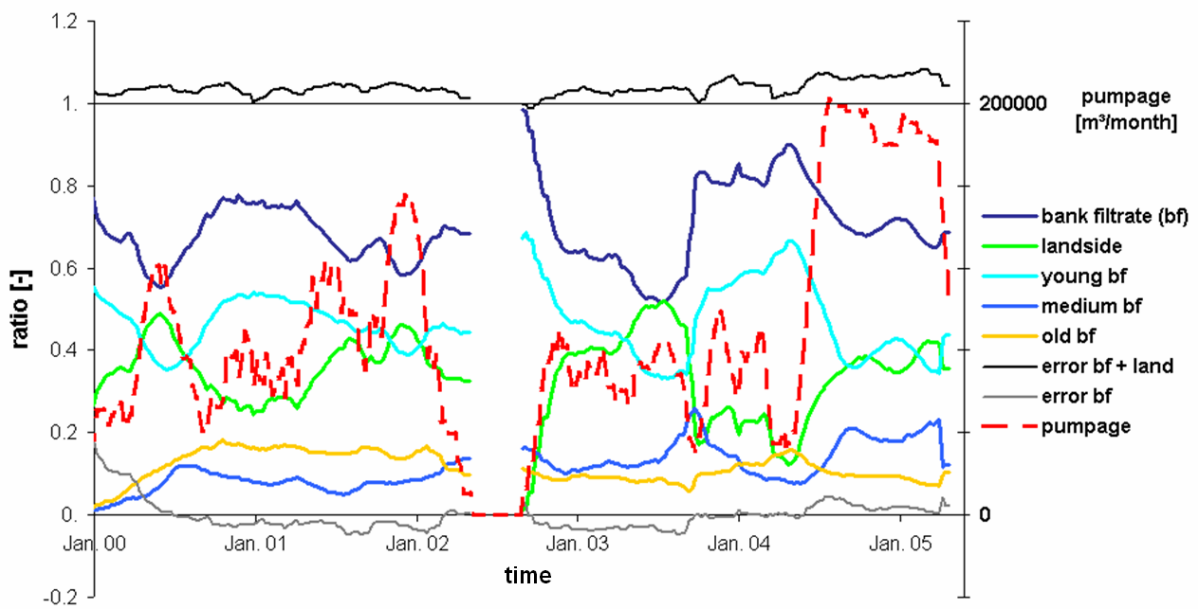

Figure 67: Fractions of water abstracted at Well 13. The dark blue line shows the total bank filtrate ratio, the green line shows the ratio of inland water, the light blue line shows the ratio of young bank filtrate (~4-6 month age) infiltrated directly in front of the transect, the indigo blue line shows the ratio of medium aged bank filtrate (~2 years age) which infiltrated north of Reiswerder, the orange line shows the ratio of old bank filtrate, infiltrated near Scharfenberg. The black and grey lines are checksums, the black shows the sum of bank filtrate and inland water which should be 1, the grey line shows difference between total bank filtrate and the sum of young, medium and old bf, which should be nil. All values are the moving average of 9 weeks. In summer 2002, the well was switched off, thus no values are available

Bank filtrate ratios also vary on a hourly time scale. When a well is switched on, the ratio of bank filtrate is high, decreasing continuously during well operation (fig. 68). Within 24 to 48 hours after the well has been switched on, the ratio of inland water increases by 20 to 30 percentage points. At the beginning, often no inland water is present in the wells. It is remarkable that the ratio may increase from almost nil to about 25% within 24 hours of well operation (1st April, fig. 68). After this time, the ratio of inland water grows more slowly with about 1.5 to 3 percent points per day. As the system does not have a steady state, variations over longer periods may not have its reason in operation of the single well. Well 12 and Well 14 (fig. App3, fig. App4, appendix) show identical mechanisms but the variations are slower and less pronounced because the model layer representing the glacial till has a higher permeability.

Regarding the periods when the wells are switched, the checksum error of bank filtrate and inland water is about 3 % to 5 % , which is far enough from the simulated ratios of 10 to 30 % inland water, to accept the results in their order of magnitude (fig. 68). The ratios for Well 12 and Well 14 are shown in figure App3 and figure App4, appendix.

After July the scattering reaches ±10%. This appears to be much, but the mean value is close to nil. This scattering probably derives because the concentration is carried by a natural

number of particles. The error occurs if a particle leaves the model at the well and the time step is small. In the following period the error is compensated systematically because then the particle concentration in the model is lower and the mass balance error is of the opposite sign. As the lengths of the time steps are only between 1 and 6 hours and the mean of the scattering is between 0.98 and 1, the results are also acceptable. The weekly mean of the checksum error is presented in fig. 69.

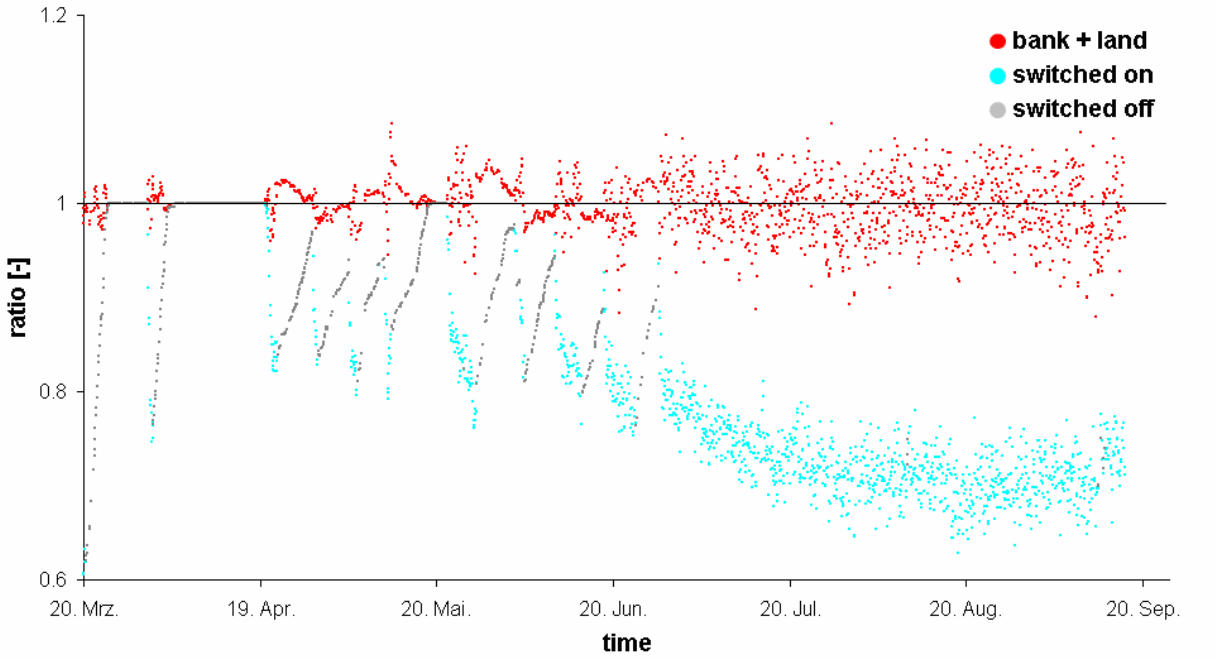

Figure 68: Ratio of bank filtrate in Well 13 in 2004, obtained by applying MT3DMS to the telescope model. Each dot represents one time step. The red dots show the sum of inland water and bankfiltrate, which should be 1. The blue dots show the ratio of bank filtrate in extracted water, the grey dots show the concentration of bank filtrate in the well when it is switched off.

3.5.3. Chemical vs. Numerical Bank Filtrate Ratios

Chemical data supports the thesis that the source of extracted water strongly depends on the elapsed time after the pump has been switched on. At the July 9th .2002 and April 9th 2003 the wells have been switched on immediately before the samples were taken. At these days the values of many physico-chemical parameters are significantly different to other sampling dates (tab. 8). The change occurs due to different ratios of bank filtrate and inland water and accord to the idea of concentrations at both sides of the well field. Deuterium and ^{18}O have much lower concentrations inland as the water is much older than bank filtrate and recharge is not affected by the Havel. AMDOPH, AMPH, phenazone and propyphenazone are indicators especially for old but also for young bank filtrate, boron for bank filtrate, magnesium and potassium show lakeside higher concentrations than inland. Chloride and sulphate concentrations are considerably higher in deep inland water. Because of the higher salinity, the conductivity of inland water is also higher, again due to the content of deep water.

Unfortunately these 2 dates do not lie within the period of the model respecting hourly exact well operation.

It appears odd to find the physico-chemical parameters electrical conductivity and temperature constant in the sampling protocol during the 15, respectively 10 min of flow before the sample is taken, since they are strongly affected by the bank filtrate ratio.

The wells and their neighbours have been out of operation for at least 3 days, as result the bank filtrate intrude deeply inland, forming cushion described above and visible in figure 66 at Well 17. As a consequence the ratios stay constant when the well is switched on, no inland water is pumped at all. Between March 20th and September 20th 2004, this effect appears at all wells and can last up to 20 hours. The behaviour of fractions of shallow and deep water is also not constant. With the present model moving interfaces between the water fractions are not respected properly since it is too short to clear initial transport conditions.

Table 8: Concentrations of dissolved substances and physico-chemical parameters which show a clear trend if the wells are switched on immediately (<1 hour) before sampling. Column 1 and 3 of each well list values obtained with normal sampling procedure, when the well is switched on at least 24 hours before sampling. At the Jul. 9th 2002 and May 9th 2003 the well has been switched on less than 1 hour before sampling, with the result that the water composition changes. The direction of this change is listed in the rightmost column. The entire time series can be found in the appendix.

	Well 12			Well 13			Well 14			
	14.6.02	9.7.02	22.8.02	19.3.03	9.4.03	21.5.03	14.6.02	9.7.02	22.8.02	change
Deuterium [vs. per mill SMOW]	-55.46	-50.66	-53.2	-52.7	-51.3	-53.4	-54.02	-50.81	-53.85	higher
18O [vs. per mill SMOW]	-6.97	-6.56	-6.98	-6.82	-6.6	-7	-6.91	-6.61	-6.93	higher
PropyPhenazone [ug/l]	0.11	0.2	0.11	0.12	0.25	0.08	0.08	0.18	0.06	higher
AMDOPH [ug/l]	1	1.3	1.1	0.85	1.3	0.8	0.76	1.3	0.71	higher
Phenazone [ug/l]	0.55	1.1	0.61	0.58	1	0.51	0.53	1.1	0.48	higher
AMPH [ug/l]	-0.05	0.26	0.12	0.11	0.23	0.06	-0.05	0.26	0.1	higher
K [mg/l]	5.24	6.52	5.4	5.81	6.77	5.17	5.54	7.43	5.15	higher
Mg [mg/l]	8.9	9.4	9.08	8.78	10	8.54	8.84	9.7	9.04	higher
B [ug/l]	120	150	120	120	140	94	130	150	110	higher
Temp [°C]	10.8	11.9	10.4	11.9	10.7	11.7	11.6	12.2	11.1	lower/higher
Na [mg/l]	38.7	33.1	38.7	36.9	31.8	36.5	39.7	34	38.3	lower
Cl [mg/l]	55	43	53	56	48	58	58	44	55	lower
Ca [mg/l]	114	96.1	112	111	100	110	106	97.3	113	lower
SO4 [mg/l]	136	108	134	129	111	133	143	109	144	lower
el. cond [mS/cm²]	790	710	790	780	710	770	810	710	800	lower

The determination of bank filtrate ratios has been included in several studies. Using concentrations of different tracers of water extracted by the wells lead to variable ratios between 57% and 90%, which are presented in table 9. The mean of all values is 11%. From a physical view the mean is meaningless as it is determined from different periods with different lengths and tracers with different accuracy. A direct comparison to modelled values is not possible for several reasons:

i. Sampling in all studies of table 9 is based on samples at one point of time. Bank filtrate ratios are highly variable on scales between hours and months. Before sampling the wells usually have been switched on at least 2 days prior to sampling. This is the time span when the ratios already had fairly stabilised. Sometimes wells are only switched on for a few hours, then bank filtrate ratios are much higher and the estimation is too low. During longer well operation this ratio may be too high. Overall, 2 days seem to be appropriate to get a fair mean value.
ii. As travel times are not known exactly, time variant concentrations of tracers indicating surface water only allow using average values.
iii. Some assumptions about the inland water have been made, as only one observation well (3304) is available. Its composition changes between May 2002 and August 2004, probably due to the breakthrough of a high proportion of stormwater runoff, which is discharged to the Airport Lake. This water contains tracers which also appear in bank filtrate and which are used in the mixing equation, which leads to errors in the calculation of bank filtrate ratios.

Nevertheless, from a more general point of view the bank filtrate ratios calculated by tracers and by modelling support each other. The mean, maximum and minimum of both methods show the same values. Please compare table 9 to table 6 and table 7.

Table 9: Ratios of bank filtrate at wells 12, 13 and 14 as determined in different studies. Single values represent average values, 2 values connected with a hyphen represent temporal variation.

Source	Period	Tracer	well 12	well 13	well 14
Fritz 2002	May 1998 - May 1999	K	80%	79%	84%
Fritz 2002	May 1998 - May 1999	Bor	88 - 90%	72 - 84%	64 - 88%
Fritz 2002	May 1998 - May 1999	EDTA	85%	87%	83%
NASRI 2004	May 2002 - Jun 2003	K	57%	56%	59%
NASRI 2004	May 2002 - Jun 2003	B	79%	73%	81%
NASRI 2004	May 2002 - Jun 2003	EDTA	66%	62%	63%
NASRI 2004	May 2002 - Jun 2003	18O	67%	67%	68%
NASRI 2004	May 2002 - Jun 2003	Deuterium	63%	66%	62%
NASRI 2005	May 2002 - Sept. 2005	K, EDTA, B, 18O, Deuterium		58 - 69%	

Pekdeger et al. (2004) determine 11% for the ratio of old bank filtrate, which agrees to simulated concentrations (tab. 6). The modelled ratio of old bank filtrate changes from 8% in autumn 2003 to 15% in spring 2004, the concentrations of AMDOPH only vary slightly from about 0.7 ug/l to 0.9 ug/l. The dynamics in the model may be too high since intrusion of young bank filtrate to the second aquifer is probably reduced by glacial till below Lake Tegel.

3.5.4. Mass Balance Regional Model vs. Telescope Model

The pumping rates of the regional model are approximated by weekly average values, but the wells are operated on an hourly scale. The discrete operation is simulated with a spatially and temporally reduced model (chapter 4.7). The present section assesses the impact of the different temporal resolution.

Computing the ratios of bank filtrate and inland water with different temporal resolution the results show some deviations. The most obvious difference is the higher portion of inland water when calculated with the regional flow model (fig. 69). This difference is not physically based, the mass checksum for the regional flow model shows a surplus, which derives from the inland water (fig. 10). Punctually differences of 10 percentage points occur (fig. 69). The deviations can not be related to a single source. As these errors preferably appear at low pumping rates, the differences to the regional model might occur, because weekly means do not reproduce the highly transient behaviour as precise as modelling the exact pattern of well operation and calculating the average afterwards. Another reason is that different pumping rates for Well 13 are applied in the two models. Setting up the regional flow model raw data from BWB was applied. Due to special operation Well 13 sometimes has been switched manually. This is respected in the telescope model.

But also other factors might affect the deviations. Short term mass balance inaccuracy of the regional flow model might contribute. Time steps are much longer than in the telescope model and fluctuations appear which can be seen at the checksum. The single errors of the checksum are up to ±10 % in the telescope model (fig. 68), but weekly sums are hardly bigger than ±2 %, while the mass checksum error of the regional flow model varies between 0% and 10%. This is acceptable, but it probably occurs because concentrations are carried by a natural number of particles, resulting in an oscillation when a particle leaves the model through the well. This view is supported by the symmetric distribution (fig. 68) and the fact, that the weekly sum of the mass balance of the telescope model is significantly smaller than for the regional model (tab. 10). Horizontal spatial discretisation of the two models is identical, but the lower aquifer of the regional model is subdivided in 5 layers, in the telescope model in 4 layers. Temporally the regional flow model is discretised in weekly periods, the telescope model in periods of 1 to 6 hours. Additionally inter- and extrapolation errors might occur when transferring data from one model to another. However, except for the inland increase in mass the other errors are of negligible magnitude. The good temporal agreement, and the similar mean value (74% / 75%) of the bank filtrate ratio supports the method of using weekly averages for most computations presented above.

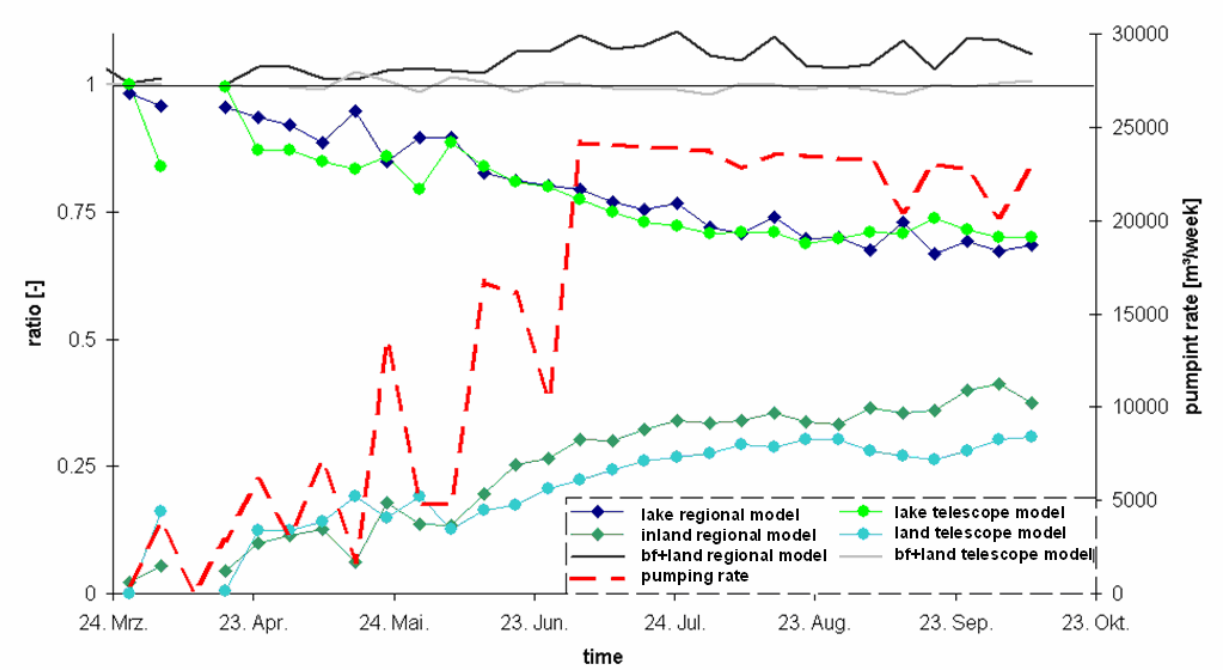

Figure 69: Bank filtrate and inland water in Well 13 in 2004, calculated with the regional flow model with weekly discretisation and the telescope model with discretisation on hourly scale. The results of the latter are summed up to weekly intervals. The dashed red line represents the pumping rate. Average bank filtration ratios are 75% / 74% for big/telescope model and 31% / 26% for inland water. The curves of the ratios are noncontinuous as around the week of April 10th no values are available as no water was abstracted.

3.5.5. Numerical Transport Error

The ratios of the different waters are determined using MT3DMS. The errors are assessed by 2 different measures: The first is considered by adding or subtracting different parts, i.e. bank filtrate and inland water are added up, the result should be always 100%, Young, medium, old and total bank filtrate are modelled as 4 species, subtracting the 3 fractions from total bank filtrate the result should be nil. These errors are presented in table 6, 7, figure 67, figure 68 and figure 69. Though these checksums sometimes reach 10 % error at hourly simulation (fig. 68), the mean normally is not more than 3 percent points from the target value. Regarding the checksum of the three bank filtrate ratios of table 6, 7 or figure 67 in Well 13 the mean error is almost nil, but it temporally varies between -5 % and 5 %. Regarding the values and variations of each ratio and regarding the error as noise, the signal to noise ratio is high enough to accept the results in their order of magnitude.

As second measure the mass balance output from MT3DMS is evaluated (Zheng et al. 1998). Unfortunately this is only considered cumulatively for the entire model domain. Uncritical errors near the outer boundary conditions accumulate in the same way as errors near the wells. Cumulative mass balance errors for MT3DMS are presented in table 10:

Table 10: Cumulative errors in the mass balance over the entire transport model domains of the telescope model (chapter 4.7) with exact times of well operation and the regional flow model with weekly average values. Inland water is named "land", bankfiltrate is named "lake".

	numerical mass balance error	
	land	lake
telescope model	+0.01 %	+0.18 %
regional model	+4.5 %	+0.45 %

The mass balance errors show uncritical values for inland water and bank filtrate considering the telescope model. Regarding the regional flow model the error in bank filtrate is acceptable with 0.45% but the error of inland water is quite high with 4.5%. As this is temporally an average value, the mass surplus of the items "error bf + land" in table 6 and 7 and fig 69 derive from inland water. The results have been checked for instability, if surplus and loss of mass equal out, which is not the case. Furthermore the error does not derive from the flow model, the error across the whole domain and in different subregions around all wells is smaller than 0.01%, which is the "detection level". Also for this measure the signal to noise ratio is high enough to accept the results in their order of magnitude.

3.5.6. Infiltration Depth

The distribution of the infiltration by depth shows considerable differences for the mean as well as for the temporal dynamics between Case2 and Case3.

Most water infiltrates between 28 m and 30 m NN with a mean at 28.7 m (fig. 70), corresponding to a water depth of 2.7 m. This value is temporally rather constant, as the classes of the depth dependent infiltration area above 29 m are each about double as large as the classes below (tab. 11). Applying Case3 the pattern of the infiltration amount is different. Between 30 m NN and 31 m NN the infiltration is about 40% higher, below 28 m the infiltration is only 50% to 80% lower. Case2 (fig. 70) better represents the amounts on a temporal scale, Case3 (fig. 71) better represents the physical processes and is more accurate regarding the depth distribution. Since anaerobic conditions seriously decrease the leakance, only a little water infiltrates in great depth. The difference can be observed in the two figures.

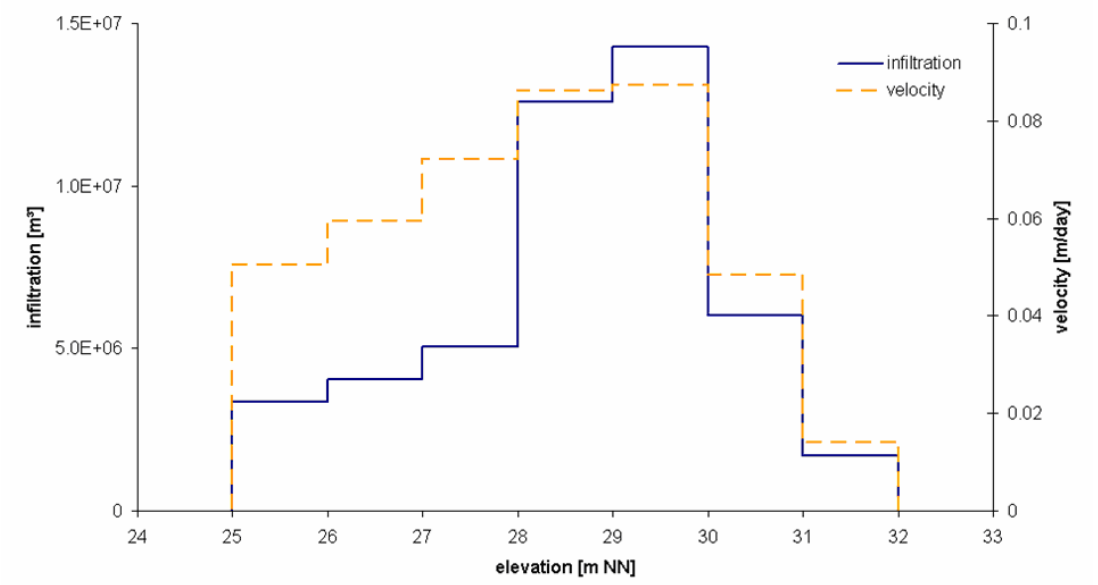

Figure 70: Classified depth of infiltration for Case2, values for the entire model period for the east bank of Lake Tegel including Reiswerder. The blue line is the infiltration amount, the orange line represents the infiltration velocity. Mean infiltration depth is 28.7 m, remaining rather constant between 28.30 m and 29 m with a standard deviation of 14 cm. The average water level is at 31.4 m. The maximal infiltration velocity varies between 27 m and 30 m.

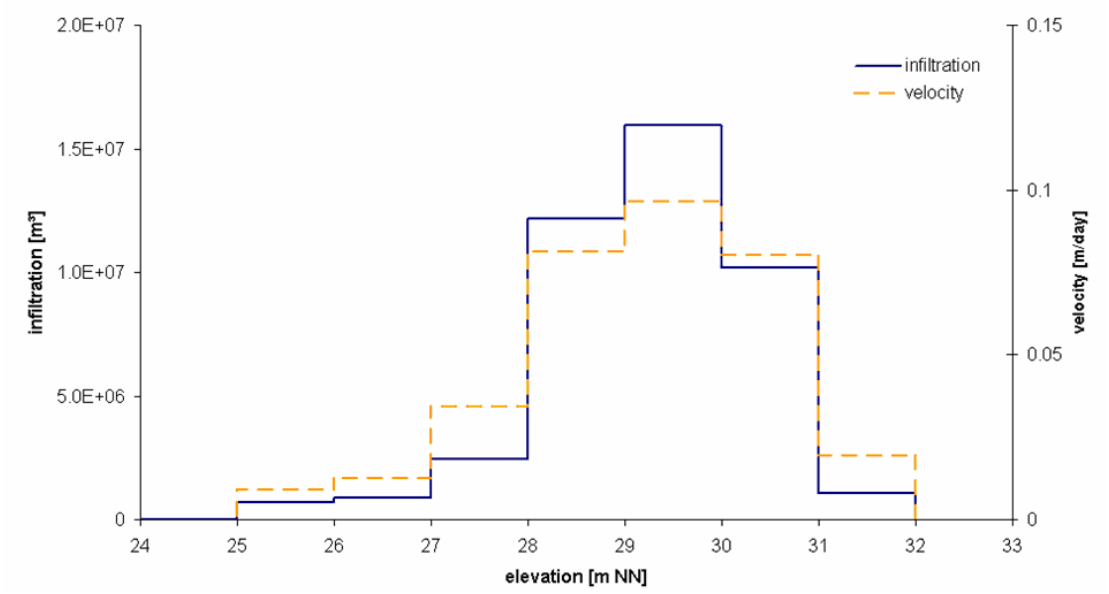

Figure 71: Classified depth of infiltration for Case3, values for the entire model period for the east bank of Lake Tegel including Reiswerder. The blue line is the infiltration amount, the orange line represents the infiltration velocity. Mean infiltration depth is 29.27 m, temporally remaining variable between 28.7 m and 29.7 m. The average water level is at 31.4 m.

Table 11: Elevations with corresponding areas for the eastern bank of Lake Tegel including Scharfenberg.

elevation [m NN]	area [m²]
31 - 32	46150
30 - 31	47400
29 - 30	62275
28 - 29	55750
27 - 28	26700
26 - 27	25875
25 - 26	25250

3.6. Transport Modelling

Concentrations of Lake Tegel generally are well defined between May 2002 and August 2004 through measurements carried out during the NASRI project (KWB 2005, Pekdeger 2006, Grünheid et al. 2005, Jekel 2006). Further measurements are available by Richter (2003) and SENSUT (2005), supplementing observations after May 2002. Moreover they provide earlier information about Lake Tegel, which has turned out as extremely valuable for a comprehensive interpretation of the system. No concentration measurements are available for outer boundary conditions, plausible boundary values are assigned, such that concentrations match observations at wells which are not or only weakly affected by young bank filtrate. This is the case for inland water (observation well 3304 and 3305) and old bank filtrate (TEG374). The fits in these observation wells show the consistent model set up and not a good performance.

3.6.1. Transport Parameters

The transport parameters are directly transferred from calibration with the hydraulic model. The distribution of the glacial till, acting as aquitard is calibrated with the telescope model (chapter 4.7).

$n_f = 0.22$ [-], effective porosity, 10 % higher than specific yield

$\alpha = 0$ [m] dispersivity

v_leak = 10^{-4} [s^{-1}] to 10^{-9} [s^{-1}], vertical leakage, (fig. 95)

(Remind: $k_f = 3.5*10^{-4}$ [m/s], horizontal hydraulic conductivity)

The effective porosity is set 10 % higher than the calibrated specific yield to account for residual water saturation during changing water tables. The dispersivity is found to be insensitive at length smaller than 1 m, as well for observation as for abstraction wells. Probably because the time between minimum and maximum of tracer input signal is between 2 and 6

month and thus in the same order of magnitude as the residence time. An additional reason may be that heterogeneities have a much higher horizontal correlation length than vertical correlation length. The strong vertical component of the flow field is unusual, inducing that the water enters and leaves regions of different conductivity faster, the time phase shift between the tracer concentrations are lower. The highly transient flow field might contribute to this effect.

3.6.2. Chloride

Chloride is an ideal tracer, it is conservative and not retarding. At the present concentrations no density driven flow occurs. A serious drawback however is that the concentration of Lake Tegel only shows one pronounced variation between May 2002 and August 2004, which is in spring 2003 (fig. 72). Meaningful results of travel times only may be obtained for the period between the shift in the surface water concentration and the shift in the corresponding observation well. In several shallow observation wells this shift could not be measured because the well screen went dry due to an extraordinary groundwater drawdown.

In general observed and modelled breakthrough curves coincide well, only observation wells 3301 and TEG372 show different behaviour. Here the surface water signal is not just phase shifted with maybe some dispersion, but the step of 25 mg/l in surface water concentration between February and April 2003 takes 6 month time to break through.

Since no measurements are available for concentration boundaries inland and below the lake, plausible boundary values are assigned, such that concentrations match observations at wells which are not or only weakly affected by young bank filtrate. This is the case for observation well 3304, 3305 and TEG374 (fig. 6). The concentration peaks in 2004 of observation well 3304 appear due to numerical oscillation of MT3DMS because of rapidly changing water levels in the partly saturated first aquifer. Cells fall dry and are rewetted again. Concentrations show numerical oscillations, MODFLOW's rewetting package obviously is not adjusted to MT3DMS. As only a small portion of abstracted water derives from the first inland aquifer, the oscillations have a negligible impact on model results in the abstraction wells.

The lack of measurements about the boundary conditions of the second inland aquifer is reflected by concentrations in abstraction wells 12, 13 and 14. Between summer 2002 and autumn 2003 concentrations are modelled about 10 mg/l too low. This may be caused by chloride concentrations of old bank filtrate and deep inland water, both are unobserved. Old bank filtrate could have had up to 80 mg/l, which would correspond to lake concentrations between 1986 and 1991 (fig. 73). With a ratio of about 13% of extracted water this only could

explain a mismatch of 3 mg/l. Additionally the ratio of old bank filtrate decreases from 18 to 7 percent from Well 12 to 14, the gap is rather constant at 10 mg/l. This indicates deep inland water to be the reason, which is the only part where chloride concentrations are completely unknown and which is very likely to be saline.

This is supported by the fact that the ratio of inland water in wells 12, 13 and 14 is elevated between winter 2002 and autumn 2003 (fig. 67, for wells 12 and 14 in the appendix) which exactly coincides with the beginning of the gap at wells 12 and 14 and its end at Well 13. Assuming half of the inland water as the unknown fraction and the ratio of this saline inland water changing proportional to the entire inland water of the 2nd aquifer, the ratio varies about by factor 3, between 7% and 20%. This results in a chloride concentration of about 140 mg/l which could explain the gap of 10 mg/l. With this assumption concentrations for the entire period would have to be 5 mg/l higher than observed. Some source of chloride is overestimated in the model, probably also due to varying inland concentration which is not fully reflected in observation well 3304 (fig. 72). Several species show strongly varying concentrations, such as ^{18}O (fig. 74, fig. App8), deuterium (fig. App9), calcium (fig. App13), sulphate (fig. App27), electrical conductivity (fig. App16) and EDTA (fig. App15).

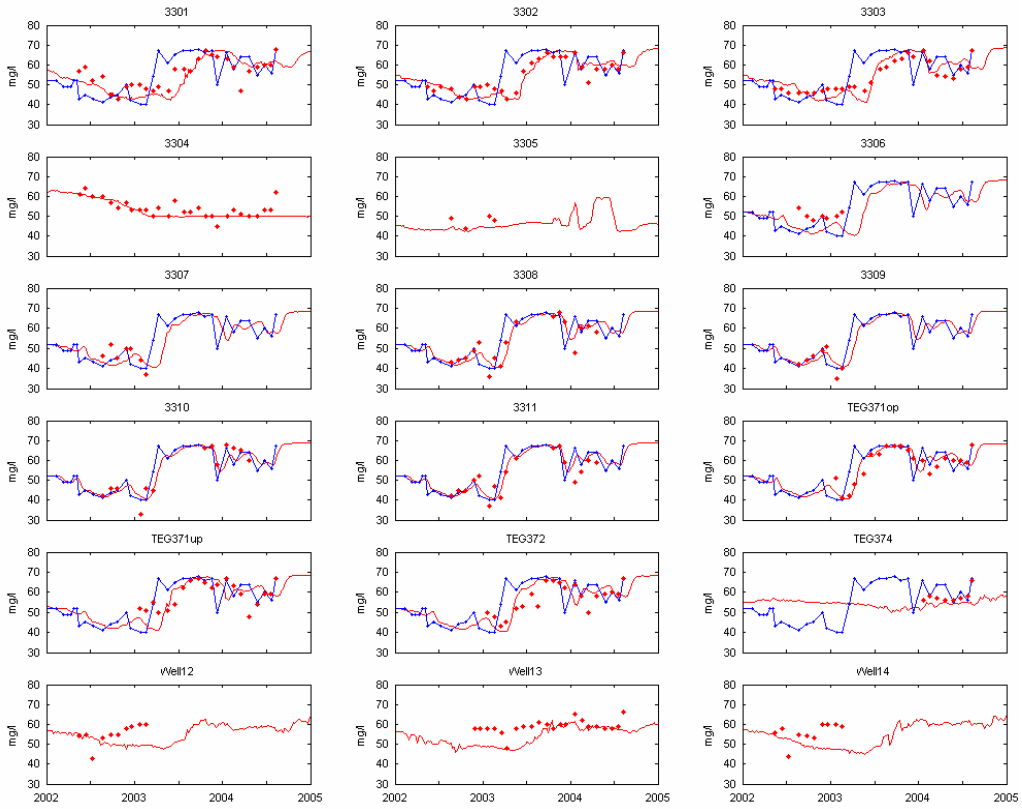

Figure 72: Observed and simulated concentrations of chloride in all sampled wells of the transect. The blue curve represents the model boundary concentration of Lake Tegel, the tiny blue dots indicate corresponding measurements. The boundary concentration is only shown at sampling wells which are highly affected by the lake. The red dots represent measured concentrations, the red curve represent the modelled concentration.

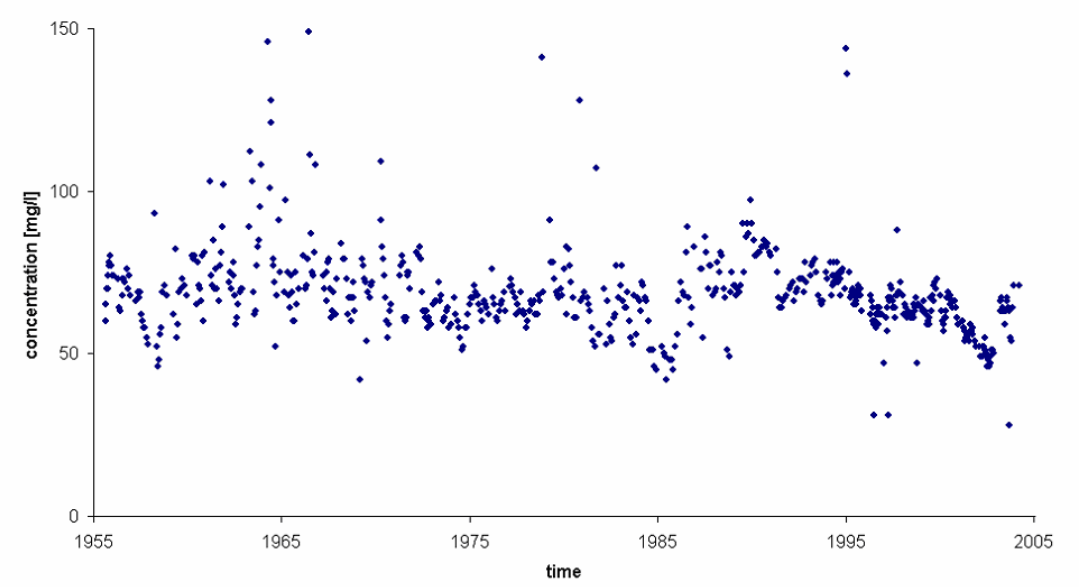

Figure 73: Concentration of chloride in Lake Tegel between 1955 and 2004. Sampling intervals varies between 2 weeks and 35 days in summer, in winter intervals usually is 1 month.

3.6.3. ^{18}O

Water is an ideal tracer. The problem of distinguishing water in water can be solved by detecting isotopic differences, in the present case the stable oxygen isotope ^{18}O is detected. The concentration is related to the concentration of ^{18}O in standard ocean water, resulting is the unit [$^{0}/_{00}$ vs. SMOW]. Since concentrations are lower, they are expressed with negative numbers. In contrast to chloride it has the advantage of having a sinusoidal concentration in Lake Tegel, making it possible to inspect the transport behaviour during the entire modelled time span. Regarding the observation wells, the fit between modelled and observed concentrations generally is good. The highest deviations appear at observation wells 3301 and 3303 in autumn/winter 2002 (fig. 74). The phase shift between observed and modelled concentrations is about 1/3 faster than the real travel time, decreasing to an almost perfect fit in 2003 and 2004. In observation well 3302 the simulations and measurements match in autumn/winter 2002 but are again about 1/3 slower in later period. The model can not reproduce the change in transport velocity. This change might occur due to changing flow directions resulting in different hydraulic conductivities upstream the observation well and thus changing travel times or mixing of medium aged or even old bank filtrate, but also may be the result of mixing flow paths with different travel times.

Transport velocity of observation well 3306 (fig. 6) is modelled about double as fast as measured values indicate, which may be caused by the glacial till distribution rather than spatial variability of the aquifer conductivity. Probably observation well 3306 is just located at the interface between bank filtrate and inland water, since the seasonal signal of ^{18}O is clearly

visible, but from August 2002 to February 2003 the temperature is almost constant, between constantly 10°C and 11°C (fig. 74).

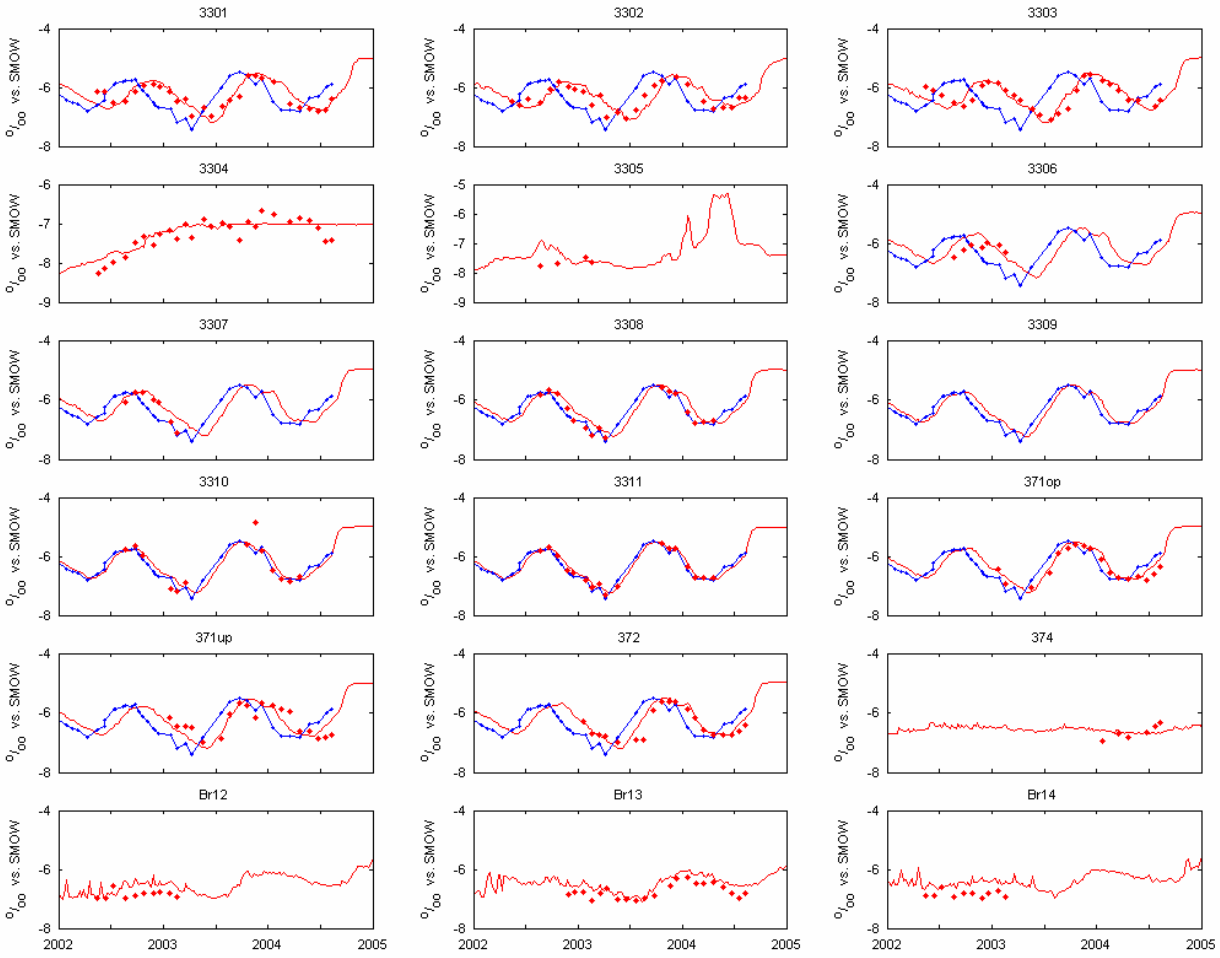

Figure 74: Observed and simulated concentrations of ^{18}O in all sampled wells of the transect. The blue curve represents the model boundary concentration of Lake Tegel, the tiny blue dots indicate corresponding measurements. The boundary concentration only is shown at sampling wells which are highly affected by the lake. The red dots represent measured concentrations, the red curve represent the modelled concentration.

Abstraction Well 12 to 14 show a rather good fit, however only with a few measurements, so solely at Well 13 the observed breakthrough is a liable indication for the correctness of travel times, also indicating the modelled transport velocity is a little fast. In average observed concentrations are 0.3 ‰ vs. SMOW (versus SMOW) lower than calculated. This means at least one source of water has a lower ^{18}O value than assumed. Old bank filtrate might contribute to this behaviour but it is not the reason, since observed concentration at TEG374 is between –6.3 ‰ SMOW and –6.9 ‰ SMOW, concentrations in precipitation within the last 20 years have only increased by about 1.5 ‰.

Inland groundwater shows concentrations as low as -8.3 ‰ SMOW, measured in spring 2002. It is not unlikely that deeper inland water has values as low as -9 ‰ SMOW as result of lower temperatures in the past, regarding the concentrations of groundwater recharge within

the last 20 years (fig. 21). Performing a mixing calculation assuming 50% of inland water with -9 ‰ ^{18}O vs. SMOW, the mismatch of 0.3 ‰ SMOW of wells 12, 13, 14 is filled.

3.6.4. Temperature

Unlike ^{18}O and chloride, temperature is not an ideal tracer. Heat exchange between the pore water and the matrix, results in a retardation coefficient $R \approx 2$. Thermal conductivity results in a diffusivity $D = 1.3*10^{-6}$ m²/s which is three orders of magnitude higher than molecular diffusivity of dissolved substances, leading to weakening of the temperature peaks with increasing travel length and time. But temperature has some considerable advantages. The input signal shows a pronounced seasonality, it is already measured during sampling of each observation well, and, most important in the present case, 10°C usually is a quite good guess for unobserved groundwater temperature.

For the interpretation, it has to be taken into account that the optical phase shift is bigger than for non retarding tracers. Due to $R \approx 2$ a misfit in simulated and real travel time of time t_1 results in a phase shift of t_1 with $R = 1$ but in a phase shift of $2*t_1$ with $R = 2$.

The fit between the modelled and observed breakthrough curves varies widely, depending on the position of the observation well. While shallow observation wells near the bank show small deviations, the fit of shallow observation wells with a larger distance to the bank, namely observation wells TEG372 and 3306 is considerably worse than the fit of chloride and ^{18}O. Apart from the virtual error due to the retardation, structural differences between observed and simulated temperature break through curve exist. TEG372 is asymmetric regarding the maximum and minimum temperature. Observation well 3306 shows peculiar behaviour. While a clear signal of ^{18}O is visible (fig. 74) the temperature is constantly at 10°C (subfigure 3306, fig. 75). This observation obviously is at the interface of bank filtrate and inland water and illustrates that temperature may have a totally different behaviour than conservative tracers.

It is also peculiar about the temperatures behaviour that the means of the observed breakthrough curves in observation well 3301, 3302 and 3303 are considerably higher than 10°C. The maximum values each year are about 17°C the minimum between 4°C and 11°C. Measurement errors seem to be improbable, the monthly measurements show a smooth curve, no seasonal deviations or scattering due to hot and sunny days can be observed. The flow in the sampling tubes is high, even direct exposition to the sun only may not increase temperature more than 0.2°C. The misfit does not appear at abstraction wells and only slightly at observation wells near the bank, thus it increases with the travel time and length. The lag between modelled and observed temperature is highly variant. Regarding observation wells

3301 to 3303 (fig. 75) in 2002, the temporal behaviour matches, in 2004 the difference is 3 months. This effect is much smaller regarding ^{18}O (fig. 74).

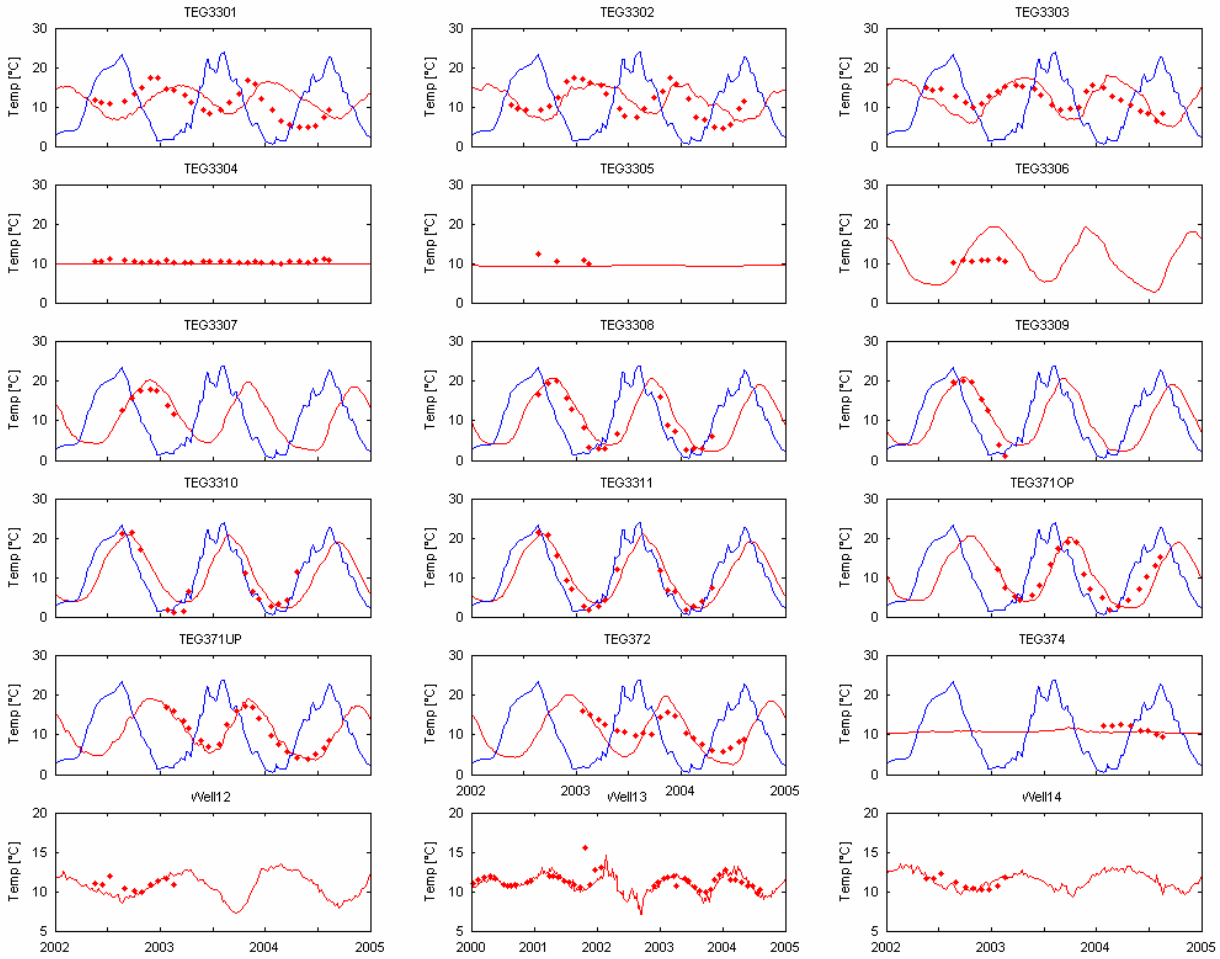

Figure 75: Observed and simulated temperature in all sampled wells of the transect. The blue curve represents the model boundary concentration of Lake Tegel, only shown at observation wells highly affected by surface water temperature. The red dots represent measured values, the red curve simulated temperature. Please note the temperature scale of observation wells and abstraction wells differs. The time scale of Well 13 already begins in 2000.

The precise estimation of the temperature of deep inland groundwater having 10°C enables the good temperature fit of the abstraction wells (fig. 75). Especially the good fit of Well 13, where measured values since 2000 are available, is a strong indication for the correct hydraulics of the model. Obviously the local heterogeneities which gain importance on a small REV (Representative Elementary Volume) which is representative for an observation well, level out each other on a big REV which is representative for an abstraction well. This is supported by simulations with stochastic conductivity fields showing almost identical results (fig. 77). In contrast to chloride and ^{18}O no offset between observed and simulated values exists, which is a further indication that the water balance is correct, the misfit occurs due to unknown concentrations of deep inland groundwater. Two reasons lead to a mean of about 11°C for abstracted water for wells 12, 13, 14:

i. The annual mean temperature of Lake Tegel varies between 10°C and 12°C between 1998 and 2005,
ii. between 2000 and 2004 infiltration in summer is higher than in winter due to seasonal pumping rates (fig. 43).

3.6.5. Stochastically Distributed Hydraulic Conductivity

In order to assess the influence of the heterogeneity of the transport model output, the smooth distribution of horizontal k_f is replaced by a stochastic conductivity field. With 10^{-6} m²/s the diffusive exchange is 1000 time higher for temperature than for dissolved substances. Diffusive temperature exchange is independent of the scale. Though dispersion for the entire system is in the same order of magnitude, it is scale dependent and thus much smaller for a small REV.

Hypothesis: Due to different exchange characteristics between regions of low and high k_f and retardation, the difference between temperature transport and ^{18}O transport is higher using a distributed conductivity field compared to a homogeneous k_f.

To each model layer an unconditioned hydraulic conductivity field with identical stochastic properties is assigned with exception of the layer which represents the glacial till. Here a hydraulic conductivity field is assigned which is obtained by regional calibration with the telescope model.

The standard deviation of the model conductivity field is similar to values of the sieve analysis (tab. 12). The mean of the field has been chosen slightly lower than the observed mean at the transect in order to match the homogeneous value from the regional model. The conservative transport of ^{18}O and chloride already produces good results. Since only the structure of the hydraulic conductivity field is of importance, it is not needed for calibration, the correlation length has been set low in order to avoid large scale effects and to focus on the differences due to the different structure.

Table 12: Field parameters used for generation of stochastic k_f fields. Observed values from Fritz (2003).

parameter	observed	model	unit
mean	$3.6*10^{-4}$	$3.2*10^{-4}$	[m/s]
standard deviation	0.44	0.5	[log10]
correlation length	n.a.	2.5	[m]

So it is not surprising that the simulations carried out with stochastically distributed hydraulic conductivity have neither improved nor deteriorated the results. But the point which

is more important is that the hypothesis can be accepted, the differences between homogeneous and stochastically distributed conductivity fields are bigger for temperature than for ^{18}O.

Small, but considerable differences between homogeneous (fig. 76) and stochastic (fig. 77) distribution occur at observation wells 3301, 3302, 3307, 3312, TEG371up and TEG372 (breakthrough curves in fig. 76, 77, locations in fig. 6). In case of observation wells 3302, 3307 and TEG372 (the latter are very similar since they are separated by a distance of only 7.5 m) a phase shift, based in the retardation of temperature, is the reason for the misfit. Looking at autumn 2001 of observation well 3303, the different structure is based in the retardation in conjunction with differences between homogeneous and stochastic conductivity. The buckling falls in the rising limb of ^{18}O but in the minimum of temperature, resulting in a different aspect of the shape. But immediately after this, in the beginning of 2002 at the same observation well, ^{18}O concentrations of homogeneous and stochastic k_f coincide perfectly, but the temperature is considerably lower/ earlier. TEG371up also shows an almost perfect match of ^{18}O but distinct differences for temperature with faster breakthrough and increased maxima and minima. The behaviour of observation well 3301 is very peculiar. The breakthrough of ^{18}O in a stochastic field is slower than in a homogeneous field, but the breakthrough for temperature is at least identical. During long intervals it is even faster.

None of the wells shows considerable differences, due to the high control volume local differences are levelled out.

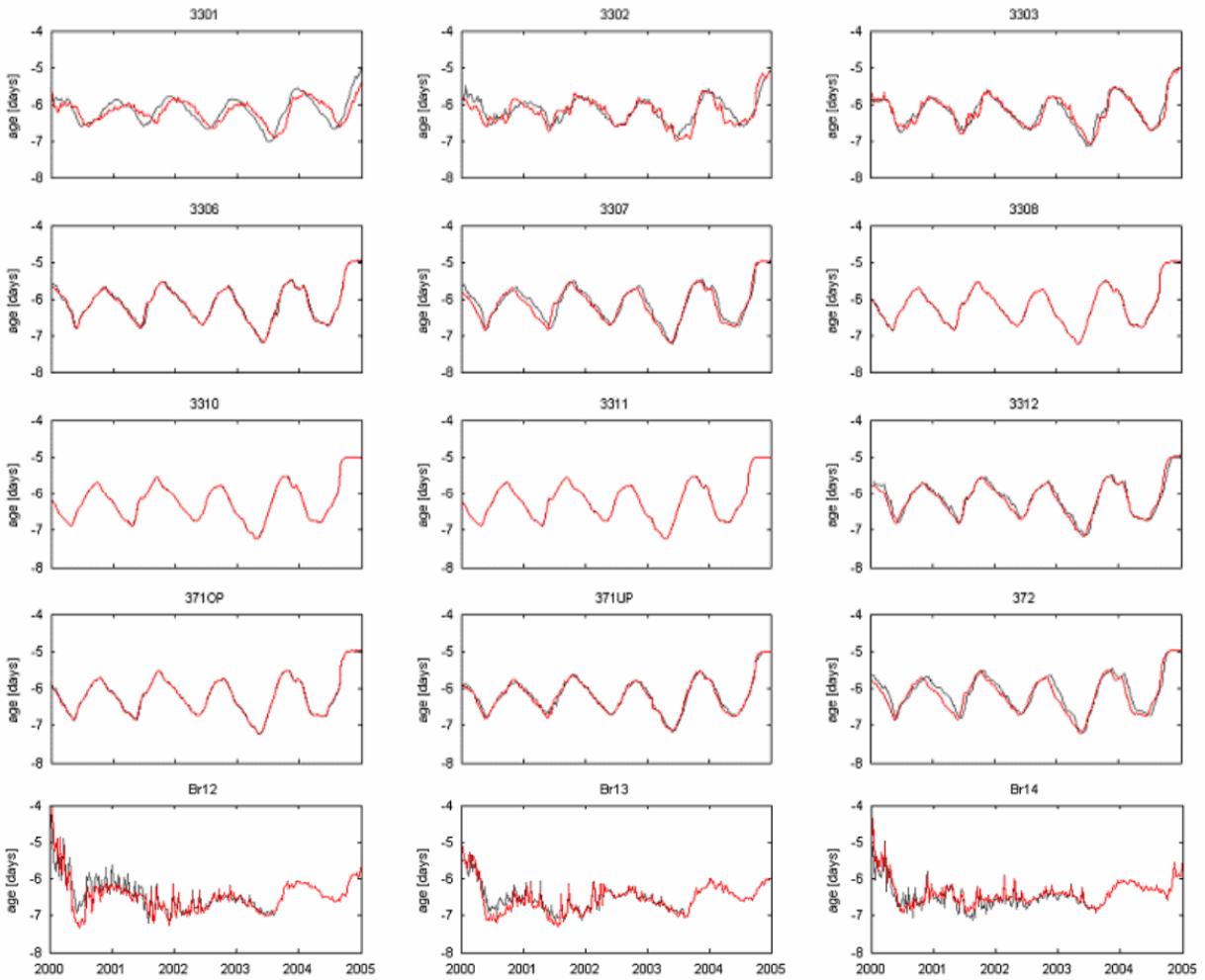

Figure 76: Concentrations of ^{18}O simulated with a homogeneous conductivity field (red curve) and with a stochastic conductivity field (grey curve) between 2000 and 2004.

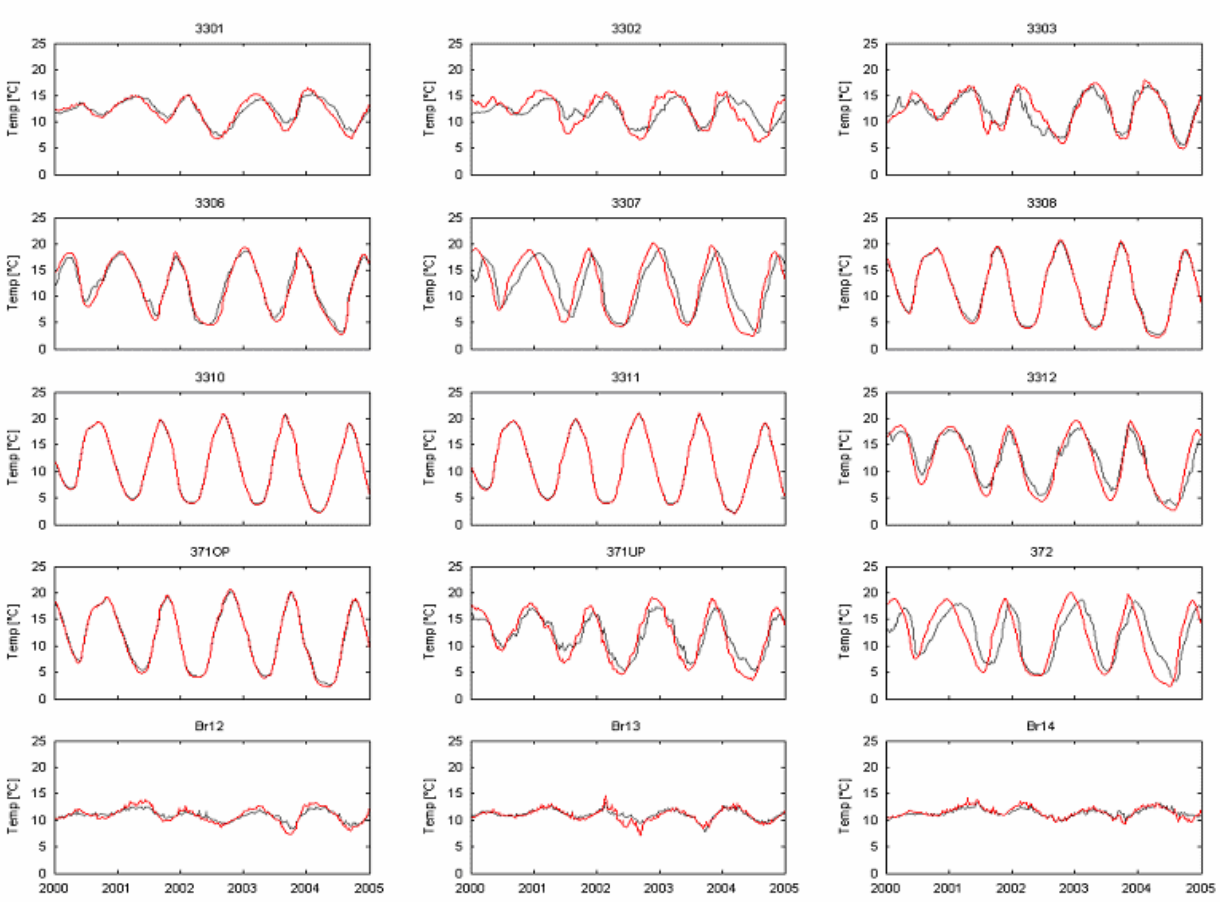

Figure 77: Temperature simulated with a homogeneous conductivity field (red curve) and with a stochastic conductivity field (grey curve) between 2000 and 2004.

Though the simulated temperature differences between stochastic and homogeneous k_f are much smaller than the differences between observed and simulated temperature, they nevertheless may be the reason. The present model is discretised too coarse for realistic simulation of heat transfer processes. A daily time scale or smaller would be appropriate for the heat transfer problem at the observed flow velocites, for 1 day the characteristic diffusion length for heat conduction is 29 cm, the flow distance is between 0.5 and 1 m. The model is discretised weekly, the horizontal block width is 5 m, the vertical block length is 3 m to 10 m. On the weekly scale the transport length with 3.5 m to 7 m is similar to the element width, but the characteristic length (eq. 17) of thermal conduction is much smaller with 77 cm. In vertical direction the insufficiency is even more obvious. Vertical discretisation is about 10 m for the first aquifer and 3 m for the second aquifer. The observed thickness of the layers with different conductivity is about 80 cm (Fritz 2002). The vertical variability is much higher than the horizontal. But since the flow is mainly directed horizontally, most of the heat probably is exchanged in vertical direction. This is not respected in the present model.

Furthermore, temperature transport affects the flow field itself by changing the viscosity, between 4°C and 18°C, as observed in observation well 3301, by factor 1.5. This mechanism is

not included in the model and probably contributes to different transport characteristics between homogeneous and heterogeneous conductivity fields for ideal tracers and especially for temperature. Density driven flow can be excluded, because the concentrations of dissolved substances as well as the temperature difference between 4°C and 18°C are too low on the present spatial scale.

3.6.6. Age

The age of bank filtrate denotes the residence time in the subsurface. It is temporally variant and depends on the pumping rates of the adjacent abstraction wells, mainly on wells 12, 13 and 14, the infiltration of lake water and the distribution of hydraulic conductivity. All observation wells of the first aquifer, namely observation wells 3306, 3307, 3308, 3309, 3310, 3311, TEG371op and TEG372 (fig. 6), show a similar shape of the age which varies up to factor 2 between 2000 and 2005, between May 2002 and August 2004 rarely more than factor 1.5 (fig. 78). The shape of the observation wells in the second aquifer shows less similarities, probably due to mixing because of local intrusion of water from the first aquifer and flow directions depending stronger on the pattern of well operation. Because the concentration gradient and the highest flux occur at the abstraction wells, and inland water is replaced by bank filtrate and vice versa, numerical inaccuracies occur which provoke the short term oscillations. Since the age is calculated using equation 11, small variations strongly affect the calculated age.

Because multiple parameters affect the age, the discussion is limited to a few points.

The modelled age of observation wells 3301 to 3303 are in reversed order: 3303, the farthest from the bank shows the youngest water, 3301 the oldest. Tracer breakthrough of ^{18}O, chloride and boron suggest the age of observation wells 3301 and 3302 is identical, but the water in observation well 3303 is younger. The difference occurs because observation wells 3301 and 3302 contain a portion of older bank filtrate, which is shows up in the age modelling, but is not visible at breakthrough curves.

Massmann (2004) determined the age by a multi tracer approach using deuterium, ^{18}O, potassium, boron, and chloride. The results of 3 months for observation well 3302, 4 months for observation well 3303 and 4-5 months for Well 13 are comparable to the modelled age.

In summer 2003 Well 13 is switched off for 168 days. Within this time the age increases from about 100 to about 200 days. One has to look carefully, because the numerical fluctuations distract the eye. Since the adjacent wells are still in operation and hydraulic pressure of the bank filtrate causes penetration to the other side of the well field, the water

body slightly moves, the increase of age is only about 60%. Beginning in June 2004, Well 13 is operated continuously, pumping rates increase by factor 3 compared to the year before. However, no clear response of the age is visible. Pumping rates of Wells 12 and 14 are decreased, the catchment of Well 13 grows. Additionally the bank filtrate ratio decreases (fig. 67)

Stochastically distributed conductivities only slightly affect the age. Deviations are similar to observations of ^{18}O (fig. 76) and temperature (fig. 77).

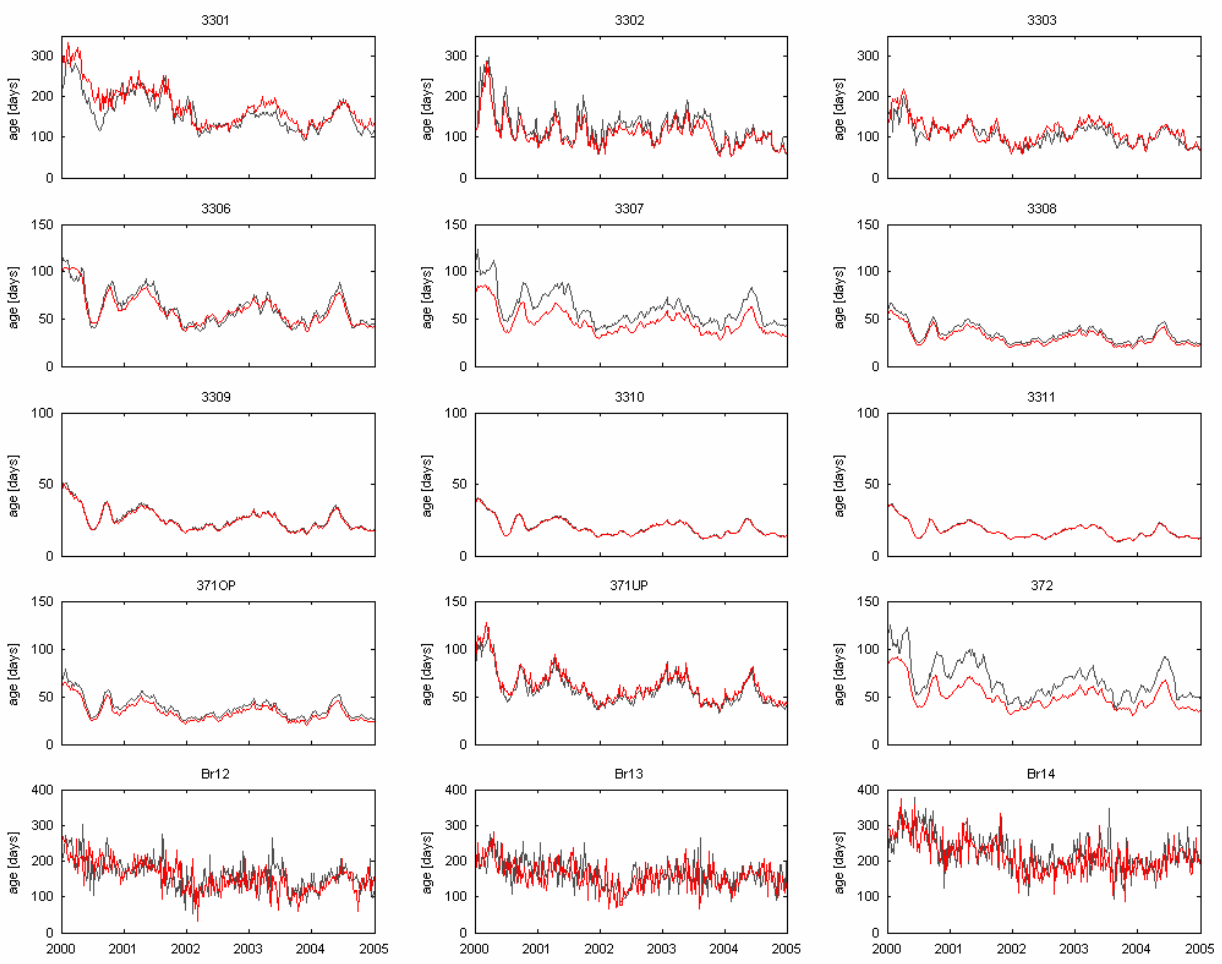

Figure 78: Age of bank filtrate which infiltrated at the eastern bank of Lake Tegel. Ratios of old bank filtrate and inland water are not respected. The red curves are obtained using a homogeneous distribution of hydraulic conductivity, the grey curve is obtained with stochastically distributed hydraulic conductivity.

Error Consideration:

Only errors specifically related to the determination of the age are discussed here, the influence of the flow regime is disregarded.

If water of different age mixes, the mixing age is underestimated in comparison to the arithmetic mean. From the viewpoint of degradation however the age calculated using eq. 11 is more realistic than the arithmetic mean, since usually a first order approach is closer to nature

than linear degradation (0^{th} order approach). This affects observation well 3301 and the abstraction wells, where young and medium aged bank filtrate mix. It potentially affects all observation wells of the lower aquifer because water from the first aquifer with a different age may intrude.

The age of the water which infiltrated near Reiswerder can only be estimated roughly. The variable height of the boundary between layer 1 and 2 as between 2 and 3 (fig. 17) follow the form of Lake Tegel and induce considerable numerical errors in calculated concentrations. Sometimes the species which decays shows higher concentrations than the conservative species. Smoothing of the high steps visible in figure 17 has not improved the accuracy. This error affects observation well 3301 and the abstraction wells.

The abstraction wells show numerical oscillations, the reasons have been already discussed above.

3.6.7. Numerical Reliability

The mass balance for each single species using MT3DMS is only available as cumulative value for the entire model domain. Normally a surplus between 0.3% and 6% occurs, increasing with higher diffusive and dispersive mass transport. Thus normally dispersion is not included, diffusion is only applied when simulating heat conduction. Due to lack of spatial and temporal resolution, the cumulative mass balance only proves limited information. For water balance purposes, a transport species from each source is assigned a dummy species of concentration 1, adding up the species gives a hint if the balance is correct. Analogue to a charge balance at ion determination this criterion only is necessary but not sufficient.

3.6.8. Synopsis Transport Modelling

Travel times estimated by breakthrough curves at the abstraction wells show a very good fit for ^{18}O and temperature. This supports the general model set up and the correct description of flow conditions. Differences of chloride concentrations can be explained by changing ratios of inland water with unobserved concentrations. By mixing calculations using the water balance it can be concluded that deep inland water contains much more chloride than the other fractions. This is plausible since significant amount of water come up from the 3^{rd} aquifer.

Analogue deep inland water has been identified to have lower ^{18}O concentrations, which is plausible with respect to the ^{18}O concentrations in precipitation since 1977.

Observation wells generally show a good fit between observed and modelled concentrations of ^{18}O and chloride. The deviations are acceptable as they do not show a general

trend of being too slow or too fast, supporting the correct modelling of the flow condition, drawn from the abstraction wells.

At the observation wells in general the fit for temperature is worse than for ^{18}O and chloride. Sometimes principally different transport characteristics are obvious. These differences are approved exemplarily by applying a stochastic conductivity field. Due to structural deficits of the model set up with respect to the modelling of heat transport, in nature temperature can be assumed to be even more dependent on heterogeneous aquifer conductivity than shown with the model.

Except for the age determination, the numerical accuracy of the solutions is regarded as sufficient. Generally observed and simulated concentrations of chloride and ^{18}O match well, indicating that the hydraulic situation is correctly described with the present model. Temperature shows only a rough match and though giving a pronounced signal it is not suitable as tracer for longer transport distances.

The concentration misfit of the abstraction wells can be explained by the unknown concentration of deep inland bank filtrate and old bank filtrate until 2003.

The question, why the minimum of temperature breakthrough is significantly increased in observation wells 3301 and 3302 remains open.

3.7. Telescope Model

Well operation at Well Field West is highly alternating with a time scale of well switching between a few hours and a few days, it is operated this way in order to satisfy the operational requirements of the waterworks Tegel. The regional flow model resolves the extremely transient hydraulic regime with weekly mean values (fig. 79). In order to describe the temporal behaviour as precisely as possible, discrete well operation is applied. The scale effect may affect water balance terms, which actually is not the case (chapter 4.5.5).

The shortly switching well operation may be regarded also as a long time multi well pumping test. Since also several observation wells exist a large quantity of data is obtained. The information within the head time curves is deeply hidden. The wells affect each other, the pumping pattern is highly alternating and switching times often are short, the hydraulic heads are highly transient which cause that identical patterns of well operation may have different results, not only because of different mean water levels but as well because the initial conditions depend on the previous patterns. The latter has to be regarded under the condition that parameters of conductivity, namely the glacial till and horizontal hydraulic conductivity, are distributed spatially and can only be estimated with some degree of non-uniqueness. The

telescope model is set up in order to simulate the short term variations of the hydraulic head and solve this Gordian knot of interdependence, non-uniqueness and transient behaviour.

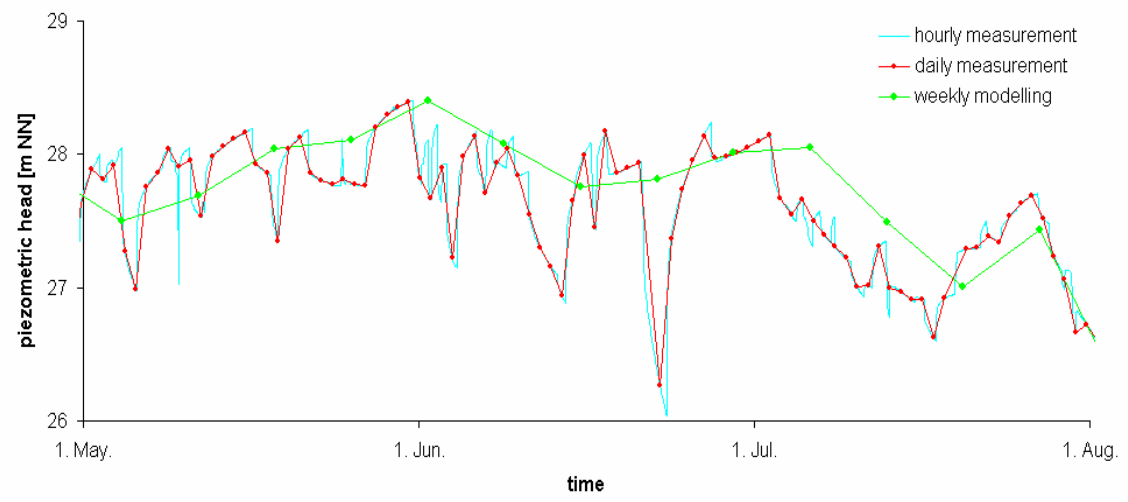

Figure 79: Piezometric heads of observation well 3301 between May and August 2004. The blue line shows piezometric heads observed hourly, the red line shows identical heads with daily observation. The green line shows simulated hydraulic heads with weekly time steps.

An important aspect to be considered is the computational model efficiency. The regional model described above is too large and unhandy and includes large regions which are not of interest. Also the temporal discretisation is not adequate, while weekly mean pumping rates are applied to the regional model, the present problem requires discrete information regarding the well operation.

In order to meet the requirements of the last paragraph, a subregion of the regional model is transformed into an independent model, called telescope model. Hydraulic heads are extracted from the regional flow model and are introduced in form of time variant specified heads as outer boundaries. The temporal resolution is increased from weekly discretisation to discrete well operation depending on the present pumping regime, with intervals between 1 h an 24 h. The horizontal discretisation from the regional model is transferred to the telescope model, since it is already fine enough and facilitates data exchange.

The present model refinement is based on the same techniques analogue to the established TMR (Telescope Mesh Refinement) method (Leake et al. 1999) as used e.g. by Hunt et al. (2001). Ironically no mesh refinement is carried out.

The subsurface shows significant heterogeneities. While aquifer hydraulic conductivities vary within 1 order of magnitude, the leakage between the aquifers, determined by the distribution of the glacial till, varies within 5 orders of magnitude (fig. 4) and thus is the principal geological factor determining the hydraulic properties at the transect.

Rötting et al. (2006) utilise cross-hole pumping tests together with stream-stage response parameters in order to determine aquifer and leakance parameters. In contrast to their approach the present model is more strictly physically based. They parameterised the stream leakance just as third type boundary condition with the conductance as calibration parameter. The area is much larger, such that spatial values represent more an average over a REV and are constrained using geostatistical data. In the present case, the leakage reacts very sensitive to the hydraulic data. It can be calibrated with a resolution in the order of the lowest borehole distance, such that geostatistic parameters would not provide additional information. In order to keep the model as sensitive to hydraulic data as possible, in accordance with Hill (1998) suggesting careful introduction of prior information, geostatistic properties have not been included, because the method itself determines structural elements of the subsurface.

3.7.1. Model Structure

Model Domain

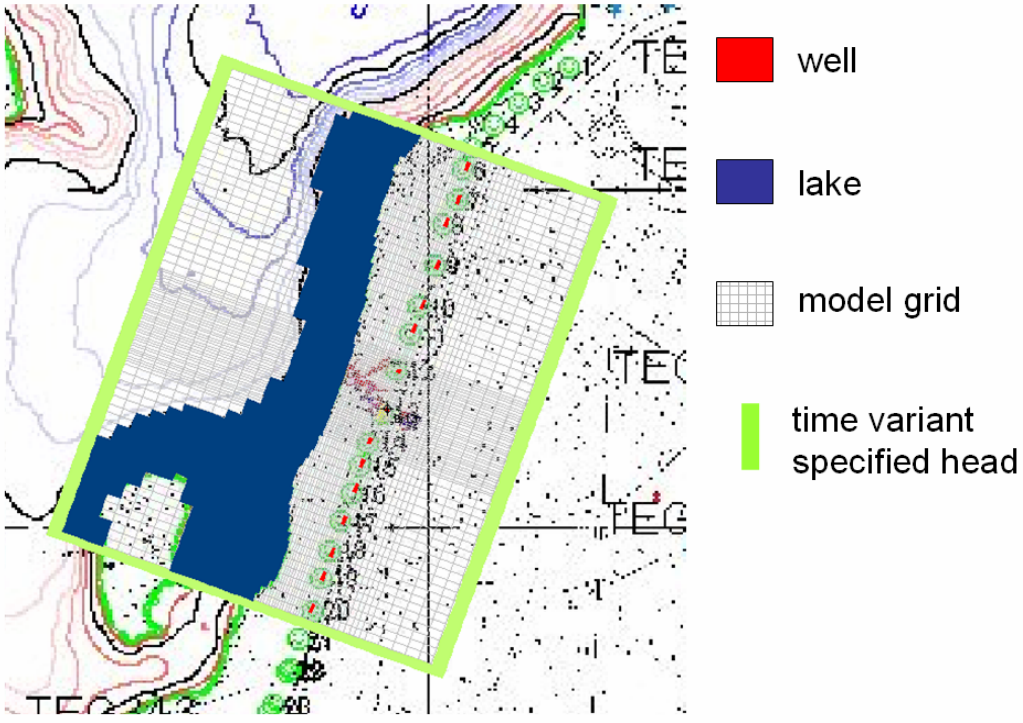

Figure 80: Extent of the telescope model. Red dots indicate wells, Lake Tegel is marked by blue areas, tiny grey lines represent the model grid. The time variant specified head boundary is marked with green colour.

The definition of the model domain should ensure that everything of importance for the flow at the transect is included. Exemplarily, the lowest detectable level of influence on the piezometric heads at the transect is switching Well 10 or 16 (fig. 80) with a magnitude of about 2 cm. The distance of these wells to the observation wells at the transect is regarded as the

maximal radius for short term changes of hydraulic heads by well operation. As a conservative estimation all wells which affect the transect have at least this distance to the boundary conditions. By this way it is ensured that the short term piezometric head changes occur within the model domain and are not affected by the boundary conditions.

Below Lake Tegel the boundary has a larger distance, since the infiltration is a transient process which directly reacts to changes of the groundwater level.

Time Variant Specified Heads

Heads from the regional model are extracted at the position of the boundary cells. Values are interpolated linearly to the beginning and end of each stress period. This means that the weekly head changes of the mother model are smoothed and no big steps occur.

Recharge

Recharge is applied as calculated for the regional model.

Lower Face

The bottom of the model is a no flow boundary

Wells

The model starts at the March 10th 2004. Until the March 17th 2004 daily mean values for pumping rates are assigned to ensure that hydraulic heads are already model dependent when the significant period starts. Between the March 17th 2004 and October 14th 2004 hourly observations and well operation were available. Intervals are set according to the operation times of wells 10 to 16 because only these wells affect the short term behaviour of the transect (see above). A new stress period starts when one of these wells is switched either on or off. Daily mean values for pumping rates are applied to wells 6 to 9 and 17 to 20.

Discretisation

The horizontal and vertical spatial discretisation of the mother model is transferred as it focuses already on the most important part. Consequently grid values could be exchanged easily between the two models. The temporal discretisation is adapted to the exact (hourly) switching times of wells 10 to 16, in total 416 stress periods covering the period between March 10th 2004 and October 13th 2004. The length of the stress periods is between 1h and 24h.

The layer where glacial till may exist is applied with a thickness of 4 m. Though the thickness is spatially variant, its contribution to horizontal flow is negligible, the constant thickness is a tolerable simplification.

3.7.2. Data and Data Pretreatment

Geological Data

Initial point of the estimation of the glacial till is the geological information obtained by boreholes. The elevation for the regarded area is between 18 m NN and 22 m NN, which is about 12 m to 16 m below ground surface. At 15 locations (11 abstraction wells, 4 observation wells) in the model domain boreholes exist which are deep enough to detect whether the till is existent. At 10 of these wells the till is existent, with a thickness of at least 2 m. At 5 wells the till is nonexistent or tiny, in observation well 3301 10 cm are found, in abstraction wells 11, 14, 19, 20 no till is found. Nevertheless it may exist with a minor thickness since the holes have a diameter of 850 mm and the used bore equipment destroys the stratification and mixes a large volume. The estimation by interpretation of the encountered till is shown in figure 81.

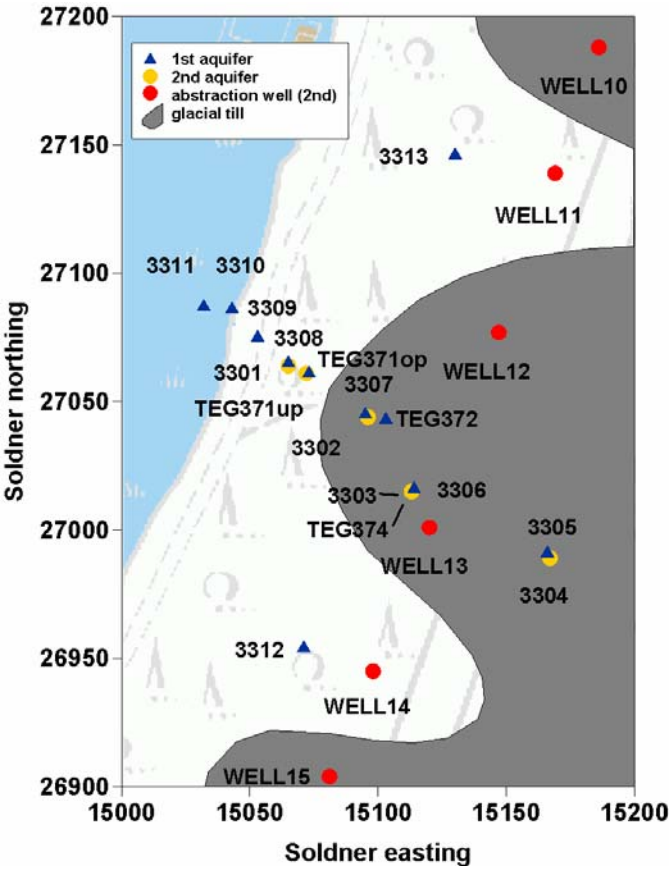

Figure 81: Estimated distribution of the glacial till at the transect, following Eichhorn (2000) and Fritz (2002). Bore profiles of abstraction wells (red circles) and deep observation wells (yellow circles) penetrate the elevation of the till and show whether it is existent.

Hydraulic Data

The parameter estimation is based on the short term hydraulic behaviour. The observed heads can not be used directly, they show deviations and offsets larger than the short term structures (chapter 4.2.2). This is caused in inexact description of infiltration by Lake Tegel

and inexact hydraulic heads inland. These values can not be varied within this model, in order to maintain a well posed parameterisation, the short term differences are parameterised. Furthermore, problems which may occur because of an offset by logger drift or errors in the reference height are avoided.

The short term drawdown is parameterised using 3 parameters. Unlike model parameters they are not estimated but form the dataset with which the model is calibrated. Parameter “a” is used to describe the jump in hydraulic heads immediately after the well is switched on. It increases with the confined state of an aquifer and is result of the head loss because the water is moving. Parameter “b” describes the unconfined behaviour, the drawdown is mitigated by the unconfined storage coefficient and because the depression cone extends. Parameter “c” is just the sum of “a” and “b” to maintain the correct shape (fig. 82). Results of a pumping test where piezometric heads are recorded with intervals of 1 minute (Fritz 2002) show that the phases “a” and “b” can not be distinguished sharply but show a smooth transition.

The data are logged with hourly intervals, the times of well switching also have hourly precision. Thus an insecurity of 1 hour exists about the exact time the wells are switched on/off. In order to minimise this error, parameter a is calculated with a difference of 2 hours. Since the head change in the second hour after switching normally is less than 20% of the head change in the first hour, the mean error by the unknown switching time is reduced to ± 10%.

The temporal model disrcetisation is adapted to the characteristic heads used to calculate parameter a, b and c. Each well switching pattern is a stress period, the first time step of each stress period has the length of 1.5 hours, which is the mean time for which “a” is calculated.

It is assumed that all wells with the same switching hour are switched at the same time. Parameter “c” is introduced in order to mitigate the error if this condition is violated and to include a fit to the general trend. It also mitigates the error if a logger may react too slow.

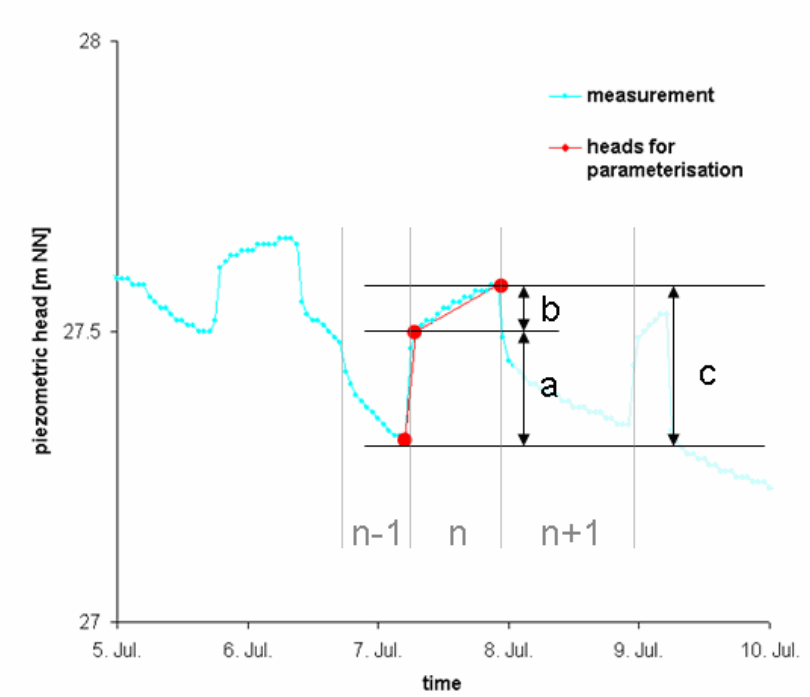

Figure 82: The blue line shows measured hydraulic heads, the red dots show the values which are used for the parameterisation. Parameter a is the head difference between the last point of the previous well switching pattern n-1 and the head 2 hours later in switching pattern n. Parameter b is the difference between the latter head and the last head of switching pattern n.

Between the Mar. 20th of and the Oct. 12th 2004 the pattern of well operation for wells 10 to 16 changes 402 times, providing a lot of information. However, many of this parameters have to be sorted out:

i. Only head data of hourly logged observation wells is included: 3301, 3302, 3303, 3304, 3312, 3313, TEG371op, TEG371up, TEG372 and Well 13 (locations in fig. 6).
ii. If the length of interval n is 2 hours or shorter no parameter is determined.
iii. If the length of interval n is 3 hours only parameter "a" is determined.
iv. Sometimes the recorded switching pattern contain errors. For some stress periods before and after a detected error no parameters are determined.
v. For Well 13 parameters are only determined if it is not switched itself.

Parameterisation

In order to assign spatial information to the entire model, pilot points (Doherty 2003) with triangular linear interpolation are used. A pilot point consists of 3 values: x and y for the spatial position and a parameter value. A triangular grid is set up, the edges of each triangle are formed by pilot points, within the triangles the parameter values are interpolated (fig. 83). In regions of high interest and high information density, each pilot point affects a smaller area and the Delauney condition is fulfilled, which means that a circle, drawn on the edges of each triangle does not comprise any edges from other triangles. In the present case the region around

the transect has the finest discretisation (fig. 83). In regions of low information and secondary interest each pilot point affects a much bigger area. The values of the pilot points are estimated using PEST. Three hydrogeologic formations are parameterised, the hydraulic conductivity of aquifer 1, the hydraulic conductivity of aquifer 2 and the leakage of the glacial till between them.

The regularisation function is a smoothing constraint:

$$\Phi_{REG} = \sum_{i=1}^{n} \sum_{j=1}^{k(i)} | \log(PP_j) - \log(PP_i) | \quad \text{eq. 34}$$

where Φ_{REG} is the regularisation objective function, n is the number of pilot points with i as counter, $k(i)$ is the number of neighbours of each pilot points. Each node is a pilot point. Values of each pilot point are interpolated linearly on the triangles to the model grid (fig. 80).

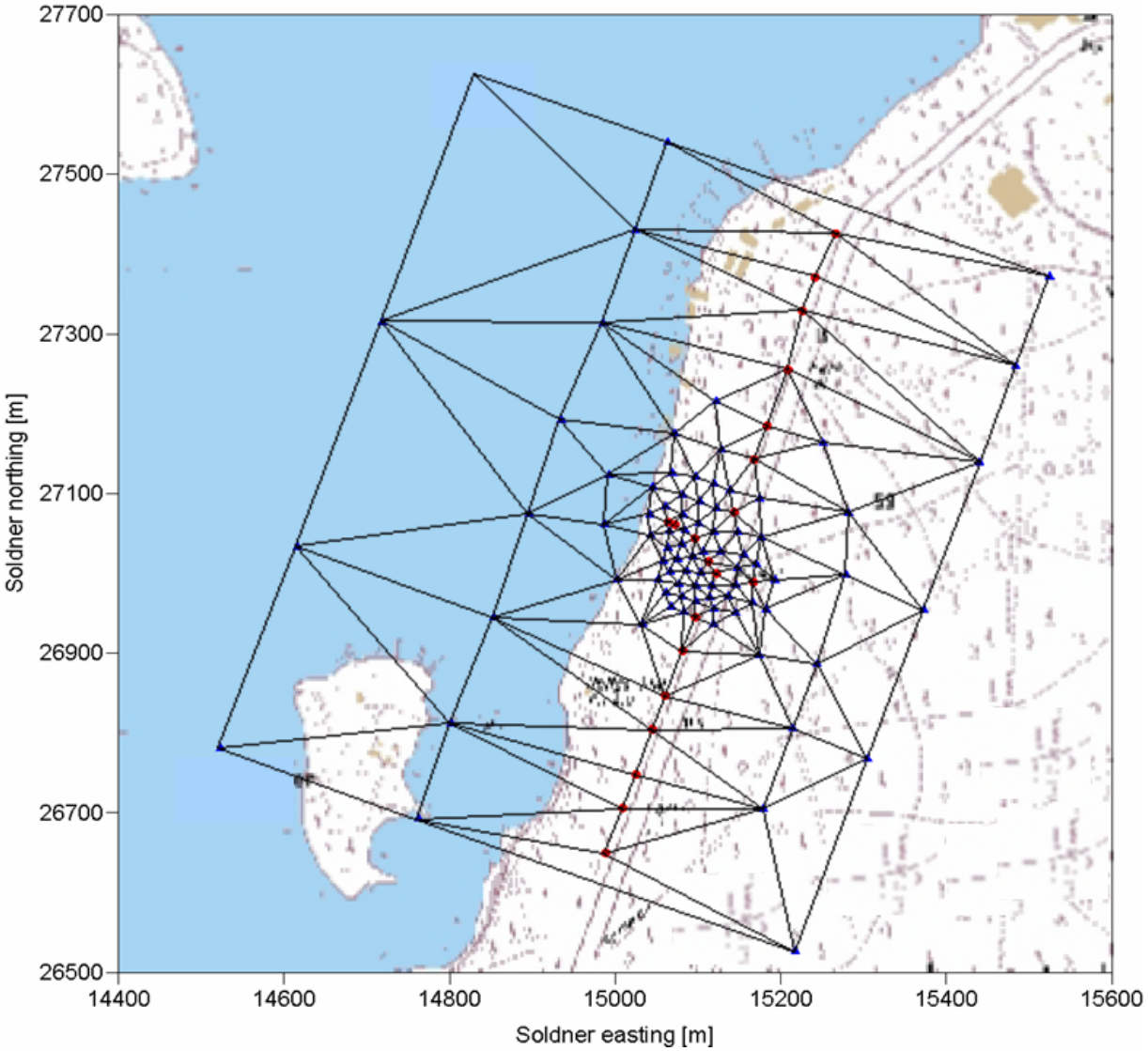

Figure 83: Location of the pilot points. Red circles indicate pilot points at the location of a deep borehole, blue triangles represent the other pilot points. The black lines show the triangles to which values are interpolated.

Every borehole deeper than 15m and thus penetrating the glacial till if existent is also location of a pilot point. If the geological profiles show that the glacial till exists, these points are taken out from parameter estimation and the leakage it set to 10^{-9} s^{-1}. An upper parameter bound of 10^{-4} s^{-1} is applied, which corresponds to a k_f of $5*10^{-4}$ m/s. The estimation of hydraulic conductivity is carried out within the bounds of $3*10^{-5}$ m/s and $3*10^{-3}$ m/s. Further values assigned are: specific yield of 0.21 [-], confined specific storage coefficient of 10^{-5} [-] and a vertical hydraulic conductivity of $3.5*10^{-4}$ m/s.

3.7.3. Results

Spatial structures of the glacial till and hydraulic conductivity could be identified (fig. 84). The most important parameter for transport and geochemistry is the distribution of the glacial till. In contrast to the assumed roughly sinusoidal shape (fig. 81) the till is shown to be expressed continuously, the areas where it is nonexistent are separated. Two holes are identified. The bigger one is located in front of Well 11 and Well 12, almost up to the observation well 3302 (fig. 81). The smaller is located between abstraction Well 14 and 3304. The till exists below the infiltration area of Lake Tegel. It has a leakage of about 10^{-6} s^{-1}. This value is about 1% of the horizontal hydraulic conductivity and can be regarded as the threshold of fully developed, i.e. impermeable glacial till. At abstraction Wells 11, 14 and observation wells 3301 and TEG371up the till has not be detected or only with a few cm thickness. The corresponding pilot points have not been constrained, but the distribution of the till is rather realistic. Though at the exact locations of wells 11 and 14 the leakage is calibrated to about 10^{-6} s^{-1}, which is just the threshold for its continuous existence, having in mind the borehole has a diameter of 850 mm tiny layers may be overseen during drilling. Areas with a high leakage are very close, indicating these wells are located in a transition zone. The boreholes of observation well 3301 and TEG371 have a smaller diameter enabling the detection of thinner layers. At 3301 10 cm of till can be detected, while at TEG371 no till is found. The calibration reproduces these details.

No constraints have been imposed on the horizontal hydraulic conductivity. In the sensitive area, the mean calibrated value is close to mean values obtained by sieve analysis by Fritz (2002) of $3.5*10^{-4}$ m/s. The variability of about ±1 order of magnitude is higher than the observed variability based on grain size distribution between 10^{-4} m/s and 10^{-3} m/s, probably this is overfitting, PEST misapplies the conductivity to compensate other deficiencies. Directly at the transect values are realistic. The large area where conductivity of aquifer 2 exceeds 10^{-3} m/s is located outside the sensitive area. Conductivities of around $3*10^{-4}$ m/s are continuous

and interconnected, lower and higher values exist as isolated areas. This means that the bulk characteristics of the aquifer are preserved.

The sensitive area is located around the transect. Because observation well 3313 is located about 200 m north14 of the transect and observation well 3312 is located about 100 m southsouthwest of the transect, it is larger towards the north. To the east it touches already the boundary condition for the parameter leakage and conductivity of aquifer 2, indicating the model domain is chosen a little too small. The criterion that the well switching should not be detectable as a discrete jump, appears to be not restrictive enough. The small areas with extremely low sensitivity of the glacial till within the transect occurs because the till is constrained to a fixed value for those pilot points where it is mapped in the corresponding bore profile.

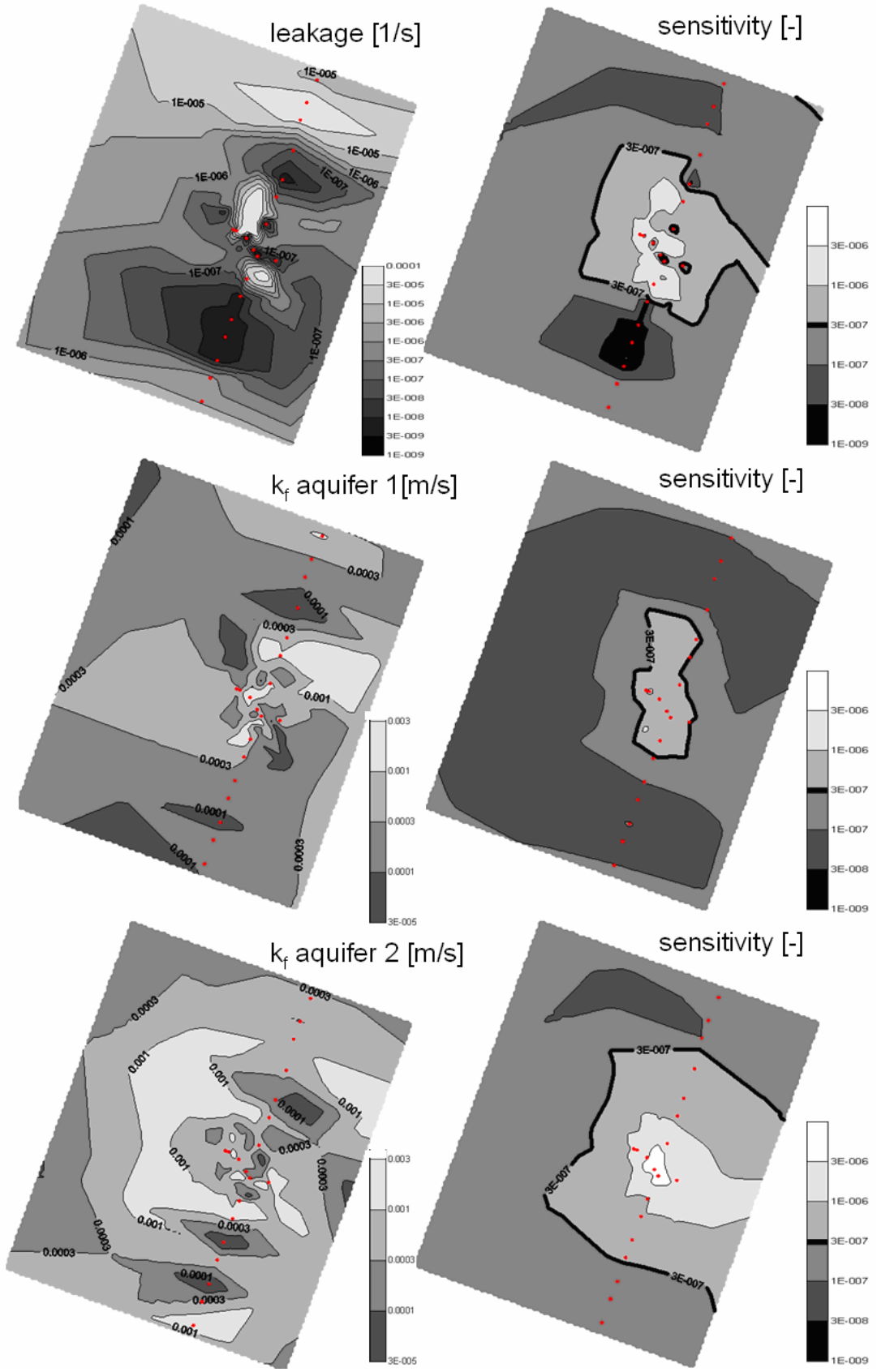

Figure 84: Calibrated spatial leakage and hydraulic conductivity and the correspondent sensitivities. The red dots show the position of all boreholes which penetrate the layer of the glacial till. Transferred to a 4 m thick layer a leakage of 10^{-4} s^{-1} corresponds to a hydraulic conductivity of $5*10^{-4}$ m/s, values below 10^{-5} m/s correspond to conductivities of the double leakage value. The bold black line surrounds the area where the model parameters are sensitive to the observations and results have a physical meaning.

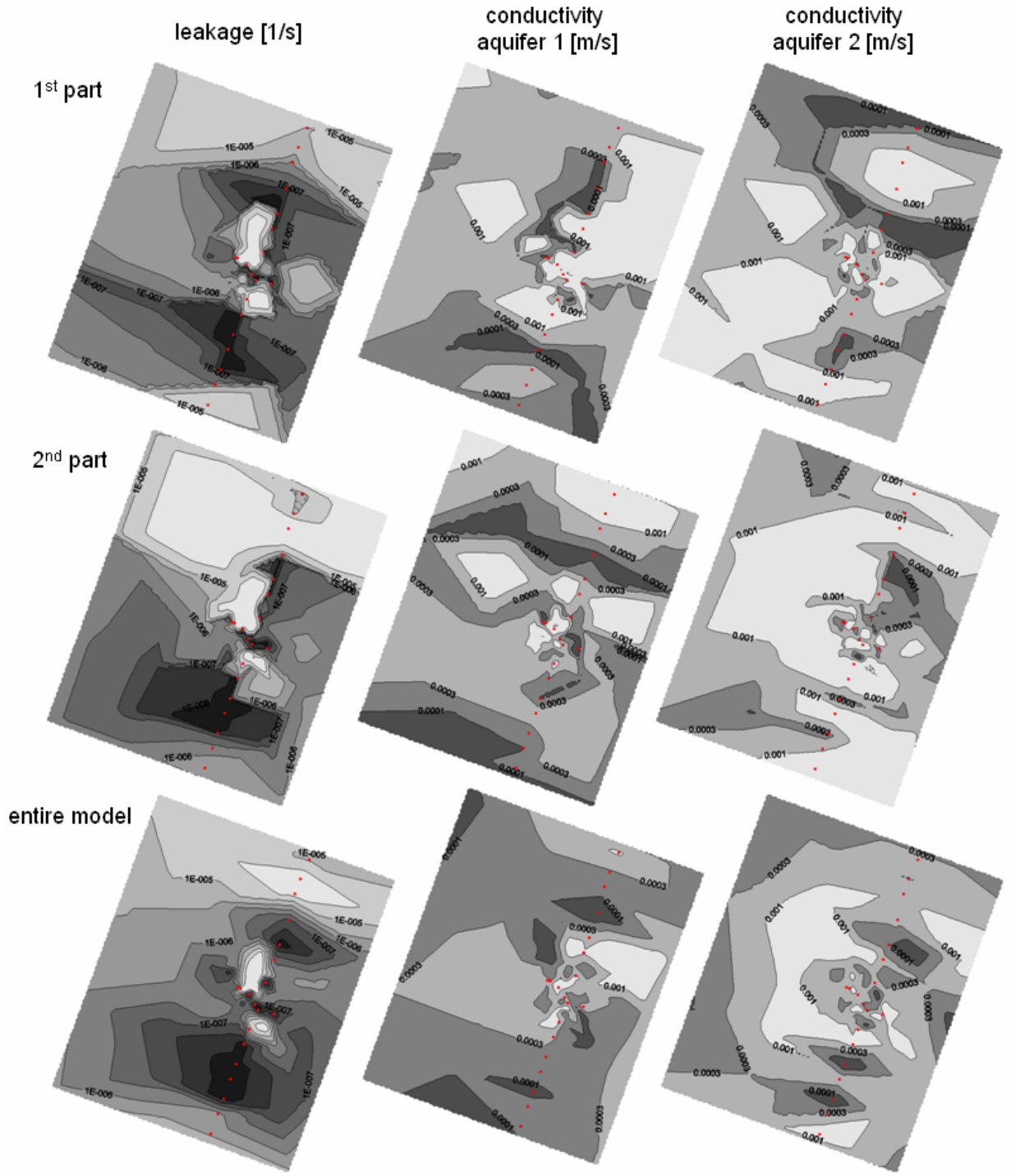

Figure 85: Cross validation of the observed model. The elements of the first row are calibrated only using observations until the 30th June, the second row is calibrated only using observations after the first of July. the last row is calibrated with the entire data set. The columns correspond to leakage, conductivity of aquifer 1 and conductivity of aquifer 2.

Cross Validation

A two fold cross validation is carried out. The calibration data set is divided into two intervals, the first between March 20th and June 30th, the second between July 1st and October 12th. For observation wells 3301, 3304 and TEG371op the hourly head observations are available for a shorter period. This way the first period only comprises 1 month of observations

for observation well 3304, the second period only comprises 6 weeks of observation well 3301 and no data of TEG371op. Calibration is performed with either of the data sets. The model itself remains unchanged.

Though lying within a sensitive region, only directly at the transect some structures are identical in the calibrated distributions, in general structures of the hydraulic conductivity only show few similarities between the 3 different calibrations. Though the hydraulic conductivity of aquifer 2 is more sensitive in a larger area than the leakage, the reliability of the calibrated results are lower. Taking into account that the variability is one magnitude higher than grain size distributions suggest, the conductivity is supposed to reach the calibrated values due to overfitting.

Both calibrations show a similar structure of the glacial till, in the vicinity of the transect, namely the existence of a big hole in front of Wells 11 and 12 and a smaller one between Well 14 and observation well 3304 (fig. 85). It is remarkable that the spatial distribution of the three calibrations only show gradual differences, since three important conditions of the calibration are different:

i. The first data set only contains 1 month of observations of observation well 3304, the second only includes 6 weeks of 3301 and no data from TEG371op.
ii. Residuals are between nil and -50 cm in the first half and between nil and 50 cm in the second half.
iii. Calibrated hydraulic conductivities show significant differences. Apparently, the spatial structures of the leakage have been calibrated physically meaningful in the vicinity of the transect.

Another calibration run has been carried out without the constraint whether the till has been found in the deep boreholes. The spatial distribution only shows gradual differences (no figure), but the low leakage in the sensitive areas hardly fell below 10^{-7} s^{-1}, since hydraulically the variation towards lower conductivities is not sensitive any more.

Goodness of Fit

The model fit of the temporal behaviour is very good. The simulated parameters a, b, c, which represent the temporal behaviour of the model show an excellent match to the characteristics of the observed hydraulic heads (fig. 86). The standard deviation of the residuals is ±3 cm. Regarding the time series curves of modelled and observed hydraulic heads, exemplary shown for observation well 3302 in figure 87 the temporal behaviour is represented very good, though simulated and observed heads differ up to ± 50 cm. Such deviations of the hydraulic heads are based in shortcomings of the water balance in the mother model. In order

to keep the model physically based this offset must not be touched by calibration, besides it is not necessary. The short term head changes are mainly determined by the abstraction rates and the hydraulic behaviour of the aquifer between confined and unconfined. However, the fact that the modelled heads until June are too high and in the second half too low might contribute to the differences in cross validation.

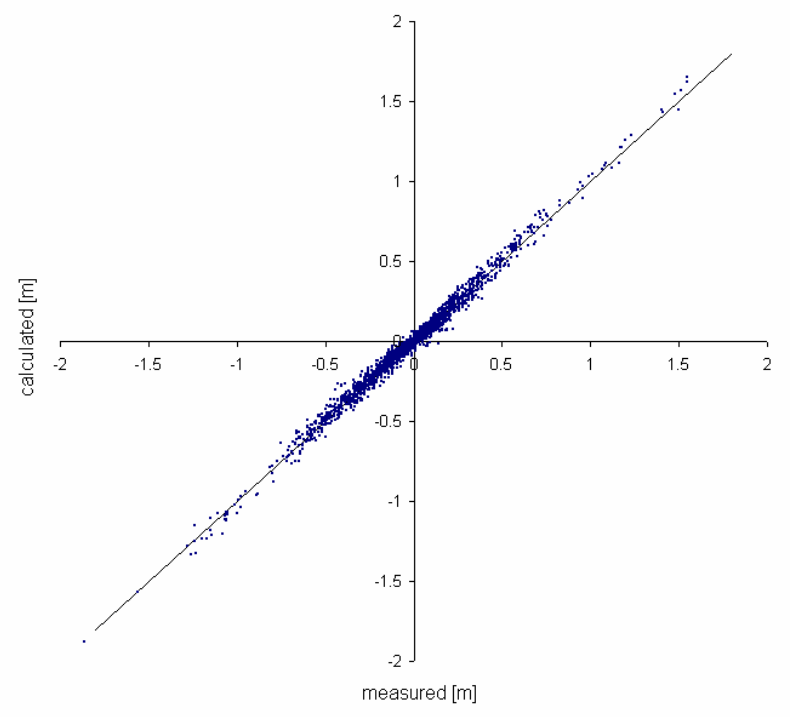

Figure 86: Scatter diagram (blue points) of the observed and simulated differences a, b, c, calculated according to figure 82. The black line indicates the ideal fit.

The modelled differences between different observation wells are most time very similar to the observed differences. However, some deviations exist. The most obvious mismatch is an offset. When most wells are switched off, the differences between the piezometers are low and should be around 0 cm, differences greater than a few cm here are based on levelling. Differences occurring when wells are switched on are model born.

Independent of an existing offset, the curves of the modelled and observed differences should have an identical shape. Normally this is fulfilled, but at some points deviations occur.

For Teg371op and TEG371up (fig. 88) the following differences can be detected:

Until the 8th April 2004 the modelled differences show a downward trend when wells are switched on and upward trend when wells are switched off. The reason is unclear.

At the 1st April a peak is visible in the measurements, but not in the modelling. Unrecorded well switching could be the reason or the logger has been temporally removed, e.g. for taking samples.

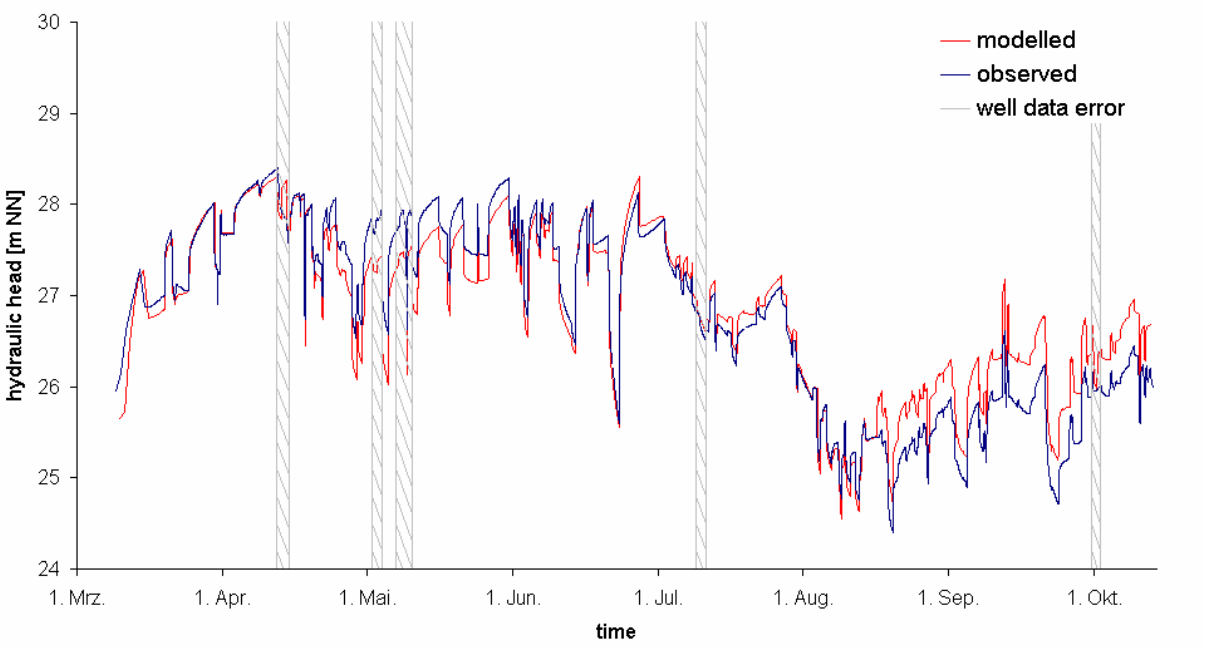

Figure 87: Observed and simulated hydraulic heads of observation well 3302 in 2004. The red line represents the modelled head, the blue line represents the observed heads, the grey rayed bars indicate times which are not respected because definite errors in well operation are detected.

The modelled differences between different observation wells are most time very similar to the observed differences. However, some deviations exist. The most obvious mismatch is an offset. When most wells are switched off, the differences between the piezometers are low and should be around 0 cm, differences greater than a few cm here are based on levelling. Differences occurring when wells are switched on are model born.

Independent of an existing offset, the curves of the modelled and observed differences should have an identical shape. Normally this is fulfilled, but at some points deviations occur.

For Teg371op and TEG371up (fig. 88) the following differences can be detected:

Until the 8th April 2004 the modelled differences show a downward trend when wells are switched on and upward trend when wells are switched off. The reason is unclear.

At the 1st April a peak is visible in the measurements, but not in the modelling. Unrecorded well switching could be the reason or the logger has been temporally removed, e.g. for taking samples.

At the March 23rd, April 19th, April 21st, April 23rd, May 18th small noses are present in the modelled but not in the observed values. The reasons probably are errors in the recorded well operation. Another reason may be the switching of remote well fields at once. In special cases it may occur that the effects of switching one well of and another one on neutralise each other.

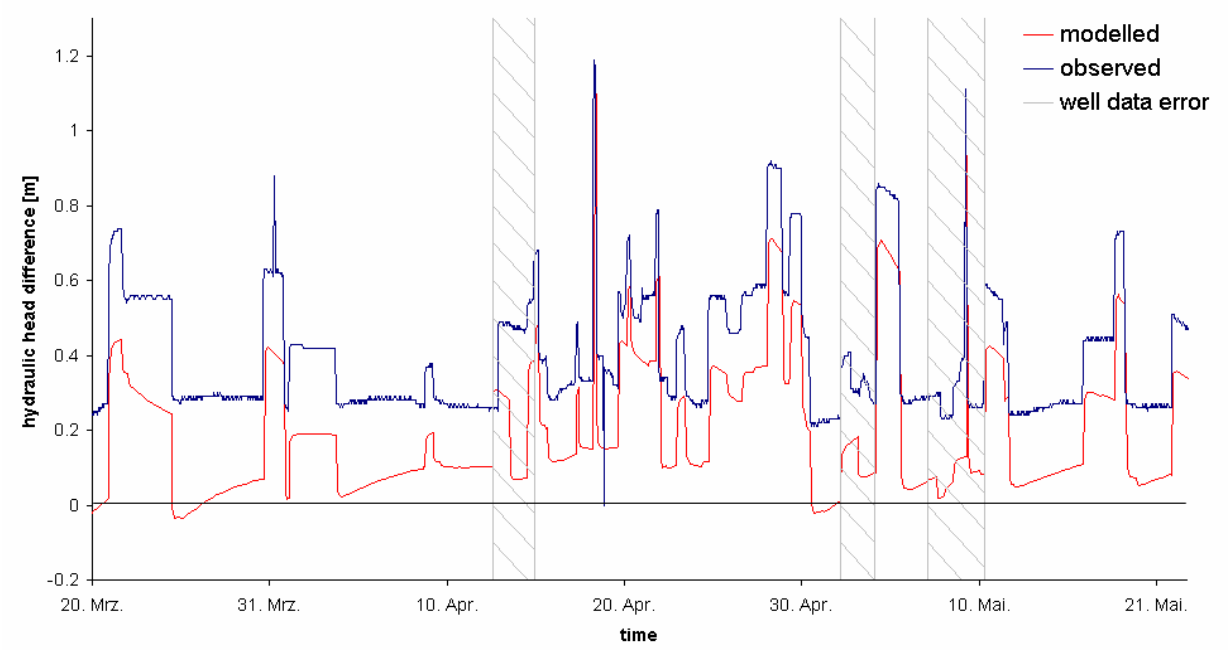

Figure 88: Observed and modelled difference between the observation wells TEG371op and TEG371up in 2004. The red line represents the modelled head, the blue line represents the observed heads, the grey rayed bars indicate times which are not respected because definite errors in well operation are detected.

Peaks of the duration of 1h in measured values probably occur due to different logger times. They occur if a well is switched between the recording of piezometric heads.

Different differences, e.g. April 26th, probably occur due to model insufficiencies. They may also occur when switching times are correct but different wells or a different number of wells are switched.

The differences between observation well 3302 and 3303 basically show the same kind of errors. The smaller ones are less obvious because of the longer interval. Some considerable differences occur around September 7th and around September 19th.

At modelled values of both well pairs negative differences occur. This means the well which normally is upstream has a higher head than the downstream well. This may occur at certain spatial and temporal well patterns in combination with the complex till distribution. However observed heads do not show such differences. Regarding March 24th (fig. 88) and April 28th (fig. 89) the model dynamics to those dates is considerably different from the observed dynamics. Probably this is not based in an offset but some structural differences between the model and reality are the reason.

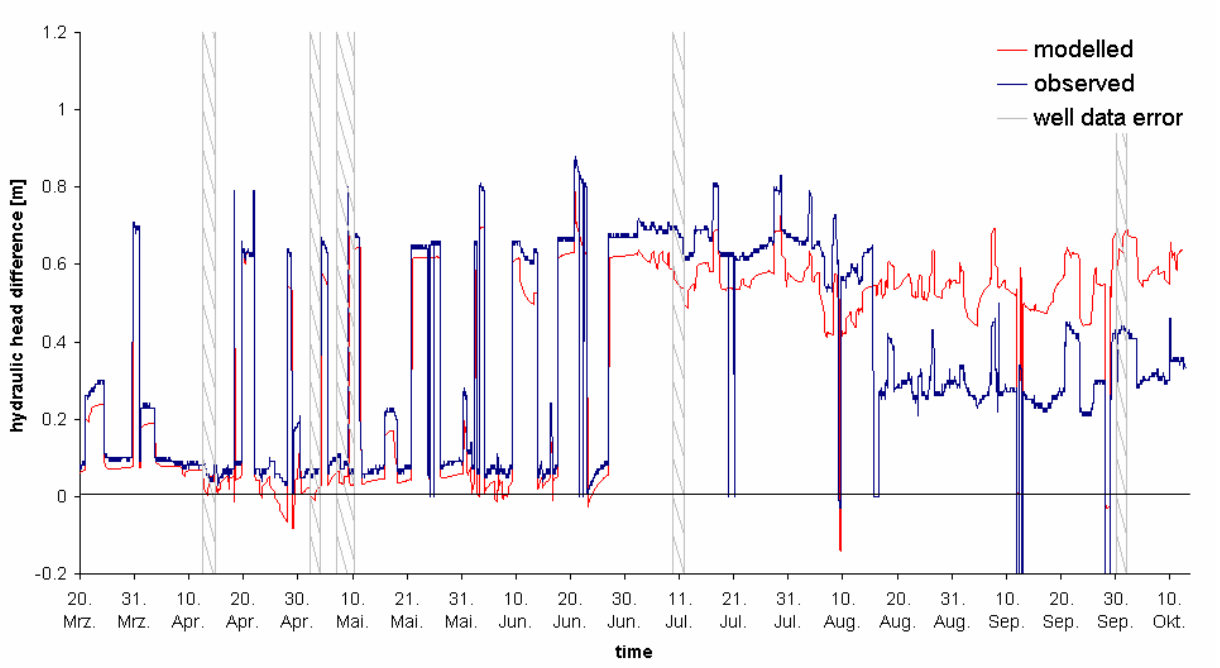

Figure 89: Observed and modelled differences between observation well 3302 and 3303 in 2004. The red line represents the modelled head, the blue line represents the observed heads, the grey rayed bars indicate times which are not respected because definite errors in well operation are detected.

Outlook

The present parameter estimation of the hydraulic properties is only based on the head differences in individual wells. It would be interesting to check if the head differences between different observation wells can be forecasted and under which conditions they provide extra information. Prediction capability and extra information on transport behaviour could also be included. This however would result in seriously increased computational effort.

The accuracy could be improved if the exact times of well operation would be known, such as a higher temporal resolution of the observed heads for extracting more information from the shape of the drawdown and recovery curve. A short pumping test carried out by BWB and Fritz (2002) provides hydraulic heads every minute, recorded in 13 observation wells of which 5 have not been included in the present study. Hereof additional information can be obtained.

In the present example only 3 spatially distributed parameters are included, but others also might contribute to the hydraulic behaviour, such as specific yield, vertical hydraulic conductivity. The impact of the accuracy of pumping rates should be assessed.

Water temperature between 5°C and 20°C results in a different viscosity of factor 1.5. Though the variability is small compared to variability of the aquifers, it could have a significant impact because it affects large areas.

In order to keep the model as sensitive to hydraulic data as possible, in accordance with Hill (1998) suggesting careful introduction of prior information, geostatistic properties have

not been included, because the method itself determines structural elements of the subsurface. However, geostatistic information from boreholes, geophysics or the model results could be incorporated

Upshot

A method has been developed which enables to detect physical meaningfully structures in the subsurface, even under conditions of limited data quality and model accuracy, based on low cost data. Only highly resolved hydraulic head data, well operational data and the general flow field are required. The logged data in conjunction with the model enables detection of errors in operational data.

It is a geophysical method which provides sensitive information about hydraulic conductivity distributions.

The position of the glacial till can be explored with shallow observation wells which may be screened above the till.

In contrast to geological profiles from Voigt et al. (2000) the glacial till is probably present below the lake and infiltration area.

3.8. Geochemical Interpretation

This chapter contains an assessment of the geochemical situation at the transect, interpreted on base of the hydraulic findings of the previous work.

In average, regarded on a big REV, the flow from Lake Tegel to the Well Field West can be regarded as a symmetric problem. Water infiltrates at the bank and flows towards the wells, in first approximation vertical mirror planes, perpendicular to the bank can be set at each well or between two wells. Though this approach is not entirely correct, especially regarding the alternating well patterns, regarding the regional flow of deeper water (chapter 4.5) and regarding the local expression of the glacial till (chapter 4.7), it seems to explain the general trend nevertheless. Tracer data for young bank filtrate suggests that this approach can be applied to aquifer 1 and to the upper part of aquifer 2, except for observation well 3301. Breakthrough curves of ^{18}O, chloride, temperature and boron show that observation wells 3311, 3310, TEG371op, TEG371up, 3302, 3303 and abstraction Well 13 (fig. 4) are ordered by increasing age. 3301 already shows different behaviour, it is located closer to the bank but tracer travel times are identical or even a little higher than for 3302, moreover mixing with old and medium aged bank filtrate is observed. Unlike in column experiments or other bank

filtration sites (Bourg and Bertain 1993) the redox zones are generally stratified vertically (Pekdeger et al. 2004, fig. 90) due to

i. oxygen input from the water table because of rapidly changing hydraulic heads and
ii. because the aquifer itself is the principal source for the degradation of organic carbon.

The DOC which infiltrated from Lake Tegel only explains about 20 % of the increase of TIC (Total Inorganic Carbon). This way organic matter can always be oxidised, the redox state still can decrease after a long flow time.

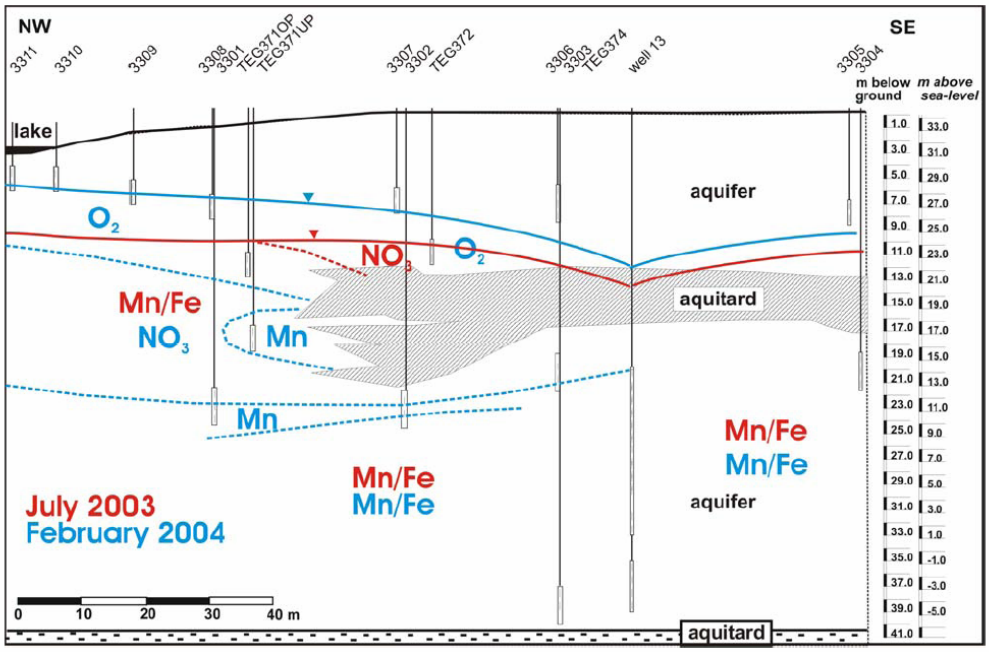

Figure 90: Approximate redox zoning as indicated by presence of dissolved O_2, NO_3^-, total dissolved Mn and total dissolved Fe as measure for Mn^{++} and Fe^{++}, red colour indicates the state in June 2003, blue colour in February 2004 (Pekdeger et al. 2004).

Observation wells in aquifer 1 can be classified in the redox zones of O_2 or nitrate. The high redox state obviously can be maintained because of oxygen input across the free water table.

3.8.1. Curios Redox Conditions

At a closer look the redox sequence appears to be mixed up, the order partially contradicts vertical zoning and as well travel times. Arranging the observation wells in order of decreasing redox potential gives the following sequence of the observation wells: 3310, 3308, TEG372, 3311, TEG371op, 3303, 3302, 3301, TEG371up. Well 13 is not included here, since the water is strongly mixed, also with inland water.

Observation wells 3308 and 3310 show very similar oxygen and nitrate concentrations, very little decreased in comparison to lake concentrations.

TEG372 is correct with respect to its spatial position. It is screened in the upper aquifer directly above the glacial till and shows very low concentrations of manganese between 0.01 and 0.08 mg/l with still considerable amounts of nitrate.

Observation well 3311 shows generally lower oxygen and nitrate concentrations than TEG372. Manganese however occurs more often in TEG372 (fig. App19, Appendix).

The redox state of TEG371op is correct with regard to its elevation and travel time from autumn 2003 on. Before the state is lower than expected, it shows Fe^{++} concentration like observation well 3302 and manganese concentrations like observation well 3301.

The reversed order of redox state for observation wells 3302 and 3303 can not be explained with the 2-D flow assumption, they are covered by glacial till. Reoxidation or the formation of a post-oxic zone, as observed by Bourg and Bertin (1993), is not possible.

Observation well 3301 is more reduced than 3302. Mixing with old and medium aged bank filtrate (chapter 4.5) might contribute to the low redox state but can not explain it fully, the amounts are too low and vary temporally, while the redox level stays rather constant.

Moreover, TEG371up has the lowest redox state of all observation wells, contradicting the flow direction as well as vertical redox zoning.

The oxygen input through the free water table is a mechanism with very high impact on redox conditions, but it is not possible to explain the mixed up order of redox states. In the following sections other factors of influence will be identified.

3.8.2. Oxygen Intrusion at the Bank

Observation well 3311 shows significantly lower concentrations of O_2 and NO_3^- than 3310. At 4 sampling dates even Mn^{++} could be detected. Observation well 3311 is located about 8 m farer from the fringe of Lake Tegel towards the middle. Due to decrease of the water table oxygen is sucked below the lake and during a rising period CO_2 is pushed out (fig. 91 and chapter 4.4.3.2). The process is highly transient, water levels vary irregularly and on different time scales (fig. 79), such that the highest exchange occurs near the fringe, decreasing towards the middle of the lake (fig. 91). This mechanism is described by (Pekdeger 2006, Grünheid 2005). The hydraulic model enables now a rather precise representation of the water table dynamic below the lake. When the water table increases during several weeks, the oxygen concentrations are very low in observation wells 3310 and 3311 (fig. 92), such as at August 20th 2003, January 28th 2003, March 17th 2003, October 20th 2003 and April 19th 2004. The water table has risen steadily during at least 3 weeks, the concentration of oxygen in both observation wells is below 2 mg/l. Concentrations in observation well 3310 however show

stronger and faster reoxidation at falling water tables, visible e.g. at Jan. 19th 2004. Concentrations in observation well 3311 are generally lower since the way is longer, thus the exchange is less intensive and the air reaching observation well 3311 has already been depleted of oxygen. The highest concentrations here occur when the water table is very low. The dead end, where no advective exchange is possible and thus oxygen is totally consumed, is far enough below the lake that it does not affect observation well 3311 any more, oxygen concentrations are high (Nov. 27th 2002, Dec. 17th 2002, Feb. 19th 2003). At May 19th 2003 the table also is very low, water already has 16 °C, probably the oxygen consumption is higher than in winter. The time series are not continuous since the lowest water tables where sampling is possible are 27.4 m NN for observation well 3310 and 27 m for observation well 3311.

Nitrate is not graphed because surface water concentrations vary between 2 mg/l and 13 mg/l. At some dates oxygen concentrations are less clearly correlated to the water table variations. Since the water table considerably varies in May on daily timescale (fig. 79), but the model only has weekly discretisation, some extent of air exchange is not obvious. This probably is of special importance to the observation well 3310. Changing oxygen consumption due to different seasonal temperature, which Grünheid et al. (2003) identified as the reason, potentially also affects concentrations, but it is dominated by the influence of the air exchange. A correlation is visible, but it is mainly based on a spurious correlation, water tables have been in average higher in winter.

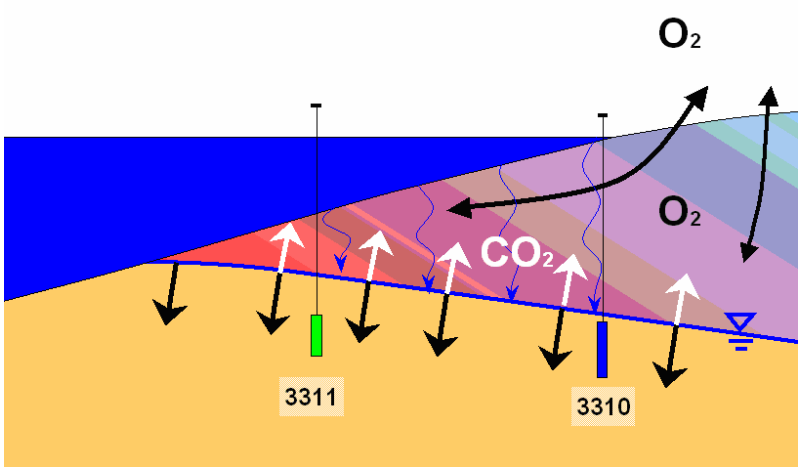

Figure 91: Cross section of the bank at the transect, schematic view of the mechanism leading to aeration of the unsaturated zone below the lake. The red colour indicates air where the oxygen is replaced by carbon dioxide, the light blue colour indicates oxygen rich air. The green colour of 3310 indicates oxic conditions, the green colour of 3311 indicate less oxic conditions, oxygen and nitrate concentrations are lower and sometimes manganese appears.

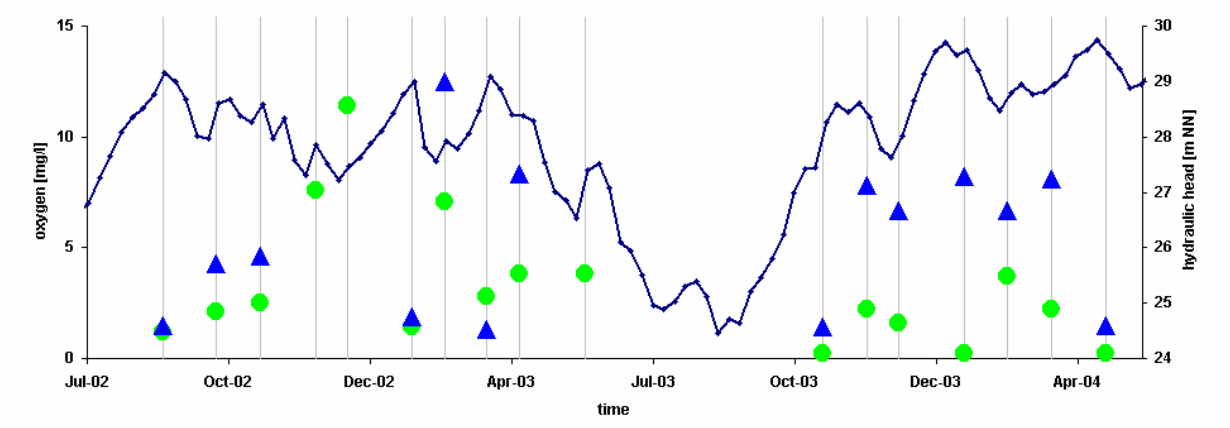

Figure 92: Oxygen concentration at observation wells 3310 (blue triangles) and 3311 (green circles). The blue curve represents the hydraulic head at observation well 3311.

Reversed Redox in Observation Wells 3303, 3302, 3301

Modelling the flow field with the spatial till distribution from figure 95 and comparing observation wells 3302 and 3303, the travel time from the bank is longer for observation well 3303, but the residence time in the second aquifer is longer for 3302 (fig. 93). This means water in observation well 3302 flows a longer time without exchange to the atmosphere and thus reaches a lower redox state. Not the horizontal position of 3302 leads to a higher residence time in the second aquifer, but the fact that the screen of 3302 is 3 m deeper than 3303. The deeper screen also enables mixing with medium aged or old bank filtrate, which contributes to the low redox state (chapter 4.5).

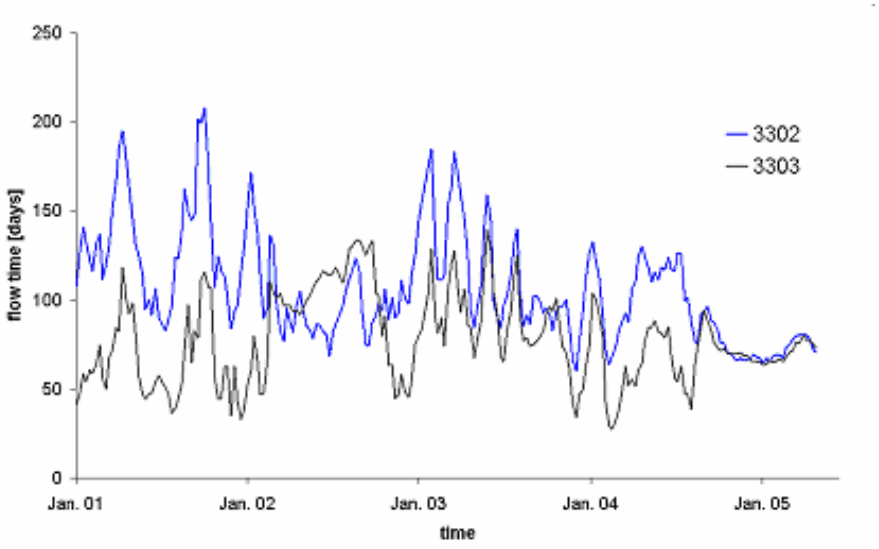

Figure 93: Residence time of young bank filtrate in aquifer 2 for observation well 3302 and observation well 3303.

For observation wells 3302 and 3301 the mechanism is similar, the simulated residence times in the second aquifer for observation well 3301 are identical or higher than for observation well 3302, and the ratio of medium aged and old bank filtrate is higher. However,

results of observation well 3301 are not as precise as results for observation wells 3302 and 3303. The tracer breakthrough is simulated with less accuracy, visible for chloride (fig. 72) and especially for temperature (fig. 75). The reason probably is that the glacial till could not be calibrated as precise here like it was possible closer to the transect, but it is very probable that observation well 3301 gets water which infiltrated in deeper regions of Lake Tegel.

The variations of DOC in surface water are not noted to induce changes in groundwater chemistry (Grünheid et al. 2005), but the surface water's chemical characteristics change significantly during and immediately after infiltration (Ludwig et al. 1997). DOC and sedimentary organic matter are still reactive, O_2 and NO_3^- as easily consumable electron acceptors are available, at later stages the organic carbon becomes less reactive and the microorganisms only can perform the less effective reduction of manganese and ferric oxides.

Farer away from the bank towards deeper water the redox state of the infiltrating water is lower (chapter 4.4.2), probably up to iron reducing conditions, but without observable sulphate reduction. Since the water which infiltrated in deeper areas of Lake Tegel stratifies below the water which infiltrated in shallow areas closer to the bank, the vertical redox zoning is not only caused by oxygen input across the water table, but already established during infiltration (fig. 94). Consequently, already aquifer 1 shows a vertical redox gradient below the infiltration area.

The combination of

i. the oxygen input across the free water surface
ii. the organic carbon being less reactive with increasing distance from the bank
iii. the lateral redox gradient during infiltration
iv. the existence of the glacial till below the infiltration area,

results in the distribution of the general redox zoning which is shown in figure 94.

The lateral redox gradient of infiltrating water may also cause the reversed redox gradient between 3301 and 3303, the nearer to the lake the observation wells are, the deeper the water already has been during infiltration and the nearer the observation wells are located to the abstraction wells, the higher the ratio of water which stayed a long time at the well aerated top of aquifer 1. Most degradation of organic matter takes places within the first metres of flow. DOC and matrix attached organic matter is less reactive. Due to the aeration across the water table the DOC and probably also sedimentary organic matter has become less reactive and 3303 also can be regarded as located within a post-oxic zone (Bourg and Bertain 1993). The slightly higher redox state of 3301 can not be explained with the 2D assumption, according to figure 94 it should have a deeper redox state than TEG371up. Below Lake Tegel the till is calibrated to be semipermeable, but results are not very sensitive and only represent a mean

value. Taking into account the glacial till forms a continuum with holes where it is nonexistent, a configuration appropriately explaining the redox state of 3301 can be easily thought of.

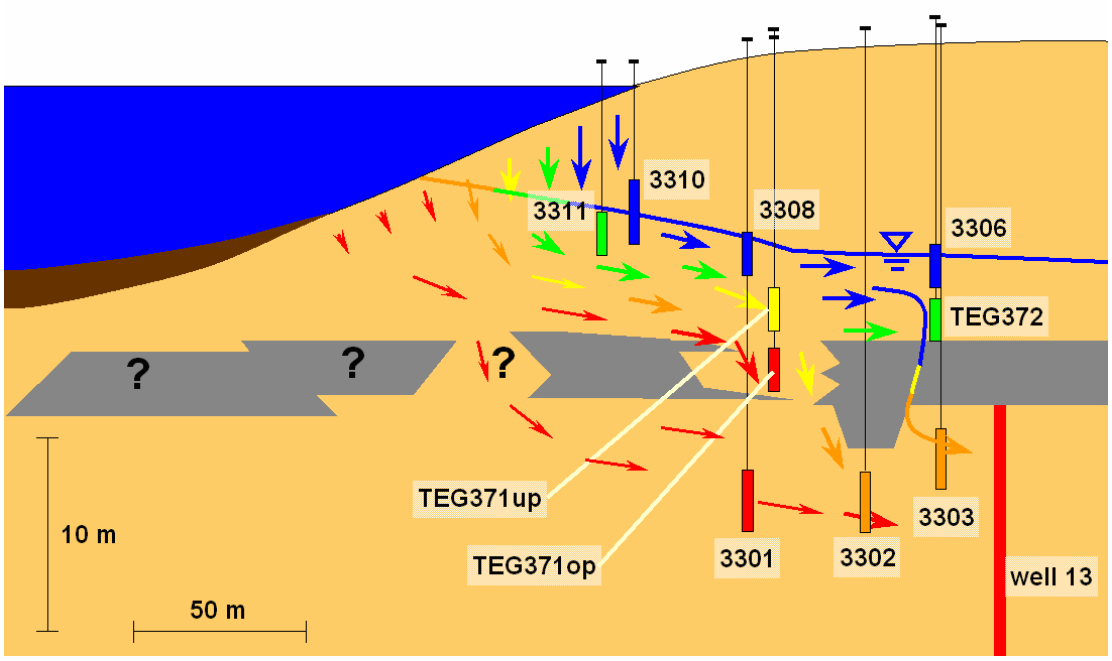

Figure 94: Almost proportional, 7 times exaggerated cross section of the transect. Arrows indicate groundwater flow, the inclined blue line represents the hydraulic head in aquifer 1. The colour ramp from blue to red corresponds with high to low redox levels. Observation wells are represented by tiny vertical lines, the screen by filled rectangles. The observation wells inland of Well 13 and some shallow observation wells are omitted for readability, also their redox state coincides with their position. The raw data can be found in the appendix, fig. App17, App19, App20 and App21.

While at observation well 3301 the glacial till still represents a considerable aquitard, at TEG371up it is already nonexistent, in that area the highly reduced water from the bottom of aquifer 1 flows downward and passes TEG371up.

Redox Level and Tracer Concentrations in Observation Well TEG371up

TEG371up shows the lowest redox state of all observation wells mainly affected by young bank filtrate. A possible interpretation is spatial heterogeneity and existence of microzones (Pekdeger et al. 2004) with reduced conductivity and/or increased organic carbon content of the sediment. However, several contraindications exist: Concentrations of boron, AMDOPH and chloride are identical or higher than in observation well 3301 showing similar temporal behaviour. Furthermore, it is doubtful if such a zone could produce high concentrations of 0.6 mg/l dissolved iron without a noticeable reduction of the hydraulic conductivity, neither in the bore profile nor in modelling. Concentrations of TIC (Total Inorganic Carbon) are similar to the other observation wells, not suggesting very strong biodegradation. These similarities to observation well 3301 indicate that the water has a similar source. The glacial till is calibrated to be nonexistent directly at the location of observation well TEG371up, but it already acts as a considerable aquitard in the direct vicinity at observation well 3301 (fig. 95). Just small spatial

shifting of the real distribution in comparison to the calibrated distribution seriously affects the source of water. The general flow direction above the glacial till is from westsouthwest to observation well TEG371up. This enhances the amount of very reduced water, because the small void acts as collecting points. Water flowing towards observation well 3302 in contrast descends to the lower aquifer more westwards. The very reduced water from the bottom of aquifer 1 just flows downward at observation well TEG371up.

Observation well TEG371up is screened between 21.7 m NN and 23.7 m NN, located between the upper and lower boundary of the till, but it shows a ratio of old and/or medium aged bank filtrate. This is a clear contradiction to the interpretation of the strong downward flow. Though in observation well 3301 the 10 cm thick glacial till is located below observation well TEG371up, at 21 m NN.

In contrast to the observed geology, the confining layer would have to be located above TEG371up, about at 24 m NN.

Another possibility is that the old/medium aged bank filtrate are already present above the glacial till. If the older bank filtrate ratios flow above the till, they become mixed with the young bank filtrate when they pass the infiltration zone. This would also explain the very similar concentrations and temporal behaviour of AMDOPH, chloride and boron to observation well 3301 and also very similar temporal behaviour in observation well 3302. Since medium aged and old bank filtrate infiltrated above the till, which probably is existent below the infiltration areas, this explanation is more elegant.

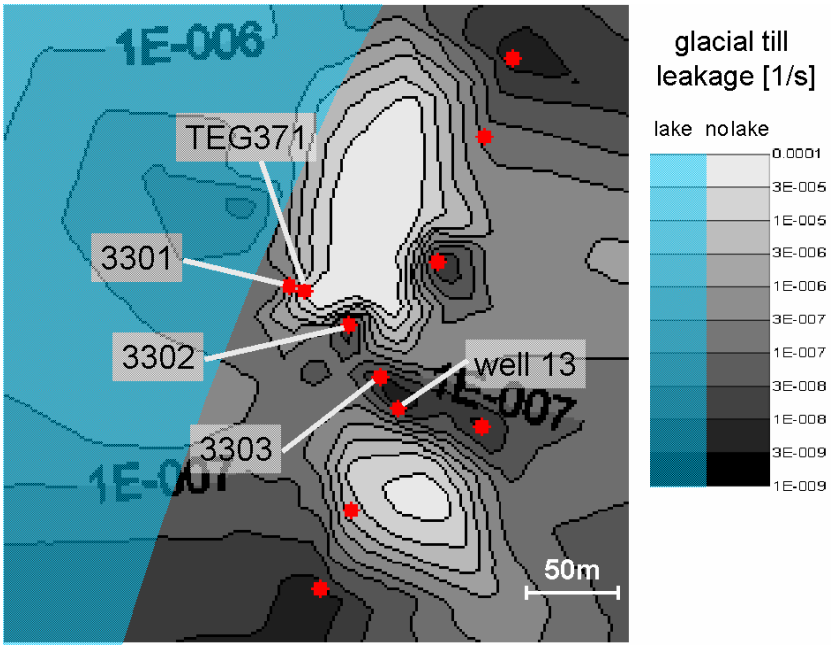

Figure 95: Calibrated glacial till at the transect. A bright tone shows high leakage, a dark tone low leakage, values below $1*10^{-7}$ s^{-1} can be regarded as effectively impermeable. Lake Tegel is indicated by a blue shaded area. All boreholes which reach the depth of the glacial till are represented by red dots.

Furthermore, the present water budget has been calculated with Case2, assuming a leakance independent of the groundwater table. But the leakance behaves more like Case3, rapidly increasing with falling hydraulic heads. Applying this to the infiltration around Reiswerder means that considerably less water infiltrates in larger distances to the bank, and that the hydraulic gradient would not be high enough to affect the lower aquifer as strong as shown in figure 59 and figure 66. The boron, chloride and AMDOPH concentrations observed possibly derive from Reiswerder.

The present behaviour illustrates that the flow paths do not follow the 2D assumption and that the differences of a 3D flow field can seriously affect geochemical reactions.

3.8.3. Drawdown Summer 2003

The groundwater at the transect is subject of considerable changes between May 2002 and August 2004. For tracers, the changes can be summarised to be induced by changing surface water concentrations, in some observation wells a small part is caused by mixing with medium aged and old bank filtrate.

The redox conditions are subject of strong changes during the observed period. Observation wells 3308, 3310 and 3311 show changes due to variations of the water table and seasonal effects, the time series of observation well 3306 is too short to judge about seasonal behaviour. The observation wells with a larger distance from the bank and deeper do not show seasonal response. But also these wells, namely observation wells TEG371op, TEG371up, 3301, 3302, 3303, 372, and Well 13 show strong changes in geochemical characteristics. Until October the most redox sensitive parameters Mn, Fe, NO_3^- and O_2 stay rather constant. Afterwards, the speciation distribution turns towards oxidising conditions. For most observation wells and species this happens sequentially (tab. 13).

Table 13: Increased redox parameters as consequence of the extreme drawdown 2003 (KWB 2005). The entire time series of can be found in the Appendix (fig. App17, App19, App20, App21).

	Fe++ [mg/l]		Mn++ [mg/l]		NO3- [mg/l]		O2 [mg/l]	
TEG371op conc.	0.23	nil	0.62	nil	nil	8.5	0.1	5.4
date	Oct-03	Nov-03	Sep-03	Feb-04	Sep-03	Nov-03	Nov-03	Feb-04
TEG371up conc.	0.65		0.75	0.15	nil		nil	sporadic
date	May-02	Aug-04	Nov-03	Jun-04	May-02	Aug-04	Oct-03	> Nov. 2003
3301 conc.	0.38	nil	0.65	0.28	nil	2.3	nil	
date	Jan-04	Feb-04	Oct-03	Feb-04	Jan-04	Feb-04	May-02	Aug-04
3302 conc.	0.23	0.06	0.5	0.2	sporadic	8.6	0.1	1.3
date	Oct-03	Apr-04	Oct-03	Jun-06	Oct-03	Apr-04	Feb-04	May-04
3303 conc.	nil		0.35	0.22	nil	3.5	0.2	1.3
date	May-02	Aug-04	Nov-03	Apr-03	Dec-03	Feb-04	Mar-04	May-04
TEG372 conc.	nil		0.05	0.01	0.3	10.3	irregular	
date	May-02	Aug-04	Aug-03	Sep-03	Aug-03	Feb-04		
well 13 conc.	~1		~0.38		nil	0.6	~0.1	2.7
date	May-02	Aug-04	May-02	Aug-04	Jan-04	Feb-04	Mar-04	Jun-04

These changes are result of hydraulic conditions, they are the consequence of the decrease of hydraulic heads between Mar. 18th 2003 and Aug. 14th 2003. At the bank, at the position of observation well 3311 the heads decrease by 5.35 m. The drawdowns are similar at all observation wells. The 4 species defining the redox zones at Lake Tegel and their behaviour as consequence of the drawdown are listed in table 13. Generally the changes behave like expected, first Fe disappears, then Mn, followed by NO_3^- and O_2 showing up. Some observation wells start at Mn reducing conditions, like observation wells 3303 and TEG371op, others do not reach the oxygen state, like observation wells TEG371up and 3301.

Usually Mn shows much slower transition than Fe, NO_3^- and O_2, probably since the reduction retreats to microzones (Murphy and Schramke 1998), when most parts of the aquifer are already characterised as nitrate zone. These zones release Mn which is only slowly reoxidised or forms metastable colloidals.

However, some particularities exist:

i. Observation well TEG371up shows constant iron concentrations but a significant reduction of manganese. The reason may be that at the void of the till with strong downward gradient different waters mix, and the deepest reduced water directly above the till has not been affected, still providing dissolved Fe, but the Mn reducing environment above decreased.

ii. Observation well 3302 shows all redox states at the same time, which only gradually change. Probably it is located within a mixing zone (chapter 4.2).

iii. Well 13 shows similar behaviour like 3302, in 2004 all 4 redox indicators are present. However nitrate concentrations are very low, though about 0.8 mg/l $NH4^+$ is present. The oxygen derives from young bank filtrate, the $NH4^+$ from old bank filtrate (36 mg/l, TEG374) and from inland water (3 mg/l, 3304).

iv. TEG372 shows irregular behaviour of oxygen concentrations since it is located near the free water surface and thus affected by oxygen input through ground air.

3.8.4. Dead Water

In chapter 4.4.2.11. it has been shown that most infiltration occurs in the unsaturated zone. The extent of the unsaturated zone is variable and mainly depends on the water table of the underlying aquifer. The thickness of the saturated zone below the lake varies between about 5 cm and 22 cm (Hoffmann and Gunkel 2006) and thus is negligible. The leakance follows equation 32, with calibrated parameters of Case3 reading:

$$L = 2.3*10^{-8}*(1+14.8*h_{usat}^{0.78})[s^{-1}] \quad \text{eq. 35}$$

Where L is the leakance and h_{usat} is the thickness of the unsaturated zone. It shall be emphasised again, that this equation is a good approximation of the process with some deviations still remaining. The important point is the principle that below a threshold depth infiltration is very low, and above infiltration is at least one order of magnitude higher. The threshold is the change between saturated and unsaturated conditions or is closely connected.

Triggered by the water level the infiltration depth decreases between Mar. 18th 2003 and Aug. 14th 2003 by about 5.5 m, up to a level of 24.5 m (fig. 96). This is about the depth where the impermeable mud begins and it is the deepest drawdown at least since 1998. Within the observed period the deepest drawdown was at Jun. 26th 2002, still 2 m higher. The slope of the bank is about 1:10, each meter of drawdown flushes a 10 m wide stripe of the aquifer. During the 2 months, when the water table decreases by 2 m until its minimum, about 2500 m³ of dead water per well are released, about 7% of the bank filtrate. This dead water is detected in the observation wells. Figure 96 illustrates the high variability of infiltrated quantities. Calculated along a cross section the following amounts infiltrate: at the 14th Aug. 2003 1.13m²/d, at the 26th June 2002 0.49 m²/d, and at the 18. Mar. 2003 only 0.054 m²/d, which means the variability is of factor 20.

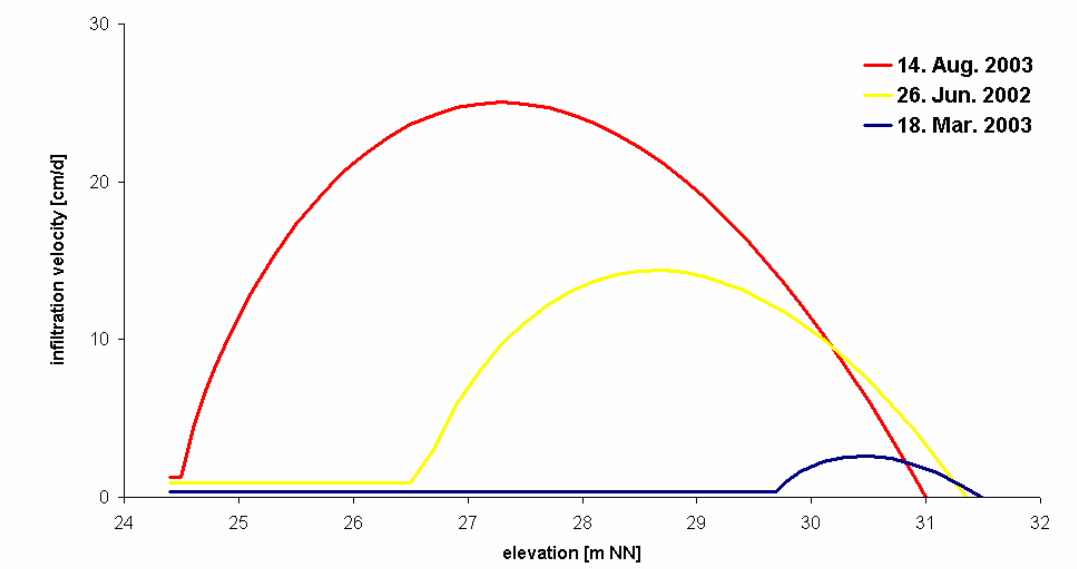

Figure 96: Curves show the depth dependent infiltration velocity at the 14th Aug. 2003 (deepest drawdown, red curve), at the Mar. 18th 2003 (highest heads in 2003, blue curve) and at the Jun. 26th 2002 (deepest previous drawdown within sampling period, yellow curve). The depth dependence is calculated with equation. 32, parameters like derived from Case3

Organic Carbon

Two parameters are used in order to identify the amount and structure of organic carbon: DOC [mg/l], which quantifies the amount of dissolved organic carbon and UV254 [m^{-1}] which is the extinction at a wavelength of 254 nm (nanometer) and quantifies the presence of aromatic atomic bounds. The ratio of UV254 and DOC is called SUVA [l mg^{-1} m^{-1}] and is a measure for the content of aromatic atomic bounds of the DOC. During the infiltration under oxic conditions preferably aliphatic (chemical single bounds) compounds are degraded, leading to an increase in SUVA, under anaerobic conditions the aromatic compounds are preferentially degraded. Such observed at the transect by Grünheid et al. (2005).

Changes in groundwater DOC at the transect do not occur due to variations in surface water but are result of geochemical processes (Grünheid 2005). The corresponding degradation reactions can be written for aerobic respiration (Greskowiak 2005) using a slightly simplified organic matter composition of Bourg and Bertain (1993):

$$CH_2O(NH_3)\ 0.15 + 1.3\ O_2 \rightarrow HCO_3^- + 0.15\ NO_3^- + 1.15\ H^+ + 0.15\ H_2O \quad \text{eq. 36}$$

and for denitrification:

$$CH_2O(NH_3)0.15 + 0.89\ NO_3^- \rightarrow HCO_3^- + 0.52\ N_2 + 0.11\ H^+ + 0.67\ H_2O \quad \text{eq. 37}$$

Just the reduction of the dissolved oxygen and nitrate from the lake water consumes 13 mg/l organic carbon. The surface water DOC decreases in average by 2.5 mg/l (fig. 97). Thus the DOC of the surface water is of minor importance. This estimation is conservative. Manganese is not considered, since it is not known which ratio derives from dissolution of

bivalent manganese and how much from reduction of tetravalent Mn. Analogue iron also is not respected for the unknown ratio of Fe(II) dissolution and Fe(III) reduction.

Principally the degradation of organic carbon can be observed in the increase of TIC. In the present case the increase of TIC by degradation of DOC is only about 15% of total TIC. Since the TIC measurements show considerable scattering and probably carbonate weathering or precipitation occurs, the amount possibly could only be determined with geochemical transport modelling and thus not in this study.

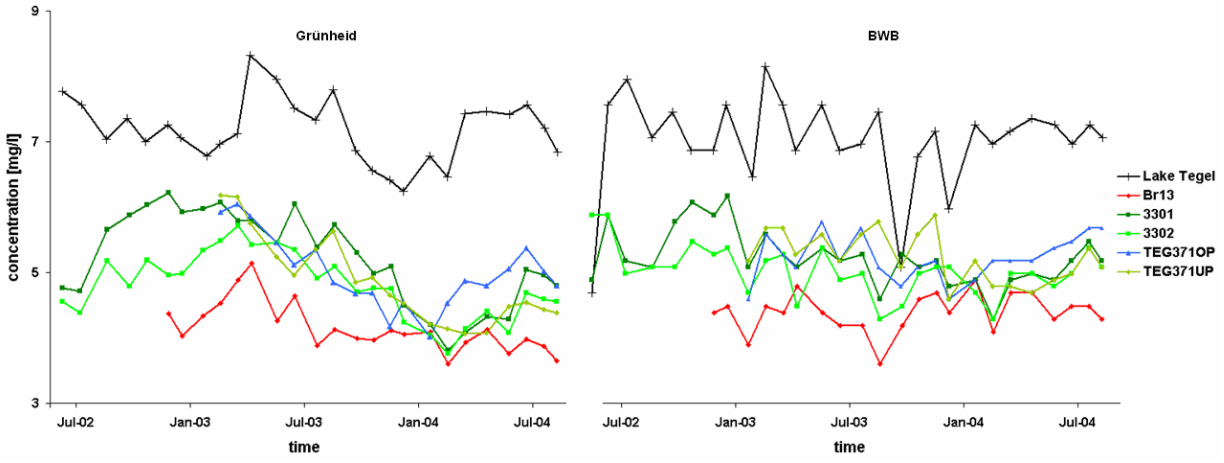

Figure 97: DOC concentrations in observation wells affected by increase in aromaticity in summer 2003.

DOC and UV254 have been analysed independently by two different laboratories: One data set was measured by Grünheid et al. (2005). The second data was measured at the laboratory of the Berlin Waterworks, BWB (2004). The parameters (fig. 97, fig. 98, fig. 99) show significant scattering within the time series and as well between the values of the two groups. The general results nevertheless are reliable, both data sets basically show the same characteristics. Also the mean values coincide, calculated over the entire period for each sampled well, they only show small deviations.

Mainly between August 2003 and November 2003 the UV254 increases, in case of observation wells TEG371up and 3301 even above the surface water level (fig. 98).

The SUVA behaves similar (fig. 99). The magnitude of this effect follows almost the same order like the redox state of observation wells. TEG371up is affected most, followed by observation wells 3301, 317op and 3302. Regarding to the average redox state the last two wells changes position, but until autumn 2003 TEG371op had slightly deeper redox conditions than 3302. This is paradox, that the observation well reach water which has been subject of intensive anaerobic degradation when the water table falls, the unsaturated zone grows and conditions should become more oxic. But during the decrease of the water level the penetration of oxygen through the free water table is reduced. The drawdown proceeds rather continuously

during 5 months (fig. 92). Therefore no CO_2 can be pushed out, large parts of the unsaturated zone contain few or no oxygen. Maybe it is more important that the interface between groundwater and ground air is small. When the water table rises residual air remains in the pore structures and enhance the penetration of oxygen by increasing the interfacial area. The increase in redox potential is beginning in August/September when the water table rises and is maintained until spring 2003.

In the beginning of 2002 the SUVA of 3301 and 3302 also is increased, supporting the elevated AMDOPH, boron and chloride concentrations as indicators for the presence of older bank filtrate (chapter 4.5).

Well 13 also shows increased SUVA values in summer 2003. This is not connected to the processes at the bank, probably this occurs due to ratio changes in the source of abstracted water.

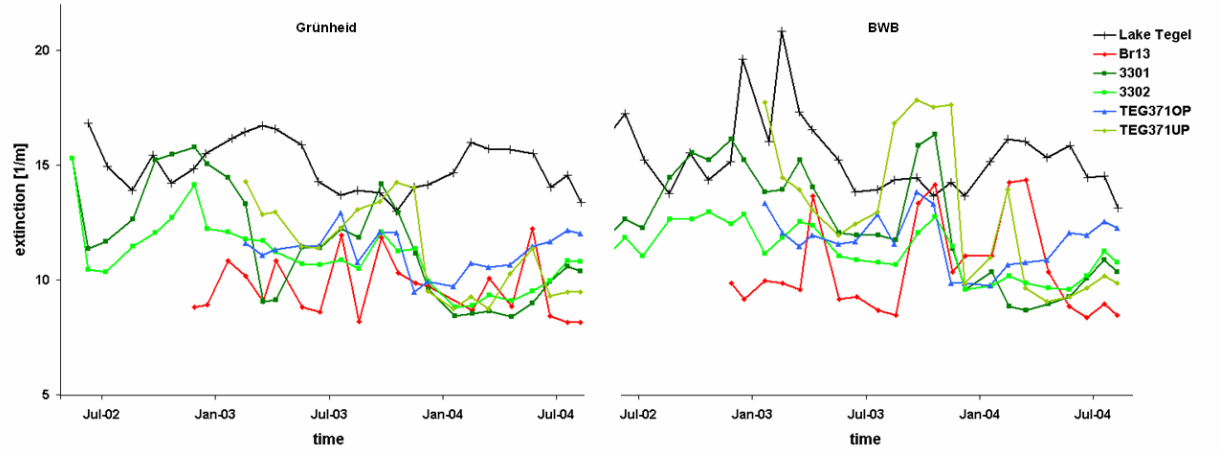

Figure 98: UV extinction at 254 nm in observation wells affected by increase in aromaticity in summer 2003.

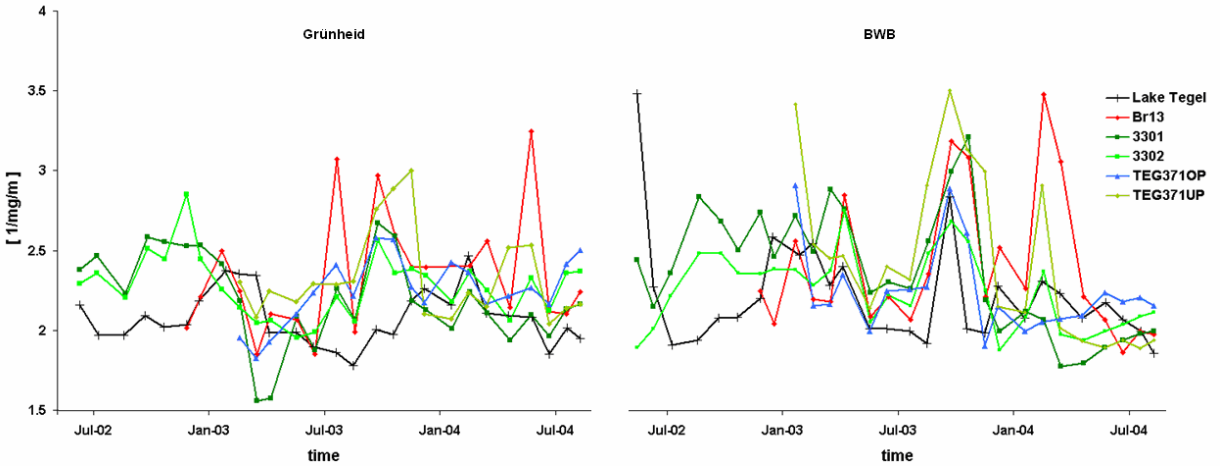

Figure 99: Ratio of UV254 and DOC concentrations in observation wells affected by increase in aromaticity in summer 2003.

Sulphate and Boron

Sulphate concentrations increase above the level surface water concentrations in many shallow and deep observation wells in Summer 2003. The highest increase can be observed at TEG371op, up to 50 mg/l between July and September higher than the input from Lake Tegel. Observation wells 3308, TEG372, TEG371up, 3301, 3302 and 3303 show values higher than surface water concentrations.

The flushed dead water contains elevated sulphate and boron concentrations (fig. 100, fig. 101). The temporal characteristics are very similar, the highest concentrations of TEG371op is between July and September 2003 with up to 200 mg/l. Such a concentration has never been measured in Lake Tegel (fig. App7, appendix). The concentration of TEG372 is maximal in September 2003. Concentrations of observation wells TEG371up, 3302 and 3303 reach their maximum between September and October 2003.

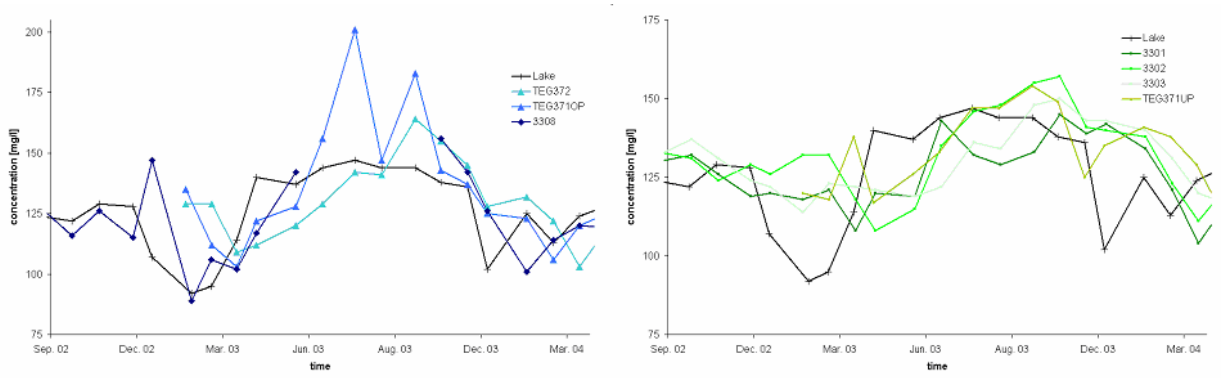

Figure 100: Concentrations of sulphate in observation wells which show particular behaviour in summer and autumn 2003. Concentrations are higher than previous lake concentrations.

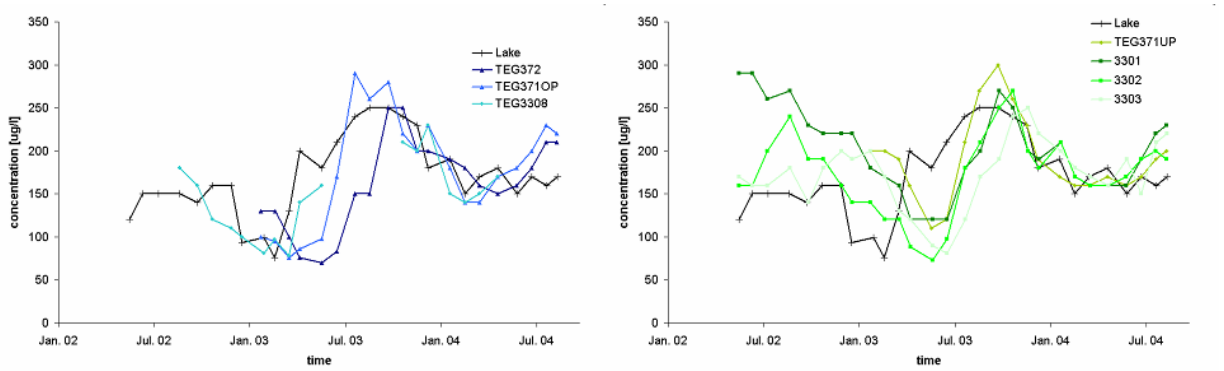

Figure 101: Boron concentrations of these observation wells also showing elevated sulphate concentrations.

The boron concentrations probably derive from elevated concentrations of infiltrated water. The time of infiltration can not be determined, since boron shows variant retardation (De Simone et al. 1997). No literature had been found that boron could be subject of retention, e.g. by complexation or chemical reaction.

The sulphate concentrations also could derive from former surface water concentrations, however, since 1996 concentrations have been around 130 mg/l or lower. Between 1994 and 1996 they have been around 175 mg/l (SENSUT 2005, fig. App7, appendix).

Since the boron concentration of the lake decreased more recently and sulphate is not subject of retardation another reason is more probable. The sulphate derives from reoxidation of sulphide, induced by the shifting of redox zones through the decrease in water level in summer 2003. The oxidation of Pyrite for example releases large amounts of H^+, simultaneously to elevated sulphate concentration the pH values decrease.

Sulphate concentrations of observation well 3301 show a pronounced depression between July and September 2003. This could be a mixing effect, but also could be result of sulphate reduction within the flushed water.

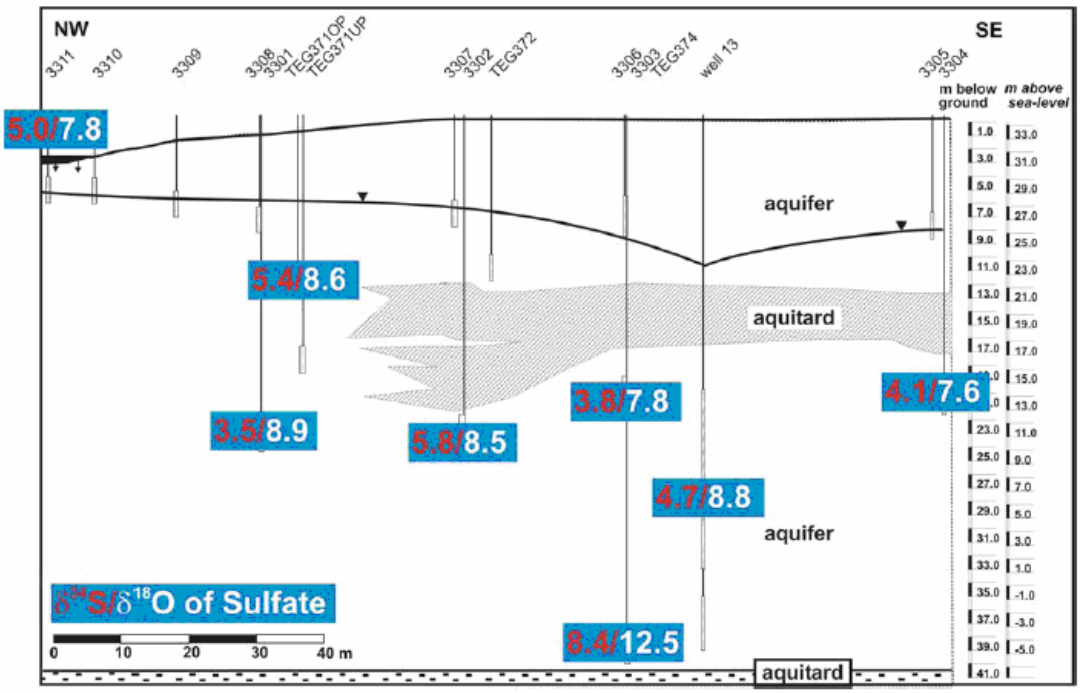

Figure 102: Concentrations of $\delta^{18}O$ [$^0/_{00}$ vs. SMOW] and $\delta^{34}S$ [$^0/_{00}$ vs. CDT] of sulphate at Jul. 20th, 2004. (Pekdeger et al. 2004).

At July 20th 2004 reaction products deriving from reoxidation of sulphidic matter had been observed. Sulphate reducing bacteria prefer the isotopic lighter sulphate molecules, leading to an enrichment of heavy sulphur and oxygen isotopes in the remaining dissolved sulphate. In the highly reduced observation well TEG374 this effect can be observed (Pekdeger et. al. 2004). This means the biologically reduced sulphur has a lighter isotopic signature. If it is oxidised again, correspondingly the released sulphate also shows lighter sulphur concentrations. The oxygen however derives from the infiltrated water, thus not showing a

lighter isotopic fingerprint. In observation wells 3301 and 3303 the lighter isotopic signature of the sulphur in the sulphate shows that it partly derives from reoxidised sulphides (fig. 102).

3.8.5. Upshot

The detailed hydraulic analysis has been essential for the understanding of the geochemical conditions. A 2D flow field is not an appropriate description for the hydraulics at the transect. The mean redox conditions and the temporal development of the redox conditions within the investigation period between May 2002 and August 2004 could be explained.

The redox gradient is roughly vertical, it is controlled by the lateral redox gradient during infiltration and oxygen input across the free water surface. The unsaturated zone below the bank is aerated by sucked air during drawdown, while the saturated zone is aerated by residual air during a rising water table.

The redox state of the unsaturated zone below Lake Tegel (observation wells 3310 and 3311) is closely connected to the variations of the water table. Temperature effects are of secondary importance.

The hypothesis of the existence of a reducing microzone around TEG371up could be rejected, instead the particular position of the glacial till guides the reduced water towards the observation well. These findings support the calibrated distribution of the glacial till. The spatial calibration shows high predictive accuracy for geochemical interpretation.

The redox conditions near the fringe of Lake Tegel are oxic, and become more anoxic towards deeper regions. The water which infiltrates in deeper regions is stronger reduced and flows earlier to the second aquifer. This induces that the water which reaches observation well 3301 already had a lower redox state during infiltration than the water in observation well 3302, the same effect causes that observation well 3302 is more reduced than observation well 3303. Furthermore, though travel time from the bank to observation well 3302 is shorter than to observation well 3303 the water has a longer residence time in the anoxic 2nd aquifer. The fact that ratios of the very reduced medium aged bank filtrate decrease from observation well 3301 to 3303.

Anoxic regions of the bank are clogged much stronger than oxic regions. This probably is induced by microbial born exopolymeric substances which are produced under sulphate reducing conditions (Okubo and Matsumoto 1979). These substances are hardly degradable under anaerobic conditions (Grünheid 2005) and convert the sediments into an almost impermeable continuum (Wood and Basset 1975). The extreme drawdown in 2003 causes aeration of these polymeric substances, which rapidly decompose under oxic conditions. DOC

is released and sulphides are reoxidised to sulphate. This different source of DOC can be observed in the highly increased UV254 and SUVA. Large amounts of reoxidised sulphate are detected in observation well TEG371op, smaller amounts in observation wells 3308, TEG372, TEG371up, 3302 and 3303.

The flushing of the remobilised, sulphate reduced dead water can be observed at decreasing sulphate concentration of observation well 3301 in autumn 2003. Since this water derives from the infiltration around Reiswerder, it is older and contains elevated concentrations of boron and chloride, showing up in observation wells TEG371op, TEG371up, 3301, 3302 and 3303. Though remobilised water can be observed in all of the observation wells which already had been reduced stronger before the drawdown, only observation well 3301 does not show increased sulphate concentrations. Obviously the water there derives from very deep infiltration areas, where too few oxygen remained for reoxidation. Under normal conditions sulphate concentrations do not suggest that sulphate reduction may occur. However, the isotopic fingerprint of sulphate in August 2004 (fig. 102, Pekdeger 2006) shows reoxidised sulphate in two observation wells.

The process is triggered by changes of the water table, namely the extreme drawdown in 2003. It was an excellent opportunity to understand this bank filtration system.

4. Synthesis

The objective of this study is to identify the relevant processes which affect bank filtration at Lake Tegel. The problem is approached by means of hydraulic modelling. It turned out that so many system characteristics have been unknown that a comprehensive hydraulic description only could be obtained by iterative development of the conceptual model and the parameterisation. Hydraulic conditions have been specified, geochemical conditions could be identified to be controlled by hydraulic processes and some important system characteristics only could be described by revealing the interaction of aquifer properties with saturated flow, unsaturated flow, and biogeochemical clogging processes. The system is highly transient on temporal scales between hours and months and spatial scales between a metre and kilometres. Large scale hydraulics and long term effects are modelled with the regional flow model. It has the smallest extent where appropriate boundary conditions can be chosen. It covers a period of a little more than 7 years. On this time scale, transport processes are only relevant on a smaller spatial scale, principally between the bank and the well field. Additionally, a good data base only exists near the transect. Consequently, transport modelling only is carried out for the direct vicinity of the transect. It is modelled on the base of the flow field of the regional model but in a smaller area. Short term hydraulics, on the scale of hours, also are only relevant in the direct vicinity of the transect. They are modelled with the telescope model.

The correct representation of infiltration processes is essential for description of bank filtration and carried out with the regional model. The leakance describes the hydraulic resistance of the surface water / groundwater interface.

4.1. Leakance

The leakance is identified to be controlled by biological and/or chemical clogging. The most important result of the study is the finding that the spatial extent as well as the magnitude of the leakance are temporally variant. At low redox levels/anaerobic conditions the leakance is very low, at high redox levels/aerobic conditions it is at least one order of magnitude higher. High degradation rates of sedimentary organic carbon in the first centimetres after infiltration induce a low redox state, sediments can be reoxidised again by air from below through the unsaturated zone. The air flow is triggered by suction and exhaust processes induced by the variations of the free groundwater surface below the bank. The result of this process is that the extent of the redox state of the clogging layer is spatially and temporally variant and affects the leakance:

(i) at high groundwater table leakance is restricted to shallow areas near the fringe and is of low magnitude,

(ii) at low groundwater levels a broad stripe up to deep water has a high leakance.

(iii) The leakance is independent of the surface water composition and physico-chemical parameters. Nitrate might be an exception, it shows some correlation to the temporal leakance.

The difference of infiltration amounts between these states can reach more than one order of magnitude. This mechanism causes that infiltration mitigates variant groundwater levels stronger than previously assumed. This finding affects all transient aspects of lake bank filtration where a correct water balance is required. It should be especially taken into account for precise prediction of groundwater levels under variable pumping rates. Furthermore, the mechanism implies that an alternating pumping pattern increases the leakance and reduces the drawdown.

Taking into account that previous approaches compensated the lack of process understanding by unrealistic description and parameterisation, the differences can be called drastic.

4.2. General Hydraulic Processes on Regional Scale

This work identified that saline water from the 3rd aquifer intrudes to the main aquifer and forms 14% of the inland water (valid for mean conditions between 1998 and 2005).

Stormwater discharge to the Airport Lake forms 36% of the inland water. Travel times are 13 years (valid for mean conditions between 1998 and 2005).

Except for pumping tests at the well Field West the glacial till dividing the 1st and 2nd aquifer is not impermeable enough to divide the aquifers effectively. In a distance greater than 400 m inland of Well Field West the maximum head difference is 20 cm. Under conditions when the entire well field abstracts water, e.g. during a pumping test, this value can be exceeded.

The hypothesis of a water divide below Lake Tegel could be rejected. A ratio of abstracted bank filtrate infiltrated at the opposite bank and is older than 10 years. This coincides with findings of Massmann et al. (2004) and WASY (2004).

The ratios of abstracted waters from all sources are subject of significant temporal variations, mainly depending on interaction between pumping rates, storage effects and leakance characteristics. These changes are triggered by the pumping rates. The effect is reversed on short and long time scales. For example, if the well(s) are switched off, bank

filtrate immediately penetrates inland. When the well(s) are switched on again, the ratio of bank filtrate is very high and can reach 100%, it can take up to a few days of pumping until ratios are approximately temporally constant. This is approved by 15 different dissolved substances or physico-chemical parameters. Their concentrations in the abstraction wells show significant differences, depending on the interval between well switching and sampling. Values either decrease or increase, each parameter consistent to the overall geochemical conditions. Switching off the wells for a longer time however would cause the bank filtrate to discharge into the lake again. The natural function of the surface water as receiving water for groundwater would be reestablished.

It is not possible to calculate scenarios because the boundary conditions are only valid for real pumping rates. However, during the modelled interval the amounts of monthly abstracted water changes on a scale up to factor 3 within a duration of more than 7 years. The induced interaction of hydraulic processes is a good indication for system behaviour under different conditions.

Though not ideally distributed, hydraulic heads have been observed with high spatial and temporal resolution. This data basis is essential for precise modelling of hydraulic processes.

The physical relevance of the processes which are included into the model is very high. A numerical sensitivity analysis was carried out. High parameter correlation only occurs due to linear interdependence in the parameterisation of the leakance, physically this is meaningless. A considerable parameter correlation exists for the depth dependence of the leakance, but showing statistical significance for higher leakance in shallow areas. The better the physical representation of key processes controlling the model is, the more the leakance is shifted to shallow water depths. The other parameter correlations are statistically of low significance. Considering all statistical parameter correlations in conjunction with the physical level of parameter uncertainty, nonuniqueness could not be detected.

The water budget error is very small, independently of temporal and spatial resolution. The telescope model (chapter 4.7) uses real times for well operation. Errors because of using weekly average values for pumping rates in the regional model could be identified as small.

4.3. Local Hydraulics

Generally the aquifers react according to their hydraulic state, the 1st aquifer is unconfined, the 2nd aquifer is confined or semiconfined. Infiltration takes place in the first aquifer, the abstraction wells are screened in the second aquifer. Thus considerable downward flow occurs. The spatial distribution of this flow is determined by the highly variant pumping patterns

interacting with the nonlinear infiltration dynamics, the latter both with the spatial distribution of the glacial till. The special situation provides an extremely rich pool of information: Wells with a capacity between 100 m³/h and 180 m³/h switched in short intervals, hydraulic heads are logged hourly in 10 observation wells. The information about the till is deeply hidden, the hydraulic heads depend on:

i. regional flow field,
ii. infiltration dynamics,
iii. actual pumping pattern, simultaneous or alternating operation of differently grouped wells,
iv. initial conditions, thus the previous pumping patterns (like last point),
v. leakage distribution of the glacial till and
vi. hydraulic aquifer conductivity.

The regional flow model resolves point 1 and 2, points 3 and 4 are resolved by an appropriate set up of the telescope model. Points 5 and partly 6 could only be resolved by development of the following new inverse modelling concept:

i. The magnitude and spatial distribution of hydraulic heads do not affect the calibration, instead temporal head differences at single locations, the shapes of the curves, respectively, are fitted. This minimises the inaccuracies introduced by the regional flow field, the observations are highly sensitive to the calibrated leakage and hydraulic conductivity.
ii. Spatial parameterisation with pilot points enables to focus effort on the sensitive areas and provides that the gradient as well as shape of the calibrated parameters is variable. This minimises computational effort and results in a continuous parameter field.
iii. The model is highly overparameterised. Apart from the ordinary objective function which accounts for the observations, a regularisation function enables that the information content of the data determines the resulting spatial resolution. In combination with point 2 this enables not only the magnitude of parameters in a area which has been previously defined, moreover spatial structures can be calibrated with high resolution.
iv. The model performance is approved by cross validation. The prediction accuracy on heads and glacial till is approved. This provides meaningful results only for automated parameter calibration.

v. The calibrated parameters enabled a high accuracy of transport modelling. This is especially remarkable as only piezometric heads are used for calibration.

Regarding the hydraulic heads, the model fit and prediction of the temporal dynamics are excellent. Subsurface structures probably have not been determined with such a resolution by any pumping test before. The calibrated hydraulic conductivity distributions are of low physical accuracy. The calibrated distribution of the glacial till, however, is unusally close to real structure. The combination of hydraulic cross validation, prediction accuracy for multispecies tracer transport and geochemical prediction capabilities is an extremely strong validation procedure, which probably has not been applied before.

The method which has been developed has a high potential for geophysical investigation at waterworks. It can be applied to investigate the geological situation of existing sites and has the potential to increase significantly the information to cost ratio at the prospect of new sites.

The calibrated configuration of the till is not only relevant within the area where it could be determined, but it also shows that glacial till has a continuous structure, the holes form islands. It is present below the infiltration areas of Lake Tegel and probably is intersected by the basin. Previously it was believed that around the basin the till is nonexistent. This finding contradicts the hypothesis that basin was geologically formed by a glacial river and supports a formation by interstitial ice. Consequently, it has to be assumed to be present around the entire lake and probably also affects other bank filtration sites.

4.4. Transport Processes

Transport is modelled successfully, not any parameter had to be calibrated. The direct transfer shows the excellent predictive performance and physical meaning of the flow model.

Dispersion occurs on a scale below the detection level of the model. Furthermore it has found to be insensitive between nil and 1m.

^{18}O, chloride and temperature are the tracers whereof physical mechanisms of subsurface transport are well known. ^{18}O and chloride show a very good fit in observation wells and slightly reduced accuracy in abstraction wells, temperature in contrast shows good fit in observation wells and an excellent fit in the abstraction wells.

^{18}O and chloride are ideal tracers, the correct description of the flow field automatically leads to a good fit of the break through curves in observation wells. Regarding the abstraction wells, the phase shift of the surface water signal is correct, but an offset exists. This derives from unknown boundary concentrations of deep water. It can be closed with mixing calculations with plausible assumptions about the concentrations of deep water in conjunction

with ratios from the transient water balance. In contrast, the fit of temperature in the observation wells is a little worse. It could be shown that heat conduction affects the transport parameters retardation and diffusivity in such way that behaviour is principally different to ideal tracers under the condition of stochastically distributed hydraulic conductivities. The fit in the abstraction wells however is excellent. The impact of heat conduction levels out because the REV of the abstraction wells is much bigger. An offset does not exist, because the temperature and thus the boundary conditions of deep water are well known.

The behaviour of other tracers is known with less accuracy. Boron is known to show variable retardation in the underground, in this study $1 \leq R \leq 1.3$ was observed. AMDOPH is detected recently, thus transport behaviour only is roughly known. It is assumed to be stable only under anaerobic conditions, retardation is assumed to be low or nonexistent. Boron, AMDOPH and chloride as well, show differences in surface water concentrations of the scale of several years. Travel times can only be roughly determined. It is much more important that these tracers show the presence of 2 additional fractions of different and significantly older bank filtrate.

In total 3 fractions of bank filtrate exist at the transect. Young bank filtrate, with an age between 3 and 6 months, is known by former investigations to be present in large parts of the aquifers. Transport modelling of this shows very good results. Within the NASRI project highly elevated concentrations of AMDOPH showed that bank filtrate older than 10 years flows in the lower regions of the second aquifer and reaches the Well Field West. Transport modelling approves the presence and the age. A medium aged fraction, with a minimum age of 2 years maybe up to 10 years, is detected by elevated concentrations of boron, chloride and AMDOPH. It is present in the upper part of the second aquifer and is found to be well mixed with the young bank filtrate. The flow is induced by extended regions of shallow water near Reiswerder, causing an infiltration surplus. The water discharges on the glacial till in the first aquifer to the north, and flows up to the transect.

4.5. Geochemistry

It is demonstrated in this study that the general geochemical conditions and as well the most significant geochemical changes are triggered by hydraulic processes. At the bank a lateral redox gradient exists, induced because oxygen is sucked, during falling groundwater tables, into the unsaturated zone below the infiltration area. The redox gradient becomes vertical because in the saturated zone the water stratifies. Oxygen concentrations below the infiltration area are shown not to be principally triggered by water table dynamics, the

hypothesis of a temperature effect can be rejected, the hypothesis that variations in surface water composition does not affect the geochemistry could be approved. It could be also approved that oxygen penetrates the free water surface in the upper aquifer during increasing water levels by entrapment of residual air. It can be summarised that the unsaturated zone is aerated during falling water tables, the saturated zone is aerated during rising water tables.

Redox zoning of observation wells TEG371up, 3301, 3302 and 3303 contradicts as well the redox chain as the generally vertical redox zoning. The behaviour is induced by the lateral redox gradient at the bank during infiltration. The configuration of the glacial till guides the water such a way, that observation well TEG371up is shows the deepest redox conditions. The reversed redox order of observation wells 3301, 3302 and 3303 occurs because water which infiltrated in deep regions infiltrates earlier to the second aquifer. The difference is enhanced because the ratio of very reduced medium aged bank filtrate decreases parallel.

Usually infiltration in deep regions of the bank, towards the middle of the lake, is very low because of bioclogging through exopolymeric substances under sulphate reducing conditions. During the extreme drawdown in 2003 these regions are aerated and become permeable. As consequence, the polymers are partly oxidised, partly converted to DOC, the sulphides are reoxidised to sulphate. The substances are flushed. The water body below has a long residence time because it formerly was hydraulically protected by the strong clogging layer. It is also flushed. Increased concentrations of boron and chloride can be observed in several observation wells, they show that the flushed water has not infiltrated recently, but has an age of several years. The oxidised DOC can be also observed in several observation wells by increased values of UV254 and SUVA, increased sulphate concentrations show reoxidation of sulphidic sediments. The extreme drawdown in summer 2003 raised many questions which led to identification and a much better understanding of the geochemical processes.

A theory for the propagation of well clogging is developed. Vertical redox stratification in the well filter is the principal factor inducing clogging. This happens in 2 stages: first water with different redox state mixes within the inner tube and precipitation of iron and manganese minerals occurs at the trenched tube of the inner well. At the second stage the permeability of the trenched tube already is significantly decreased. The water which enters the gravel filter can not flow radial but flows vertically. This way oxic and anoxic water mix within the gravel filter where the minerals precipitate.

4.6. Relevance for Waterworks

The present work reveals central processes of bank filtration which previously have not been expected to exist and which are of major importance for drinking water abstraction. A new method of geophysical exploration of hydraulic conductivities, just requiring hydraulic heads from normal well operation is developed.

Infiltration Dynamics

It is revealed that the infiltration reacts with a higher elasticity than previously assumed using a $2^{nd}/3^{rd}$ type or a 3^{rd} type boundary. This is a crucial point and should be respected as well for simulation of hydraulic conditions of the past and especially for predictions. This mechanism implies that hydraulic heads are significantly less affected by changing pumping rates than previously assumed. Due to reduced water abstraction, inland water levels as well as water levels between the well field and the lake will rise significantly less than modelled until now. The relevance for cellars, infrastructure, flow direction and velocity at contaminated sites and vegetation is obvious.

The infiltration of surface water increases with the intrusion of oxygen below the infiltration zone. A transient pumping pattern, which results in high head variations at the infiltration zone, causes less drawdown than a continuous pumping pattern.

Airport Lake

In average 36% of the inland water at Well Field West derive from stormwater discharge of the city are of Tegel, the mean travel time to the Well Field West is 13 years. Since the stormwater runoff contains several undesired constituents, the drinking water quality is adversely affected. Compared to infiltration at Lake Tegel, the biogeochemical processes at the interface between the Airport Lake and the groundwater are quite different:

i. The water levels in the Airport Lake and at the adjacent aquifers are very similar. The extend of the unsaturated zone is only a few centimetres.
ii. Due to the large distance from the well field, water levels vary considerably less, the advective oxygen input to the unsaturated zone is considerably smaller than at Lake Tegel.
iii. The Airport Lake has a depth of 40 m. It is a former gravel pit and thus very well connected as well to the first as to the second aquifer.

As consequence of these points, the ratio of water not passing an aerated unsaturated zone is much higher than at Lake Tegel, probably most of the water infiltrates through the saturated zone. This means the purification is less effective than at the bank filtration site. Even if no

prescriptive limits are violated, the precautionary principle requires to minimise the undesired constituents in this part. Taking into account that all stormwater discharge of the district Tegel is distributed as drinking water to Berlin the protection of this resource is of high importance.

Chemical Clogging

Precipitation of iron and manganese minerals, also called chemical clogging, requires high maintenance effort for abstraction wells and the delivery tubes. It occurs if water with dissolved iron or manganese mixes with oxic water. A theory for chemical clogging is developed. The following mechanisms are possible:

i. At the horizontal interface between oxic and underlying anoxic water precipitation occurs. This effect probably is very small, since the concentration gradients are small. Compared to the iron and manganese clogging in the wells, the precipitation in the aquifer, if existent, is considerably smaller, a strong indication that this effect is negligible.
ii. Redox gradients occur along flow paths, e.g. induced by the extreme drawdown 2003. The gradients are spatially even smaller than vertical gradients, thus negligible.
iii. If water tables are lower in the inner tube of the well than the top of the well screen, oxygen intrudes from the wellhead. If the water entering the well at this elevation contains iron or manganese, they precipitate, presumably predominantly at the trenched tube.
iv. If water with high redox potential enters the well at the upper screen and water with low redox potential enters the well at the lower screen, the redox difference between the mixed water in the inner tube and in the gravel filter increases with the elevation. Iron and manganese precipitate, predominantly at the trenched tube.

The precipitated minerals at the trenched tube should be removed before they affect the permeability, because:

v. Assuming, the trenched tube has become low- or impermeable at the top, oxic water which flows to the well, enters the gravel filter but the horizontal exit to the well is clogged. It flows downward. In these deeper regions anoxic water enters. The coarse grained structure of the trenched tube provides excellent mixing conditions, like a static mixer known from chemical engineering. Heavy precipitation of the gravel filter occurs, which hardly can be removed. Since as well the redox difference as the amount of downward flowing water increases, the precipitation velocity of iron and manganese oxides increases disproportionately high with the impermeable length of the trenched tube.

It can be concluded that the presence of a vertical stratification of waters with oxidation capacity at the top and with dissolved iron and manganese in lower regions is the principal reason for clogging. Since it is not possible to remove iron and manganese from the lower aquifers, the only promising strategy is to minimise the presence of oxidation capacity, namely oxygen and nitrate, from the shallow areas of the aquifer. Other techniques, like inhibiting mineral precipitation in the trenched tubes by using copper plated materials, only displaces the process from the wells downstream to pumps and delivery tubes.

The coverage with glacial till can significantly reduce the oxidation state of water at the top of the aquifer. If this water is shielded against reoxidation by the free water table, the dissolved oxygen can be degraded. If also nitrate is degraded, ideally already during infiltration, or during the passage below the glacial till, precipitation of minerals is inhibited. This can be achieved by a pumping regime adapted to the general hydraulic conditions, in interaction with the glacial till providing oxygen free water by inhibition of reoxidation. This would also prevent the precipitation of the delivery tubes to the waterworks.

Determination of the Distribution of the Glacial Till

In chapter 4.7 a method is described, how the distribution of the glacial till can be determined. The effort is low, because hydraulic information of existing piezometers can be used to determine the extent of the glacial till. Each abstraction well may also serve as piezometer. It is remarkable that piezometers may not even scratch the glacial till, it is enough that they are screened in the saturated zone to provide spatial and sensitive information about its location. The combination of using already existing abstraction wells and shallow observation wells as piezometers is a promising method for accurate and cost effective determination of the spatial distribution of aquitards.

4.7. Outlook

Infiltration and Clogging

The new insights on the most important region during bank filtration, the water sediment interface, provide a view of the general hydraulic behaviour. The mathematical description is not yet mechanistic. It underestimates the long term variability and overestimates the short term variability. The discovered interdependence of hydraulic and biological processes determines the infiltration amounts. Since most geochemical changes occur in the infiltration zone these processes probably seriously affect the purification capacity of bank filtration. Further research is required on:

i. the air transport processes in the subsurface
ii. the way the air oxidises the sediments from below
iii. the temporal and spatial structures of infiltration
iv. the biogeochemical processes during infiltration
v. the impact of nitrate

With high probability and due to the hydraulic situation at Lake Wannsee, the observed mechanism also triggers infiltration there. The observed infiltration structure on a riverbank filtration field site described by Schubert (2002) suggests that the same mechanism could be of importance. Since no consistent and quantitative clogging theory of riverbank filtration exists until now, the discovered mechanism is worthwhile to be further investigated. The discovered clogging mechanism could be of worldwide relevance for bank filtration and artificial groundwater recharge.

Local Hydraulics

It has been demonstrated that local geology has a very high impact on the distribution of geochemical information recovered by observation wells and also on the clogging processes in abstraction wells. The developed method for spatial calibration is very promising as it provides reliable results for the location of the aquitard. The capabilities of the method should be further investigated:

i. calibration of the glacial till inland
ii. the possibility to provide sensitive information with a reduced number of observation wells, e.g. only hydraulic information of an existing well field
iii. the level of spatial information which can be obtained by a higher level of integration, i.e.:
    a) increased temporal resolution of hydraulic heads
    b) reliable information about spatial head differences
    c) coupled transport modelling, with conservative tracers and temperature
    d) including regulary measured temperature profiles
iv. subsequent geochemical modelling in order to determine operational state and system design to ensure the absence of oxygen and nitrate in the wells

The developed method has a high potential for geophysical investigation at waterworks. It can be applied to investigate the geological situation of existing sites and as well significantly increase the information to cost ratio in the prospect of new sites.

Temperature as Tracer

Because of seasonal variations with high magnitude and high flow rates, temperature breakthrough deeply penetrates into the aquifer. As consequence, the relevance of temperature data is higher than for any other aquatic subsurface system. It can be regarded as missing link between conservative tracers and hydraulic data. Data of ideal tracers are relevant for a small REV, hydraulic heads for a very big REV, because of heat conduction temperature is of relevance for a REV in between. In natural aquifers with spatially distributed hydraulic conductivity, temperature can provide a new quality of information about the subsurface. Further investigation about the following items is required:

i. the impact of the viscosity effect
ii. the impact of heat conduction in spatially inhomogeneous aquifers

Within a multi tracer approach temperature has a high potential of contributing substantially different kinds of information. Evaluation of the data requires inverse modelling.

Field Measurements

In addition to the many kinds of data with high spatial and temporal resolution which have been collected, the following field measurements should be carried out:

i. temperature profiles, especially in deep observation wells - this information would be of importance for spatial hydraulic and hydrogeologic structures
ii. continuous observation of key parameters of well water quality after switching - the information would clarify the inland intrusion of bank filtrate. The contrary effect of pumping on short and long temporal scale could be specified
iii. measurement of spatial and temporal infiltration dynamics, in conjunction with oxygen measurements in the unsaturated zone - this is necessary to understand the clogging mechanisms, which are a key factor in bank filtration

The author believes these measurements provide very important information with relatively low effort.

Geochemical Modelling

In conjunction with the determination of glacial till distribution, geochemical modelling can be used to adapt operation and design of bank filtration sites with respect to well clogging. In this context two different kinds of oxygen intrusion should be quantified:

i. oxygen intrusion exchange with the unsaturated zone by suction at falling water levels
ii. oxygen input to the infiltrated water below the infiltration area

iii. oxygen input to the groundwater across the free water table

Within this study geochemical data only have been regarded qualitative. The present work could be the starting point for meaningful to reactive geochemical transport, evaluating the field measurements at the test sites in conjunction with chemical properties of pharmaceutical residues and other xenobiotic compounds.

Glossary

Abstraction: synonym for extraction of water

Airport Lake: Lake at the eastern model boundary, german name: Flughafensee

AMDOPH: Derivate of the analgesic phenazone, stable at low redox stages, concentrations in old bank filtrate below Lake Tegel are much higher than in younger bank filtrate.

BF: bank filtrate

BOD 1/BOD 5: Biological Oxygen Demand, oxygen consumption by biological degradation within 1/5 days.

BWB: Berlin Water Works (Berliner Wasser Betriebe)

Case1: Scenario of flow model, assumes linear trend of leakance between 1998 and 2005. Model fit is almost as good as Case2, but for some reasons it is not assumed to be a valid expression of the physical processes.

Case2: Scenario of flow and transport model, used for almost all flow and transport calculations. The leakance is temporally variant and is roughly proportional to pumping rates of Well Field West.

Case3: Scenario of flow model. The leakance is higher in the unsaturated zone and triggered by its thickness. Decrease of the biological and/or chemical clogging by aerobic conditions is assumed to be the underlying physical process.

DOC: Dissolved Organic Carbon, after filtration through 0.45 µm.

GWA: Groundwater recharge facility in Tegel using ponded infiltration, located west of the airport, german name: Grundwasseranreicherungsanlage

HSM/HSM Tegel: Hydrogeological structural model of the upper two aquifers around the waterworks Tegel. The present model area is entirely included. It is set up by FUGRO (2000).

Hyporheic Zone: Water saturated zone directly below the water sediment interface. Exchange rates the surface water is high, concerning water, dissolved substances and hydrobiology.

Leakance: The ratio K'/b', in which K' and b' are the vertical hydraulic conductivity and the thickness, respectively, of the confining beds (Lohman et al., 1972). The leakage in contrast is calculated for the transfer between two adjacent layers (WebTech306, 2005). The term is not used following the definition of the International Glossary of Hydrology (2006): Quantity of water that flows across a unit area of the boundary between the main aquifer and its overlying or underlying semi-confining layer per unit head difference across this semi-confining layer.

Medium aged bank filtrate: aged about 1,5 to 4 years. Infiltrated near Scharfenberg and flows in bend streamlines to Well 12 and 13. Water which infiltrates around Scharfenberg is also abstracted by wells 14 to 26, but for these wells

NASRI: Natural and Artificial Systems for Recharge and Infiltration, investigation project on bank filtration and artificial groundwater recharge, May 2002 – June 2006

Old bank filtrate: bank filtrate aged >10 years, infiltrated near Scharfenberg or near Well Field North. It shows elevated concentrations of Phenazone derivates, as e.g. AMDOPH

Phenazone: analgesic. Today it is still in use and is found as well as its derivates (e.g. AMDOPH) in Lake Tegel, but concentratios in the past had been at least 10 times higher than 2002-2005.

Pumpage: synonym of pumping rate

Reiswerder: Island in Lake Tegel, southwest of the Well 13 and the transect. Around Reiswerder much groundwater is recharged due to extended regions of shallow water.

Relative leakance: Parameterisation describing the temporal variant behaviour, approximated by linear trends of 2 month length forming a continuous curve.

Residual: Difference between observed and simulated hydraulic head (Res = Meas – Calc).

REV: Representative Elementary Volume, can take values between pore scale and regional scale, of importance for the relevance of scale dependent processes

Scharfenberg:Large island in Lake Tegel.

Secchi Depth: Method for determination of the viewing depth in a surface water, a disc with cross ordered 2 black and 2 white fields is submerged, the depth when it disappears is the Secchi Depth.

SMOW: Sea Mean Ocean Water, standard water used for calculation of reference concentrations of the stable isotopes ^{2}H and ^{18}O.

Stress period: interval with constant boundary conditions, comprises one or more time steps.

SUVA: UV extinction at 254 nm, used for detection of the aromatic compounds of DOC.

Telescope model: spatial and temporal submodel of the main model, calculated on hourly basis with real well switching times.

TIC: total inorganic carbon

Time step: Numerical calculation interval, also output interval of piezometric heads.

Well 13: Well no. 13 of Well Field West, NASRI investigations concentrated on this well and the pertaining transect

Young bank filtrate: water with an age of about 4 to 8 month, infiltrated directly in front of the corresponding well

Literature

Bates and Anderson 2001; Bates, P., D., and Anderson, M., G.; Validation of Hydraulic Models; Model Validation – Perspectives in Hydrological Science; Chichester UK, 2001

Bear 1972; Bear. J.; Dynamics of fluids in porous media; American Elsevier, New York, 1972

Bourg and Bertain 1993; Bourg, A. C. M., and Bertain, C.; Biogeochemical Processes during the Infiltration of River Water into and Alluvial Aquifer; Envion. Sci. Technol.; 27; pp.661-666,

Bouwer and Rice 1989; Bouwer, H. and Rice, R. C.; Effect of water depth in groundwater recharge basins on infiltration; J. Irrig. and Drain. Eng.; 115; pp.556-567,

Brühl et al. 1986; Brühl, H.; Sommer-von Jarmersted, C; Ergebnisbericht: Baugrunduntersuchung auf der Kabeltrasse im Tegeler See (Wasserwerk Tegel – Trafostation Tegelort); Institut für Angewandte Geologie der Freien Universität Berlin; unpublished work, 1986

Brusseau et al. 1998; Brusseau, Mark L.; Non-ideal transport of reactive solutes in heterogeneous porous media: 3. model testing and data analysis using calibration versus prediction; Journal of Hydrology; 209; pp.147-165,

BWB 2002-2005; Berliner Wasser Betriebe; kind provision of Data: Piezometric heads, well operational hours, pumping test data, amounts of abstracted water from entire WW Tegel, precipitation; 2002-2005

Chiang 1993; Chiang, W. H.; Water Budget Calculator - A computer code for calculating global and subregional water budget using results from MODFLOW; Kassel University,Germany; 1993

Chorus et al. 2006; Chorus, I., Bartel, H.; Retention and elimination of cyanobacterial toxins (microcystins) through artificial recharge and bank filtration; NASRI – Final Project Report; Kompetenzzentrum Wasser Berlin; 2006

DeSimone et al. 1997; DeSimone L.A.; Howes B.L.; Barlow P.M.; ass-balance analysis of reactive transport and cation exchange in a plume of wastewater-contaminated groundwater; Journal of Hydrology; 203; *1*, pp.228-249,

Dillon et al. 1999; Dillon, P. Pavelic, P.Toze, S. Ragusa, S.,Wright, M., Peter, P. Martin, R., Gerges, N., and Rinck-Pfeiffer, S.; Storing recycled water in an aquifer: benefits and risks; AWWA J.Water; 26; *5*, pp.21-29,

Doherty 2003; Doherty, J.; Groundwater model calibration using Pilot Points and Regularisation; Ground Water; 41; *2*, pp.170-177,

Doherty 2005; Doherty, J.; PEST – Model-Independent Parameter Estimation User Manual 5th Edition; Watermark Numerical Computing; 2005 pp.336,

Doussan et al. 1993; Doussan, C., Toma, A., Paris, B., Poitevin, G., Ledoux, E., Detay, M.; Coupled use of thermal and hydraulic head data characterize river-groundwater exchanges; Journal of Hydrology; 153; pp.215-229,

Doyle 1890; The Sign of Four; Lippincott's Monthly Magazine; 2; 1890

Eichhorn 2000; Eichhorn, S.; Numerische Strömungsmodellierung der Uferfiltration am Tegeler See; Diplomarbeit; Institut für Geologie, Geophysik und Geoinformatik FU Berlin; 2000

Frey 1975; Frey, W.; Zum Tertiär und Pleistozän des Berliner Raumes; Zeitschrift der Deutschen Gesellschaft für Geowissenschaften; 126; pp.281-292,

Fritz 2002; Fritz, B.; Untersuchungen zur Uferfiltration unter verschiedenen wasserwirtschaftlichen, hydrogeologischen und hydraulischen Bedingungen; Dissertation; Fachbereich für Geowissenschaften, FU Berlin; 2002

Fritz 2003; Fritz; Detailed data collected during the doctoral thesis: Fritz (2002); personal communication; 2003

Fugro 2000; FUGRO GmbH, im Auftrag BWB; Hydrogeologisches Strukturmodell für das Wasserwerk Tegel; unpublished work; 2000

Greskowiak et al. 2005; Greskwiak, J., Prommer, H., Massmann, G., Johnston, C. D., Nützmann, G., Pekdeger, A.; The impact of variably saturated conditions on hydrogeochemical changes during artificial recharge of groundwater; Applied Geochemistry; 20; pp.1409-1426,

Grünheid 2005; Grünheid, S., Amy, G., Jekel, M.; Removal of bulk dissolved organic carbon (DOC) and trace organic compounds by bank filtration an artificial recharge; Water Research; 39; pp.3219-3228,

Hannappel 2002; Hannappel, S., Asbrand, M.; Entwicklung eines Hydrogeologischen Modells im unterirdischen Einzugsgebiet eines Wasserwerks im Lockergestein; Schriftenreihe der Deutschen Geologischen Gesellschaft; 24; 2002 pp.55-86,

Harbaugh et al. 2000; Harbaugh AW, Banta ER, Hill MC and McDonald MG ; MODFLOW-2000, The U.S. Geological Survey modular ground-water model User guide to Modularization concepts and the ground-water flow process, U. S. Geological Survey, Open-file report 00-92; Hunter, 2000

Hill 1998; Hill, M. C. ; Methods and Guidelines for Effective model effective Model Calibration, U.S. Geological Survey Water-Resources Investigations Report 98-4005; Denver, Colorado, 1998

Hoelen et al. 2006; Hoelen TP, Cunningham JA, Hopkins GD, Lebron CA, Reinhard M; Bioremediation of cis-DCE at a sulfidogenic site by amendment with propionate; Ground Water Monitoring and Remediation; 36; *3*, pp.82-91,

Hoffmann et al. 2006; Hoffmann, A., Gunkel, G.; Dynamik und Funktionalität des sandigen Interstitials unter dem Einfluss induzierter Uferfiltration; Proceedings DGL 2006, Dresden; 2006

Holländer et al. 2005; Holländer, Hartmut M , Boochs Peter W., Billib, Max, Panda, Sudhindra N.; Labor-Säulenversuche zur Untersuchung von Clogging-Effekten im Grundwasserleiter—Einfluss von physikalischen An- und Ablagerungen, Gasblasen und biologischer Aktivität; Grundwasser; 10; *4*, pp.205-215, 1430-483X.

Holzbecher 2005; Holzbecher, E.; The Lake Dagow Coupled Model for Groundwater and Surface Water; Coupled Models for the Hydrological Cycle - integrating Atmosphere, Biosphere, and Pedosphere; Bronstert A/ Carrera J./ Kabat P./ Lütkemeier S.; Springer Publ., 2005 pp.225-230,

Holzbecher et al. 2006; Holzbecher, E., Engelmann, F., Nützmann, G.; The viscosity effect on infiltrating surface water, Hydrogeology Journal; Hydrogeology Journal; in Review; 2006

Hunt et al. 2001; Hunt, R.J., Steuer, J.J., Mansor M.T., Bullen T.D.; Delineating a recharge area for a spring using numerical modeling, Monte Carlo techniques, and geochemical investigation; Ground Water; 39; *5*, pp.702-712,

IAEO 2006; International Atomic Energy Association; Stable oxygen and hydrogen isotopes of precipitation in Berlin between 1978 and 2001; www.iaeo.org.

Jekel 2006; Jekel, M.; Organic Substances in Bank filtration and Groundwater Recharge - Process Studies; NASRI – Final Project Report; Kompetenzzentrum Wasser Berlin; 2006

Kühn and Müller 2000; Kühn, W., and Müller, U.; Riverbank filtration. An overview; J. AWWA; 92; *12*, pp.60-69,

Kuhr 2001; Kuhr, M.; Grobwurzelarchitektur in Abhängigkeit von Baumart, Alter, Standort und sozialer Stellung; Dissertation; Georg-August-Universität Göttingen, Fakultät für Forstwissenschaften und Waldökologie; 2001

KUP 2006; Ingenieurgesellschaft Prof. Kobus und Partner GmbH; Development Leakage Meter; 2006 http://www.kobus-partner.com/index1.html.

KWB 2005; complete NASRI data base, in ownership of KWB (Kompetenzzentrum Wasser Berlin) and BWB (Berliner Wasser Betriebe); 2005

Lane et al.2001; Lane, Stuart N., Richards, Keith S.; The 'Validation' of Hydrodynamic Models: Some Critical Perspectives; Model Validation – Perspectives in Hydrological Science; John Wiley & Sons Ltd, Chichester UK, 2001

Langguth and Voigt 2004; Langguth, Voigt; Hydrogeologische Methoden; Springer Verlag, Heidelberg, Germany,

Leake et al. 1999; Procedures and Computer Programs for Telescopic Mesh Refinement Using MODFLOW, USGS Open-file Report 99-238; Tucson Arizona, 1999

Lin et al. 2003; Lin, C., Greenwald, D., Banin, A.; Temperature Dependence of Infiltration Rate During Large Scale Water Recharge Into Soils; Soil Sci. Soc. Am. J.; 67; pp.487-493,

Lohman 1972; Lohman, S.W.; Ground-water hydraulics: U.S. Geological Survey Professional Paper 708; pp.67,

Ludwig et al. 1997; Ludwig, U., Grischek, T., Nestler, W., Neumann, V.; Behaviour of Different molecular-weight Fractions of Elbe River Water during River Bank Infiltration; Acta Hydrochim. Hydrobiol.; 25; pp.145-150,

Massmann et al. 2004; Massmann, G., Knappe, A., Richter, D., Pekdeger, A.; Investigating the Influence of Treated Sewage on Groundwater and Surface Water Using Wastewater Indicators in Berlin, Germany; cta hydrochim. hydrobiol.; 32; *4-5*, pp.336-350,

Miettinen et al. 1997; Miettinen, I., Vartiainen, T. and Martikainen P.J.; Microbial growth and assimilable organic carbon in Finnish drinking waters; Water Science Technology; 35; pp.301-306,

Morel-Seytoux 2001; Morel-Seytoux; Groundwater; Model Validation – Perspectives in Hydrological Science; John Wiley & Sons Ltd, Chichester UK, 2001

Müller 1999; Müller, T.; Wörterbuch und Lexikon der Hydrogeologie; Springer Verlag Berlin Heidelberg, 3-540-65642-1.

Murphy and Schramke; Murphy, E. M., and Schramke, J. A.; Estimation of microbial respiration rates in groundwater by chemical modeling constrained with stable isotopes; Geochim. Cosmochim. Acta; 62; *21/22*, pp.3395-3406,

National Research Council 1990; National Research Council; Groundwater Models; Scientific and Regulatory Applications; National Academy Press, Washington, 1990 pp.303,

Neumann 1984; Neumann SP; Adaptive Eulerian-Lagrangian finite element method for advection-dispersion; Int. J. Numerical Method in Engineering; 20; pp.321-337,

Nogeitzig 2005; Nogeitzig, A.; Processes during infiltration at the water sediment interface; Diplomarbeit; nstitut für Geologische Wissenschaften, Arbeitsbereich Hydrogeologie an der Freien Universität Berlin; 2005 http://web.fu-berlin.de/hydrogeologie/pdf/da_alex_nogeitzig.pdf.

Nützman 2006; Nützmann G.; Integrated modelling concepts for bank filtration processes: coupled ground water transport and biogeochemical reactions; NASRI – Final Project Report; Kompetenzzentrum Wasser Berlin; 2006

Nützmann et al. 2003; Nützmann, G., Holzbecher E., Pekdeger A.,; Evaluation of water balance of Lake Stechlin with the help of chloride data; Arch. Hydrobiol. Spec. Issues Advanc. Limnol.; 58; pp.11-23,

Okubo and Matsumoto 1979; Okubo T., and Matsumoto J.; Effect of infiltration rate on biological clogging and water quality changes during artificial recharge; Water Resour. Res.; 15; *6*, pp.1536-1542,

Okubo and Matsumoto 1983; Okubo T., and Matsumoto J.; Biological Clogging of Sand and Changes of Organic Constituents During Artificial Recharge; Water Research; 17; *7*, pp.813-821,

Olsthoorn et al. 2002; Olsthoorn T., Poeter E., Moorman J.; Lessons from Analyzing Trial-and-Error Calibrated Models for Prediction Reliability; Acta Uneversitatis Carolinae – Geologica; 46; *2/3*, pp.183-189,

Oreskes and Belitz 2001; Oreskes N., and Belitz K.; Philosophical Issues in Model Assessment; Model Validation – Perspectives in Hydrological Science; John Wiley & Sons Ltd; Chichester UK, 2001

Pachur and Haberland 1977; Pachur, H. J., Haberland W.; Untersuchungen zur morphologischen Entwicklung des Tegeler Sees; Die Erde; 108; *4*, pp.320-341,

Parchur 1987; Pachur H.-J.; Die Seen Berlins als Objekte geographischer Forschung – Ergebnisse und Aspekte; Verhandlungen des Deutschen Geographentages, Bd. 45; Stuttgart, 1977

Parkhurst and Appelo 1999; Parkhurst, D. L., and Appelo, C. A. J.; User's Guide to PHREEQC (Version 2) – a computer program for speciation, batch-reaction, one-dimensional transport, and inverse geochemical calculations. U.S. Geological Survey Water-Resources Investigation Report 99-4259; Denver, Co., U. S. A.,, pp.312,

Parkhurst and Petkewich 2002; Parkhurst, D. L., and Petkewich, M. D; Geochemical Modeling of an Aquifer Storage Recovery Experiment, Charleston, South Carolina; Artificial Recharge Workshop Proceedings, U.S. Geological Survey; Sacramento, California, 2002

Pekdeger 2003; Pekdeger A.; Piezometric heads of several observation wells at the transect around Well 13 of Well Field West, waterworks Tegel; personal communication; 2003

Pekdeger 2006; Pekdeger A.; Hydrogeologicalhydrogeochemical processes during bank filtration and ground water recharge using a multi tracer approach; NASRI – Final Project Report; Kompetenzzentrum Wasser Berlin; 2006

Pekdeger et al. 1999; Pekdeger A., Brühl, H., Sommer- von Jarmersted, C., Fritz B., Franke P., Przybylski I., Schumacher F., Skripalle J.; Ermittlung der einzugsbezogenen Fördermengenanteile von Uferfiltrat an der Grundwasserförderung der Berliner Wasserbetriebe sowie Untersuchungen zur langfristigen güteseitigen Stabilität der Uferfiltratgewinnung vor dem Hintergrund der rapiden Abnahme der Spree-Wasserführung und einer anzustrebenden Kreislaufwirtschaft der Oberflächenwässer. – Projekt Uferfiltration Berlin, Abschlussbericht.; Im Auftrag der Senatsverwaltung für Stadtentwicklung, Umweltschutz und Technologie. Arbeitsgemeinschaft Uferfiltration Berlin; 1999

Pekdeger et al. 2004; Pekdeger A., Massmann G., Ohm B.; Hydrogeological-hydrogeochemical processes during bank filtration and ground water recharge using a multi tracer approach; 2st periodic report, Jan. to Dec. 2003, unpublished report form the NASRI project (Natural and Artificial Systems or Recharge and Infiltration); Kompetenzzentrum Wasser Berlin; 2004

Poeter et al. 1998; UCODE Program Manual. USGS Water Resources Investigation Report 98-4080; 1998

Popper 1959; Popper K.; The Logic of Scientific Discovery; Basic Books, New York,

Prommer 2002; Prommer H.; A reactive multicomponent transport model for saturated porous media. Draft of user's manual version 1.0; contaminated land assessment and remediation research centre, the university of Edinburgh; 2002 http://www.pht3d.org.

Prommer and Barry 2005; Prommer H. and Barry D. A; Modeling bioremediation of contaminated groundwater; In Bioremediation: Microbial solutions for real-world environmental cleanup; R. M. Atlas and J. Philp ; ASM press, Washington DC., pp.108-138,

Prommer et al. 2005; Prommer H., and Stuyfzand P. J.; Identification of temperature-dependent water quality changes during a deep well injection experiment in a pyritic aquifer; Environ. Sci. and Technol.; 39; *7*, pp.2200-2209,

Ray et al. 2002; Ray, C., Melin, G., Linsky, R. B.; Riverbank filtration – Improving Source-Water Quality; Kluwer Academic Publishers; Dordrecht, 2002

Richter 2003; Richter, D.; Untersuchung des Gewässersystems von Spree und Havel im Berliner Westen mit Hilfe verschiedener Tracer; Diplomarbeit; Freie Universität Berlin; 2003

Ripl et al. 1987; Ripl W., Heller S., and Linnenweber C; Limnologische Untersuchungen an den Sedimenten des Tegeler Sees; Eigenverlag Fachgebiet Limnologie, Technische Universität Berlin; 1987

Rötting et al. 2006; Rötting T. S., Carrera J., Bolzicco J., Salvany J. M.; Stream-Stage Response Tests and Their Joint Interpretation with Pumping Tests; Groundwater; 44; *3*, pp.371-385,

Rümmler 2003; Rümmler J.; 2-Dimensional-horizontal-ebene Simulation der Grundwasserströmungsverhältnisse unter Uferfiltrationsbedingungen; Diplomarbeit; Mathematisch-Naturwissenschaftliche Fakultät 2, Geographisches Institut, Humboldt-Universität zu Berlin; 2003

Schley 1981; Schley A.; Bestimmung der Durchlässigkeiten am Beispiel von Seesedimenten des Tegeler Sees; Unveröffentl. Diplomarbeit; FB Geowissenschaften, FU Berlin; 1981

Schubert 2002; Schubert, J.; Hydraulic aspects of riverbank filtration – field studies; Journal of Hydrology; *266*, pp.145-161,

Seifert et al. 2005; Seifert D., Engesgaard P.; Biological clogging of porous media: Tracer studies of non-uniform flow patterns; ISMAR5 – 5th international symposium on Management of Aquifer Recharge, 12-16 June ; Berlin, Germany, 2005

Sensut 2002-2005; Water levels of Lake Tegel and Airport Lake, physico-chemical Parameters of Lake Tegel; let from Senatsverwaltung für Stadtentwicklung des Landes Berlin; 2002-2005

Shaw et al. 1990; Shaw R. D., Shaw J. F. Fricker H. H., Prepas E. E.; Integrated Approach to Quantify Groundwater Transport of Phosphorus to Narrow Lake; Alberta Limnology and Oceanography; 35; *4*, pp.870-886,

Sivers 2001; Sievers, J.; Geochemische und hydraulische Untersuchungen an Mudde- und Sandkernen aus dem Tegeler See; unveröffentlichte Diplomarbeit; Institut für Geowissenschaften, FU Berlin; 2001

Stuyfzand et al. 2004; Stuyfzand P. J., Juhàsz-Holterman M. H. A., de Lange W. J.; Riverbank filtration in the Netherlands: well fields, clogging and geochemical reactions; NATO Advanced Research Workshop: Clogging in Riverbank Filtration; Bratislava, 2004

Umweltatlas Berlin; Senatsverwaltung für Stadtentwicklung des Landes Berlin; Digitaler Umweltatlas Berlin; 2002-2006 http://www.stadtentwicklung.berlin.de/umwelt/umweltatlas/.

Vandevivere and Baveye 1992; Vandevivere P. and Baveye P.; aturated Hydraulic conductivity reduction caused by aerobic bacteria in sand columns; Soil Science Society of America Journal; 56; *1*, pp.1-13,

Voigt et al. 2000; Voigt I., Eichberg M.; Hydrogeologische Übersichtsprofile Nr.1- Nr.10; erstellt von der Fugro im Auftrag der BWB; Berlin, 2000

von Gunten et al. 1994; von Gunten H. R., Karametaxas G., Keil R.; Chemical Processes in Infiltrated Riverbed Sediments; Envion. Sci. Technol.; 28; pp.2078-2093,

Wasserschutzgebietsverordnung Tegel 1995; Senat Berlin; Verordnung zur Festsetzung des Wasserschutzgebietes für das Wasserwerk Tegel; pp.753-1-13,

WASY 2004; WASY; Hydrogeologisches Fachgutachten zur Auswirkung grundlegender Änderungen des Betriebs zur Grundwasseranreicherung Wasserwerk Tegel; unpublished work; WASY Gesellschaft für wasserwirtschaftliche Planung und Systemforschung mbH; Berlin, 2004

WebTech360 2005; WebTech360; Processing MODFLOW Pro – Users Manual; WebTech360; 20 Fairbanks, Suite 187 Irvine, CA 92618, U.S., 2005 http://www.webtech360.com.

Wiese et al. 2004; Wiese B., Holzbecher E., Rümmler J, and Nützmann G.; Effects of Oscillating Pumping Regimes of Bank-Filtration Galleries; Proc. International Conference on Finite-Element Models, FEM-MODFLOW, MODFLOW and more 2004; Carlovy Vary, Czech Republic, 2004 pp.411-414,

Wolf 2004; Wolf, P.; Die Grundwasserströmungsverhältnisse im Bereich des WW Beelitzhof (Großer Wannsee) – ein numerisches Strömungsmodell. ; Diplomarbeit; Fachbereioch Geowissenschaften Universität Hannover;

Wood and Basset 1975; Wood W. W., and Bassett R. L.; ater Quality Changes Related to the Development of Anaerobic Conditions During Artificial Recharge; Water Resour. Res.; 11; *4*, pp.553-558,

Zheng et al. 1998; Zheng C., and Wang P. P.; MTD3MS, A modular three-dimensional transport model. ; US Army Corps of Engineers Watewrways Experiment Station; Vicksburg, Miss., U.S.A.,

Ziegler 2001; Ziegler, D.; Untersuchungen zur nachhaltigen Wirkung der Uferfiltration im Wasserkreislauf Berlins; Dissertation; Fakultät Prozesswissenschaften, Technische Universität Berlin; 2001

Appendix

Well 12 – water balance

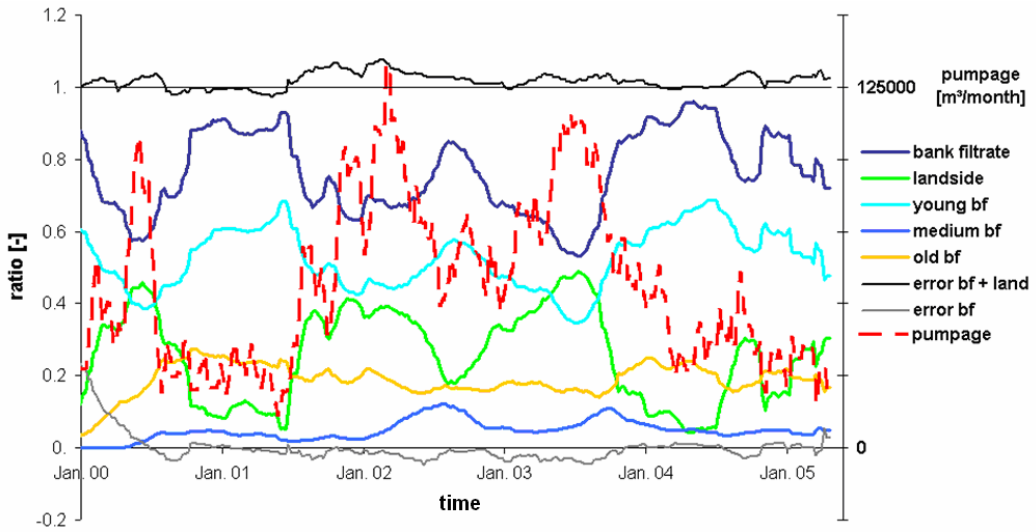

Figure App1: Fractions of water abstracted at Well 12. The dark blue line shows the total bank filtrate ratio, the green line shows the ratio of inland water, the light blue line shows the ratio of young bank filtrate (~4-6 month age) infiltrated directly in front of the transect, the indigo blue line shows the ratio of medium aged bank filtrate (~2 years age) which infiltrated north of Reiswerder, the orange line shows the ratio of old bank filtrate, infiltrated near Scharfenberg. The black and grey lines are checksums, the black shows the sum of bank filtrate and inland water which should be 1, the grey line shows difference between total bank filtrate and the sum of young, medium and old bf, which should be nil. The dashed red line is the pumping rate and belongs to the right y-axis. All values are the moving average of 9 weeks.

Well 14 – water balance

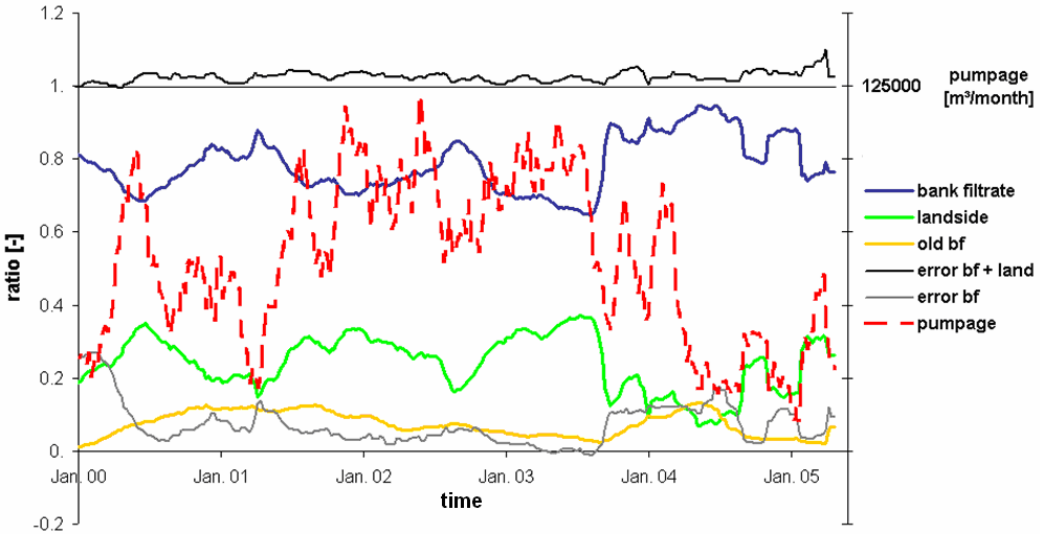

Figure App2: Fractions of water abstracted at Well 14. The dark blue line shows the total bank filtrate ratio, the green line shows the ratio of inland water, the orange line shows the ratio of old bank filtrate, infiltrated near Scharfenberg. The black and grey lines are checksums, the black shows the sum of bank filtrate and inland water which should be 1, the grey line shows difference between total bank filtrate and the sum of young, medium and old bf, which should be nil. The dashed red line is the pumping rate and belongs to the right y-axis. All values are the moving average of 9 weeks.

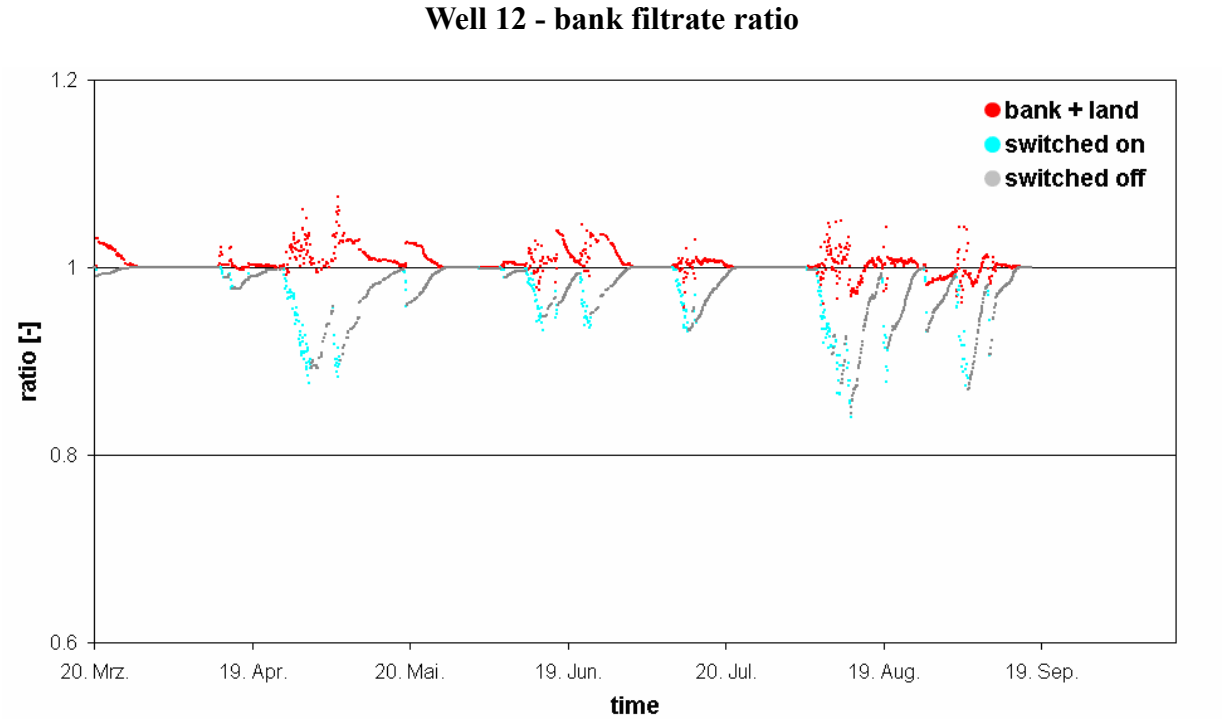

Figure App3: Ratio of bank filtrate in Well 12 in 2004, obtained by applying MT3DMS to the telescope model. Each dot represents one time step. The red dots show the sum of inland water and bankfiltrate, which should be 1. The blue dots show the ratio of bank filtrate in extracted water, the grey dots show the concentration of bank filtrate in the well when it is switched off.

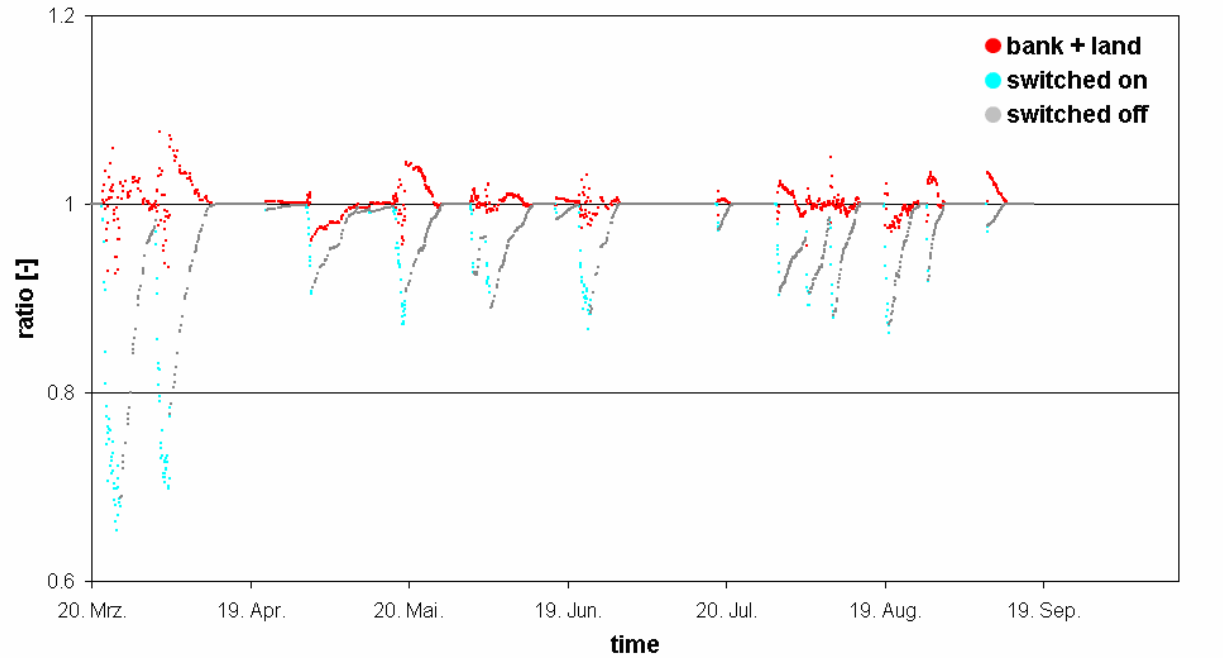

Figure App4: Ratio of bank filtrate in Well 14 in 2004, obtained by applying MT3DMS to the telescope model. Each dot represents one time step. The red dots show the sum of inland water and bankfiltrate, which should be 1. The blue dots show the ratio of bank filtrate in extracted water, the grey dots show the concentration of bank filtrate in the well when it is switched off.

Lake Tegel Boron

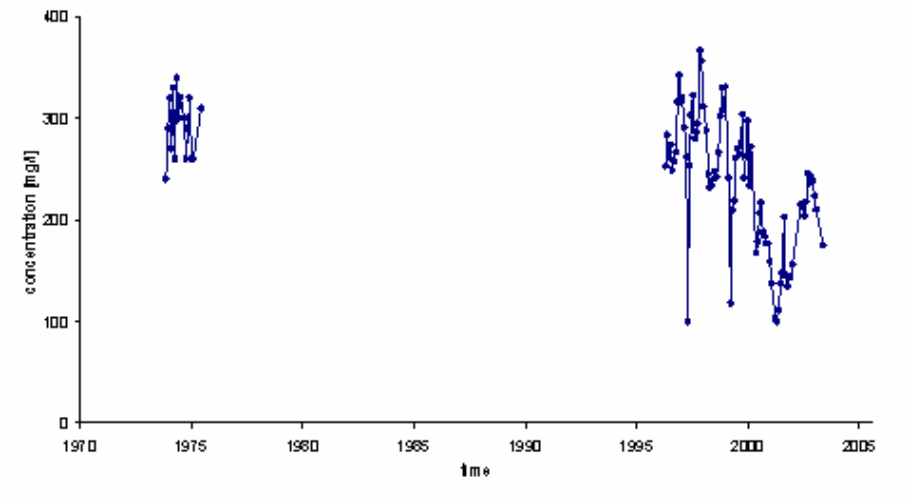

Figure App5: Concentration of boron in Lake Tegel (SENSUT 2005)

Lake Tegel Chloride

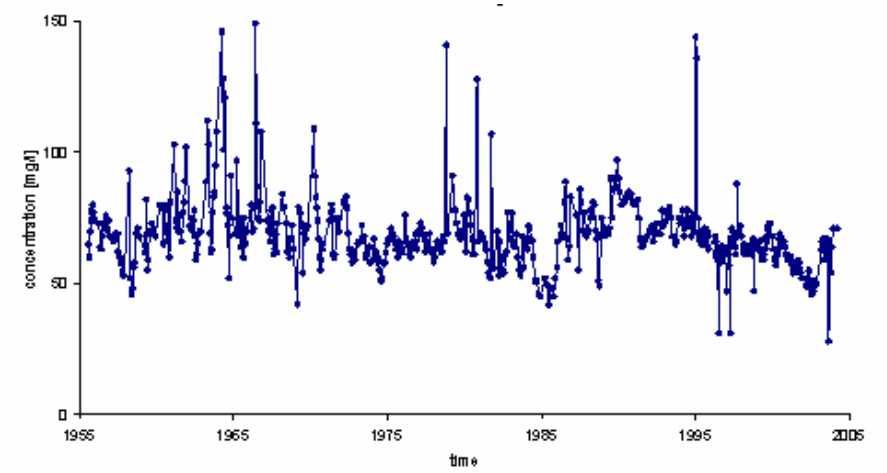

Figure App6: Concentration of chloride in Lake Tegel (SENSUT 2005)

Lake Tegel Sulphate

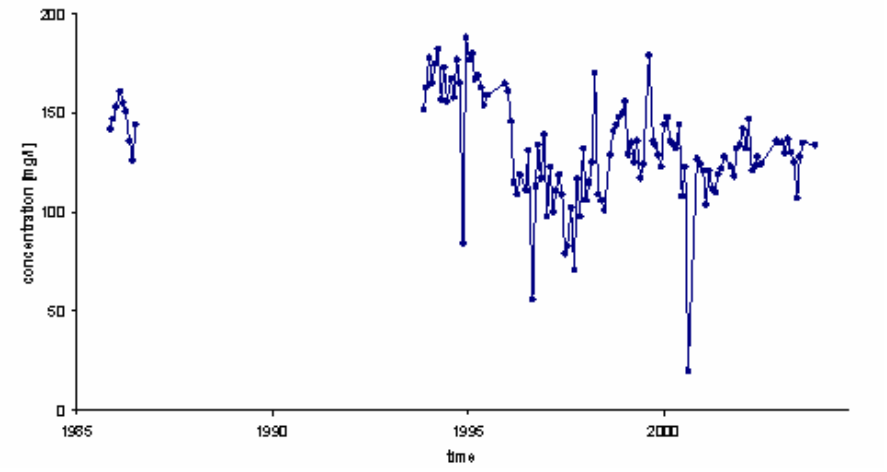

Figure App7: Concentration of sulphate in Lake Tegel (SENSUT 2005)

^{18}O

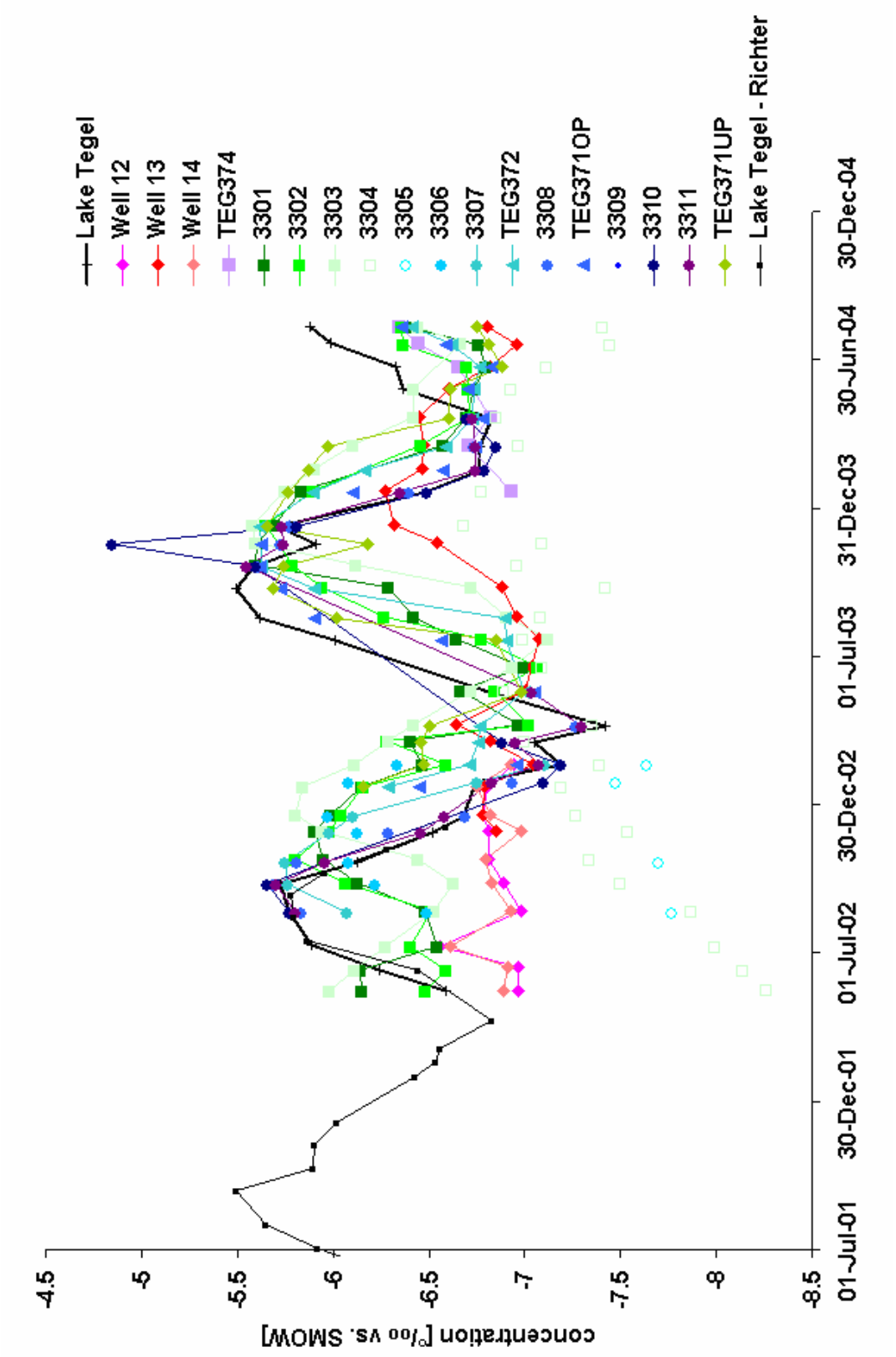

Figure App8: Concentrations of ^{18}O in Lake Tegel, observation wells and abstraction wells 12, 13, 14 (KWB 2005)

^{2}H

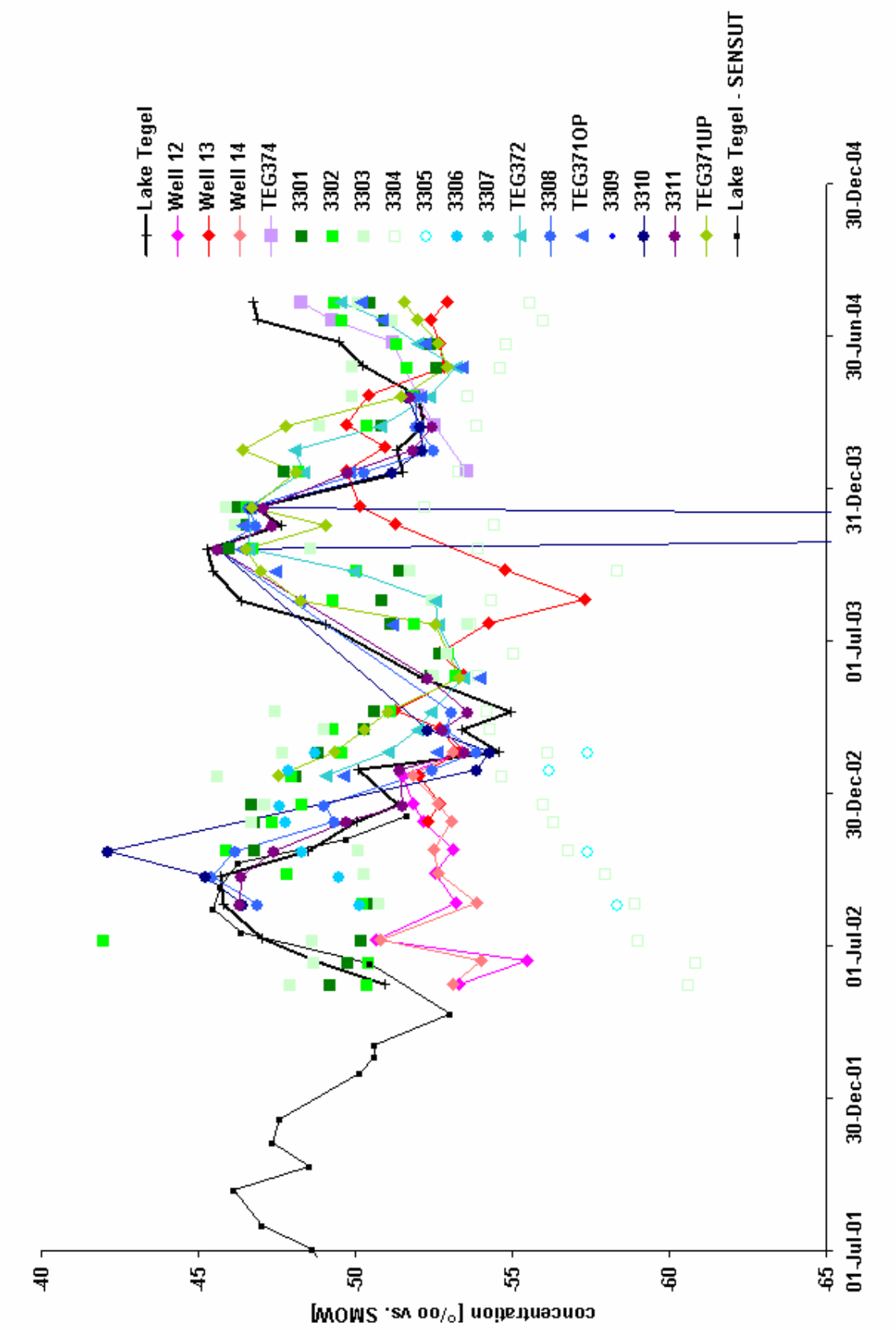

Figure App9: Concentrations of Deuterium in Lake Tegel, observation wells and abstraction wells 12, 13, 14 (KWB 2005).

AMDOPH

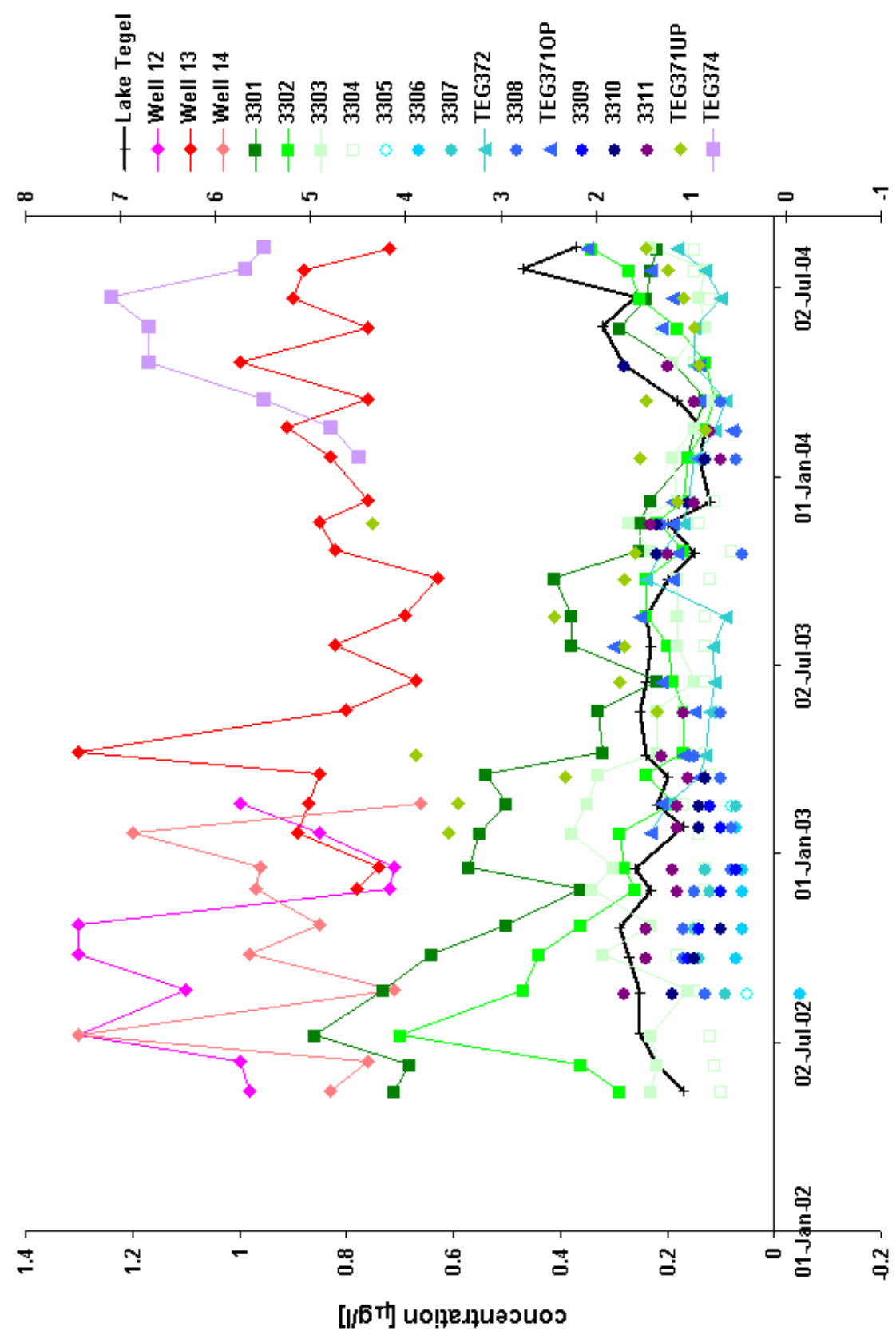

Figure App10: Concentrations of AMDOPH in Lake Tegel, observation wells and abstraction wells 12, 13, 14 (KWB 2005).

AMPH

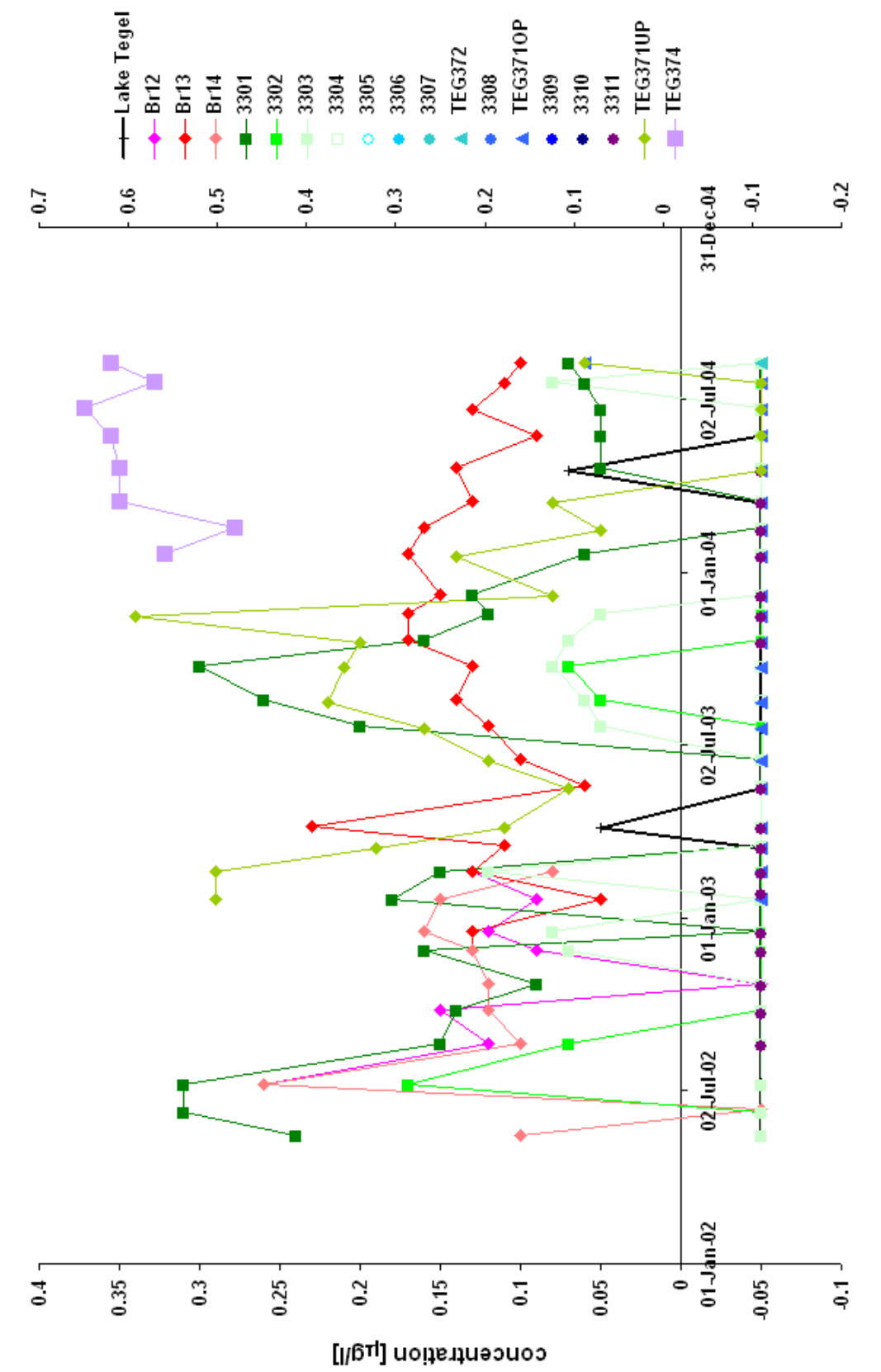

Figure App11: Concentrations of AMPH (Aminophenazone) in Lake Tegel, observation wells and abstraction wells 12, 13, 14 (KWB 2005). The value of negative concentrations indicate the level of detection.

Boron

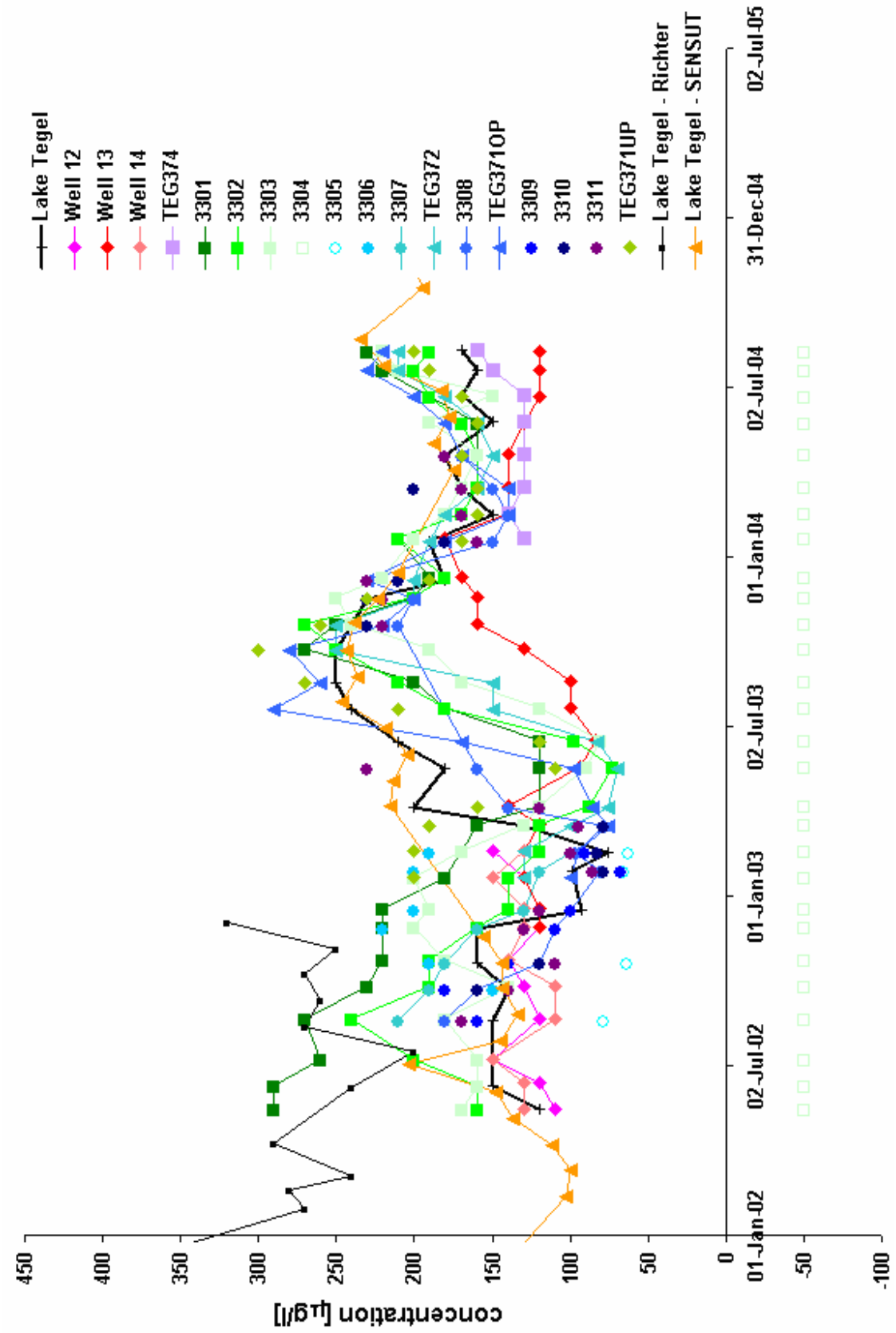

Figure App12: Concentrations of Boron in Lake Tegel, observation wells and abstraction wells 12, 13, 14 (KWB 2005, Richter 2003, SENSUT 2005).

Calcium

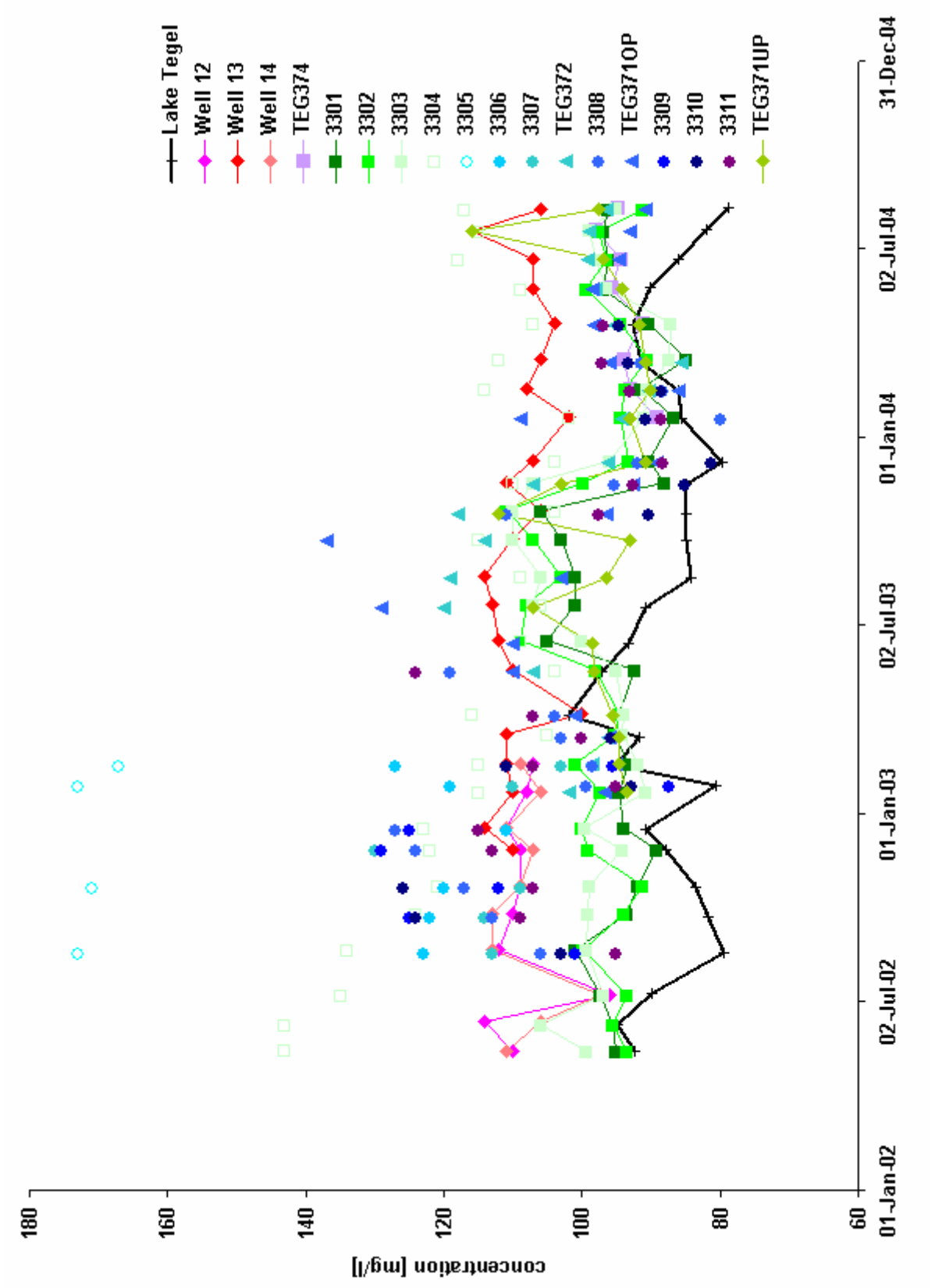

Figure App13: Concentrations of Calcium in Lake Tegel, observation wells and abstraction wells 12, 13, 14 (KWB 2005).

Chloride

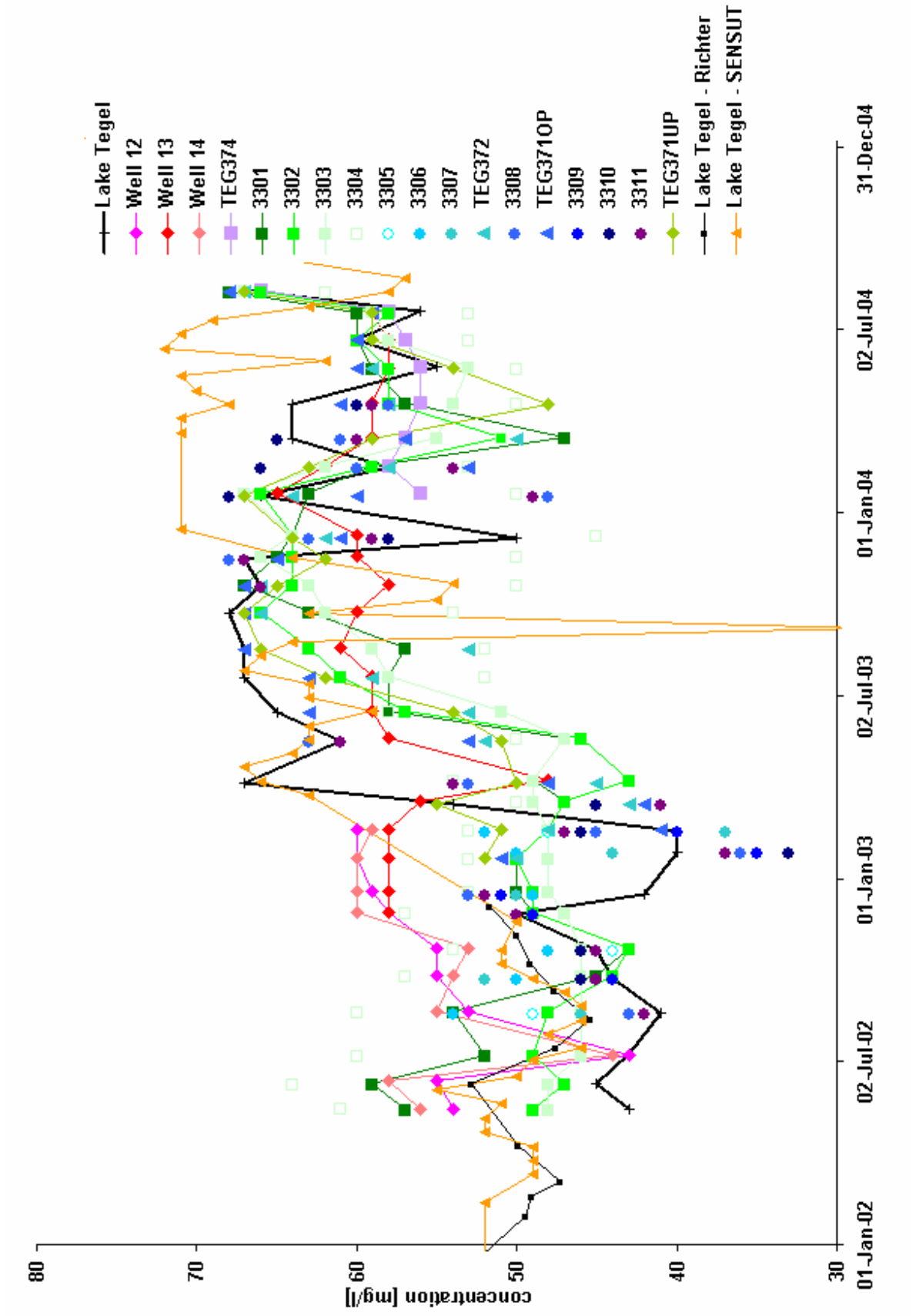

Figure App14: Concentrations of chloride in Lake Tegel, observation wells and abstraction wells 12, 13, 14 (KWB 2005, Richter 2003, SENSUT 2005).

EDTA

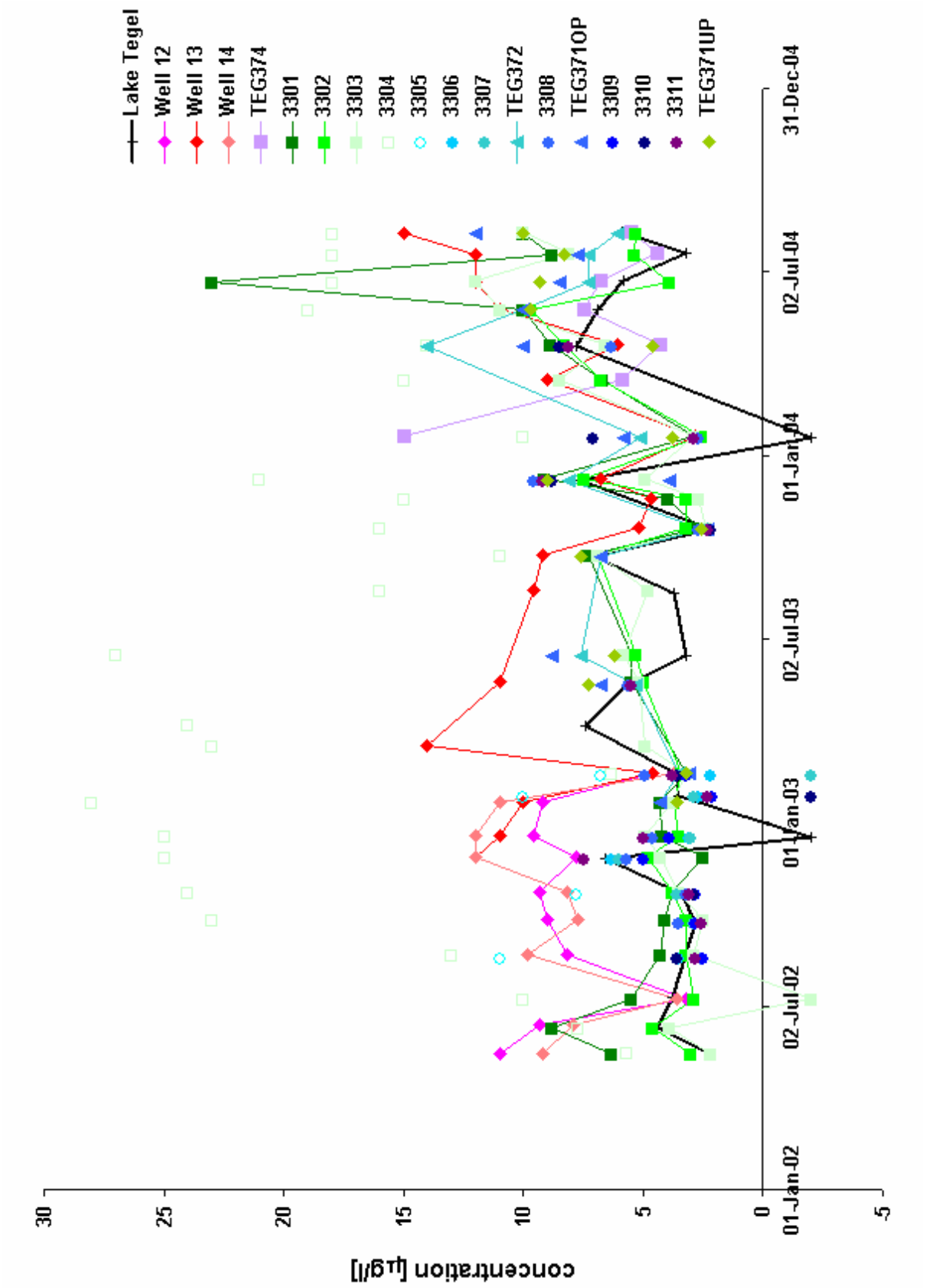

Figure App15: Concentrations of EDTA in Lake Tegel, observation wells and abstraction wells 12, 13, 14 (KWB 2005). The value of negative concentrations indicate the level of detection.

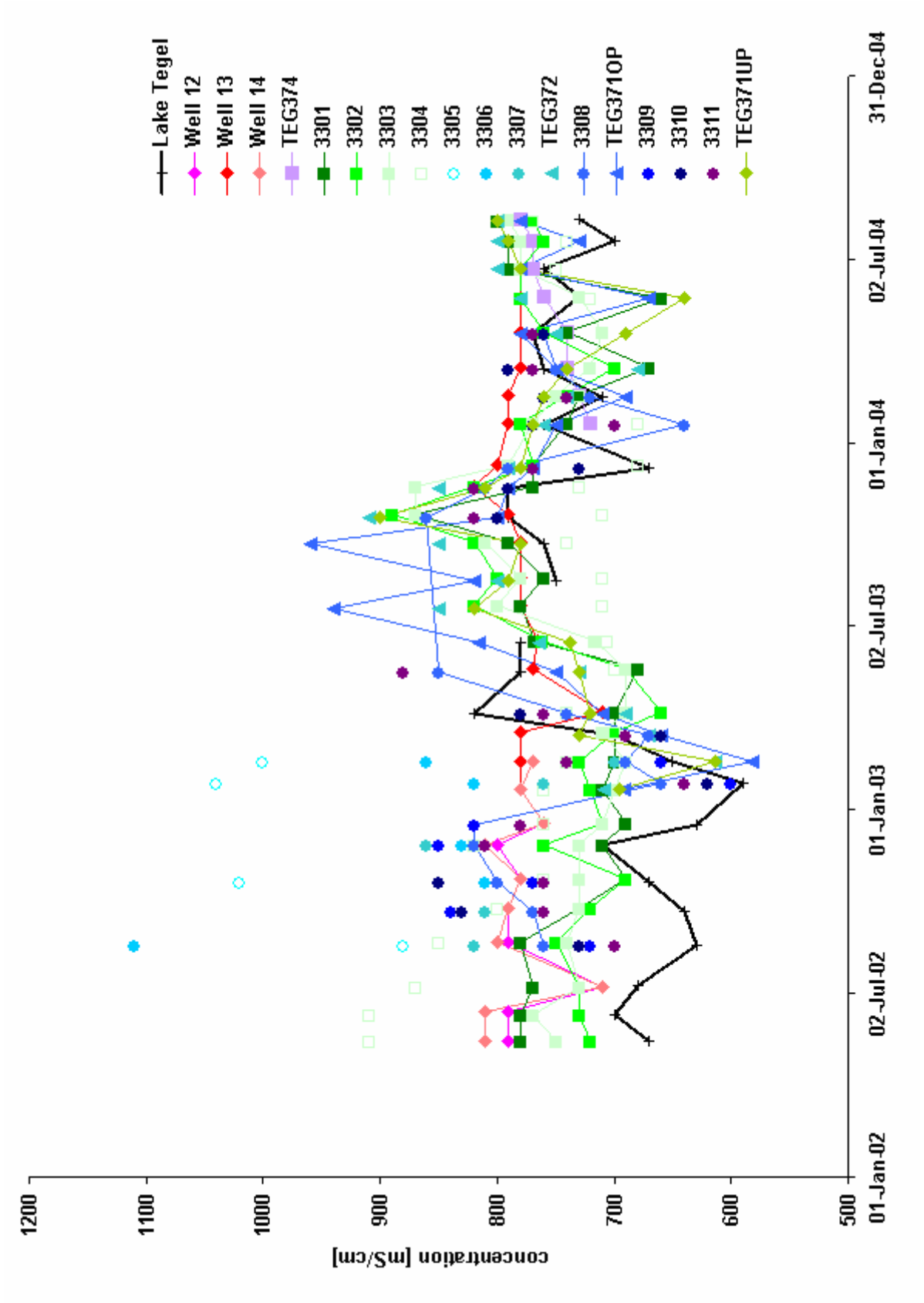

Figure App16: Concentrations of electrical conductivity in Lake Tegel, observation wells and abstraction wells 12, 13, 14 (KWB 2005).

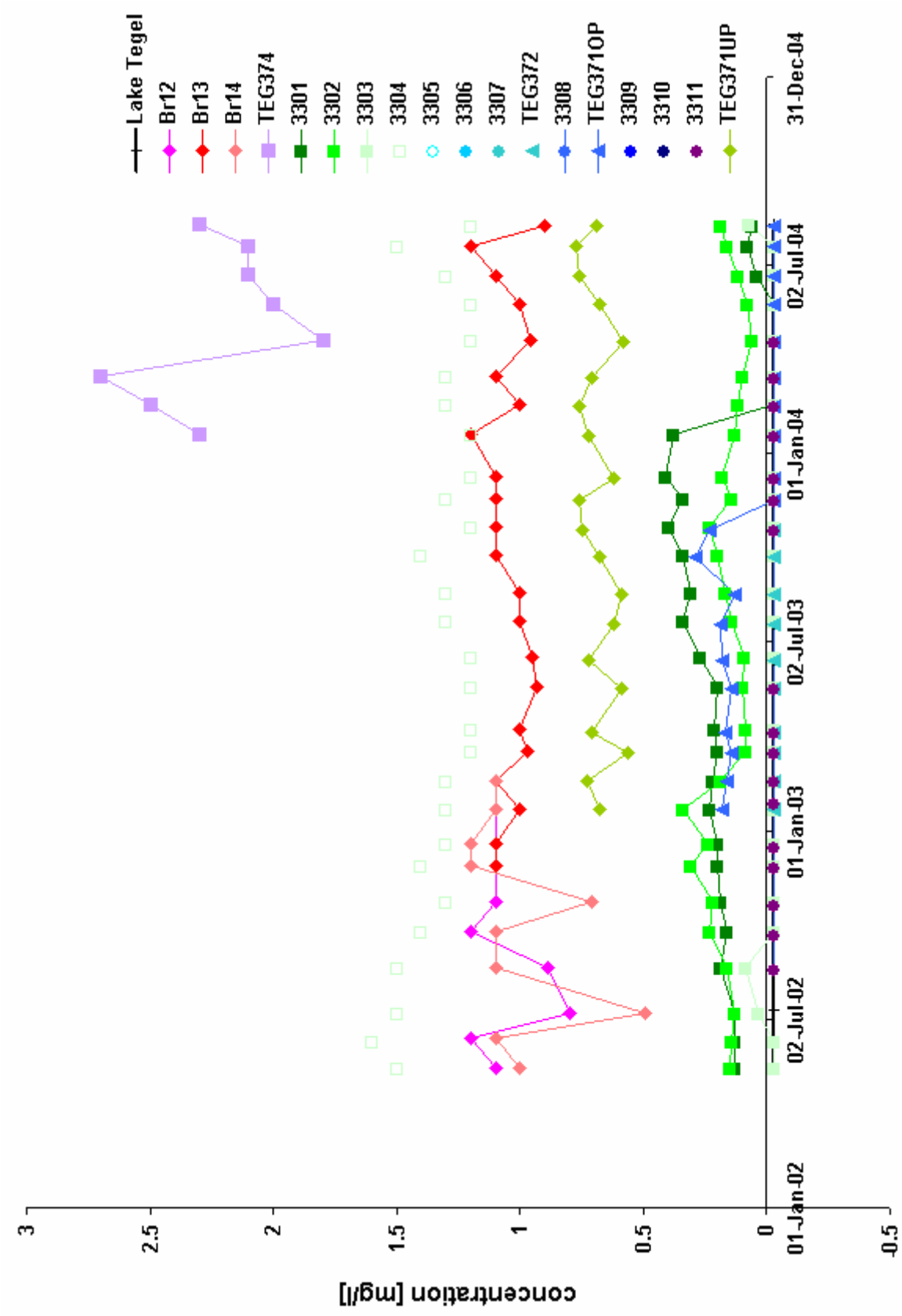

Figure App17: Concentrations of total iron in Lake Tegel, observation wells and abstraction wells 12, 13, 14 (KWB 2005). The value of negative concentrations indicate the level of detection.

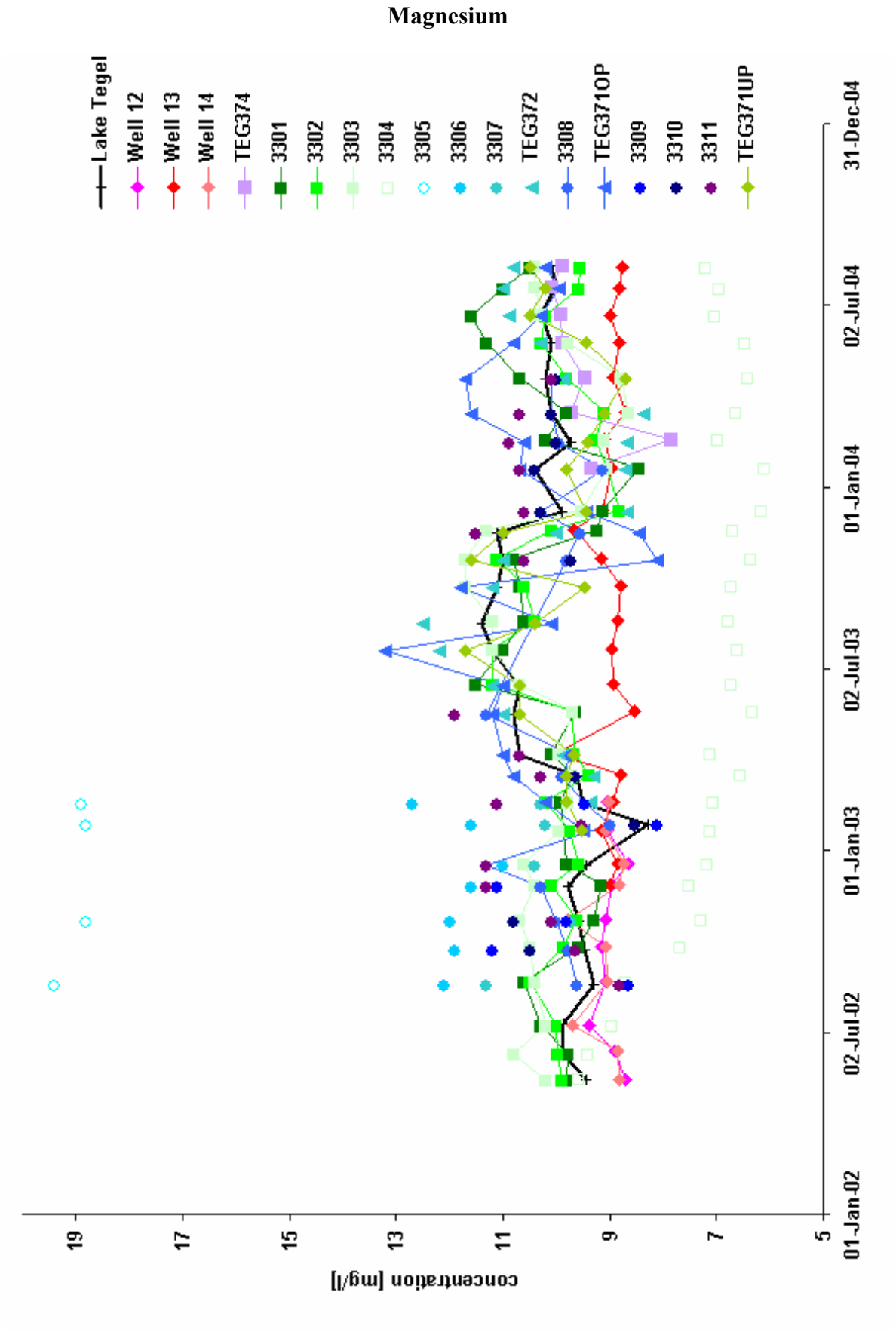

Figure App18: Concentrations of Magnesium, measured during the NASRI project (KWB 2005).

Manganese

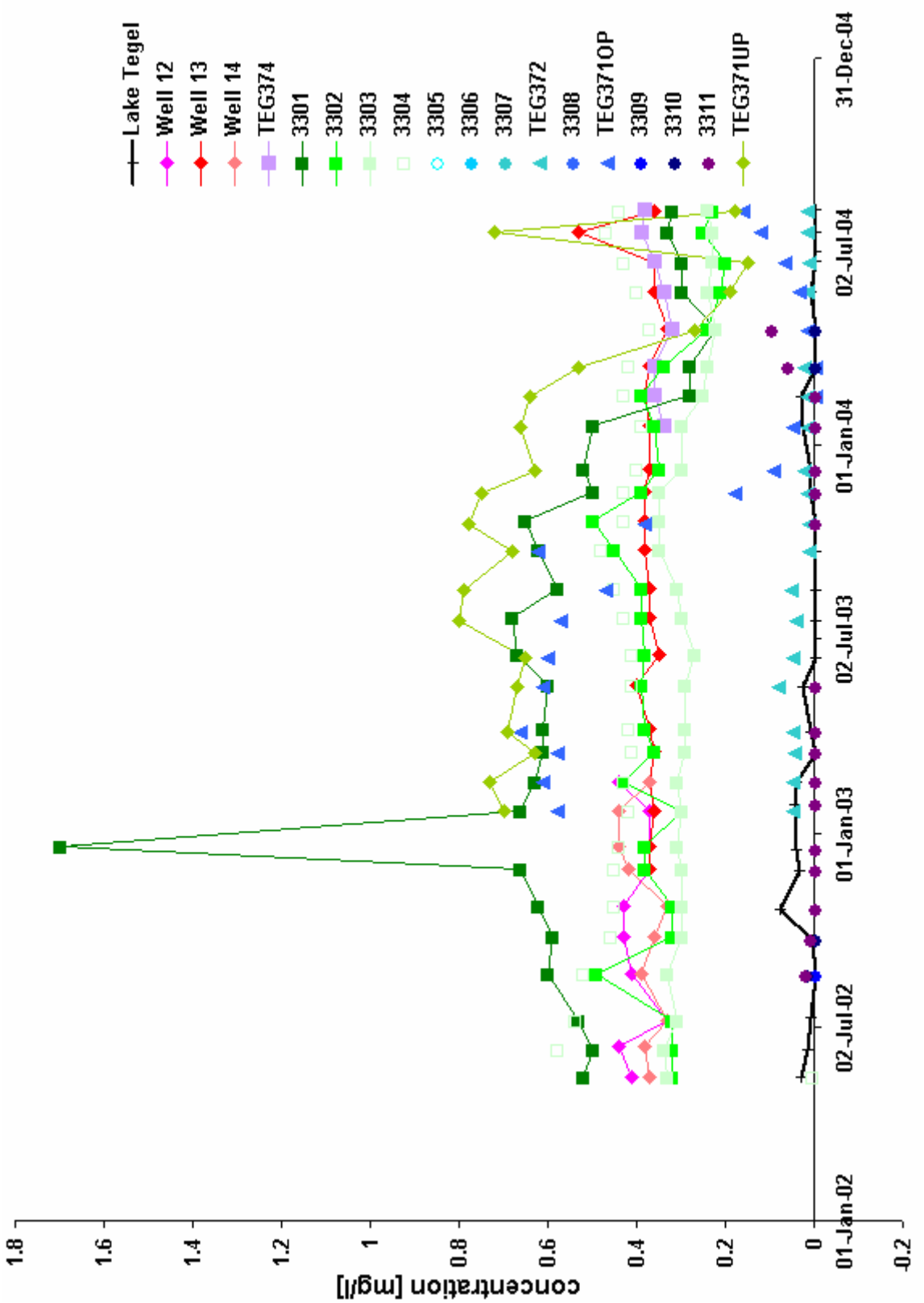

Figure App19: Concentrations of Manganese, measured during the NASRI project (KWB 2005). The value of negative concentrations indicate the level of detection.

Nitrate - N

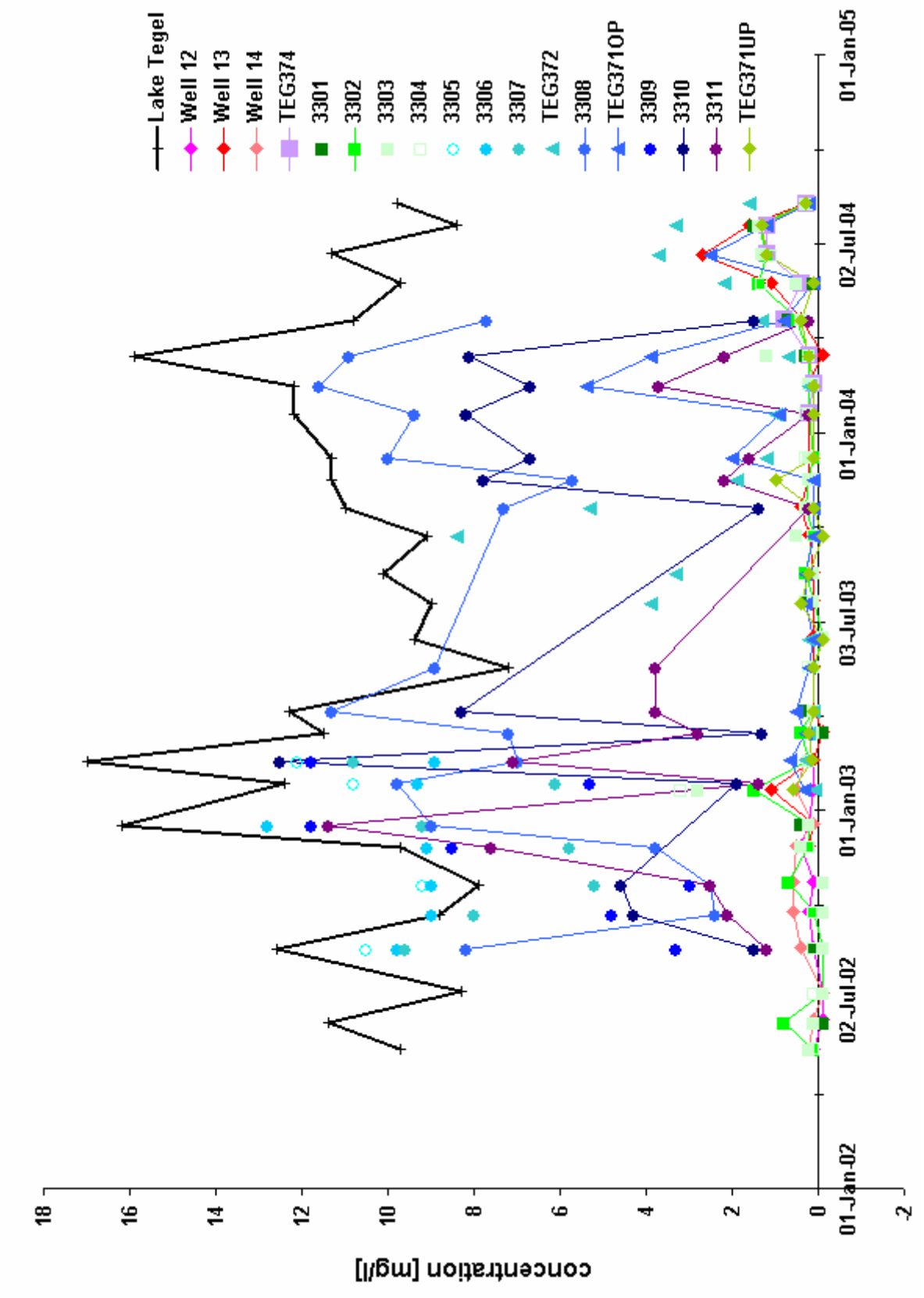

Figure App20: Concentrations of nitrate-N, measured during the NASRI project (KWB 2005). The value of negative concentrations indicate the level of detection.

Oxygen

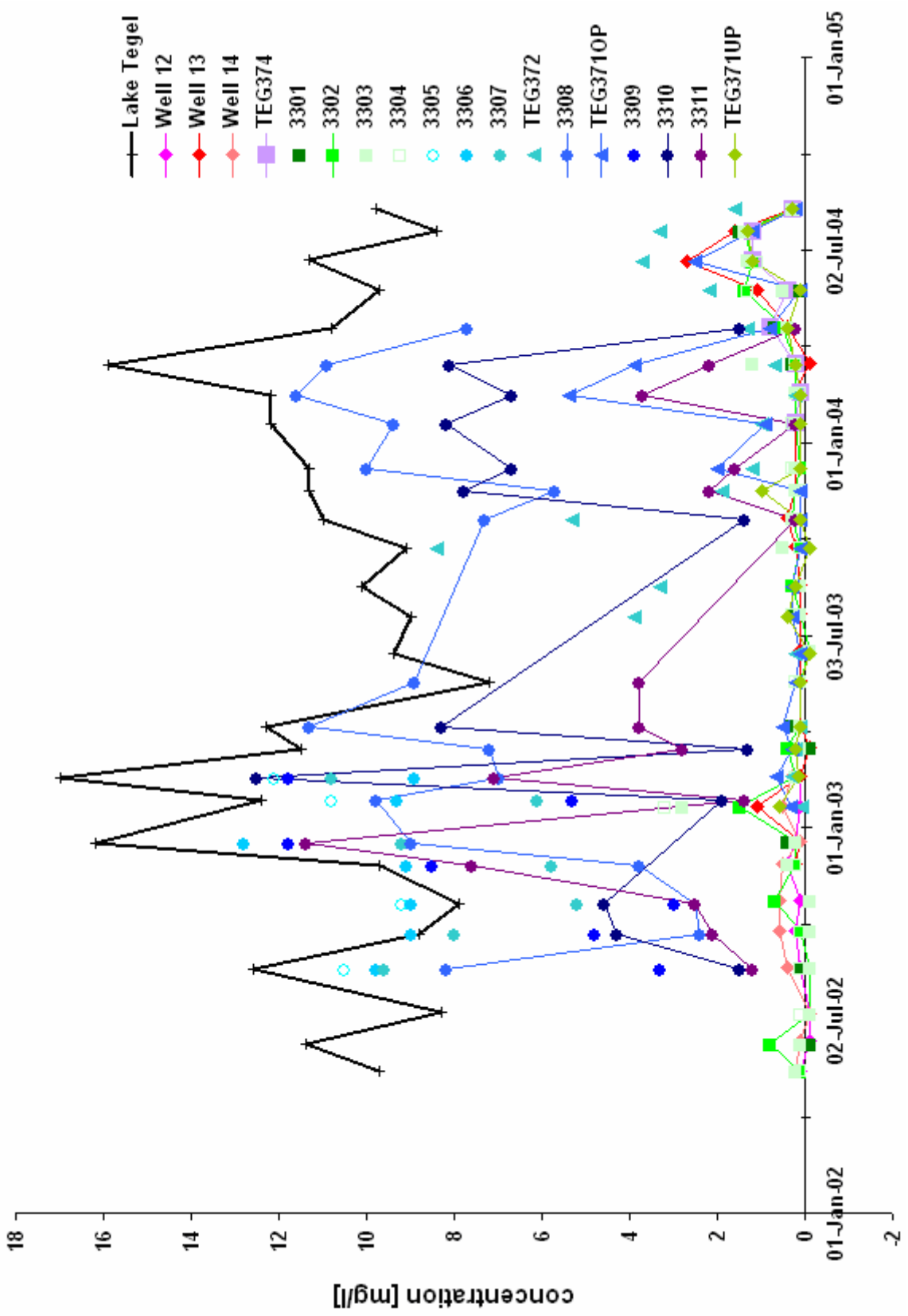

Figure App21: Concentrations of oxygen, measured during the NASRI project (KWB 2005). The value of negative concentrations indicate the level of detection.

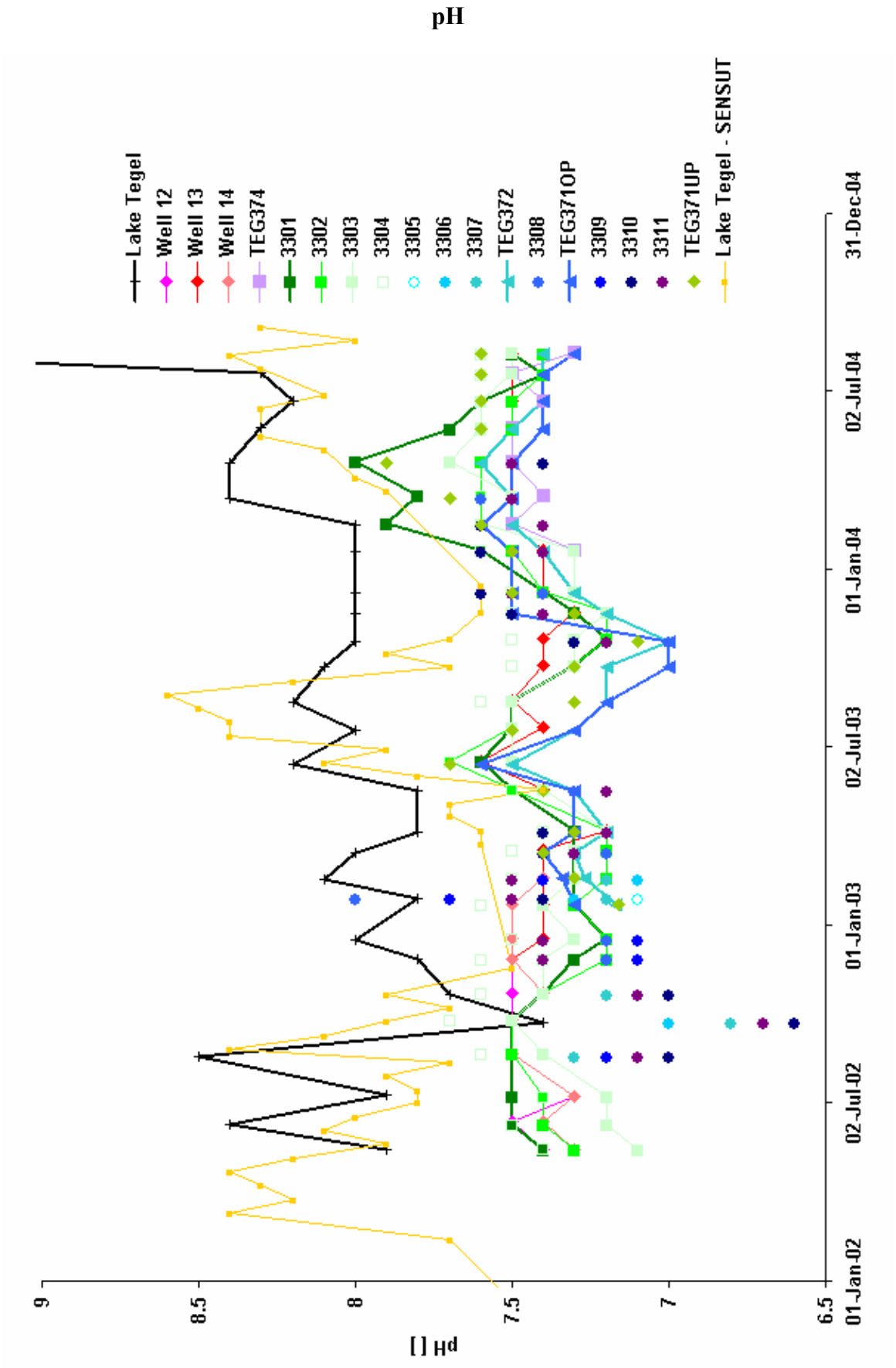

Figure App22: pH values, measured during the NASRI project (KWB 2005) and (SENSUT2005).

Phenazone

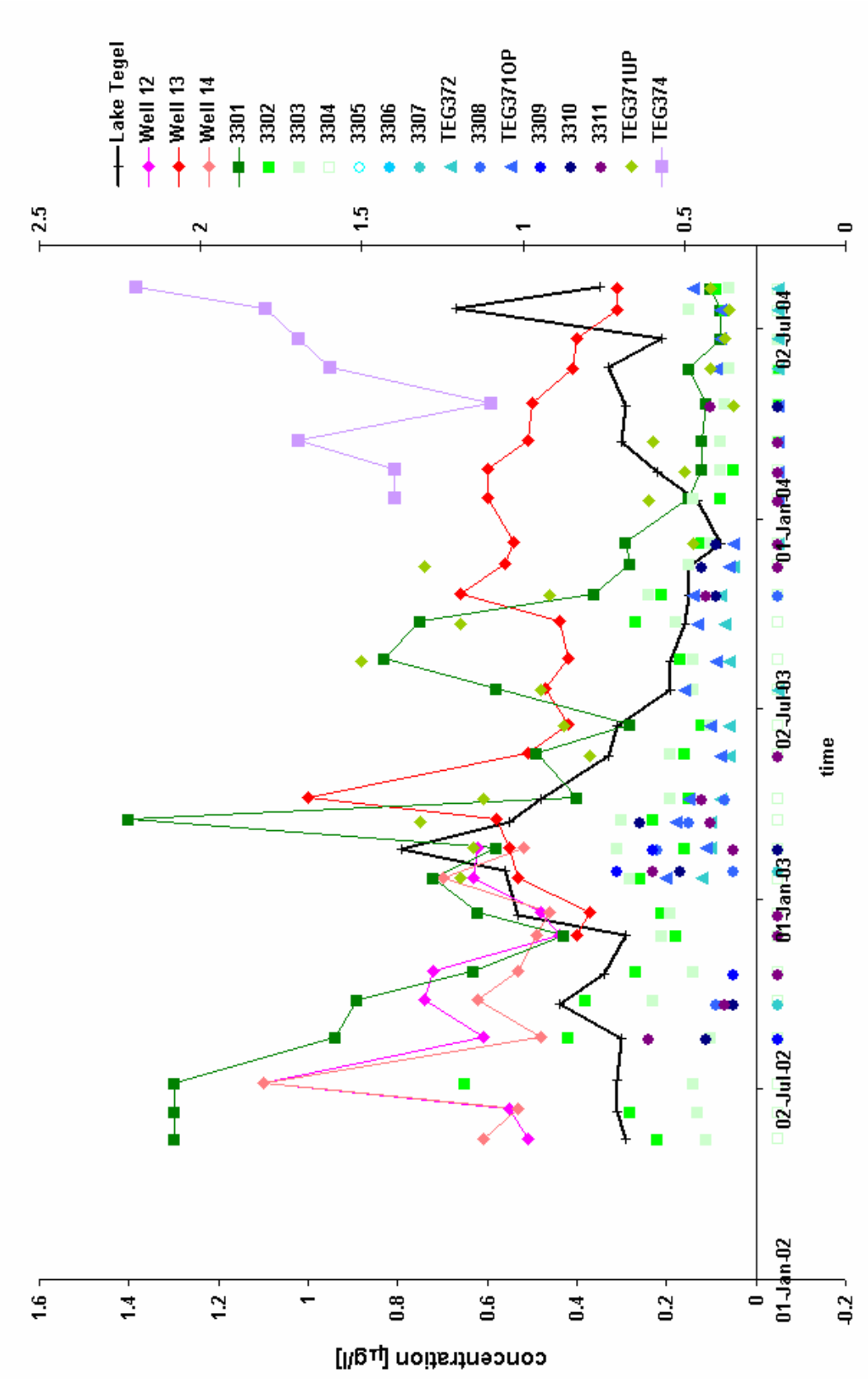

Figure App23: Concentrations of phenazone, measured during the NASRI project (KWB 2005). TEG374 is plotted to the right y-axis. The value of negative concentrations indicate the level of detection.

Potassium

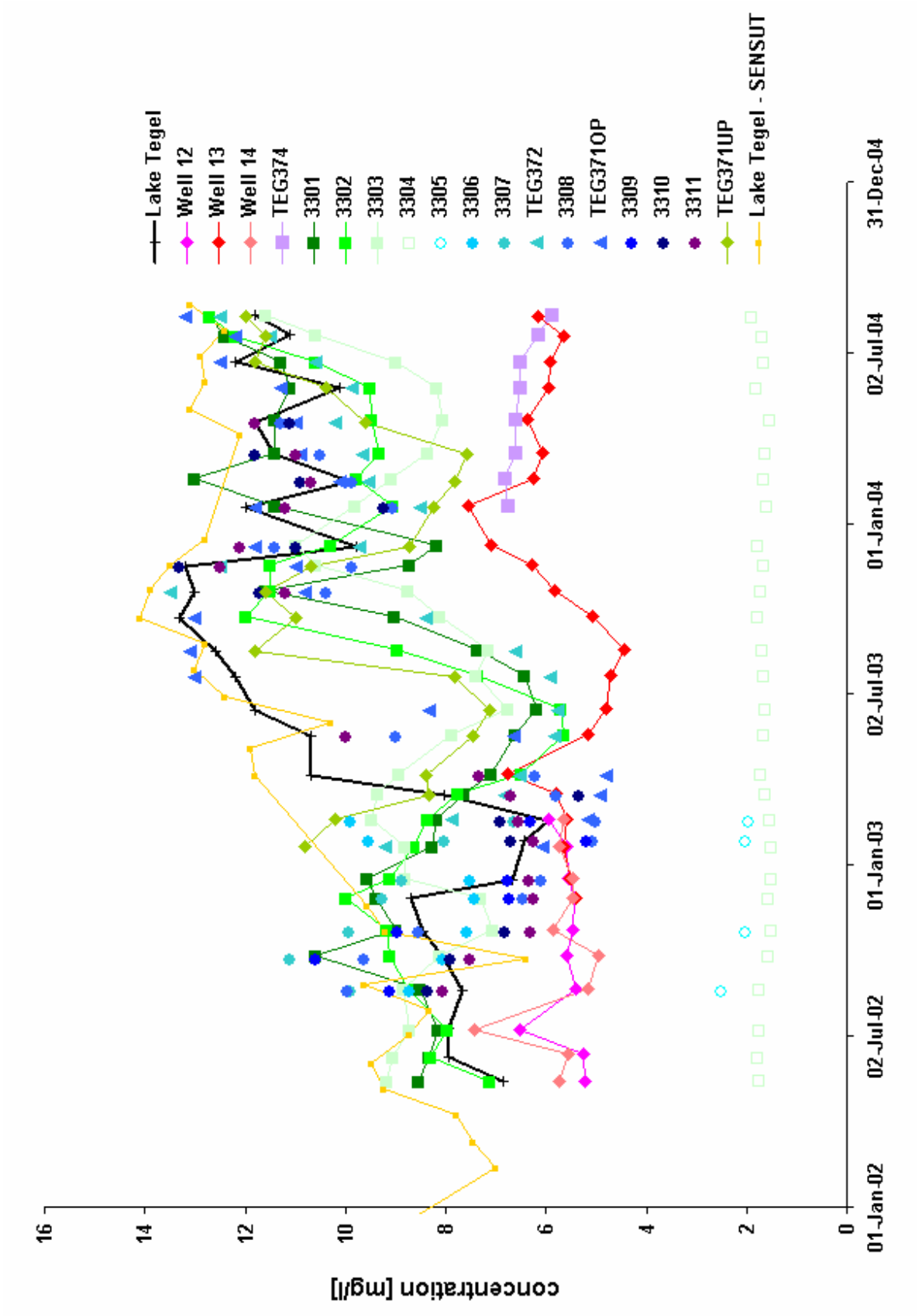

Figure App24: Concentrations of potassium in Lake Tegel, observation wells and abstraction wells 12, 13, 14 (KWB 2005, SENSUT 2005).

Propyphenazone

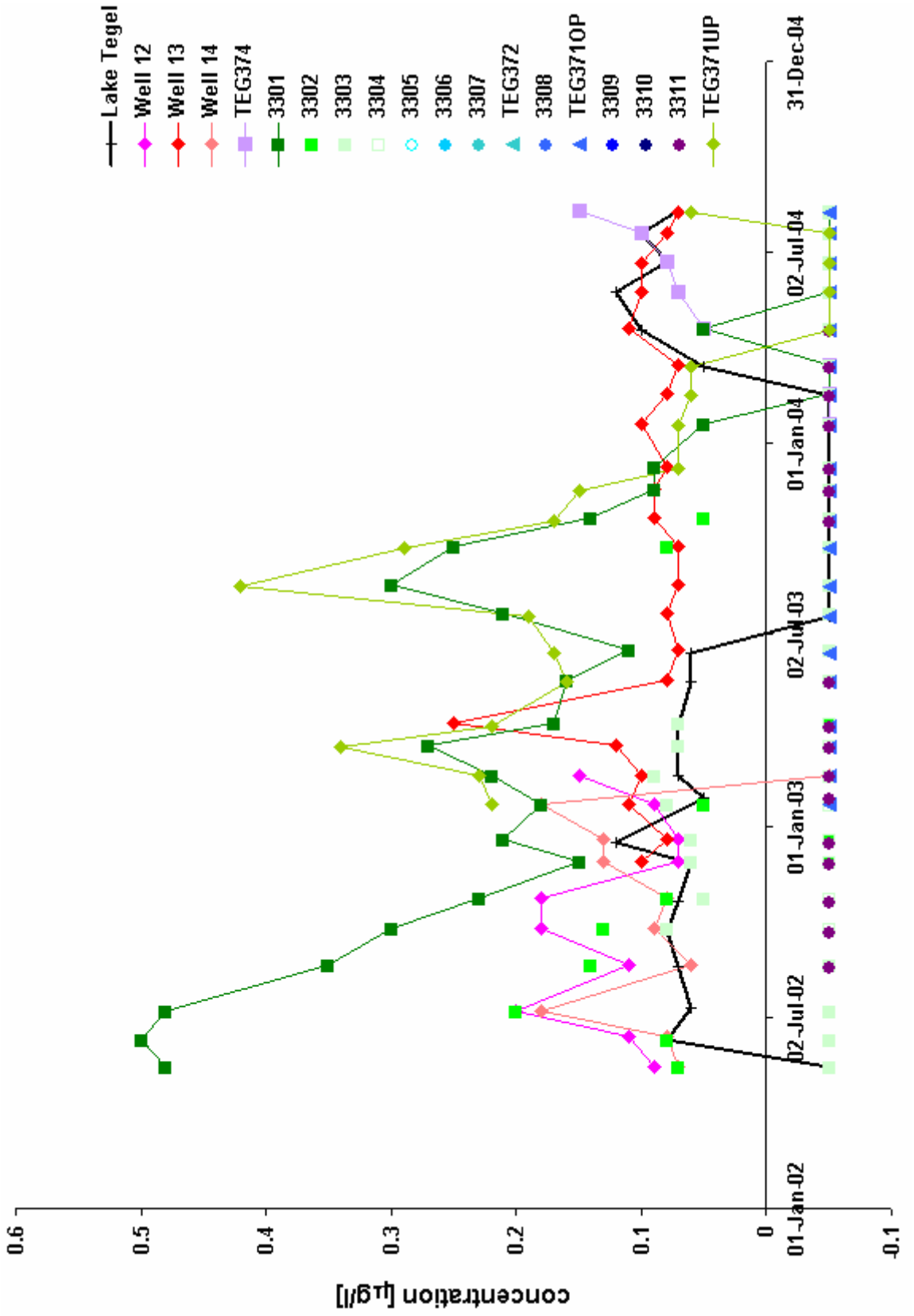

Figure App25: Concentrations of propyphenazone, measured during the NASRI project (KWB 2005). The value of negative concentrations indicate the level of detection.

Sodium

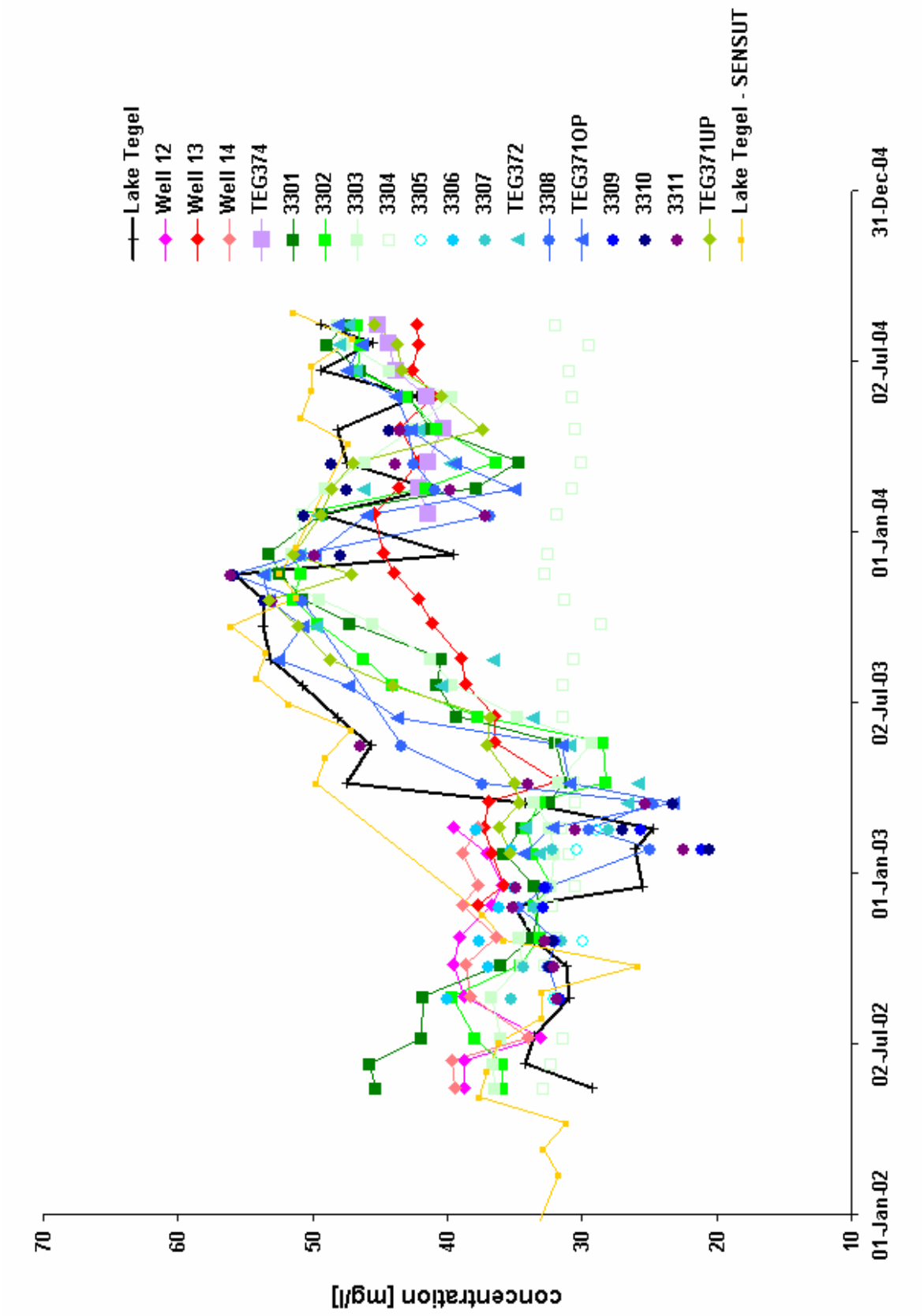

Figure App26: Concentrations of sodium in Lake Tegel, observation wells and abstraction wells 12, 13, 14 (KWB 2005, SENSUT2005).

Sulphate

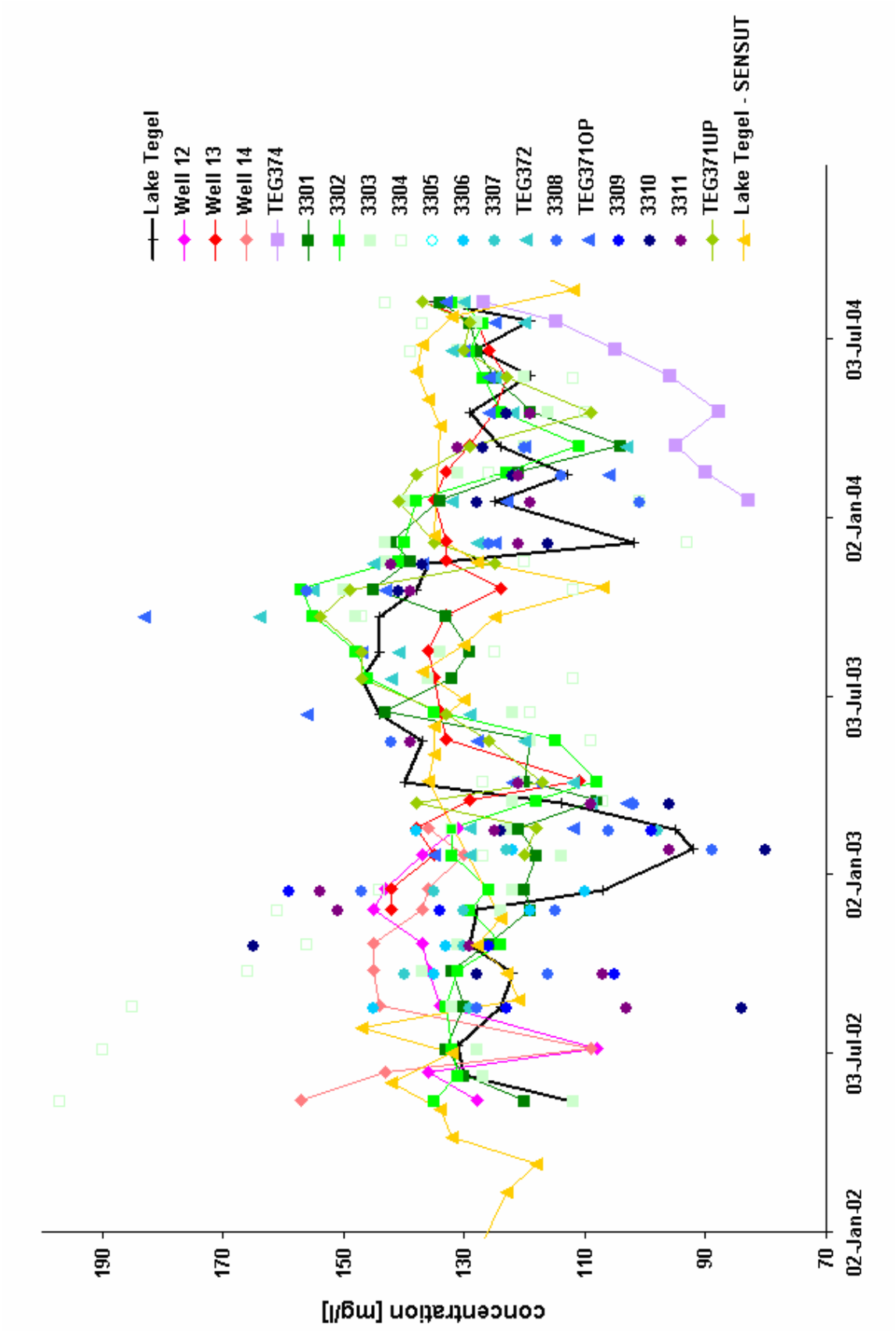

Figure App27: Concentrations of sulphate in Lake Tegel, observation wells and abstraction wells 12, 13, 14 (KWB 2005, SENSUT2005).

Temperature

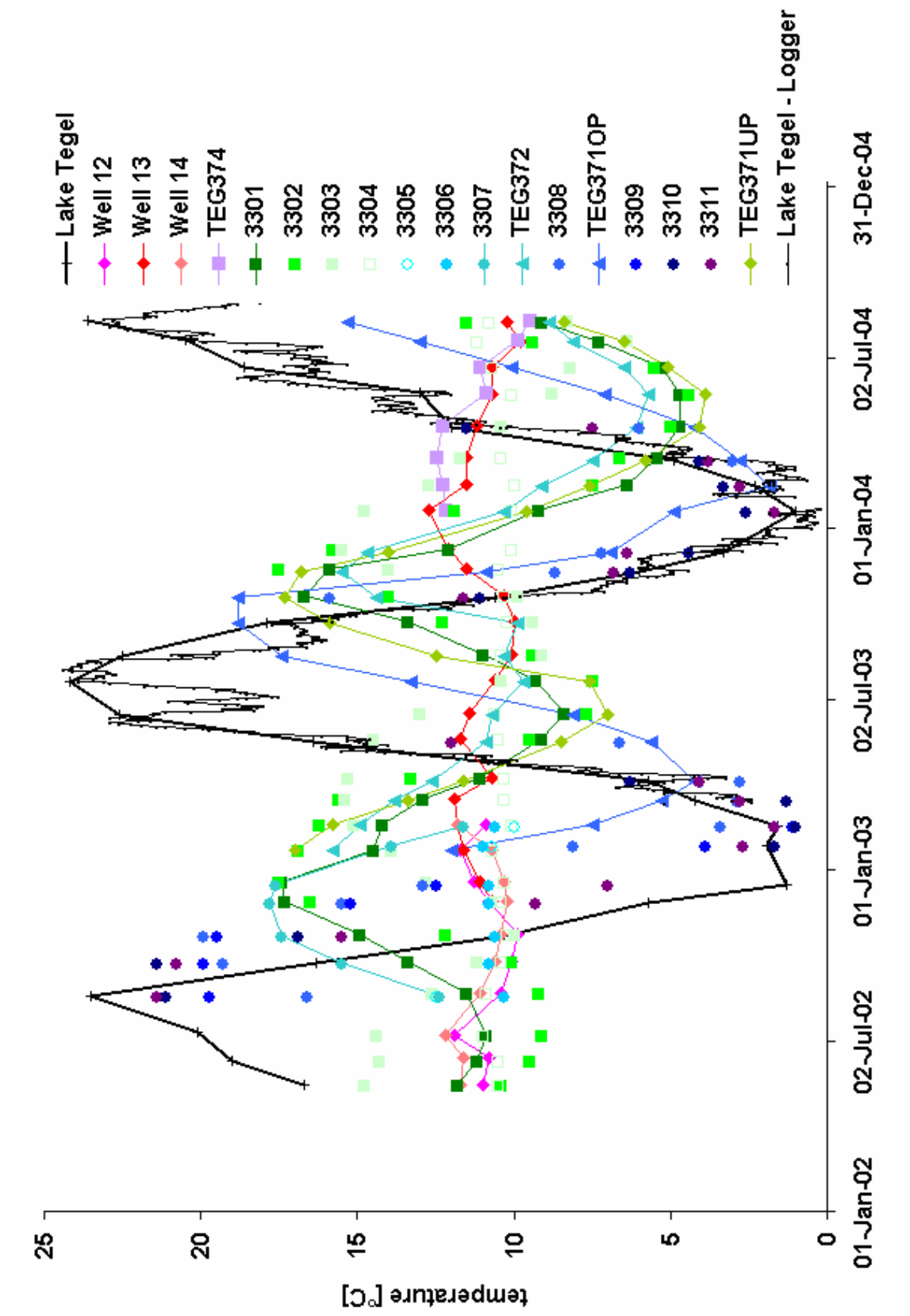

Figure App28: Temperature in Lake Tegel, observation wells and abstraction wells 12, 13, 14 (KWB 2005).

Total Inorganic Carbon

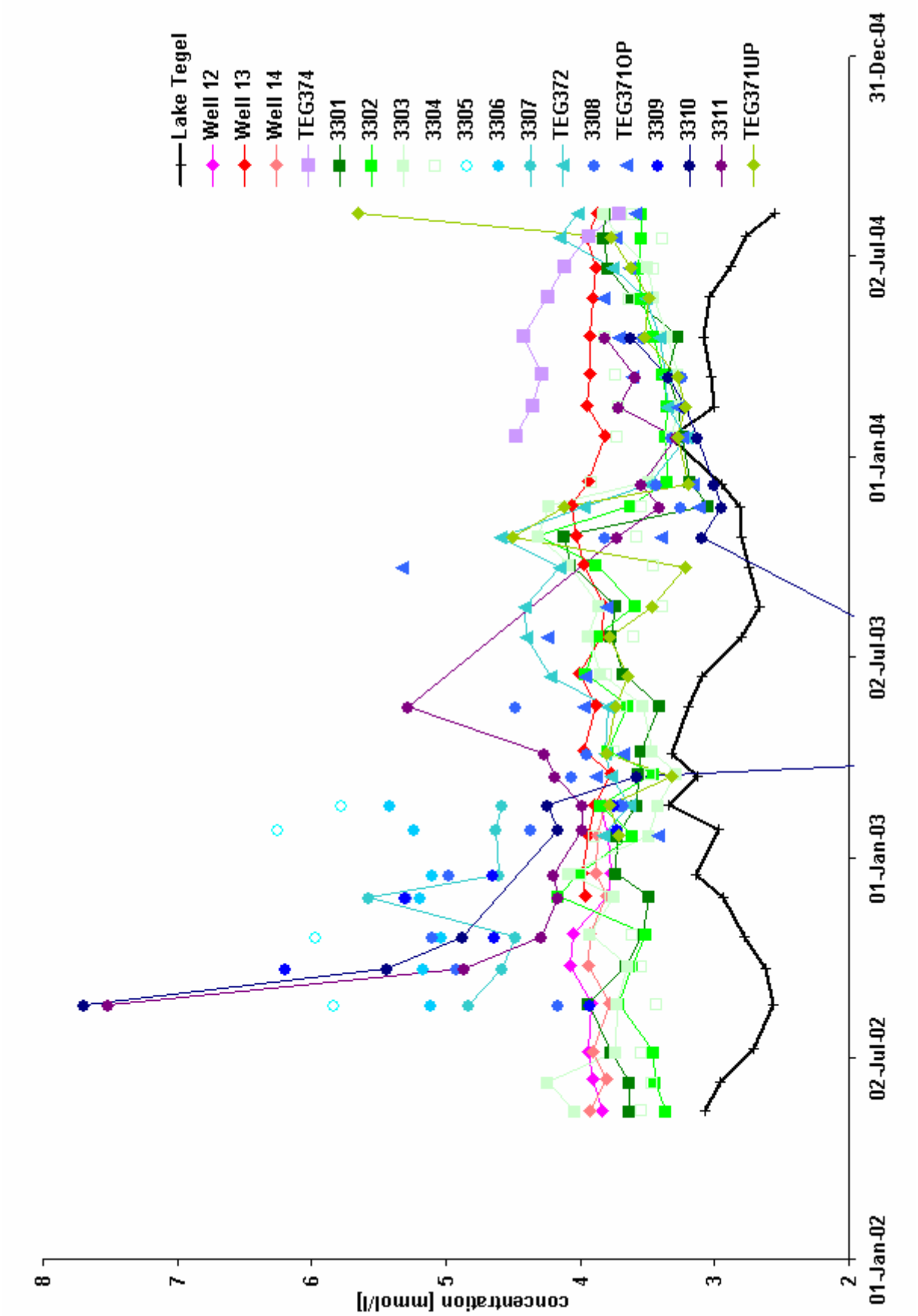

Figure App29: Total inorganic carbon in Lake Tegel, observation wells and abstraction wells 12, 13, 14 (KWB 2005).

Acknowledgements

I would like to thank all the persons which supported this work. Special thanks to my supervisor Gunnar Nützmann for his steady support and trustfulness during the entire thesis, Janek Greskowiak for the answers to many geochemical questions, and Reinhard Hinkelmann for his very careful review and methodical hints which substantially improved this work, and Ekkehard Holzbecher for the short-term review. Asaf Pekdeger for his amply support in hydrogeologic questions

The possibility to use recent and unpublished data from Anja Hoffmann significantly improved the density of interpretation. Many thanks as well to Danijela Markoviç for review, discussions about matrix operations and long time mental support. The latter two points also refer to the help of Rainer Brüggemann. Thorsten Strube's cookie sessions provided several kinds of energy for many late hours. Johannes Hochschild and Fritz installed the extra bits of computational power. Alexander Nogeitzig provided voluntary support and the deepest dive at the infiltration measurements. The discussions with Gudrun Massmann, Frank Engelmann and Thomas Taute raised many questions, revealed inconsistencies and led to a better understanding of the system. Birgit Fritz crawled deeply in the treasure chest of her investigations with large benefit for the present thesis.